frontiers | Research Topics

Case reports in neurogenetics, volume III - 2023

Edited by
Huifang Shang

Published in
Frontiers in Neurology

ISSN 1664-8714
ISBN 978-2-8325-4950-6
DOI 10.3389/978-2-8325-4950-6

About Frontiers

Frontiers is more than just an open access publisher of scholarly articles: it is a pioneering approach to the world of academia, radically improving the way scholarly research is managed. The grand vision of Frontiers is a world where all people have an equal opportunity to seek, share and generate knowledge. Frontiers provides immediate and permanent online open access to all its publications, but this alone is not enough to realize our grand goals.

Frontiers journal series

The Frontiers journal series is a multi-tier and interdisciplinary set of open-access, online journals, promising a paradigm shift from the current review, selection and dissemination processes in academic publishing. All Frontiers journals are driven by researchers for researchers; therefore, they constitute a service to the scholarly community. At the same time, the *Frontiers journal series* operates on a revolutionary invention, the tiered publishing system, initially addressing specific communities of scholars, and gradually climbing up to broader public understanding, thus serving the interests of the lay society, too.

Dedication to quality

Each Frontiers article is a landmark of the highest quality, thanks to genuinely collaborative interactions between authors and review editors, who include some of the world's best academicians. Research must be certified by peers before entering a stream of knowledge that may eventually reach the public - and shape society; therefore, Frontiers only applies the most rigorous and unbiased reviews. Frontiers revolutionizes research publishing by freely delivering the most outstanding research, evaluated with no bias from both the academic and social point of view. By applying the most advanced information technologies, Frontiers is catapulting scholarly publishing into a new generation.

What are Frontiers Research Topics?

Frontiers Research Topics are very popular trademarks of the *Frontiers journals series*: they are collections of at least ten articles, all centered on a particular subject. With their unique mix of varied contributions from Original Research to Review Articles, Frontiers Research Topics unify the most influential researchers, the latest key findings and historical advances in a hot research area.

Find out more on how to host your own Frontiers Research Topic or contribute to one as an author by contacting the Frontiers editorial office: frontiersin.org/about/contact

Case reports in neurogenetics, volume III - 2023

Topic editor
Huifang Shang — Sichuan University, China

Citation
Shang, H., ed. (2024). *Case reports in neurogenetics, volume III - 2023*. Lausanne: Frontiers Media SA. doi: 10.3389/978-2-8325-4950-6

Table of contents

frontiers | Frontiers in Neurology

TYPE Case Report
PUBLISHED 01 June 2023
DOI 10.3389/fneur.2023.1161940

OPEN ACCESS

EDITED BY
Giorgio B. Boncoraglio,
IRCCS Carlo Besta Neurological Institute Foundation, Italy

REVIEWED BY
Barbara Garavaglia,
IRCCS Carlo Besta Neurological Institute Foundation, Italy
Annie Chiu,
Hong Kong Children's Hospital, Hong Kong SAR, China

*CORRESPONDENCE
Cláudia Falcão Reis
✉ claudiafalcaoreis@chporto.min-saude.pt

RECEIVED 08 February 2023
ACCEPTED 10 May 2023
PUBLISHED 01 June 2023

CITATION
Sousa E, Abreu M, Tkachenko N, Rocha J and Falcão Reis C (2023) Case report: Mohr-Tranebjaerg syndrome: hearing impairment as the onset of an insidious disorder with high recurrence risk. *Front. Neurol.* 14:1161940. doi: 10.3389/fneur.2023.1161940

Case report: Mohr-Tranebjaerg syndrome: hearing impairment as the onset of an insidious disorder with high recurrence risk

Eulalia Sousa[1], Maria Abreu[2], Nataliya Tkachenko[2], João Rocha[3] and Cláudia Falcão Reis[2,4,5]*

[1]Pediatrics Department, Centro Hospitalar Tâmega e Sousa, Penafiel, Portugal, [2]Medical Genetics Unit, Centro de Genética Médica Jacinto Magalhães, Centro Hospitalar Universitário de Santo António, Porto, Portugal, [3]Neurology Department, Centro Hospitalar Tâmega e Sousa, Penafiel, Portugal, [4]Life and Health Sciences Research Institute (ICVS), School of Medicine, University of Minho, Braga, Portugal, [5]ICVS/3B's-PT Government Associate Laboratory, Braga, Portugal

Mohr-Tranebjaerg syndrome (MTS) is an X-linked recessive disorder caused by *TIMM8A* loss of function. It is characterized by sensorineural hearing loss in childhood, progressive optic atrophy in early adulthood, early onset dementia and psychiatric symptoms of variable expressivity. We present a family with 4 affected males, explore age-related and interfamilial variability and review the literature.

Case report: A 31 years-old male developed psychiatric symptoms at age 18 and presented early onset dementia. Sensorineural hearing loss had been diagnosed in childhood. At 28yo, he developed dysarthria, dysphonia, dysmetria, limb hyperreflexia, dystonia, and spasticity following an acute encephalopathic crisis. WES revealed a hemizygous novel likely pathogenic variant in *TIMM8A*, c.45_61dup p.(His21Argfs*11), establishing the diagnosis of MTS. Genetic counseling of the family allowed the diagnosis of three other symptomatic relatives —3 nephews (11yo and two 6yo twins), children of a carrier sister. The oldest nephew had been followed since 4yo due to speech delay. Sensorineural hearing loss was diagnosed at 9yo, and hearing aids were prescribed. The two other nephews were monozygotic twins, and both had unilateral strabismus. One of the twins had macrocephaly and hypoplasia of the anterior temporal lobe, as disclosed by an MRI performed due to febrile seizures. Both had developmental delays, with the language being the most affected area. Their audiograms confirmed hearing loss. All three nephews were hemizygous for the familial *TIMM8A* variant.

Discussion: Hearing loss, an early sign of MTS due to auditory neuropathy, can often be overlooked until more severe features of the disorder manifest. Recurrence risk is high for female carriers, and reproductive options should be offered. Early monitoring of hearing and vision loss and neurological impairment in MTS patients is mandatory since early interventions may positively impact their development. This family showcases the importance of performing a timely etiological investigation of hearing loss and its impact on genetic counseling.

KEYWORDS

MTS, deafness-dystonia syndrome, hearing loss, epilepsy, X-linked

Introduction

Mohr-tranebjaerg syndrome (MTS), also known as deafness-dystonia-optic neuronopathy, is a rare X-linked recessive neurodegenerative disease characterized by pre-lingual or post-lingual sensorineural hearing impairment in early childhood, followed by slowly progressive dystonia or ataxia and optic atrophy in adolescence or adulthood (1, 2).

MTS is progressive, and other signs and symptoms may appear throughout the patient's life, such as pyramidal signs, cognitive decline, dementia, or psychiatric disorders (1–3). However, there is considerable clinical heterogeneity since both intrafamilial and interfamilial phenotypic variations have been described (4).

This syndrome is caused by hemizygous deleterious variants in *TIMM8A* or by a contiguous gene deletion at Xq22.1 encompassing *TIMM8A*. This gene encodes a small protein that localizes to the intermembrane space in mitochondria and is a component of the translational system for the import and assembly of mitochondrial inner membrane proteins (5–7). When the contiguous gene deletion includes *BTK*, located telomeric to *TIMM8A*, it additionally results in X-linked agammaglobulinemia (2, 8).

This article presents a family with four males with MTS (Figure 1) and explores age-related and interfamilial variability. Informed consent was obtained from the mothers, the legal guardians of the patients. Institutional Review Board of Centro Hospitalar Universitário do Porto granted a waiver from review.

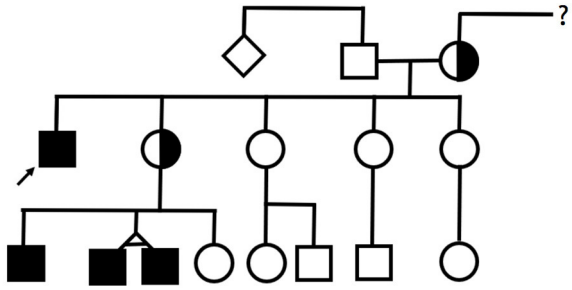

FIGURE 1
Pedigree. Filled squares represent individuals with a molecularly confirmed diagnosis of MTS.

Cases report

Case 1

The index patient, a 31-year-old male, was the first child of non-consanguineous and Caucasian parents. He had four younger sisters, and there was no family history of congenital disease.

During childhood, he presented a neurodevelopmental delay, especially in language acquisition, but no motor development delay. He was diagnosed with sensorineural hearing loss from an early age and began using hearing aids. By the age of 10 years, he was diagnosed with generalized epilepsy. He maintained convulsive episodes despite being medicated in the 1st years after diagnosis, but after 16 years old had a seizure-free period of several years. He was medicated with valproic acid through adolescence and adulthood, having recently switched levetiracetam and lacosamide.

He began having severe behavioral problems in late adolescence, associated with progressive cognitive decline, and requiring several hospitalizations due to psychiatric decompensation.

At age 27, during a psychiatric hospitalization due to self and hetero-aggressiveness, he presented generalized tonic-clonic seizures and developed severe and prolonged encephalopathy with conscious level depression associated with severe nosocomial pneumonia. Non-convulsive status epilepticus and central nervous system lesions were excluded by magnetic resonance imaging (MRI). During the following weeks, with infection resolution, his conscious level improved, but his neurological state never fully recovered to the previous state. His neurological examination revealed a well-awake and aware patient with limited speech and typical dysarthria of the hearing impaired. Severe dysphagia was present during the following weeks after the encephalopathic period, and percutaneous gastrostomy was needed but removed in less than a year. He did not present any motor deficit but had a generalized increase in muscle tone, especially in the lower limbs, with moderate spasticity and hyperreflexia, with a spastic gait that was impossible without assistance. There was also slight right-hand dystonia but without functional limitation. Whenever he became severely ill by systemic disease, his neurologic deficits worsened, and there was a rapid functional decline during the following 5 years.

The following investigation was carried out: normal metabolic, endocrine, and autoimmune panels; cerebral and spinal MRI with no focal lesions or atrophy. Electromyography revealed a slight axonal type of sensory neuropathy. Mitochondrial DNA sequencing was also negative for any pathological mutation. Ophthalmologic evaluation at age 29 was normal.

As the previous etiological investigation was inconclusive, whole exome sequencing was performed and revealed a hemizygous novel likely pathogenic variant in *TIMM8A*, c.45_61dup p.(His21Argfs*11), establishing the diagnosis of Mohr-Tranebjaerg syndrome. This variant has not been described in the literature nor in the gnomAD and ClinVar databases.

Subsequently, the patient's family was referred for genetic counseling. The same variant was found in the mother and one of the four sisters. Genetic counseling also allowed the diagnosis of other symptomatic relatives: three nephews (cases 2–4) who were children of a carrier sister. All three nephews were hemizygous for the familial *TIMM8A* variant.

Case 2

The oldest nephew was an 11-year-old boy, the first son of a non-consanguineous couple, born full-term after a supervised pregnancy. In the neonatal period, he performed otoacoustic emissions that were normal. At age 4, he was referred to a pediatric consultation due to a delay in developing expressive language. A global developmental delay was diagnosed, with the language area most severely affected. Afterward, behavioral problems were also

reported. He started speech and occupational therapy with some progress and improvements.

At 8 years old, he underwent a cognitive assessment (Weschler Intelligence Scale for Children—WISC III) that revealed a full scale intelligence quotient (IQ) of 55, verbal IQ of 51 and performance IQ of 65.

After irregular and incomplete attendance at medical appointments and diagnostic tests, sensorineural hearing loss (70 dB bilaterally) was diagnosed at 9 years Hearing aids were prescribed, which led to a slight improvement, but without full recovery of language delay.

His neurological examination was always normal, and he had no dysmorphic features.

Cases 3 and 4

The two other nephews were 6-year-old monozygotic twins, younger brothers of patient 2. They were born at 39 weeks, and no complications were described in the neonatal period. They performed the universal newborn hearing screening through otoacoustic emissions with a "pass" result in both ears.

Both had unilateral strabismus, one with onset in the 1st months of life and the other at around 2 years of age, with follow-up in ophthalmology.

One of the twins (case 3) was referred for a developmental consultation at 11 months due to macrocephaly (head circumference >99th percentile) and two simple febrile seizures at 7 and 10 months, without recurrence of seizures subsequently. In this context, he performed a cerebral MRI that only revealed an arachnoid cyst in the left middle fossa and associated hypoplasia of the anterior aspect of the temporal lobe. At 6 years of age, the other twin (case 4) had an episode of cervical dystonia.

Both had behavioral problems and global developmental delays. At 5 years old, they were evaluated by the Griffiths Mental Development Scale (GMDS), which revealed a general quotient of 64 and 70 in patients 3 and 4, respectively. The language subscale had the lowest developmental quotient: 38 and 52 for cases 3 and 4, respectively. The audiograms of both seem to confirm hearing loss but are non-specific due to lack of cooperation. Brainstem auditory evoked potentials while sedated have been scheduled for both.

Discussion

MTS is characterized by a great phenotypic variability, including intrafamilial, as demonstrated by the description of these four clinical cases. Nevertheless, all these cases had in common a neurodevelopmental delay and hearing loss with onset in the first decade of life.

The hearing impairment results from auditory neuropathy. As expected, many patients with MTS have intact otoacoustic emissions, indicating normal outer hair cells, at least in the early stages of the disease, as seen in the nephews (cases 2–4) (2, 8). Hearing impairment is often the presenting manifestation, and according to the literature, it appears to be more consistent in the age of onset and progression compared to neurological, visual, and psychiatric symptoms, which vary in degree and rate of severity (2, 8). Even so, it is sometimes overlooked and underdiagnosed until more severe features of the disorder manifest. Therefore, the hearing impairment investigation is essential because an early etiological diagnosis allows for anticipating and managing other symptoms and proper family genetic counseling.

The neurological features of MTS are usually characterized by progressive movement disorder that can appear either as dystonia and ataxia, or pyramidal signs as spasticity (2, 4). The onset of dystonia and pyramidal symptoms is variable, ranging from childhood to much later (up to the sixth decade), and there is a predilection for onset in the upper limbs or craniocervical region (4, 5). The same was verified in this family with two patients who developed dystonia, one in the first decade of life and the other in adulthood but with pyramidal symptoms as the predominant picture. Some patients may also develop dysphagia, mild peripheral sensory neuropathy (2). Index patient had a slight axonal sensory neuropathy and developed periods of severe and prolonged dysphagia during a systemic infection episode.

Another characteristic of MTS is the development of neuropsychiatric symptoms. Behavioral or neuropsychiatric problems, such as mild intellectual disability, personality changes, anxiety, reduced impulse control, aggressiveness, and compromised concentration ability, may be present from childhood. Later, some patients may present paranoid psychiatric features or gradually develop dementia (2, 8). In this family, all affected males presented delayed cognitive development with developmental speech or language disorders and behavioral problems. The index case developed more severe psychiatric features and aggressive outbursts in late adolescence.

Optic neuropathy, another feature of this syndrome, may be subclinical for many years (2). Visual impairment usually manifests between the second and fourth decades of life (5). In this family, none of the affected individuals have been diagnosed with optic neuronopathy to date.

Although epilepsy has not been associated to MTS, it is a sufficient prevalent diagnosis in the general population to be a concomitant diagnosis in our index patient. Patient 3 did not develop epilepsy up to this point, having had only simple febrile seizure episodes. The authors also argue that this newly described variant could have epileptic seizures as a phenotypic manifestation. As MTS encompasses a neurodevelopment disorder, the association with epilepsy could be one to be traced in the future, as the incidence of neurodevelopmental disorders in patients with epilepsy is higher than that in the general population (9).

Genetic diagnosis is essential as it may offer opportunities for anticipatory management. The treatment of this genetic syndrome is symptomatic, consisting in managing its manifestations (8). Thus, early monitoring of hearing and vision loss and neurological impairment in MTS patients is essential since early interventions may positively impact psychomotor development and quality of life. For this purpose, regular follow-up by a multidisciplinary team is paramount.

MTS is inherited in an X-linked manner. Consequently, the recurrence risk is high for female carriers, as seen in this family. Genetic counseling should be offered to affected or at-risk individuals, including discussion of the potential risk to offspring and reproductive options. Once the pathogenic variant has been

identified in the family, preimplantation genetic testing and prenatal testing are possible (2).

Conclusion

In conclusion, Mohr-Tranebjaerg syndrome should be suspected in a family with male elements affected with hearing loss at a young age, associated with dystonia or behavioral or neuropsychiatric disorders. This family illustrates the importance of timely etiological investigation of hearing impairment and its impact on genetic counseling.

Data availability statement

The original contributions presented in the study are included in the article/Supplementary material, further inquiries can be directed to the corresponding author.

Ethics statement

Written informed consent was obtained from the legal guardians of the patients, for the publication of any potentially identifiable images or data included in this article.

Author contributions

CF was the attending geneticist of the family and all MTS patients and reviewed and edited the manuscript. JR was the attending neurologist of the index patient and reviewed and edited the manuscript. NT was the initial attending geneticist of the monozygotic twin younger nephews. ES was the attending pediatrician resident. MA was the attending medical genetics resident. ES and MA drafted the manuscript. All authors revised the manuscript critically for important intellectual content and approved the final version of the manuscript.

Conflict of interest

The authors declare that the research was conducted in the absence of any commercial or financial relationships that could be construed as a potential conflict of interest.

Publisher's note

All claims expressed in this article are solely those of the authors and do not necessarily represent those of their affiliated organizations, or those of the publisher, the editors and the reviewers. Any product that may be evaluated in this article, or claim that may be made by its manufacturer, is not guaranteed or endorsed by the publisher.

Supplementary material

The Supplementary Material for this article can be found online at: https://www.frontiersin.org/articles/10.3389/fneur.2023.1161940/full#supplementary-material

References

1. Wang H, Wang L, Yang J, Yin L, Lan L, Li J, et al. Phenotype prediction of Mohr-Tranebjaerg syndrome (MTS) by genetic analysis and initial auditory neuropathy. *BMC Med Genet.* (2019) 20:11. doi: 10.1186/s12881-018-0741-3

2. Tranebjærg L. Deafness-dystonia-optic neuronopathy syndrome. In: MP Adam, DB Everman, GM Mirzaa, RA Pagon, SE Wallace, LJH Bean, et al., editors, *GeneReviews®*. Seattle, WA: University of Washingto (2003). p. 2.

3. Kojovic M, Pareés I, Lampreia T, Pienczk-Reclawowicz K, Xiromerisiou G, Rubio-Agusti I, et al. The syndrome of deafness-dystonia: Clinical and genetic heterogeneity. *Mov Disord.* (2013) 28:795–803. doi: 10.1002/mds.25394

4. Ha AD, Parratt KL, Rendtorff ND, Lodahl M, Ng K, Rowe DB, et al. The phenotypic spectrum of dystonia in Mohr-Tranebjaerg syndrome. *Mov Disord.* (2012) 27:1034–40. doi: 10.1002/mds.25033

5. Aguirre LA, Pérez-Bas M, Villamar M, López-Ariztegui MA, Moreno-Pelayo MA, Moreno F, et al. A Spanish sporadic case of deafness-dystonia (Mohr-Tranebjaerg) syndrome with a novel mutation in the gene encoding TIMM8a, a component of the mitochondrial protein translocase complexes. *Neuromuscul Disord.* (2008) 18:979–81. doi: 10.1016/j.nmd.2008.09.009

6. Neighbors A, Moss T, Holloway L, Yu SH, Annese F, Skinner S, et al. Functional analysis of a novel mutation in the TIMM8A gene that causes deafness-dystonia-optic neuronopathy syndrome. *Mol Genet Genomic Med.* (2020) 8:e1121. doi: 10.1002/mgg3.1121

7. Penamora-Destriza JM, Domingo A, Schmidt TGPM, Westenberger A, Klein C, Rosales R. First report of a filipino with Mohr-Tranebjaerg syndrome. *Mov Disord Clin Pract.* (2015) 2:417–9. doi: 10.1002/mdc3.12210

8. Shenny B, Vishwajyoti B, Deepika S. Deafness dystonia optic neuronopathy syndrome—A case report. *J Dental Medical Sci.* (2016).

9. Shimizu H, Morimoto Y, Yamamoto N, Tayama T, Ozawa H, Imamura A. Overlap between epilepsy and neurodevelopmental disorders: Insights from clinical and genetic studies. In: SJ Czuczwar, editor, *Epilepsy*. Brisbane, QLD: Exon Publications (2022). p. 10.

frontiers | Frontiers in Neurology

TYPE Case Report
PUBLISHED 15 June 2023
DOI 10.3389/fneur.2023.1139047

OPEN ACCESS

EDITED BY
Félix Javier Jiménez-Jiménez,
Hospital Universitario del Sureste, Spain

REVIEWED BY
Yuto Uchida,
Johns Hopkins Medicine, United States
Fiore Manganelli,
University of Naples Federico II, Italy
Ylenia Vaia,
University of Milan, Italy
Amanda Nagy,
Massachusetts General Hospital and Harvard Medical School, United States

*CORRESPONDENCE
Tai-Seung Nam
✉ nts0022@hanmail.net

RECEIVED 06 January 2023
ACCEPTED 22 May 2023
PUBLISHED 15 June 2023

CITATION
Kang Y-R, Nam T-S, Kim J-M, Kang KW, Lee S-H, Choi S-M and Kim M-K (2023) Older adult-onset Alexander disease with atypical clinicoradiological features: a case report. *Front. Neurol.* 14:1139047. doi: 10.3389/fneur.2023.1139047

Older adult-onset Alexander disease with atypical clinicoradiological features: a case report

You-Ri Kang [1], Tai-Seung Nam [1,2*], Jae-Myung Kim [1], Kyung Wook Kang [1,2], Seung-Han Lee [1,2], Seong-Min Choi [1,2] and Myeong-Kyu Kim [1,2]

[1]Department of Neurology, Chonnam National University Hospital, Gwangju, Republic of Korea, [2]Department of Neurology, Chonnam National University Medical School, Gwangju, Republic of Korea

Alexander disease (AxD) is a rare autosomal dominant astrogliopathy caused by mutations in the gene encoding for glial fibrillary acidic protein. AxD is divided into two clinical subtypes: type I and type II AxD. Type II AxD usually manifests bulbospinal symptoms and occurs in the second decade of life or later, and its radiologic features include tadpole-like appearance of the brainstem, ventricular garlands, and pial signal changes along the brainstem. Recently, eye-spot signs in the anterior medulla oblongata (MO) have been reported in patients with elderly-onset AxD. In this case, an 82-year-old woman presented with mild gait disturbance and urinary incontinence without bulbar symptoms. The patient died 3 years after symptom onset as a result of rapid neurological deterioration after a minor head injury. MRI showed signal abnormalities resembling angel wings in the middle portion of the MO along with hydromyelia of the cervicomedullary junction. Herein, we report the case of this patient with older adult-onset AxD with an atypical clinical course and distinctive MRI findings.

KEYWORDS

age of onset, Alexander disease, brainstem atrophy, magnetic resonance imaging, medulla oblongata

Introduction

Alexander disease (AxD) is an inherited progressive neurodegenerative disease caused by a mutation in the gene encoding for glial fibrillary acidic protein (GFAP). AxD has traditionally been classified into three types based on age at onset (AAO): infantile-onset (from birth to 2 years), juvenile-onset (2–14 years), and adult-onset (>14 years) (1). However, another classification system based on statistical analyses of 215 AxD cases was proposed in 2011 (2). According to this system, type I AxD manifests cerebral symptoms and signs occurring before the age of 4 years and cerebral white matter (WM) abnormalities with frontal predominance, while type II usually manifests bulbospinal symptoms in the second decade of life or later and posterior fossa WM abnormalities (2). A tadpole-like form of brainstem atrophy is the most typical manifestation of type II AxD; this can be caused by significant atrophy of the medulla oblongata (MO) and upper cervical spinal cord (3). Other radiologic findings include pial fluid-attenuated inversion recovery (FLAIR) signal changes in the brainstem (4), ventricular garlands (5), and the "eye-spot" sign in the anterior portion of the MO (6).

We managed a patient with older adult-onset AxD who presented with mild gait disturbance and urinary incontinence and without bulbar symptoms. The patient died 3 years after symptom onset as a result of post-traumatic neurological deterioration. MRI showed signal abnormality in the middle portion of the MO and hydromyelia of the cervicomedullary junction (CMJ), findings that have not been previously described. Herein, we report the case of this patient with type II AxD with an atypical clinical course and distinct MRI findings.

Case description

An 82-year-old woman with diabetes mellitus presented with a several-month history of unsteady gait and urinary incontinence. Neurological examination showed mild spasticity in the lower limbs and generalized hyperreflexia, but no Babinski sign or ankle clonus was present. We observed no bulbar symptoms or signs, including dysarthria, dysphagia, or dysphonia, and the results of tests for extrapyramidal symptoms, ocular movements, and parkinsonism were unremarkable. Her mini-mental state examination score was 25/30. A urodynamic study revealed dysfunction during the storage phases, suggesting neurogenic detrusor overactivity. Normal pressure hydrocephalus was initially suspected based on the triad of symptoms of gait disturbance, cognitive impairment, and urinary incontinence. Brain MRI showed periventricular and deep WM signal changes in the FLAIR image with no ventricular enlargement (Evans index = 0.26) (Figure 1A). Electrodiagnostic studies, including a nerve conduction study, needle electromyography, and evoked potentials, were conducted to evaluate amyotrophic lateral sclerosis or cervical spondylotic myelopathy, but these showed unremarkable results except for prolonged central motor conduction time to the upper and lower limbs in motor-evoked potentials (MEPs). In the spine MRI, mild atrophy of the MO was suspected; the ratio of the sagittal diameter of the MO to that of the pons was 0.43 (Figure 1B). No pial FLAIR signal changes were observed, nor was the eye-spot sign in the anterior MO. Intriguingly, hydromyelia in the CMJ and signal abnormalities radiating laterally from the central canal in the middle portion of the caudal MO were observed (Figure 2). GFAP gene sequencing revealed a heterozygous missense mutation (c.197G > A, p.Arg66Gln) previously reported to be pathogenic (2), and the patient was ultimately diagnosed with type II AxD. Although mild gait unsteadiness persisted, the patient could walk independently without assistance for approximately 2 years after the diagnosis. However, after a minor head injury resulting from a slip and fall, the patient became unable to walk, and dysarthria and dysphagia developed. Follow-up brain MRI showed no evidence of intracranial hemorrhage. There were no notable changes in the diameters of the sections of the brainstem, although the diameter of the MO was slightly decreased (Figure 1C). Eventually, the patient died of recurrent episodes of pneumonia 3 years after symptom onset.

Discussion

Type II AxD usually manifests bulbospinal symptoms and signs in the second decade of life or later (2). In our patient, neurological symptoms developed after the age of 80 years and remained mild, without apparent progression until the patient experienced head trauma, which is consistent with the previous speculation that advanced age of onset is associated with a milder clinical course (2). Conversely, our patient died 3 years after symptom onset, which is in line with a previous report that patients with older adult-onset AxD aged >65 years may experience more rapid disease progression than those with younger adult-onset AxD and become dependent within 2 years of onset (8). Even a minor head injury has been reported to cause acute neurological deterioration in AxD (9), which is similar to the case of our patient who died within 8 months of post-traumatic neurological exacerbation. The association between AAO and disease course in adult-onset AxD remains unclear and inconclusive. However, our case of older adult-onset AxD highlights the fact that extrinsic factors, including head trauma, physical immobility, or infections, may accelerate disease progression or contribute to poor prognosis.

Among the various MRI features observed in later-onset AxD, the most typical finding is brainstem and spinal cord atrophy (3). In our case, the ratio of the sagittal diameter of the MO to that of the pons was slightly decreased, which is consistent with one

FIGURE 1
Brain MRI of the patient. **(A, B)** MRI performed at the initial examination. **(A)** Axial T2-weighted image reveals periventricular and deep white matter hyperintensities. **(B)** Diameters of the midbrain, pons, and medulla oblongata (MO) are 14.9 mm, 23.3 mm, and 10.1 mm, respectively, on the midsagittal T1-weighted image. **(C)** MRI performed after a minor head injury shows no prominent changes. The diameters of the brainstem sections were measured as the anteroposterior distance according to the method proposed by Yoshida et al. (7).

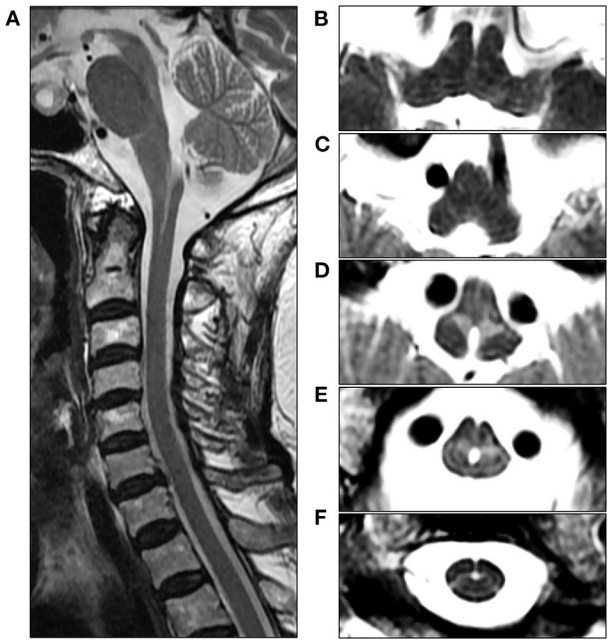

FIGURE 2
Cervical spine MRI of the patient at the initial examination. **(A)** Sagittal T2-weighted image reveals unevenly shaped hydromyelia at the cervicomedullary junction (CMJ). **(B, C)** Axial T2-weighted images at the level of the rostral medulla oblongata (MO) show normal findings in the absence of signal abnormalities in the pyramids. **(D)** Axial T2-weighted image at the level of the caudal MO reveals bilaterally symmetric hyperintensities around the central canal, resembling angel wings. **(E)** Axial T2-weighted image at the level of the CMJ reveals a hydromyelia and signal abnormalities radiating laterally from the central canal. **(F)** Axial T2-weighted image at the C2 vertebral level shows the cervical cord with normal appearance.

of the MRI parameters suggested for distinguishing adult-onset AxD from other neurological disorders (7). However, tadpole-like brainstem atrophy was not distinctly evident. The most distinctive MRI findings in our case were the signal abnormalities resembling "angel wings" radiating from the central canal (Figures 2D, E) and hydromyelia of the CMJ, which have not yet been reported. Recently, a signal abnormality in the anterior portion of MO, referred to as the "eye-spot sign," has been reported in elderly-onset AxD with mild MO atrophy and has been speculated to reflect myelin loss in the bilateral pyramids (6). In this case, our patient exhibited the pyramidal signs and MEP abnormalities, and thus the angel-wings-like signal change may be understood as being caused by the dysmyelination of the corticospinal fibers in the section where pyramidal tracts on both sides enter the spinal cord immediately after pyramidal decussation. However, this signal abnormality is located not in the medullary pyramids but in the middle portion of the MO, which suggests that it could not be simply explained by the hypothesis proposed by Yoshida et al. (6). Furthermore, the contiguity of signal change and hydromyelia at the caudal MO may indicate the contribution of the central canal to this distinctive MRI finding. The central canal is lined by the ependymal cell layer, surrounded by subependymal regions comprised of glial cells (10). Intriguingly, in an autopsy report of an 85-year-old AxD patient with no focal neurological deficit, the intense gliosis accompanied by abundant Rosenthal fibers was limited to the subependymal regions of the central canal, third ventricle, and fourth ventricle in the absence of macroscopic brainstem atrophy. Accordingly, the angel-wings-like signal change might reflect gliosis extending from the subependymal area of the central canal deep into the medullary parenchyma (11). Moreover, hydromyelia might be explained by the passive widening of the central canal secondary to the regional neurodegeneration of the subependymal area. Unfortunately, our hypotheses could not be substantiated since a postmortem examination was not performed in this case.

In summary, our case highlights several interesting characteristics of older adult-onset type II AxD, including mild spastic gait and urinary incontinence in the absence of bulbar symptoms, with rapid disease progression after a minor head injury. Radiologically, angel-wings-like signal abnormalities along with hydromyelia at the level of CMJ may be another feature of type II AxD. This case helps us understand the clinical and radiologic features of older adult-onset AxD.

Data availability statement

The datasets presented in this article are not readily available because of ethical and privacy restrictions. Requests to access the datasets should be directed to the corresponding author.

Ethics statement

The studies involving human participants were reviewed and approved by Institutional Review Board at Chonnam National University Hospital. The patients/participants provided their written informed consent to participate in this study. Written informed consent was obtained from the individual(s) for the publication of any potentially identifiable images or data included in this article.

Author contributions

Y-RK: data curation and writing of original draft. T-SN: conceptualization, writing (review and editing), and supervision. J-MK, KK, and S-MC: formal analysis. S-HL: data curation and formal analysis. M-KK: formal analysis and supervision. All authors contributed to the article and approved the submitted version.

Funding

This work was supported by grants from Chonnam National University Hospital Biomedical Research Institute (BCRI 19049 and 21025).

Conflict of interest

The authors declare that the research was conducted in the absence of any commercial or financial relationships that could be construed as a potential conflict of interest.

Publisher's note

References

1. Russo LS, Aron A, Anderson PJ. Alexander's disease: a report and reappraisal. *Neurology.* (1976) 26:607–14. doi: 10.1212/WNL.26.7.607

2. Prust M, Wang J, Morizono H, Messing A, Brenner M, Gordon E, et al. GFAP mutations, age at onset, and clinical subtypes in Alexander disease. *Neurology.* (2011) 77:1287–94. doi: 10.1212/WNL.0b013e3182309f72

3. Namekawa M, Takiyama Y, Honda J, Shimazaki H, Sakoe K, Nakano I. Adult-onset Alexander disease with typical "tadpole" brainstem atrophy and unusual bilateral basal ganglia involvement: a case report and review of the literature. *BMC Neurol.* (2010) 10:21. doi: 10.1186/1471-2377-10-21

4. Graff-Radford J, Schwartz K, Gavrilova RH, Lachance DH, Kumar N. Neuroimaging and clinical features in type II (late-onset) Alexander disease. *Neurology.* (2014) 82:49–56. doi: 10.1212/01.wnl.0000438230.33223.bc

5. van der Knaap MS, Ramesh V, Schiffmann R, Blaser S, Kyllerman M, Gholkar A, et al. Alexander disease: ventricular garlands and abnormalities of the medulla and spinal cord. *Neurology.* (2006) 66:494–8. doi: 10.1212/01.wnl.0000198770.80743.37

6. Yoshida T, Mizuta I, Saito K, Kimura Y, Park K, Ito Y, et al. Characteristic abnormal signals in medulla oblongata-"eye spot" sign: Four cases of elderly-onset Alexander disease. *Neurol Clin Pract.* (2015) 5:259–62. doi: 10.1212/CPJ.0000000000000124

7. Yoshida T, Yasuda R, Mizuta I, Nakagawa M, Mizuno T. Quantitative evaluation of brain stem atrophy using magnetic resonance imaging in adult patients with alexander disease. *Eur Neurol.* (2017) 77:296–302. doi: 10.1159/000475661

8. Yoshida T, Mizuta I, Yasuda R, Mizuno T. Clinical and radiological characteristics of older-adult-onset Alexander disease. *Eur J Neurol.* (2021) 28:3760–7. doi: 10.1111/ene.15017

9. Benzoni C, Aquino D, Di Bella D, Sarto E, Moscatelli M, Pareyson D, et al. Severe worsening of adult-onset Alexander disease after minor head trauma: Report of two patients and review of the literature. *J Clin Neurosci.* (2020) 75:221–3. doi: 10.1016/j.jocn.2020.03.033

10. Saker E, Henry BM, Tomaszewski KA, Loukas M, Iwanaga J, Oskouian RJ, et al. The Human central canal of the spinal cord: a comprehensive review of its anatomy, embryology, molecular development, variants, and pathology. *Cureus.* (2016) 8:e927. doi: 10.7759/cureus.927

11. Soffer D, Horoupian DS. Rosenthal fibers formation in the central nervous system. Its relation to Alexander's disease. *Acta Neuropathol.* (1979) 47:81–4. doi: 10.1007/BF00698278

frontiers | Frontiers in Neurology

TYPE Case Report
PUBLISHED 20 July 2023
DOI 10.3389/fneur.2023.1199095

OPEN ACCESS

EDITED BY
Andrew Anthony Hicks,
Eurac Research, Italy

REVIEWED BY
Jae Ho Jung,
Seoul National University Hospital, Republic of Korea
Davide Vecchio,
Bambino Gesù Children's Hospital (IRCCS), Italy

*CORRESPONDENCE
Claudia Ciaccio
✉ claudia.ciaccio@istituto-besta.it

RECEIVED 02 April 2023
ACCEPTED 28 June 2023
PUBLISHED 20 July 2023

CITATION
Hafdaoui S, Ciaccio C, Castellotti B, Sciacca FL, Pantaleoni C and D'Arrigo S (2023) Case report: A novel pathogenic FRMD7 variant in a Turner syndrome patient with familial idiopathic infantile nystagmus. *Front. Neurol.* 14:1199095. doi: 10.3389/fneur.2023.1199095

Case report: A novel pathogenic FRMD7 variant in a Turner syndrome patient with familial idiopathic infantile nystagmus

Sara Hafdaoui[1], Claudia Ciaccio[1]*, Barbara Castellotti[2], Francesca L. Sciacca[3], Chiara Pantaleoni[1] and Stefano D'Arrigo[1]

[1]Department of Pediatric Neurosciences, Fondazione IRCCS Istituto Neurologico Carlo Besta, Milan, Italy, [2]Department of Medical Genetics and Neurogenetics, Fondazione IRCCS Istituto Neurologico Carlo Besta, Milan, Italy, [3]Laboratory of Cytogenetic, Neurological Biochemistry and Neuropharmacology Unit, Department of Diagnostic and Technology, Fondazione IRCCS Istituto Neurologico Carlo Besta, Milan, Italy

Infantile idiopathic nystagmus (IIN) is an oculomotor disorder characterized by involuntary bilateral, periodic ocular oscillations, predominantly on the horizontal axis. X-linked IIN (XLIIN) is the most common form of congenital nystagmus, and the FERM domain-containing gene (*FRMD7*) is the most common cause of pathogenesis, followed by mutations in *GPR143*. To date, more than 60 pathogenic *FRMD7* variants have been identified, and the physiopathological pathways leading to the disease are not yet completely understood. *FRMD7*-associated nystagmus usually affects male patients, while it shows incomplete penetrance in female patients, who are mostly asymptomatic but sometimes present with mild ocular oscillations or, occasionally, with clear nystagmus. Here we report the first case of a patient with Turner syndrome and INN in an XLIIN pedigree, in which we identified a novel frameshift mutation (c.1492dupT) in the FRMD7 gene: the absence of one X chromosome in the patient unmasked the presence of the familial genetic nystagmus.

KEYWORDS

FRMD7, idiopathic nystagmus, Turner syndrome, X-linked IIN, X-linked nystagmus

1. Introduction

The *FRMD7* gene is located in the Xq26.2 chromosomal region; it consists of 12 exons encoding a 714-residue protein, FRMD7, whose cellular function is still debated (1–3). It is known that the FRMD7 protein contains a FERM domain at the N-terminus, indicating its possible participation in signal transduction between the cell membrane and the cytoskeleton (4), similar to other FERM domain proteins (5, 6).

The gene is expressed in various tissues, namely in the brain areas responsible for eye movement control (such as the midbrain and cerebellum) and the retina. Studies in mice have detected *FMRD7* mRNA in the ventricular layer of the forebrain, suggesting that the protein plays a role in the development of nerve cells in these areas of the brain and retina (7, 8).

More than 60 *FRMD7* variants have been described in X-linked infantile nystagmus, most of them missense variants; pathogenic variants of the gene are likely to result in the production of an unstable protein that is unable to perform its normal functions, therefore disrupting nerve cell development in the expected areas of influence (2, 7). This malfunctioning of the brain areas that control eye movements, along with retinal

misdevelopment, is thought to cause the involuntary side-to-side eye movements that are characteristic of X-linked infantile nystagmus (7, 9, 10).

Genetic studies of nystagmus are increasingly being reported, expanding the clinical and molecular knowledge of this disorder.

Turner syndrome is a chromosomal abnormality caused by the deletion or non-functioning of one X chromosome in a phenotypically female individual. In about 50% of cases, it is caused by an X monosomy (45,X0 karyotype), while the other half are mosaic patients carrying an X monosomy component and a normal component (45,X0/46,XX or 45,xo/46,XY); in addition, in rare cases, Turner syndrome can result from peculiar chromosomal abnormalities leading to a non-functional X chromosome, such as isochromosome Xq (an X chromosome composed of two copies of the long arm of the X chromosome linked together), ring X with partial loss of genetic material in both the long and short arms, or Xp/ Xq deletions (11, 12). With an incidence of 1/2,500 births, it is one of the most common chromosomal anomalies observed. Two main random pathogenic mechanisms are known to cause the disorder: a nondisjunction event occurring during germ cell development, with the creation of an egg or sperm cell lacking an X chromosome, which, together with a normal germ cell, generates an embryo with an anomalous number of chromosomes and an error during the cell division cycles of early fetal development, resulting in a mosaic asset with a part of cells with a normal karyotype and a part of cells with an X0 alteration (11). It is typically a *de novo* condition, because most patients are infertile, but in extremely rare cases it can be transmitted from one generation to the next (12). The phenotype of Turner syndrome arises from X-linked genes that escape inactivation: short stature and Madelung's deformity result from mutations in the *SHOX* gene (13), while gonadal dysgenesis involves genes such as *USP9X*, *RPS4X*, and *DIAPH2* (12, 14).

The X chromosome also contains several genes responsible for X-linked disorders, which typically manifest in male subjects and are masked in female subjects by the presence of a normally functioning gene on the other X. The absence of an X chromosome may therefore expose Turner's patients to the occurrence of familial genetic disorders that do not usually affect female individuals.

2. Case presentation

A 5-month-old girl was referred to our center because of early-onset nystagmus. Her family history was positive for nystagmus, present in the maternal uncle and a male cousin of the mother (Figure 1).

The girl was born from a heterozygous twin pregnancy; her female twin and an older sister were reported to be in good general health, as were her parents. The pregnancy was complicated by gestational hypertension, and a cesarean section was performed at 35 + 3 weeks gestation. At birth, she showed normal growth parameters (weight 2,070 g, length 47 cm, head circumference 31 cm) and no perinatal distress (Apgar score 10/10), but she later experienced poor sucking for a few days and an anterior ectopic anus was detected.

At the age of 3 months, her father started noticing anomalous horizontal eye movements; the girl underwent an ophthalmologic examination, which confirmed the presence of a pendular nystagmus of low frequency and good amplitude, without convergence problems or fundus oculi alterations.

Clinical examination revealed good general health and normal growth (length 62 cm =25–50°, weight 6.3 kg = 25–50°, head circumference 40.5 cm = 10–25°). Dysmorphic facial features were present (bitemporal narrowing, epicanthus, simplified and protruding ears), in addition to mild telethelia, inverted nipples, the previously reported anteriorly displaced anus, a hairless sacral dimple, and a congenital melanocytic nevus on the right leg covered with hair and measuring 6 × 3 cm. Neurological examination showed bilateral pendular horizontal nystagmus, mildly increased muscular tone, and mild motor developmental delay.

The patient underwent several diagnostic examinations, including routine blood work, metabolic screening (plasma amino acids and urine organic acids), brain MRI, EEG, and evoked potentials (VEP, ERG, BAEP), all with normal results; in particular, brain MRI showed no signs of optic nerve atrophy, and VEP and ERG showed no alterations. Once again, the girl underwent an ophthalmologic evaluation, which confirmed normal fundus oculi,

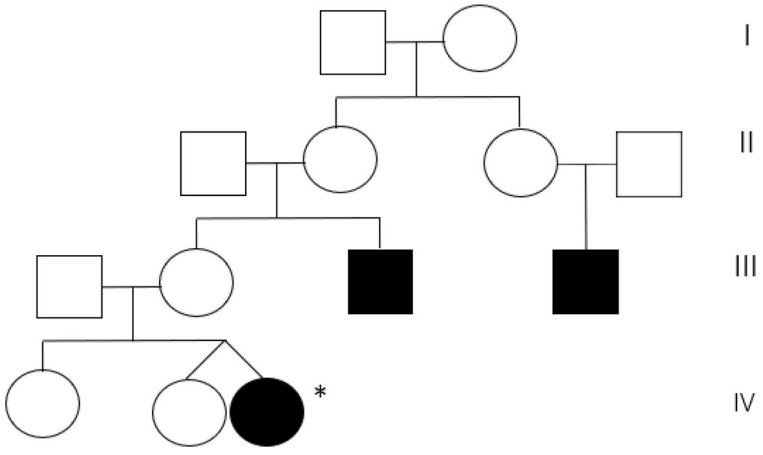

FIGURE 1
Maternal pedigree of the patient. Proband is marked with an asterisk.

no photophobia, and no additional pathologic findings other than the nystagmus.

All the data pointed to a genetic condition. Array CGH was performed with an ISCA resolution of 19 kb, with the following result: Xp22.33q28 (16961_155208387)x1, meaning a deletion of an entire heterosome. Therefore, we also asked for a karyotype, performed on 16 metaphases with a resolution of 550 bands, which confirmed an X monosomy (Turner syndrome) in all analyzed metaphases. Nystagmus is an uncommon feature in Turner's patients, with a variable prevalence depending on the study, ranging from 4 up to 20% (15, 16). Given the family history and the genotype of the baby, we hypothesized that the nystagmus could be a symptom of an X-linked condition caused by the loss of one of the sex chromosomes and, in particular, an alteration in the *FRMD7* gene.

Sequencing of the *FMRD7* gene was performed by NGS technology and highlighted the presence of a hemizygous frameshift variant (c.1492dupT), which determines the production of an aberrant and prematurely truncated protein (p.Tyr498Leufs*15), and is classified as probably pathogenic according to the ACMG guidelines (17) (PVS1, PM2 criteria). The same variant was detected in the healthy mother, while the male relatives, living abroad, were not available for testing. The nystagmus was therefore confirmed to be caused by this mutation, which was revealed by Turner syndrome.

3. Discussion

45,X0 is the most common karyotype in patients with Turner syndrome, accounting for ∼50% of all cases (12, 18). Typical manifestations of the condition include short stature, hypogonadism, and/or other types of gonadal dysplasia (often with primary amenorrhea), a webbed neck, mammary hypoplasia with spaced and inverted nipples, heart malformations (most commonly bicuspid aortic valve, aortic coarctation, and aortic valvulopathy), and skeletal (shield-like chest, cubitus valgus, scoliosis) or genitourinary abnormalities (horseshoe kidney, anus imperforatus, anal atresia) (11, 12, 18). The phenotype can be very different among patients and mostly depends on the karyotype, with X0 individuals having the most severe presentation and mosaic individuals showing severity and gonadal differentiation depending on the ratio of 45,X0/normal cells (12, 18).

Ophthalmologic defects are not typical of Turner syndrome, and the most common features emerging from the few available studies are ametropia and strabismus, both of which are also known to be common in the general pediatric population (19). Nystagmus has been listed in the group of "uncommon ophthalmological defects" (prevalence 5%−25%) in a paper by Denniston and Butler (15) and estimated at 4% in a study by Wikiera et al. (16).

In our case, the family history was suggestive of hereditary nystagmus, given the presence of two affected male relatives in the maternal line.

FRMD7 variants are among the most common causes of hereditary nystagmus.

The gene was first suspected to be involved in the condition in 2006, following a work published by Tarpey et al. (3) that identified an *FMRD7* variant in 15 of 16 families with congenital nystagmus. The gene is now known to be a member of the protein 4.1 superfamily and to have a highly conserved NH2-terminus containing the B41 and the FERM-C domains (20–22). The FERM domain at the N-terminus is also present in other proteins, such as FARP1 and FARP2, and studies in rats have demonstrated that it modulates the length and branching of neurites in embryonic cortical neurons and reorganizes the cytoskeleton (7, 21). In adult humans, the FRMD7 protein is absent in ocular tissues but has been detected during embryonic stages in the developing neural retina and in brain regions that control eye movements (forebrain, midbrain, cerebellar primordium) (3–6). Recently, foveal hypoplasia and developmental abnormalities of the optic nerve head have been reported in patients with *FRMD7* pathogenic variants as a result of retinal neuronal migratory disorders due to impaired growth cone guidance, which is consistent with the expression patterns observed in the developing retina and optic nerve (23). The dysfunction of FRMD7 may contribute to the absence of the horizontal optokinetic reflex through the loss of horizontal direction selectivity. These findings suggest that the abnormal development of the afferent visual system may be associated with *FRMD7* variants and may affect neural circuits within the oculomotor system, leading to abnormal eye movements and gaze instability (22). Taken together, these data provide strong evidence that the FRMD7 protein plays a role in the neural development of visual circuits.

Although we did not perform a functional analysis of the protein, a review of the FRMD7 literature shows that in mice, null mutations in FRMD7 alter neurite length and the branching process of neurons in the midbrain, cerebellum, and retina. This is a plausible explanation for how defects in the protein coded by *FRMD7* cause disease (4, 24).

FRMD7-related infantile nystagmus is characterized by either the onset of horizontal, conjugate, gaze-dependent, or time-dependent nystagmus in the first 6 months of life or periodic alternating nystagmus (with cyclic changes in nystagmus direction) with infantile onset. Binocular vision and color vision are normal, and visual acuity is usually good (>6/12). In total, 15% of affected individuals have an abnormal head posture as the consequence of a continuous attempt to reach an eccentric null point (a point of gaze where oscillation is minimally present) (25, 26). The optokinetic response is abnormal, and both low gains and reversal patterns have been described (25). No particular genotype-phenotype has been described regarding such ophthalmologic features; indeed, studies have shown extensive intra- and interfamilial variability in the clinical presentation (8, 25, 27).

In our case, once the patient was found to have Turner syndrome, the most likely condition to explain her nystagmus was an *FMRD7* alteration. Considering other XL conditions associated with nystagmus, the little girl did not show the iris hypopigmentation that is usual in type 1 ocular albinism; there were no symptoms or signs of photophobia present, as expected in blue cone monochromatism; and dark adaptation was normal, thus ruling out congenital stationary night blindness.

FRMD7 sequencing was therefore performed, confirming the presence of the pathogenic variant c.1492dupT (p.Tyr498LeufsTer15) that, consistent with family history, was inherited from her healthy mother.

XLIIN shows an incomplete penetrance in carrier females (27–29), probably as a consequence of the skewed X inactivation pattern, resulting in an unbalanced inactivation of the paternal and maternal X chromosomes established in embryonic life (28–30).

In our family, we did not study the X inactivation pattern and FRMD7 testing was not performed in the two patient siblings for ethical reasons (they are both healthy minors).

4. Conclusions

We presented the case of a girl with a phenotype mimicking that of a more severe condition and found it to be the consequence of a double diagnosis of Turner syndrome plus familial *FRMD7*-related nystagmus.

Given the phenotype, the first diagnostic hypothesis was that a single disease could justify all the clinical features of the girl. Array-CGH analysis revealed the diagnosis of Turner syndrome, which explains almost all the symptoms (spaced and inverted nipples, anal anomaly, etc.) but not the nystagmus. Moreover, the maternal family history was positive for nystagmus in male relatives, which is extremely relevant to anamnestic data. *FRMD7*-related nystagmus was confirmed by the targeted molecular analysis, which identified the maternal frameshift variant in exon 12 c.1492dupT (p.Tyr498LeufsTer15), not previously described and predicted *in silico* to be pathogenic. Other frameshift variants in the same exon are described and analyzed in different studies, highlighting the important role of the highly conserved C-terminal region of FRMD7 (31, 32). These findings lead us to the diagnosis of *FRMD7* X-linked nystagmus with Turner syndrome.

With the advent of NGS, we have access to extremely sophisticated genetic methods that have allowed us to make great strides in the knowledge of genetics and pathologies; in fact, international genetic guidelines recommend WES as a first-step analysis in the case of psychomotor delay and intellectual disability. However, it is useful to remember that the techniques of classical and molecular cytogenetics must not be abandoned, as in this case they led to a simplified diagnostic algorithm.

In conclusion, our results broaden the mutation spectrum of FRMD7. Finally, this work highlights the importance of a sequential and precise diagnostic algorithm that, starting from a careful collection of anamnestic data and clinical examination, facilitates the achievement of a diagnosis without bias or waste of resources.

Data availability statement

The datasets presented in this article are not readily available because of ethical and privacy restrictions. Requests to access the datasets should be directed at: the corresponding author.

Ethics statement

Ethical review and approval was not required for the study on human participants in accordance with the local legislation and institutional requirements. Written informed consent to participate in this study was provided by the participants' legal guardian/next of kin. Written informed consent was obtained from the individual(s), and minor(s)' legal guardian/next of kin, for the publication of any potentially identifiable images or data included in this article.

Author contributions

SH: patient evaluation and manuscript writing. CC: patient evaluation, manuscript writing, and editing. BC and FLS: genetic testing performance and manuscript revision. CP and SD: supervision, manuscript revision, and editing. All authors had access and approved the final version of the manuscript.

Funding

The study was funded by Fondazione Pierfranco e Luisa Maria and Banca d'Italia.

Acknowledgments

The authors from the Department of Developmental Neurology of the Institute are members of ITHACA ERN.

Conflict of interest

The authors declare that the research was conducted in the absence of any commercial or financial relationships that could be construed as a potential conflict of interest.

The reviewer DV declared a shared parent affiliation with the authors to the handling editor at the time of review.

Publisher's note

References

1. Zhao H, Huang X-F, Zheng Z-L, Deng W-L, Lei X-L, Xing D-J, et al. Molecular genetic analysis of patients with sporadic and X-linked infantile nystagmus. *BMJ Open.* (2016) 6:e010649. doi: 10.1136/bmjopen-2015-010649

2. Chen J, Wei Y, Tian L, Kang X. A novel frameshift mutation in FRMD7 causes X-linked infantile nystagmus in a Chinese family. *BMC Med Genet.* (2019) 20:5. doi: 10.1186/s12881-018-0720-8

3. Tarpey P, Thomas S, Sarvananthan N, Mallya U, Lisgo S, Talbot CJ, et al. Mutations in FRMD7, a newly identified member of the FERM family, cause X-linked idiopathic congenital nystagmus. *Nat Genet.* (2006) 38:1242–4. doi: 10.1038/ng1893

4. Betts-Henderson J, Bartesaghi S, Crosier M, Lindsay S, Chen H-L, Salomoni P, et al. The nystagmus-associated FRMD7 gene regulates neuronal outgrowth and development. *Hum Mol Genet.* (2010) 19:342–51. doi: 10.1093/hmg/ddp500

5. Cho W, Stahelin RV. Membrane-protein interactions in cell signalling and membrane trafficking. *Annu Rev Biophys Biomol Struct.* (2005) 34:119–51. doi: 10.1146/annurev.biophys.33.110502.133337

6. Sun CX, Robb VA, Gutmann DH. Protein 4, 1. tumour suppressors: getting a FERM grip on growth regulation. *J Cell Sci.* (2002) 115(Pt 21):3991–4000. doi: 10.1242/jcs.00094

7. Watkins RJ, Thomas MG, Talbot CJ, Gottlob I, Shackleton S. The role of FRMD7 in Idiopathic Infantile Nystagmus. *J Ophtalmol.* (2012) 460957. doi: 10.1155/2012/460956

8. Self J, Haitchi HM, Griffiths H, Holgate ST, Davies DE, Lotery A. Frmd7 expression in developing mouse brain. *Eye.* (2010) 24:165–9. doi: 10.1038/eye.2009.44

9. Pu J, Li Y, Liu Z, Yan Y, Tian J, Chen S, et al. Expression and localization of FRMD7 in human fetal brain, and a role for F-actin. *Mol Vis.* (2011) 17:591–7.

10. Pu J, Mao Y, Lei X, Yan Y, Lu X, Tian J, et al. FERM domain containing protein interacts with the Rho GDP Dissociation inhibitor and specifically activates Rac1 signalling. *PLoS ONE.* (2013) 8:e73108. doi: 10.1371/journal.pone.0073108

11. Ranke MB, Saenger P. Turner's syndrome. *Lancet.* (2001) 28:358. doi: 10.1016/S0140-6736(01)05487-3

12. Shankar Kikkeri N, Nagalli S. *Turner's Syndrome.* [Updated 2022 Jun 20]. In: StatPearls [Internet]. Treasure Island, FL: StatPearls Publishing (2022).

13. Ogata T, Matsuo N, Nishimura G. SHOX haploinsufficiency and overdosage: impact of gonadal function status. *J Med Genet.* (2001) 38:1–6. doi: 10.1136/jmg.38.1.1

14. Yuan X, Zhu Z. Turner syndrome with rapidly progressive puberty: a case report and literature review. *J Int Med Res.* (2020) 48:300060519896914. doi: 10.1177/0300060519896914

15. Denniston AKO, Butler L. Ophthalmic features of Turner's syndrome. *Eye.* (2004) 18:680–4. doi: 10.1038/sj.eye.6701323

16. Wikiera B, Mulak M, Koltowska-Haggstrom M, Noczynska A. The presence of eye defects in patients with Turner syndrome is irrespective of their karyotype. *Clin Endocrinol.* (2015) 83:842–8. doi: 10.1111/cen.12794

17. Richards S, Aziz N, Bale S, Bick D, Das S, Gastier-Foster J, et al. Standards and guidelines for the interpretation of sequence variants: a joint consensus recommendation of the American College of Medical Genetics and Genomics and the Association for Molecular Pathology. *Genet Med.* (2015) 17:405–24. doi: 10.1038/gim.2015.30

18. Sybert VP, McCauley E. Turner's syndrome. *N Engl J Med.* (2004) 351:1227–38. doi: 10.1056/NEJMra030360

19. Huang J, Basith SST, Patel S, Goetsch Weisman A, Brickman W, Mets MB, et al. Ocular findings in paediatric Turner syndrome. *Ophthalmic Genet.* (2022) 43:450–3. doi: 10.1080/13816810.2022.2045512

20. Li N, Wang L, Cui L, Zhang L, Dai S, Li H, et al. Five novel mutations of the FRMD7 gene in Chinese families with X-linked infantile nystagmus. *Mol Vis.* (2008) 14:733–8.

21. Baines AJA. A FERM-adjacent (FA) region defines a subset of the 4.1 superfamily and is a potential regulator of FERM domain function. *BMC Genomics.* (2006) 7:85. doi: 10.1186/1471-2164-7-85

22. Du W, Bu J, Dong J, Jia Y, Li J, Liang C, et al. A novel frame-shift mutation in FRMD7 causes X-linked idiopathic congenital nystagmus in a Chinese family. *Mol Vis.* (2011) 17:2765–8.

23. Thomas MG, Crosier M, Lindsay S, Kumar A, Araki M, Leroy BP, et al. Abnormal retinal development associated with FRMD7 mutation. *Hum Mol Genet.* (2013) 22:4086–93. doi: 10.1093/hmg/ddu122

24. Pu J, Lu X, Zhao G, Yan Y, Tian J, Zhang B. FERM domain containing protein 7 (FRMD7) upregulates the expression of neuronal cytoskeletal proteins and promotes neurite outgrowth in Neuro-2a cells. *Mol Vis.* (2012) 18:1428–35.

25. Thomas S, Proudlock FA, Sarvananthan N, Roberts EO, Awan M, McLean R, et al. Phenotypical characteristics of idiopathic infantile nystagmus with and without mutations in FRMD7. *Brain.* (2008) 131:1259–67. doi: 10.1093/brain/awn046

26. Thomas MG, Crosier M, Lindsay S, Kumar A, Thomas S, Araki M, et al. The clinical and molecular genetic features of idiopathic infantile periodic alternating nystagmus. *Brain.* (2011) 134:892–902. doi: 10.1093/brain/awq373

27. Shiels A, Bennett TM, Prince JB, Tychsen L. X-linked idiopathic infantile nystagmus associated with a missense mutation in FRMD7. *Molec Vis.* (2007) 13:2233–41.

28. Kaplan Y, Vargel I, Kansu T, Akin B, Rohmann E, Kamaci S, et al. Skewed X inactivation in an X linked nystagmus family resulted from a novel, p.R229G, missense mutation in the FRMD7 gene. *Br J Ophthalmol.* (2008) 92:135–41. doi: 10.1136/bjo.2007.128157

29. Zhang B, Liu Z, Zhao G, Xie X, Yin X, Hu Z, et al. Novel mutations of the FRMD7 gene in the X-linked congenital motor nystagmus. *Mol Vis.* (2007) 13:1674–9.

30. Pereira G, Dória S. X-chromosome inactivation: implications in human disease. *J Genet.* (2021) 100:63. doi: 10.1007/s12041-021-01314-1

31. Schouten JP, McElgunn CJ, Waaijer R, Zwijnenburg D, Diepvens F, Pals G. Relative quantification of 40 nucleic acid sequences by multiplex ligation-dependent probe amplification. *Nucleic Acid Res.* (2002) 30:e57. doi: 10.1093/nar/gnf056

32. AlMoallem B, Bauwens M, Walraedt S, Delbeke P, De Zaeytijd J, Kestelyn P, et al. Novel FRMD7 mutations and genomic rearrangement expand the molecular pathogenesis of X-linked idiopathic infantile nystagmus. *Invest Ophtalmol Vis Sci.* (2015) 56:1701–10. doi: 10.1167/iovs.14-15938

frontiers | Frontiers in Neurology

TYPE Case Report
PUBLISHED 26 July 2023
DOI 10.3389/fneur.2023.1228810

OPEN ACCESS

EDITED BY
Félix Javier Jiménez-Jiménez,
Hospital Universitario del Sureste, Spain

REVIEWED BY
Pedro J. Garcia-Ruiz,
University Hospital Fundación Jiménez Díaz, Spain
Luciana Chessa,
Sapienza University of Rome, Italy

*CORRESPONDENCE
Jing Zhang
✉ zhangj096@yeah.net
Zhaonan Yu
✉ yuzhaonan870213@163.com

†These authors have contributed equally to this work

RECEIVED 25 May 2023
ACCEPTED 04 July 2023
PUBLISHED 26 July 2023

CITATION
Shao L, Wang H, Xu J, Qi M, Yu Z and Zhang J (2023) Ataxia-telangiectasia in China: a case report of a novel *ATM* variant and literature review. *Front. Neurol.* 14:1228810. doi: 10.3389/fneur.2023.1228810

Ataxia-telangiectasia in China: a case report of a novel *ATM* variant and literature review

Li Shao[1†], Haoyi Wang[2,3†], Jianbo Xu[4], Ming Qi[2,5], Zhaonan Yu[2,6*] and Jing Zhang[1*]

[1]Department of Child Healthcare, Jinhua Maternity and Child Health Care Hospital, Jinhua, Zhejiang, China, [2]Hangzhou D.A. Medical Laboratory, Hangzhou, Zhejiang, China, [3]Central Laboratory, Precision Diagnosis and Treatment Center of Jinhua City, Jinhua, Zhejiang, China, [4]Department of Laboratory Medicine, Jinhua Maternity and Child Health Care Hospital, Jinhua, Zhejiang, China, [5]Department of Cell Biology and Medical Genetics, School of Medicine, Zhejiang University, Hangzhou, Zhejiang, China, [6]Medical College of Tianjin University, Tianjin, China

Background: Ataxia-telangiectasia (A-T) is a multisystem genetic disorder involving ataxia, oculocutaneous telangiectasia, and immunodeficiency caused by biallelic pathogenic variants in the *ATM* gene. To date, most *ATM* variants have been reported in the Caucasian population, and few studies have focused on the genotype–phenotype correlation of A-T in the Chinese population. We herein present a Chinese patient with A-T who carries compound heterozygous variants in the *ATM* gene and conducted a literature review for A-T in China.

Case presentation: A 7-year-old Chinese girl presented with growth retardation, ataxia, medium ocular telangiectasia, cerebellar atrophy, and elevated serum alpha-fetoprotein (AFP) level, which supported the suspicion of A-T. Notably, the serum levels of immunoglobulins were all normal, ruling out immunodeficiency. Exome sequencing and Sanger sequencing revealed two likely pathogenic *ATM* variants, namely NM_000051.4: c.4195dup (p.Thr1399Asnfs*15) and c.6006 + 1G>T (p.?), which were inherited from her father and mother, respectively. From the Chinese literature review, we found that there was a marked delay in the diagnosis of A-T, and 38.9% (7/18) of A-T patients did not suffer from immunodeficiency in China. No genotype–phenotype correlation was observed in this group of A-T patients.

Conclusion: These results extend the genotype spectrum of A-T in the Chinese population and imply that the diagnosis of A-T in China should be improved.

KEYWORDS

ataxia-telangiectasia, *ATM* gene, cerebellar atrophy, case report, literature review

Introduction

Ataxia-telangiectasia (A-T; OMIM no. 208900) is a rare multisystem disorder characterized by ataxia, oculocutaneous telangiectasia, global developmental delay, immunodeficiency, radiation hypersensitivity, and/or increased susceptibility to malignancy particularly of lymphoid origin (1–3). This condition is caused by biallelic pathogenic variants in the *ATM* gene located at chromosome 11q22.3 (1–3). The phenotype of A-T is associated with some degree of preservation of ATM kinase activity. The classical form of A-T is a severe multisystem disorder with an early onset, progressive, and neurodegenerative course due to biallelic loss-of-function variants in the *ATM* gene, whereas the milder type of A-T, characterized by slow neurological progression and/or later onset and designated "variant A-T", is caused by biallelic variants with at least one non-truncating variant (missense or splice site variant) resulting in the presence of residual ATM kinase activity

10.3389/fneur.2023.1228810

(3). The *ATM* gene harbors 66 exons and encodes a PI3K-family kinase with 3,050 amino acid residues. Hitherto, more than 1,400 unique variants have been identified in the *ATM* gene (https://www.lovd.nl/ATM).

However, studies investigating *ATM* variants and A-T in China are scarce (4–9). Herein, we describe a Chinese female patient affected by A-T with compound heterozygous variants in the *ATM* gene, one of which is novel. Furthermore, we review the literature on the genotype–phenotype spectrum of A-T in the Chinese population.

Case presentation

Clinical report

The proband, a 7-year-old Chinese girl, was referred to our hospital for the evaluation of growth retardation. Her weight and height were below the 3rd percentile, and she exhibited medium ocular telangiectasia since the age of 5. Neurological examinations revealed progressive limb and truncal ataxia, diagnosed on the basis of gait instability, dysarthria, spasticity, and delayed cognitive and motor development. At the last follow-up visit, the 9-year-old patient was not wheelchair-bound. The parents reported that the proband initially developed symptoms of ataxia at the age of 2. Laboratory tests showed that the serum levels of α-fetoprotein (AFP), lactic dehydrogenase (LDH), and carbohydrate antigen 199 (CA199) were significantly elevated, whereas the serum levels of carcinoembryonic antigen (CEA) and immunoglobulins (IgA, IgG, IgM, and IgE) levels were within the normal range (Table 1). Brain magnetic resonance imaging (MRI) unveiled cerebellar atrophy with the enlargement of cerebellar sulci (Figure 1). The parents were both normal, and no relatives were reported to have neurodegenerative diseases except for the grandpa's cousin who presented amentia. A-T was suspected based on the clinical features of ataxia, cerebellar atrophy, ocular telangiectasia, and elevated serum AFP level. Given the absence of immunodeficiency and the conservative wishes of the parents, we decided to follow up with the patient at present. Medical interventions will not be administered until the disease progresses.

Genetic analysis

To validate the clinical suspicion of A-T, exome sequencing was performed using the peripheral blood from the patient. The procedures of genetic analysis and the filtering condition for variants were described by Shalash et al. (10). We identified compound heterozygous variants in the *ATM* gene, NM_000051.4 (*ATM*): c.4195dup and c.6006 + 1G>T. The intronic variant c.6006 + 1G>T (ClinVar Variation ID: 2029577) was expected to disrupt RNA splicing by affecting a donor splice site in intron 40 of the *ATM* gene, thereby it was classified as pathogenic in the ClinVar database. The variant c.4195dup located at exon 28 led to a frameshift at residue 1399, which was predicted to produce a truncated protein of 1,412 amino acids (p.Thr1399Asnfs*15) lacking

TABLE 1 Clinical and laboratory features of the patient.

	Ataxia-age at onset (years)	Telangiectasias-age at onset (years)	Age at diagnosis (years)	Cerebellar atrophy	Serum AFP (ng/ml)	Serum CA199 (U/ml)	Serum LDH (U/L)	Serum CEA (ng/ml)	IgA (g/L)	IgG (g/L)	IgM (g/L)	IgE (kU/L)
Patient	2	5	7	Atrophied	319.61	52.73	283	<0.5	1.48	12.8	1.8	<2.0
Normal value					0–8.1	0–37	109–245	0–5	0.70–4.00	7.00–16.00	0.40–2.30	<100

AFP, α-fetoprotein; LDH, lactic dehydrogenase; CA199, carbohydrate antigen 199; CEA, carcinoembryonic antigen.

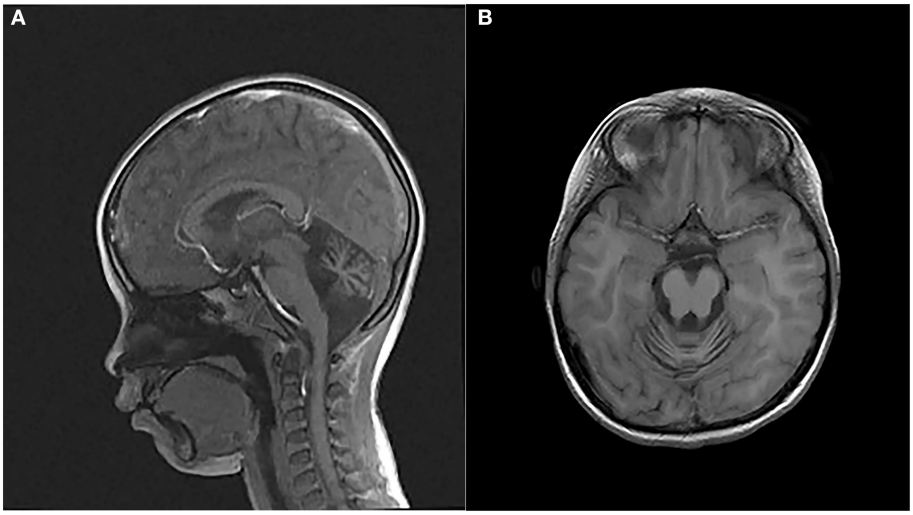

FIGURE 1
Magnetic resonance images (MRIs) of the patient's brain. **(A)** Sagittal T2-weighted brain MRI. **(B)** Axial T1-weighted brain MRI.

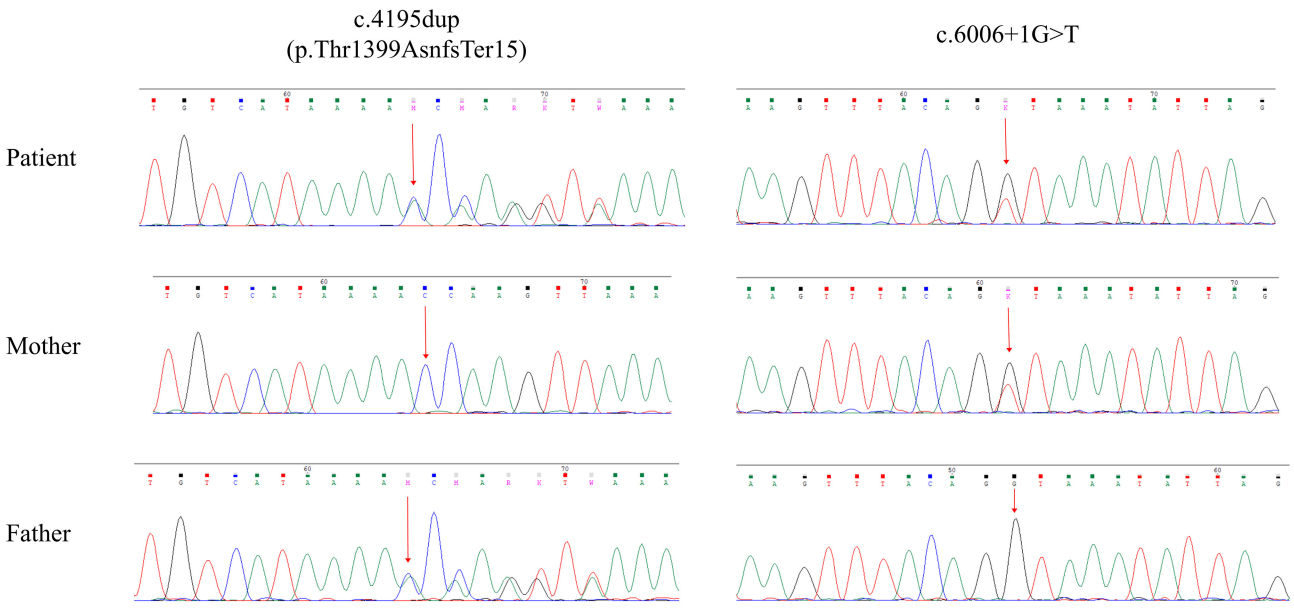

FIGURE 2
Sanger sequencing validation of the *ATM* variants of all family members.

the FAT, PI3K/PI4K catalytic, and FATC domain. The CADD and GERP scores were 33 and 4.22, respectively, both of which exceeded the threshold for pathogenicity. Using the MutationTaster tool, both variants were predicted to be disease causing. Familial segregation analysis was verified using Sanger sequencing. The compound heterozygous variants, c.4195dup and c.6006 + 1G>T, were inherited from the unaffected father and mother, respectively (Figure 2). The frameshift variant c.4195dup was not included in the gnomeAD, HGMD, and 1000G databases, thereby confirming its novelty. We did not identify any pathogenic variants in other nervous system-related genes.

Chinese literature review

Seventeen Chinese cases with A-T from six studies were collected to reveal the genotypic and phenotypic features of A-T in China (Table 2) (4–9). Combined with the case in this article, we found that there was a delay of ≥5 years in diagnosis since the onset of clinical presentations in most cases. With regard to the *ATM* genotype, compound heterozygosity is the major allelic type in China possibly due to the legal prohibition of consanguineous marriage in our country. Most cases had at least one *ATM* truncated (frameshift or non-sense) variant, which is in agreement with the classical clinical signs of A-T. Seven cases did not present

TABLE 2 Literature review for Chinese patients with ataxia-telangiectasia.

Family	Patient	Nucleotide change	Protein effect	Allele	Ataxia	Telangiectasias	Cerebellar atrophy	Elevated α-fetoprotein	Immune manifestations	Ataxia-age at onset (years)	Telangiectasias-age at onset (years)	Age at diagnosis (years)	References
I	1	c.1346G>C	p.Gly449Ala	hom	+ (severe)	+	+	+	IgA deficiency and T-cell defect	7	7	15	(4)
II	2	c.610G>T and c.6679C>T	p.Gly204* and p.Arg2227Cys	CH	+ (moderate)	+	+	+	agammaglobulinemia and T-cell defect	10	10	15	
III	3	c.1464G>A and c.56–1G>A	p.Trp448* and Splice acceptor	CH	+	+	+	+	IgG deficiency	2	3	13	(5)
	4									1.5	2	4	
IV	5	c.2680delG and c.7166C>G	p.Asp894 Ilefs*4 and p.Ser2389*	CH	+	+	+	+	-	2.5	3	14	
	6									1.5	1	7	
V	7	c.3174G>A and Exon 63 deletion	p.Trp1058* and N/A	CH	+	+	+	+	-	4	1	13	
VI	8	c.2152_2154 delinsAAAC and c.8713_ 8714insCA	p.Cys718Lysfs*19 and p.Val2906Glnfs*32	CH	+	+	+	+	-	1.5	2	8	
VII	9	c1402_1403delAA and c.2413C>T	p.Lys468Glufs*17 and p.Arg805*	CH	+	+	+	+	IgG deficiency	2	2	8	
VIII	10	c.6885G>T and c.3742_3743 insGGAGGTTCT	p.Val1248Phe and p.Tyr1248Trpfs*10	CH	+	+	+	+	-	2	2	7	
IX	11	c.50_72 + 7del	p.Asp18_L ys24delins(23)	hom	+(severe)	+	+	+	-	2.5	NR	13	(6)
	12				+ (moderate)	+	+	+	High IgM	6.5	NR	12	
	13				+ (moderate)	+	+	+	-	6.5	NR	11	
X	14	c.5939–5948del and c.2639–384A>G	p. Ile980fs and p.Gly880 Glufs*14	CH	+ (moderate)	+	-	NR	Low IgA and IgG, high IgM, B- and T-cell lymphopenia	7	7	7	(7)
	15				+ (severe)	+	+	NR	Mild lymphopenia with IgA defect	5	6	15	
XI	16	c.6679C>T and c.5773delG	p.Arg2227Cys and p.Gly1925 Glufs*12	CH	+	+	+	+	Increased leukocyte count and agammaglobulinemia	2	NR	7	(8)
XII	17	c.1402_1403delAA	p.Lys468Glufs*18	hom	+ (severe)	+	+	+	Low IgA and IgG	2	4	10	(9)
XIII	18	c.4195dup and c.6006 + 1G>T	p.Thr1399Asnfs*15 and splice donor	CH	+	+	+	+	-	2	5	7	This study

+, present; -, not present; NR, not reported; ho, homozygosity; CH, compound heterozygosity. * indicates termination codon.

10.3389/fneur.2023.1228810

immunodeficiency, which is one of the cardinal clinical indications in A-T. No genotype–phenotype correlation was found in this group of A-T patients.

Discussion

We report a Chinese patient affected by A-T with compound heterozygous *ATM* genotype; one of the identified variants is unreported. In China, patients are suspected of A-T only when classical clinical signs, namely ataxia and oculocutaneous telangiectasia are present. However, the onset age of ataxia and oculocutaneous telangiectasia is sometimes different. Some manifestations may even occur prior to ataxia and oculocutaneous telangiectasia, such as recurrent infections of unknown origins (7). These factors, combined with the extremely low prevalence of A-T at 1:40,000–1:300,000 (3), collectively lead to a delay in the diagnosis of A-T in China. According to the Chinese literature review (Table 2), it takes more than 5 years in China to complete the diagnosis of A-T since the onset of symptoms; therefore, great efforts are still warranted to ameliorate the diagnosis of this rare genetic disorder. Devaney et al. (11) reported the presentation and diagnostic delay in A-T, which further consolidated our conclusions.

The early measurement of serum AFP is an easily detectable and reliable biological hallmark of A-T (3). As expected, the serum AFP level is elevated in all reported Chinese patients with A-T (Table 2), except for two patients whose AFP levels were not reported (7). Immunodeficiency is also an important indicator for A-T, which is associated with ATM protein dysfunction in immunoglobulin class-switch recombination (CSR), V(D)J recombination, and B- and T-cell homeostasis (12, 13). It has been reported that immunodeficiency is present in approximately two-thirds of A-T patients (1, 3). The Chinese literature review (Table 2) shows that 38.9% (7/18) of Chinese patients with A-T, including the one in our case, have normal immune status at the time of diagnosis, which is in agreement with the literature data. For these patients who have no signs of immunodeficiency, elevated serum AFP levels and neurological manifestations are the most suggestive.

Conclusion

In conclusion, our findings extend the genotype spectrum of A-T in the Chinese population and suggest that the diagnosis of A-T in China should be improved in clinical practice. The limitations of our study are the small number of patients and a lack of functional investigation.

Data availability statement

The datasets presented in this article are not readily available because of ethical and privacy restrictions. Requests to access the datasets should be directed to the corresponding authors.

Ethics statement

The studies involving human participants were reviewed and approved by the Ethics Committee of Jinhua Maternity and Child Health Care Hospital. Written informed consent to participate in this study was provided by the participants' legal guardian/next of kin. Written informed consent was obtained from the individual(s) and minor(s)' legal guardian/next of kin, for the publication of any potentially identifiable images or data included in this article. Written informed consent was obtained from the participant/patient(s) for the publication of this case report.

Author contributions

JX, LS, and JZ were the patient's physicians. HW and MQ reviewed the literature and contributed to manuscript drafting. HW and ZY performed the mutation analysis. JX and JZ conceptualized and designed the study, coordinated and supervised data collection, and critically reviewed the manuscript for important intellectual content. HW, ZY, and JZ were responsible for the revision of the manuscript for important intellectual content. All authors contributed to the article and approved the submitted version.

Conflict of interest

The authors declare that the research was conducted in the absence of any commercial or financial relationships that could be construed as a potential conflict of interest.

Publisher's note

References

1. Rothblum-Oviatt C, Wright J, Lefton-Greif MA, McGrath-Morrow SA, Crawford TO, Lederman HM. Ataxia telangiectasia: a review. *Orphanet J Rare Dis.* (2016) 11:159. doi: 10.1186/s13023-016-0543-7

2. Amirifar P, Ranjouri MR, Yazdani R, Abolhassani H, Aghamohammadi A. Ataxia-telangiectasia: a review of clinical features and molecular pathology. *Pediatr Allergy Immunol.* (2019) 30:277–88. doi: 10.1111/pai.13020

3. Amirifar P, Ranjouri MR, Lavin M, Abolhassani H, Yazdani R, Aghamohammadi A. Ataxia-telangiectasia: epidemiology, pathogenesis, clinical phenotype, diagnosis, prognosis and management. *Expert Rev Clin Immunol.* (2020) 16:859–71. doi: 10.1080/1744666X.2020.1810570

4. Jiang H, Tang B, Xia K, Hu Z, Shen L, Tang J, et al. Mutation analysis of the *ATM* gene in two Chinese patients with ataxia

telangiectasia. *J Neurol Sci.* (2006) 241:1–6. doi: 10.1016/j.jns.2005.09.001

5. Huang Y, Yang L, Wang J, Yang F, Xiao Y, Xia R, et al. Twelve novel *Atm* mutations identified in Chinese ataxia telangiectasia patients. *Neuromolecular Med.* (2013) 15:536–40. doi: 10.1007/s12017-013-8240-3

6. Chen W, Liu S, Hu H, Chen G, Zhu S, Jia B, et al. Novel homozygous ataxia-telangiectasia (A-T) mutated gene mutation identified in a Chinese pedigree with A-T. *Mol Med Rep.* (2019) 20:1655–62. doi: 10.3892/mmr.2019.10402

7. Gu C, Wang H, Shu J, Zheng J, Li D, Cai C, et al. RNA sequencing combining with whole exome sequencing reveals a compound heterozygous variant in *ATM* in a girl with atypical ataxia-telangiectasia. *Clin Chim Acta.* (2021) 523:6–9. doi: 10.1016/j.cca.2021.08.026

8. Li XL, Wang YL. Ataxia-telangiectasia complicated with Hodgkin's lymphoma: A case report. *World J Clin Cases.* (2020) 8:2387–91. doi: 10.12998/wjcc.v8.i11.2387

9. Zhang L, Jia Y, Qi X, Li M, Wang S, Wang Y. Trihexyphenidyl for treatment of dystonia in ataxia telangiectasia: a case report. *Childs Nerv Syst.* (2020) 36:873–5. doi: 10.1007/s00381-019-04399-3

10. Shalash AS, Rösler TW, Salama M, Pendziwiat M, Müller SH, Hopfner F, et al. Evidence for pathogenicity of variant *ATM* Val1729Leu in a family with ataxia telangiectasia. *Neurogenetics.* (2021) 22:143–7. doi: 10.1007/s10048-021-00639-4

11. Devaney R, Pasalodos S, Suri M, Bush A, Bhatt JM. Ataxia telangiectasia: presentation and diagnostic delay. *Arch Dis Child.* (2017) 102:328–30. doi: 10.1136/archdischild-2016-310477

12. Bakkenist CJ, Kastan MB, DNA. Damage activates ATM through intermolecular autophosphorylation and dimer dissociation. *Nature.* (2003) 421:499–506. doi: 10.1038/nature01368

13. Driessen GJ, Ijspeert H, Weemaes CM, Haraldsson Á, Trip M, Warris A, et al. Antibody deficiency in patients with ataxia telangiectasia is caused by disturbed B- and T-cell homeostasis and reduced immune repertoire diversity. *J Allergy Clin Immunol.* (2013) 131:1367–75. doi: 10.1016/j.jaci.2013.01.053

frontiers | Frontiers in Neurology

TYPE Case Report
PUBLISHED 13 September 2023
DOI 10.3389/fneur.2023.1242472

OPEN ACCESS

EDITED BY
Huifang Shang,
Sichuan University, China

REVIEWED BY
Cigdem Koroglu Altok,
National Institute of Diabetes and Digestive and Kidney Diseases (NIH), United States
Antonio Orlacchio,
Santa Lucia Foundation (IRCCS), Italy

*CORRESPONDENCE
Jiang Cheng
✉ chengjiangnx@163.com
Zhenhai Wang
✉ wangzhenhai1968@163.com

†These authors have contributed equally to this work and share first authorship

RECEIVED 19 June 2023
ACCEPTED 22 August 2023
PUBLISHED 13 September 2023

CITATION
Li H, Xuan T, Xu T, Yang J, Cheng J and Wang Z (2023) SIGMAR1 variants in ALS–PD complex cases: a case report of a novel mutation and literature review.
Front. Neurol. 14:1242472.
doi: 10.3389/fneur.2023.1242472

SIGMAR1 variants in ALS–PD complex cases: a case report of a novel mutation and literature review

Haining Li[1,2†], Tingting Xuan[1,3†], Ting Xu[4], Juan Yang[1,2], Jiang Cheng[1,2*] and Zhenhai Wang[5,6*]

[1]Department of Neurology, General Hospital of Ningxia Medical University, Yinchuan, China, [2]Diagnosis and Treatment Engineering Technology Research Center of Nervous System Disease of Ningxia Hui Autonomous Region, Yinchuan, China, [3]School of Clinical Medicine, Ningxia Medical University, Yinchuan, China, [4]Department of Neural Electrophysiology, Cardiovascular and Cerebrovascular Disease Hospital, General Hospital of Ningxia Medical University, Yinchuan, China, [5]Institute of Medical Sciences, General Hospital of Ningxia Medical University, Yinchuan, Ningxia, China, [6]Ningxia Engineering Technology Research Center for Diagnosis and Treatment of Nervous System Diseases, Neurology Center, General Hospital of Ningxia Medical University, Yinchuan, Ningxia, China

Amyotrophic lateral sclerosis (ALS) is a devastating neurodegenerative disease characterized by progressive degeneration of upper and lower motor neurons, with occasional involvement of the extrapyramidal system. Mutations in the sigma non-opioid intracellular receptor 1 (*SIGMAR1*) gene have been identified as one of the causes of ALS. Here, we present a case of a 49-year-old man diagnosed with ALS–Parkinson's disease (PD) complex. The patient exhibited bradykinesia and tremor, and whole-exome sequencing revealed homozygous mutations in the *SIGMAR1* gene (c.446-2A>T). In addition, we conducted an investigation into the clinical and molecular phenotype of previously reported variants of *SIGMAR1* associated with ALS. This case report aims to raise awareness among physicians regarding atypical phenotypes of amyotrophic lateral sclerosis and to encourage further research on the factors leading to *SIGMAR1* mutations in patients.

KEYWORDS

amyotrophic lateral sclerosis, Parkinson's disease, *SIGMAR1*, genotype, phenotype

Introduction

Amyotrophic lateral sclerosis (ALS) represents the most common form of motor neuron disease, characterized by the degeneration of upper and lower motor neurons. ALS is classified into two types: familial (fALS) and sporadic (sALS), with the latter accounting for 90–95% of cases, while fALS comprises only 5–10%. The etiology of sALS remains largely unknown although it is believed to involve both genetic and environmental factors. Genetic factors, in particular, play a significant role in the occurrence of sALS. To date, more than a hundred ALS-related genes have been identified, with approximately 30 genes primarily associated with ALS (1). Among Asians, Cu/Zn superoxide dismutase (SOD1) gene mutations are the most prevalent, whereas pathogenic mutations in the sigma non-opioid intracellular receptor 1 (*SIGMAR1*) gene are rare in Asian patients with familial or sporadic ALS. While mutations in the *SIGMAR1* gene have been reported in association with ALS, with or without frontotemporal dementia or juvenile ALS, no instances of this mutation in the ALS–Parkinson's disease (PD)

complex have been described until now. Here, we present the case of a 49-year-old patient with ALS–PD complex, exhibiting slowly progressing motoneuron disease that may be linked to a homozygous *SIGMAR1* mutation. Additionally, we conduct a comprehensive review of cases of ALS patients with mutations in this gene, as reported in the relevant scientific literature.

Case report

A 49-year-old man presented to our neurology department with complaints of involuntary shaking in both upper limbs for the past 3 years, along with slowness of movement for the past 2 years. He exhibited rest and action tremors in both upper limbs, along with simultaneous occurrence of bradykinesia and rigidity. Subsequently, he experienced unresponsiveness, memory decline, and choking while drinking, and his speaking rate began to slow down. Additionally, his facial expressions started to diminish, as noticed by his wife. In April 2021, the patient received a diagnosis of Parkinsonian syndrome at a local hospital. Initial treatment with levodopa at a daily dosage of 100 mg, gradually increased to 200 mg, resulted in partial improvement in involuntary shaking, but showed no significant overall improvement. Over the next year, his symptoms rapidly worsened, with progressive aggravation of stiffness and the appearance of mental irritability. Neurological examinations revealed decreased spontaneous facial expressions, poor eye movement in all directions, horizontal nystagmus, mildly increased muscle tone in the neck and limbs, and deep tendon reflexes in the biceps and triceps (1+). A positive Babinski sign was observed bilaterally. Symmetric muscle atrophy of the calves was also noted, which he reported experiencing for as long as he could remember (Figure 1A). Additionally, it was noted that he had planovalgus deformities of both feet since the age of 5 years (Figure 1B), a condition similar to that of his uncle's feet. The strength of his upper and lower extremities, as well as proximal and distal muscles, was assessed as 5 on the Medical Research Council Muscle Scale. Brain magnetic resonance imaging revealed only mild atrophy, and his cognitive functions were deemed normal, scoring 28 on the standardized Mini-Mental State Examination and 23 points on the Montreal Cognitive Assessment. Further cervical and thoracic spine MRI showed degenerative changes, and electromyography revealed chronic denervation in both upper and lower extremities. Motor nerve conduction studies demonstrated reduced conduction velocity, amplitude, and distal latency in the left median nerve, as well as in the bilateral tibial and peroneal nerves. Sensory nerve conduction testing revealed normal sensory nerve action potential but showed delayed F-wave latencies in the left median and tibial nerves. However, anal sphincter electromyography was normal. The somatosensory-evoked potential showed abnormalities in the bilateral lower limbs, indicating a conduction block in the somatosensory pathway from the spinal cord to the cortex. Moreover, the bilateral visually evoked potential and bilateral auditory brainstem response were also found to be abnormal. The visually evoked potential showed prolonged P100 latency in both eyes. The auditory brainstem response suggested that bilateral ears were stimulated, but the waveform on both sides was relatively poor. The ambulatory electroencephalogram monitoring was normal. The routine cerebrospinal fluid (CSF) analysis showed normal pressure, cell counts, and levels of protein and glucose. Finally, whole-exome sequencing was performed using MyGenostics. In this study, four steps were employed to select potential pathogenic mutations for downstream analysis: (i)

FIGURE 1
(A) Atrophy of bilateral calves more pronounced distally giving a "stork leg" appearance akin to Charcot-Marie-Tooth disease. **(B)** Planovalgus deformities of both feet.

mutations with read counts less than 5 and mutation ratios below 30% were excluded; (ii) mutations with a frequency greater than 5% in 1,000 g, ESP6500, and Inhouse databases were removed; (iii) mutations present in the InNormal database (MyGenostics) were also discarded; (iv) synonymous mutations not listed in the HGMD database were excluded. The remaining mutations were considered potential pathogenic mutations for further analysis (Figure 2). Genomic DNA was extracted from the patient's whole blood, and subsequent sequencing analysis identified a novel splice site mutation in intron 3 of SIGMAR1 gene (c.446-2A>T), which was further confirmed by Sanger sequencing (Figures 2, 3A). A review of the patient's medical history revealed a longstanding presence of planovalgus deformities in both feet for over 40 years. Physical examination revealed muscle atrophy of both lower limbs at 10 years old, and he complained of mild discomfort while walking. However, his general condition was normal. The patient did not pursue further examination or treatment at that time. During the current clinical examination, upper and lower motor neuron damage was observed, and all the above findings were consistent with the diagnosis of ALS. At that time, the Unified Parkinson's Disease Rating Scale-Part III motor score (in the morning without antiparkinsonian therapy) was 40. Next, we conducted a levodopa load test, and he showed a good response to levodopa. Based on the findings, the patient was eventually diagnosed with ALS–PD complex. Further exploration of the patient's family history revealed that his parents were close relatives as they were second cousins. Unfortunately, his father was dead. Genetic testing was conducted on the mother, and it revealed that she has the same SIGMAR1 variant as detected in the proband (Figure 3B). Subsequently, a pedigree analysis was performed (Figure 3C). At the 3-month follow-up examination, the symptoms were observed to have remained relatively stable.

Review of previously reported cases of ALS patients with SIGMAR1 mutations

A literature review was conducted by searching PubMed and China National Knowledge Infrastructure (CNKI) databases from their inception until May 2023 using the keywords "*SIGMAR1*," "ALS," and "amyotrophic lateral sclerosis." Relevant articles describing cases of ALS with *SIGMAR1* mutations were selected. Among the articles, eight described studies of interest, three reported cases of familial ALS (fALS), and five reported cases of sporadic ALS (sALS). Various mutations in the *SIGMAR1* gene were identified in affected individuals, including a mutation (c.67251G > T) in the 3′-untranslated region in the FTLD-MND pedigree and mutations (c.304G > C, c.67231A > G, c.505 T > A, c.622C > T, c.283dupC, c.58 T > C, c.125 > G) in the *SIGMAR1* gene in affected ALS patients. The phenotypes of each of these cases are presented in Table 1 and Figure 4.

Discussion and conclusion

According to the revised El Escorial criteria, patients with ALS may exhibit extrapyramidal involvement in addition to upper and lower motor neuron symptoms and signs (8). When ALS is associated with PD, it is known as Brait–Fahn–Schwartz syndrome or ALS–PD complex. Parkinsonism in these patients typically resembles PD and shows a response to levodopa. ALS–parkinsonism is more common than ALS–PD complex and refers to the presence of extrapyramidal findings that do not respond to levodopa treatment in ALS patients (8). Mutations in the *SIGMAR1* gene have previously been linked to different forms of ALS, including juvenile (onset age < 20 years old) and adult-onset (early

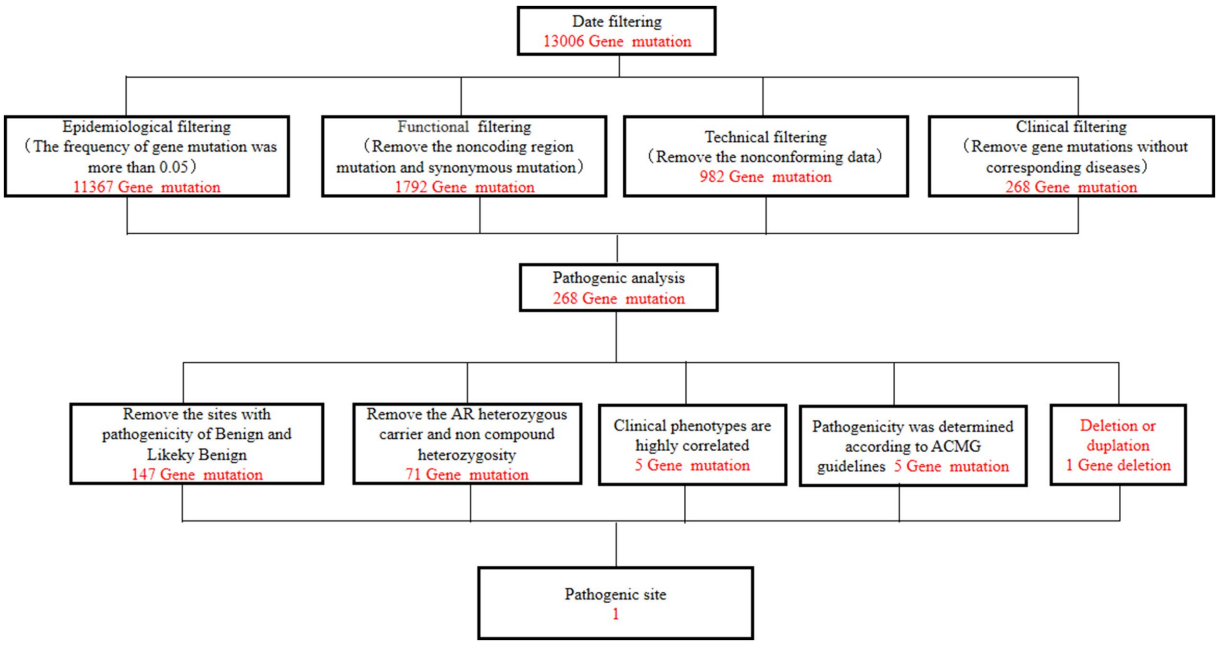

FIGURE 2
Filtering steps for the variant calls in whole-exome sequencing.

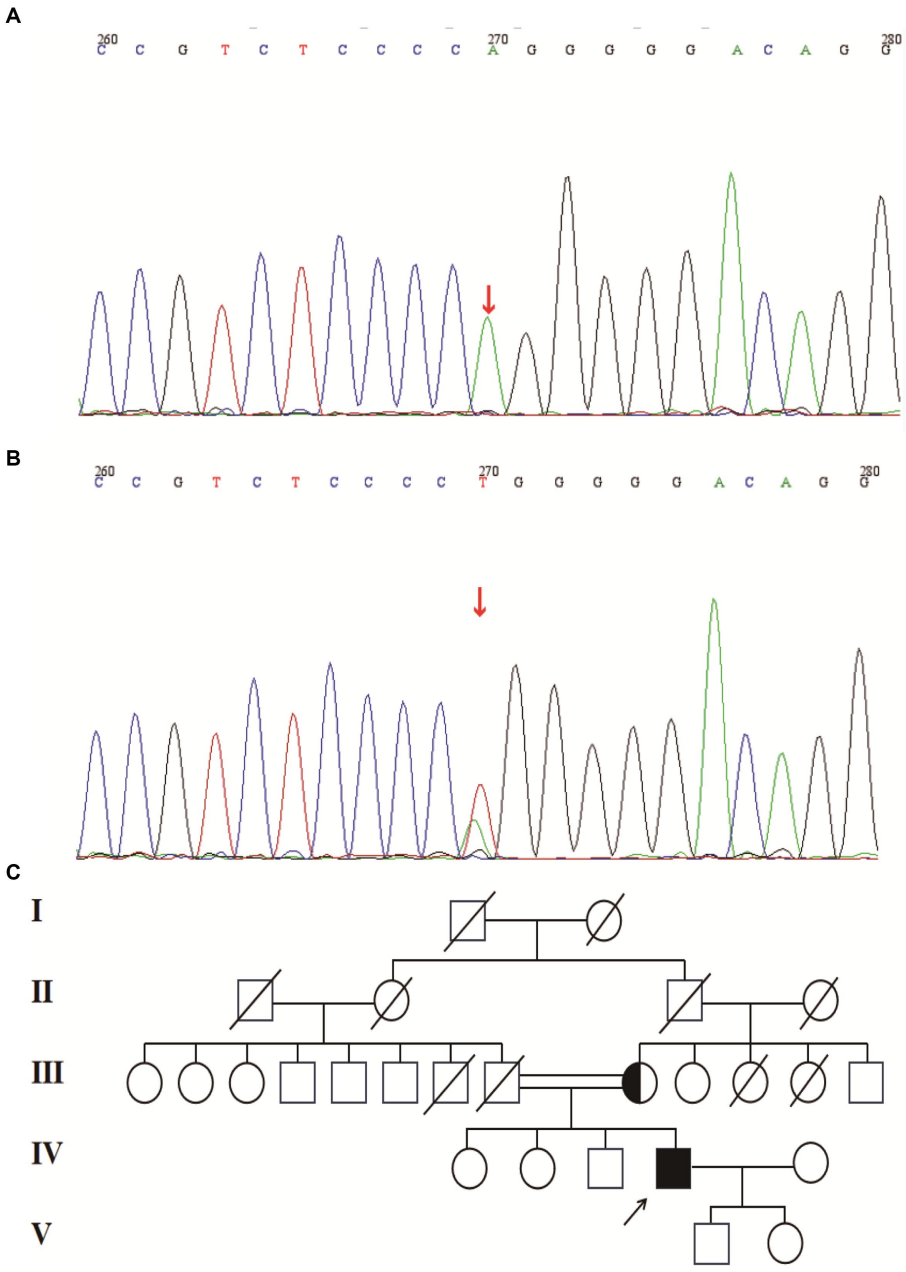

FIGURE 3
(A) Splice site mutation in the SIGMAR1 identified in our patient. Sanger sequencing was performed using cDNA generated from the patient. **(B)** Mutation in the SIGMAR1 identified in our patient's mother. **(C)** Mutant pedigree map of familial mutations. Circles = females; squares = males; and slashes = deceased.

onset within 20–60 years and late onset >60 years) cases (9). Most SIGMAR1-related ALS cases present with a typical ALS phenotype, but the SIGMAR1 c.672*51G > T variant was identified in an Australian familial FTLD cohort with ALS, presenting as an ALS-frontotemporal dementia (FTD) phenotype (3). In this report, we present a case of ALS–PD complex in a patient with juvenile onset. We identified a potentially new pathogenic variant (c.446-2A > T) located in intron 3 of the *SIGMAR1* gene. The sequencing data was saved in FASTQ format, and MGI sequencing adapters and low-quality reads (<80 bp) were filtered using the cutadapt software.[1] The clean reads were then mapped to the UCSC hg19 human reference genome using the BWA parameter of the Sentieon software.[2] Next, we removed duplicated reads using the driver parameter of Sentieon software, which also corrected the base to improve the quality of the output BAM file reads, making

1 http://code.google.com/p/cutadapt/
2 https://www.sentieon.com/

TABLE 1 Clinical phenotypes of patients with SIGMAR1 mutations.

References	Source	Clinical diagnosis	Nucleotide change	Phenotype	Initial symptoms	Mode of inheritance	Age of onset (years or median years)
Al-Saif et al. (2)	Saudi Arabia	ALS	c.304G>C	fALS	Lower limb spasticity and weakness	AR	(1.5)
Luty et al. (3)	Australia	ALS-FTLD/FTD	c.672*51G>T	fALS	NA	AD	NA
Ullah et al. (4)	Pakistani	ALS	c.672*31A>G	fALS	Progressive weakness of the upper limbs	AR	30
Izumi et al. (5)	Japan	ALS	c.505T>A c.622C>T	sALS	Slowly progressive gait disturbance	NA	80
Karasozen et al. (6).	USA	ALS	c.283dupC	sALS	An orthopedist for toe walking	Uniparental disomy	4
Kim et al. (7)	Korea	ALS	c.58T>C	sALS	Slowly progressive limb weakness	NA	47
Tripolszki et al. (1)	Hungary	ALS	c.125T>G	sALS	Tetraparesis	NA	(67.5)

ALS, amyotrophic lateral sclerosis; fALS, familial ALS; sALS, sporadic ALS; AR, autosomal recessive; AD, autosomal dominant; NA, no information available.

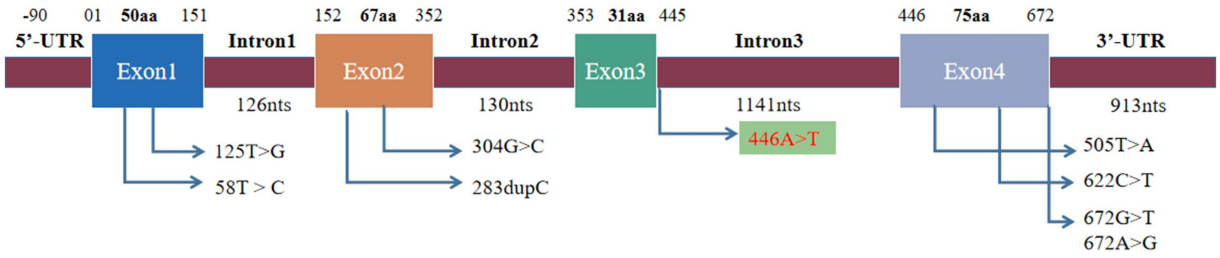

FIGURE 4
Mutation site of SIGMR1. The previously reported mutation site was located in exons and 3'-UTR, and the mutation site was located in intron.

them closer to the real probability of mismatch with the reference genome. The mapped reads were used for variation detection. Variants of SNP and InDel were identified using the driver parameter of the Sentieon software. The data were then transformed into VCF format. To further analyze the variants, we used ANNOVAR software[3] to annotate and cross-reference multiple databases, including 1,000 genome, ESP6500, dbSNP, EXAC, Inhouse (MyGenostics), HGMD, SIFT, PolyPhen-2, MutationTaster, and GERP++. Based on the ACMG guidelines, this variant was predicted to be likely pathogenic (PVS1+PP3+PM2). To the best of our knowledge, this is the first reported case of *SIGMAR1*-related ALS presenting as ALS–PD complex.

Compared to previously reported cases, the patient in this report exhibited distinct clinical phenotypes. While muscle weakness is the most commonly observed clinical feature in patients with *SIGMAR1* mutations (10), the patient in our case presented with no symptoms of muscle weakness but instead displayed extrapyramidal symptoms, including bradykinesia, rigidity, and tremor. It is noteworthy that in the majority of ALS patients, motor nerve conduction velocities and terminal latencies are normal. However, this particular patient showed decreased conduction velocity, amplitude, and distal latency in the left median nerve, bilateral tibial, and peroneal nerves, which may be particularly relevant to the long-term atrophy of the lower limbs. Through our literature review, we found cases of ALS patients with *SIGMAR1* mutations presenting with ALS either with or without frontotemporal dementia as well as cases of juvenile ALS. Nevertheless, this is the first reported case, where an association between ALS–PD phenotype and *SIGMAR1* mutations has been observed.

SIGMAR1 is comprised of four exons and three introns, located on chromosome 9p13.3. This gene exhibits ubiquitous expression in various human tissues, including the brain (cerebellum), retinal ganglion cells, astrocytes, liver, and placenta. Particularly, it is prominently expressed in motor neurons found in the brainstem and spinal cord. The *SIGMAR1* gene plays diverse roles in different cells and organs, encompassing ion channel regulation, chaperone function, regulation of mitochondrial morphology, dynamics, and function, as well as involvement in autophagy and endoplasmic reticulum (ER) stress response (10, 11). A common pathological feature in ALS is the disruption of the ER-associated membrane, where the ER-resident chaperone protein is predominantly localized (12, 13). Consequently, changes in *SIGMAR1* function may alter ER morphology and impact ER stress responses, resulting in abnormal mitochondrial damage and the initiation of cellular autophagy, thereby contributing to the pathogenesis of ALS. PD, another prevalent neurodegenerative disease, has also been associated with alterations in *SIGMAR1* functions. Studies

3 http://annovar.openbioinformatics.org/en/latest/

by Finsterer et al. (9) demonstrated that *SIGMAR1* agonist treatment in mice with 6-hydroxydopamine lesions reduced neuroinflammation, increased the density of dopaminergic fibers in denervated striatal regions, and elevated the levels of neurotrophic factors. Furthermore, Hong et al. (14) revealed that *SIGMAR1* deficiency reduced 1-methyl-4-phenyl-1,2,3,6-tetrahydropyridine-induced death of dopaminergic neurons and parkinsonism. Thus, pharmacological activation/inhibition of *SIGMAR1* may potentially slow down the progression of PD. Overall, *SIGMAR1* activation has demonstrated protective effects in neurodegenerative diseases by modulating various cellular pathways, including the regulation of mitochondrial function, autophagy, calcium homeostasis, and chaperone function.

SIGMAR1 activation has been found to induce potent neuroprotective effects, promote neuronal survival, and restore neuronal plasticity, leading to a deceleration of disease progression in neurodegenerative conditions. Moreover, it has shown promise in ameliorating the clinical symptoms of these diseases. On the contrary, dysfunction of *SIGMAR1* may exacerbate the advancement of neurodegenerative disorders. Positioned at the interface of two crucial organelles commonly implicated in the majority of neurodegenerative disorders—the mitochondria and the ER—*SIGMAR1* emerges as a robust therapeutic target with significant potential for intervention.

Data availability statement

The datasets presented in this article are not readily available because of ethical and privacy restrictions. Requests to access the datasets should be directed to the corresponding authors.

Ethics statement

The studies involving human participants were reviewed and approved by the General Hospital of Ningxia Medical University. The patients/participants provided their written informed consent to participate in this study. Written informed consent was obtained from the individual(s) for the publication of any potentially identifiable images or data included in this article.

Author contributions

TXua examined the patient clinically. JY performed and analyzed neuroradiologic imaging studies. TXu analyzed electromyography results. HL analyzed performed genetic analyses. HL and TXua wrote the manuscript. JC and ZW analyzed and interpreted the data and revised the manuscript. All authors contributed to the article and approved the submitted version.

Funding

This research study was supported by the Key Research and Development Program of Ningxia Hui Autonomous Region (grant number 2022BEG03130), the Natural Science Fund project in Ningxia (grant number 2022AAC03561), and the National Nature Science Foundation of China (grant number 81960245).

Conflict of interest

The authors declare that the research was conducted in the absence of any commercial or financial relationships that could be construed as a potential conflict of interest.

Publisher's note

References

1. Tripolszki K, Gampawar P, Schmidt H, Nagy ZF, Nagy D, Klivényi P, et al. Comprehensive genetic analysis of a Hungarian amyotrophic lateral sclerosis cohort. *Front Genet*. (2019) 10:732. doi: 10.3389/fgene.2019.00732

2. Al-Saif A, Al-Mohanna F, Bohlega S. A mutation in sigma-1 receptor causes juvenile amyotrophic lateral sclerosis. *Ann Neurol*. (2011) 70:913–9. doi: 10.1002/ana.22534

3. Luty AA, Kwok JB, Dobson-Stone C, Loy CT, Coupland KG, Karlström H, et al. Sigma nonopioid intracellular receptor 1 mutations cause frontotemporal lobar degeneration-motor neuron disease. *Ann Neurol*. (2010) 68:639–49. doi: 10.1002/ana.22274

4. Ullah MI, Ahmad A, Raza SI, Amar A, Ali A, Bhatti A, et al. *In silico* analysis of SIGMAR1 variant (rs4879809) segregating in a consanguineous Pakistani family showing amyotrophic lateral sclerosis without frontotemporal lobar dementia. *Neurogenetics*. (2015) 16:299–306. doi: 10.1007/s10048-015-0453-1

5. Izumi Y, Morino H, Miyamoto R, Matsuda Y, Ohsawa R, Kurashige T, et al. Compound heterozygote mutations in the SIGMAR1 gene in an oldest-old patient with amyotrophic lateral sclerosis. *Geriatr Gerontol Int*. (2018) 18:1519–20. doi: 10.1111/ggi.13506

6. Karasozen Y, Sheikh KA, Mancias P, Nguyen TP. Uniparental Disomy leading to a rare juvenile form of ALS. *J Pediatr Perinatol Child Health*. (2020) 4:107–10. doi: 10.26502/jppch.74050049

7. Kim HJ, Kwon MJ, Choi WJ, Oh KW, Oh SI, Ki CS, et al. Mutations in UBQLN2 and SIGMAR1 genes are rare in Korean patients with amyotrophic lateral sclerosis. *Neurobiol Aging*. (2014) 35:1957.e7–8. doi: 10.1016/j.neurobiolaging.2014.03.001

8. Swinnen B, Robberecht W. The phenotypic variability of amyotrophic lateral sclerosis. *Nat Rev Neurol*. (2014) 10:661–70. doi: 10.1038/nrneurol.2014.184

9. Finsterer J, Burgunder JM. Recent progress in the genetics of motor neuron disease. *Eur J Med Genet*. (2014) 57:103–12. doi: 10.1016/j.ejmg.2014.01.002

10. Aishwarya R, Abdullah CS, Morshed M, Remex NS, Bhuiyan MS. Sigmar1's molecular, cellular, and biological functions in regulating cellular pathophysiology. *Front Physiol*. (2021) 12:705575. doi: 10.3389/fphys.2021.705575

11. Su TP, Hayashi T, Maurice T, Buch S, Ruoho AE. The sigma-1 receptor chaperone as an inter-organelle signaling modulator. *Trends Pharmacol Sci*. (2010) 31:557–66. doi: 10.1016/j.tips.2010.08.007

12. Sakai S, Watanabe S, Komine O, Sobue A, Yamanaka K. Novel reporters of mitochondria-associated membranes (MAM), MAMtrackers, demonstrate MAM disruption as a common pathological feature in amyotrophic lateral sclerosis. *FASEB J*. (2021) 35:e21688. doi: 10.1096/fj.202100137R

13. Watanabe S, Ilieva H, Tamada H, Nomura H, Komine O, Endo F, et al. Mitochondria-associated membrane collapse is a common pathomechanism in SIGMAR1- and SOD1-linked ALS. *EMBO Mol Med*. (2016) 8:1421–37. doi: 10.15252/emmm.201606403

14. Hong J, Sha S, Zhou L, Wang C, Yin J, Chen L. Sigma-1 receptor deficiency reduces MPTP-induced parkinsonism and death of dopaminergic neurons. *Cell Death Dis*. (2015) 6:e1832. doi: 10.1038/cddis.2015.194

frontiers | Frontiers in Neurology

TYPE Case Report
PUBLISHED 14 September 2023
DOI 10.3389/fneur.2023.1235909

OPEN ACCESS

EDITED BY
Félix Javier Jiménez-Jiménez,
Hospital Universitario del Sureste, Spain

REVIEWED BY
Ana Westenberger,
University of Lübeck, Germany
Jean-Baptiste Demoulin,
Université Catholique de Louvain, Belgium

*CORRESPONDENCE
Jamal Al Ali
✉ jamalalali04@gmail.com

RECEIVED 06 June 2023
ACCEPTED 30 August 2023
PUBLISHED 14 September 2023

CITATION
Al Ali J, Yang J, Phillips MS, Fink J, Mastrianni J and Seibert K (2023) A case report of a patient with primary familial brain calcification with a *PDGFRB* genetic variant. *Front. Neurol.* 14:1235909. doi: 10.3389/fneur.2023.1235909

A case report of a patient with primary familial brain calcification with a *PDGFRB* genetic variant

Jamal Al Ali[1]*, Jessica Yang[2], Matthew S. Phillips[2], Joseph Fink[2], James Mastrianni[1] and Kaitlin Seibert[1]

[1]Department of Neurology, University of Chicago, Chicago, IL, United States, [2]Department of Psychiatry and Behavioral Neuroscience, University of Chicago, Chicago, IL, United States

Fahr's disease, or primary familial brain calcification (PFBC), is a rare genetic neurologic disease characterized by abnormal calcification of the basal ganglia, subcortical white matter and cerebellum. Common clinical features include parkinsonism, neuropsychiatric symptoms, and cognitive decline. Genes implicated in Fahr's disease include *PDGFB*, *PDGFRB*, *SLC20A2*, *XPR1*, *MYORG*, and *JAM2*. We present the case of a 51-year-old woman who developed subacute cognitive and behavioral changes primarily affecting frontal-subcortical pathways and parkinsonism in association with extensive bilateral calcifications within the basal ganglia, subcortical white matter, and cerebellum on neuroimaging. Relevant family history included a paternal aunt with parkinsonism at age 50. Normal parathyroid hormone and calcium levels in the patient's serum ruled out hypoparathyroidism or pseudohypoparathyroidism as causes for the intracranial calcifications. Genetic panel sequencing revealed a variant of unknown significance in the *PDGFRB* gene resulting in a p.Arg919Gln substitution in the tyrosine kinase domain of PDGFRB protein. To our knowledge this is the first report of a p.Arg919Gln variant in the *PDGFRB* gene associated with PFBC. Although co-segregation studies were not possible in this family, the location of the variant is within the tyrosine kinase domain of PDGFRB and pathogenicity calculators predict it is likely to be pathogenic. This report adds to the list of genetic variants that warrant functional analysis and could underlie the development of PFBC, which may help to further our understanding of its pathogenesis and the development of targeted therapies for this disorder.

KEYWORDS

Fahr's disease, missense variant, PDGFRB gene variant, primary familial brain calcification (PFBC), tyrosine kinase

Introduction

Primary familial brain calcification (PFBC), also known as Fahr's Disease, is a genetically and phenotypically heterogenous neurodegenerative disorder (1–3). Clinically, patients with PFBC experience a variable combination of neuropsychiatric (4–10) and motor symptoms (2, 11, 12), including parkinsonism, dystonia, seizures, ataxia, chorea, dementia, psychosis, and frontal-subcortical cognitive dysfunction. Radiologically, abnormal calcification is present within the bilateral basal ganglia, but also the subcortical white matter, cerebellum, thalamus, and brainstem (1–3).

Six genes contribute to the genetic heterogeneity of PFBC, four of which follow autosomal dominant inheritance: *PDGFB*, *PDGFRB*, *SLC20A2*, and *XPR1* (3, 12–15) and two are autosomal

recessive: *MYORG*, and *JAM2*; (12, 16, 17). We describe a case of a 51-year-old woman with cognitive, behavioral, and radiographic features of Fahr's disease who harbored a variant (Rs14571770) (18) of the *PDGFRB* gene (Platelet Derived Growth Factor Receptor beta). The transition c.2756G>A resulted in a glutamine substitution of arginine (p.Arg919Gln) in exon 20, within the tyrosine kinase domain of the PDGFRB protein (Figure 1) (19).

Three gene panels were used to screen for genetic variants in a total of 70 genes implicated in neurodegeneration and PFBC (Supplementary material). Genes implicated in PFBC were *SLC20A2, PDGFB, PDGFRB and XPR1.* At the time of testing, available panels did not include sequencing for the two autosomal recessive genes *MYORG* and *JAM2.* All 3 panels used next generation sequencing of the exons; and analyzed the sequences for missense variants, insertions, deletions, and copy number variations.

Detection of this variant in *PDGRFB* assisted in diagnosis and management of this patient, emphasizing the importance of genetic testing in patients with neuropsychiatric symptoms, parkinsonism and neuroimaging characteristics suggestive of PFBC.

Case presentation

A 51-year-old Filipina woman with a history of hypertension and systemic lupus erythematosus (SLE) presented with subacute cognitive changes over the course of 4 weeks. The patient reported feeling occasionally disoriented at work, with difficulty concentrating, and depressed, which were noticed by her family and coworkers. Additional symptoms noted by her family included dysarthria, dysphagia, gait instability, and trouble following conversations. She had no personal psychiatric or neurologic history. Family history was significant for several family members with rheumatoid arthritis and SLE, and a paternal aunt with parkinsonism at the age of 50, for whom an autopsy was not done. The patient's father died at age 74 from small cell lung carcinoma and her mother died at age 70 from cardiac arrest. Neither parent had parkinsonian or cognitive symptoms, although a paternal aunt was diagnosed with Parkinson's Disease at age 50. Evaluation at a local hospital included a computerized tomography (CT) scan of the head, which showed extensive hyperintensity throughout the basal ganglia, cerebellum, central pons, and periventricular subcortical white matter. Initial magnetic resonance imaging (MRI) of the brain with gadolinium showed diffuse abnormal susceptibility signal within the deep white matter in the cerebellar and cerebral hemispheres, relatively minimal abnormal fluid-attenuated inversion recovery (FLAIR) signal, and no contrast enhancement. Lumbar puncture was performed to assess for inflammation in the setting of possible neuropsychiatric SLE (NPSLE); cerebrospinal fluid (CSF) testing was non-inflammatory, with white blood cell count 3 (nL = 0–5 cells/mm^3), Glucose 76 (nL = 40–70 mg/dL), Protein 35 (nL = 15–45 mg/dL), and negative results for Gram stain and culture, West Nile virus, Herpes Simplex Virus (HSV), Measles, Mumps, Varicella Zoster Virus (VZV), and Coccidioidomycosis. Serum studies showed a positive Antinuclear Antibody (ANA) titer of: 1:2,560 (nL = <1:40) speckled, negative double stranded deoxyribonucleic acid (dsDNA) Antibody < 1 (nL = <4 iU/mL), normal complement component 3 (C3): 123 (87–200 mg/dL), and normal complement component 4 (C4): 32 (19–52 mg/dL). Based on a concern for NPSLE, she was treated with intravenous methylprednisolone 1 g/kg/day for 3 days followed by a prolonged oral prednisone taper. For depressive symptoms, she was prescribed citalopram 20 mg. A neuropsychological evaluation was ordered, and she was referred to a tertiary center for further diagnosis and management. A timeline of the patient's symptoms, diagnostic workup, and interventions is represented in Figure 2.

The patient underwent the neuropsychological evaluation but did not follow up in clinic until 15 months later. At that time, she presented with concerns of symptom progression. She reported trouble with fine movements, especially writing, slowing of her gait, and falling. Her dysarthria worsened and she developed dysphonia and dysphagia. Behavioral changes included new impulsivity and episodes of uncontrollable bouts of laughter or anger. On neurological examination, the patient was alert and oriented to person, place, and time, her speech was slow, deliberate and aprosodic. She exhibited normal naming, comprehension, and repetition, with no paraphasic errors. Ideomotor apraxia was demonstrated in both hands. She scored 16 on a Montreal Cognitive Assessment (MoCA), missing points for Trails B (−1), cube copy (−1), clock draw (−2), animal naming (−1), backward digit repetition (−1), serial seven subtraction (−2), sentence repetition (−2), phonemic fluency (−1), abstraction (−2), and delayed recall of one of five words (−1), although she retrieved the word with a semantic cue. Cranial nerve evaluation demonstrated oculomotor apraxia with hypermetric saccades and impaired smooth pursuit, hypophonia, and hypokinetic dysarthria. The motor exam showed paratonic upper extremities, bradykinesia and diffuse hyperreflexia. Plantar reflexes were flexor bilaterally. Primitive reflexes of grasp., glabellar, palmomental, and snout were present. Dysmetria was

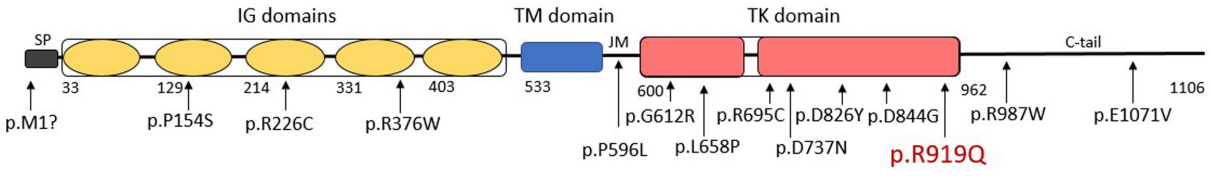

FIGURE 1
A schematic representation of Platelet Derived Growth Factor Receptor beta (PDGFRB) protein including a signal peptide (SP), five extracellular Ig-like (IG) domains, a transmembrane (TM) domain, a juxtamembrane domain (JM), an intracellular split tyrosine kinase (TK) domain, and a C-terminal tail (C-tail). Previously reported variants affecting the PDGFRB protein are presented according to their approximate position in the protein amino-acid chain. The patient's p.R919Q variant is shown in red.

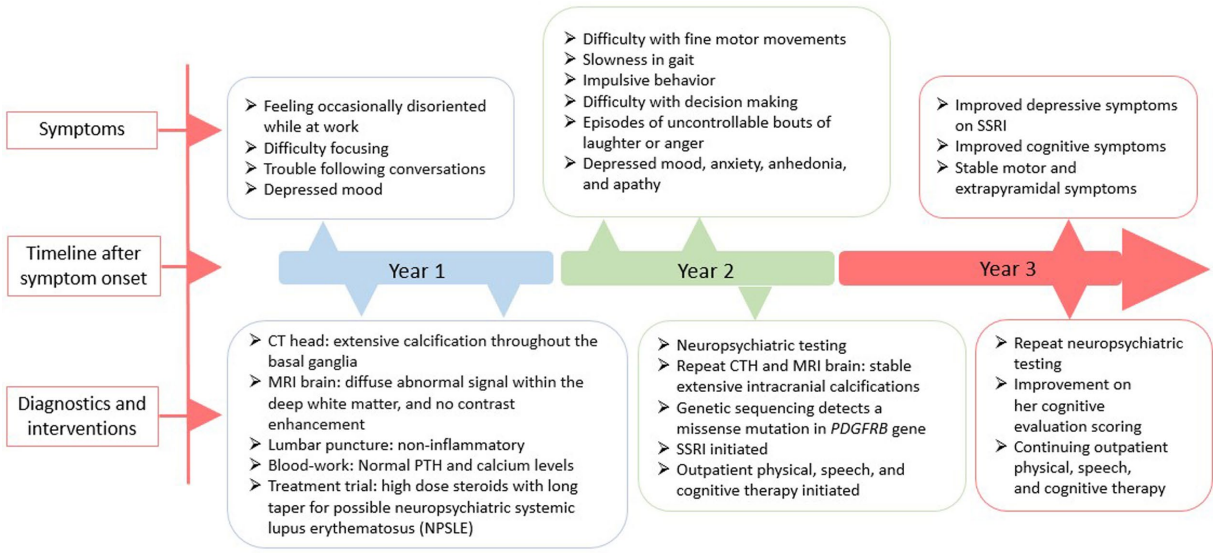

FIGURE 2
A schematic timeline of the patient's symptoms, diagnostic workup, and interventions, presented in years after presentation.

present bilaterally, although more prominent on the left. Her posture was narrow-based, upright, but with reduced stride and absent arm swing on the left. Sensory exam was normal.

Initial blood work was ordered to exclude metabolic etiologies that might lead to brain calcifications, including parathyroid hormone, calcium, magnesium and phosphate, all of which were normal. A repeat CT scan of the head showed diffuse hyperdense foci favored to represent extensive calcifications throughout the bilateral corona radiata, basal ganglia, cerebellar hemispheres, and midbrain (Figure 3A), comparable to the patient's initial neuroimaging 15 months prior. A repeat MRI brain without contrast showed extensive susceptibility effect and high T1 and T2 signal in the bilateral cerebral, brainstem, and cerebellar deep gray nuclei and white matter (Figure 3B).

The neuropsychological evaluation (Table 1) done 15 months prior revealed prominent impairment in attention and processing speed that contributed to variably impaired new learning and memory. Impairments were also evident with problem solving, speeded verbal fluency and naming tasks. On a self-report measure of depression (Beck Depression Inventory, 2nd Edition), she endorsed elevated level of depressive symptoms, with feelings of sadness, thoughts of suicide, anhedonia, irritability, and significant fatigue. On a self-report measure of behavioral symptomatology associated with frontal networks functioning (Frontal Systems Behavior Scale), when compared with that at the time of initial presentation, 2 months prior to the neuropsychological evaluation, she endorsed a decrease in measures of apathy, disinhibition, and executive dysfunction, although her partner endorsed no significant changes in these symptoms. A repeat neuropsychological evaluation, approximately one and a half years after the initial evaluation (Table 1), was generally consistent with the findings described in the previous evaluation, although the patient demonstrated some improvement in measures of immediate and delayed memory and recognition; increased difficulty on select measures of visual memory and psychomotor processing speed were also noted (Table 1). She was switched from citalopram 20 mg to sertraline 50 mg daily due to her unresolved depressive symptoms, and was provided physical, speech, and cognitive therapy.

Based on the neuropsychiatric findings, clinical parkinsonism, basal ganglia calcifications, and family history of parkinsonism, the suspicion for PFBC was high which prompted us to search for a possible genetic cause, using a directed approach that focused on genes implicated in PFBC. We detected a c.2756G>A change in the *PDGFRB* gene, which results in a glutamine (Gln) substitution of arginine (Arg) at residue 919 (Figure 1).

Discussion

We report here the clinical, neuroimaging and neuropsychological features of 51-year-old Filipina woman with PFBC who was found to harbor a missense variant in the *PDGFRB* gene. Using next generation genetic sequencing, we detected a c.2756G>A, p.Arg919Gln substitution in the tyrosine kinase domain of PDGFRB protein (19). Using available computational models, the variant is predicted to be "probably damaging" (PolyPen: 0.981), "deleterious" (SIFT: 0.03), "likely deleterious" (CADD: 32), and "damaging" (MetaLR: 0.56). This variant [NM_002609.4, ENST00000261799.4, chr5: 149499072 (GRCh37/hg19)] is reported in dbSNP (Rs145717708, http://www.ncbi.nlm.nih.gov/snp/) (18), and was found in 33 individuals in gnomAD (SNV 5-149,499,072-C-T, https://gnomad.broadinstitute.org) (20), with a low minor allele frequency of 0.0001202 in the general population and 0.001595 (>0.1%) in the "Other East Asian" population, but has never been reported in association with PFBC or any other pathology. Following the ACMG criteria for scoring genetic variants (21), we would classify this as a variant of unknown significance (VUS) because it satisfies contradictory criteria for being a benign (BS1, the allele frequency is greater than expected for the disorder) and a pathogenic variant (PP3, the variant is located in a

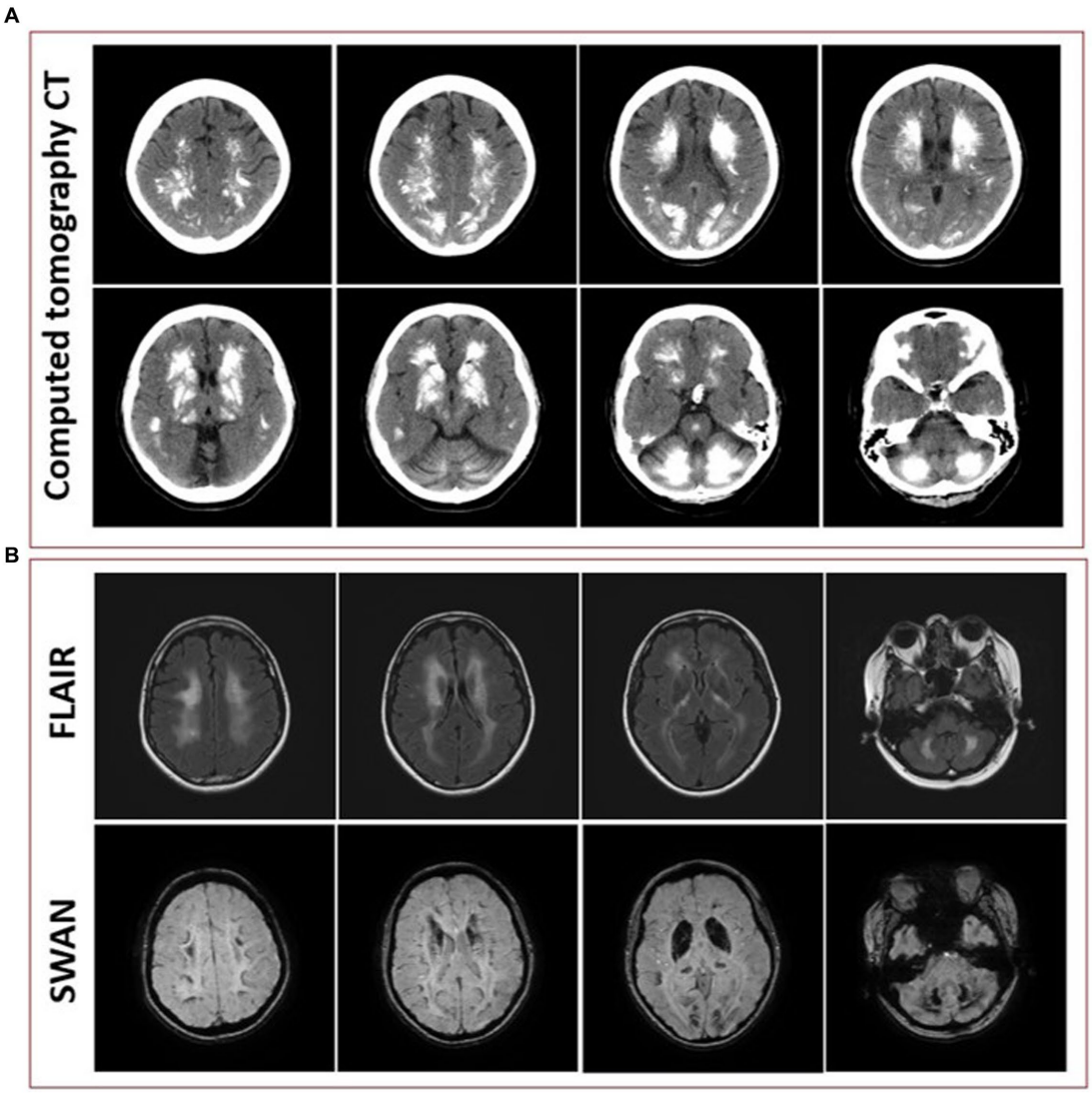

FIGURE 3
(A) Representative axial cuts from the patient's computed tomography (CT) scan 15 months after symptom onset, showing diffuse hyperdense foci favored to represent extensive calcifications throughout the bilateral corona radiata, basal ganglia, cerebellar hemispheres, and midbrain.
(B) Representative axial cuts from the patient's magnetic resonance imaging (MRI) 15 months after symptom onset, fluid-attenuated inversion recovery (FLAIR) sequence showing high T2 signal in the bilateral cerebral, brainstem, and cerebellar deep gray nuclei and white matter and susceptibility-weighted angiography (SWAN) sequence showing extensive susceptibility effect.

well-established functional domain and that multiple lines of computational evidence support a deleterious effect on the protein).

PDGFRB gene is known for its pleiotropism, making it central to different molecular systems and implicated in a diverse array of neurological syndromes including infantile myofibromatosis, Kosaki/overgrowth syndrome, Penttitnen syndrome, Sporadic Port-Wine Stain, Moyamoya syndrome, Cornelia de Lange syndrome and PFBC (19). The PDGFRB protein is a widely expressed pericyte marker (22), integral in maintaining the blood–brain barrier (BBB). Dysfunction within the BBB can lead to deposition of aberrant materials in the brain, such as the calcifications seen in PFBC (8).

Among the 13 variants in *PDGFRB* that are reported to be associated with PFBC (Figure 1) (8, 23–29), six are missense variants lie within the tyrosine-kinase domain between exons 13 and 20 (8, 24, 26–29). In cell-based experiments, two missense variants affecting the tyrosine-kinase domain (p.L658P, p.R695C) were shown to directly interfere with PDGFRB autophosphorylation, leading to defective downstream signaling (27, 30, 31). A recent study showed that 4 of the 6 known missense variants in the tyrosine-kinase domain (p.G612R, p.L658P, p.D826Y, p.D844G) resulted in complete loss of tyrosine-kinase activity (29), one variant (p.R695C) had a partial effect on receptor autophosphorylation, and one variant (p.D737N) did not lead to any significant functional defect. The p.R919Q variant we present here warrants further study to investigate its functional effect on the tyrosine-kinase activity of PDGFRB protein.

10.3389/fneur.2023.1235909

TABLE 1 Neuropsychological test data comparing 2019 evaluation with 2021 evaluation.

Domain	Measure	2019 evaluation *z*-scores	2021 evaluation *z*-scores
Estimated premorbid function	Word reading	0.90	0.75
Attention/ working memory	WAIS-IV WMI[1]	−0.55	−0.95
	Digit span	−0.67	−0.67
	Arithmetic	−2.00	−1.00
	WAIS-IV PSI[2]	−1.75	−1.60
	Symbol search	−2.33	−1.67
	Coding	−1.00	−1.33
	Stroop word	−1.50	−3.00
	Stroop color	−1.60	−2.10
	Trails A	−2.40	−2.40
Memory	CVLT-II[3]		
	Total	−1.20	−0.70
	Short delay free recall	−1.50	−1.00
	Short delay cued recall	−3.50	−2.00
	Long delay free recall	−2.00	−1.00
	Long delay cued recall	−2.50	0.00
	RCFT[4]		
	Immediate recall	0.50	−0.40
	Delayed recall	0.50	−1.30
	Recognition trial	−2.95	−2.00
	WMS-IV[5]		
	Logical memory I	−1.67	−0.67
	Logical memory II	−1.00	0.00
	Recognition trial	36%–50%tile	51%–75%tile
Language	Naming	−3.00	−2.67
	Fluency		
	Phonemic	−1.33	−0.33
	Semantic	−1.75	−1.67
Executive functioning	Stroop color-word	−1.60	−1.80
	WCST[6]		
	Categories	6%–10%tile	11%–16%tile
	Errors	−1.60	−1.70
	Perseverative Responses	−1.50	−0.90
	Trails B	−1.90	−2.30
Motor functioning	Grooved pegboard		
	Dominant hand	−2.70	−2.20
	Non-dominant hand	−2.80	−2.00
	Grip strength		
	Dominant hand	−1.90	−1.90
	Non-dominant hand	−1.30	−1.40
Behavioral functioning	FrSBe[7] (self)	Before/after *(T-score)*	Before/after *(T-score)*
	Apathy	78/58	91/95
	Disinhibition	83/64	75/63
	Executive dysfunction	61/45	96/57
	Total	79/57	95/74
	FrSBe (informant)		
	Apathy	44/51	47/97
	Disinhibition	50/52	48/54
	Executive dysfunction	50/54	46/69
	Total	48/53	47/76

1. Wechsler Adult Intelligence Scale, 4th Edition Working Memory Index; 2. Wechsler Adult Intelligence Scale, 4th Edition Processing Speed Index; 3. California Verbal Learning Test, 2nd Edition; 4. Rey-Osterrieth Complex Figure Test; 5. Wechsler Memory Scale, 4th Edition; 6. Wisconsin Card Sorting Test; 7. Frontal Systems Behavior Scale.

In a recent systematic review on phenotype–genotype relationships of 516 patients with PFBC, 26 (5%) from 9 families were reported to carry PDGFRB variants, eight of which carried a unique missense variant (12). All 26 carriers had calcification of the basal ganglia and 12 of the 26 variant carriers (46%) were clinically affected. As in the case of our patient, calcifications in other affected areas including thalamus, cerebellum, and white matter were commonly found in symptomatic carriers (12). The median age at onset of PFBC in a PDGFRB carrier in this series was 48 years (range 11–54) (12), which is consistent with our patient who developed symptoms at age 51. The most common motor signs reported included parkinsonism and bradykinesia (17% each), and the most frequent nonmotor signs were headache (33%) and cognitive deficits (25%) (12). In our case, the patient's predominant symptoms were neuropsychological (cognitive, behavioral, and psychiatric) with only mild motor manifestations (bradykinesia and dysarthria).

The clinical work up of brain calcifications include ruling out an endocrinological source of abnormal calcium homeostasis. We confirmed normal serum parathyroid hormone and calcium levels in our patient, ruling out hypoparathyroidism or pseudohypoparathyroidism as causes. Our patient's history of SLE also raised concerns for NPSLE. NPSLE is known to present with multiple neuropsychological symptoms including acute confusional states, cognitive, anxiety, and mood disorders; however, less than 1% of patients present with motor symptoms and the diagnosis remains largely a diagnosis of exclusion (32). In our patient, the presence of parkinsonism on exam and the extensive intracranial calcification supports the diagnosis of PFBC over NPSLE. Other adult-onset neurodegenerative conditions with intracranial calcifications include spinocerebellar ataxia type 20 (SCA20) which is associated with pronounced cerebellar calcifications affecting the dentate nucleus without involvement of the basal ganglia; polycystic lipo-membranous osteo-dysplasia (PLOSL) characterized by fractures, frontal lobe syndrome, and progressive dementia

beginning in the fourth decade, with bilateral calcifications of the basal ganglia, most often in the putamina; and dystonia, parkinsonism, hypermanganesemia, polycythemia, and chronic liver disease, which is a movement disorder resulting from manganese accumulation in the basal ganglia. This disease results from biallelic loss-of-function variants in SLC30A10 and basal ganglia calcifications may mimic those seen in individuals with PFBC (3).

Several case reports and reviews have explored the neuropsychological profiles of individuals with PFBC (4, 5, 7, 33–35). Psychiatric manifestations including mood disorders and psychotic symptoms are frequently present. Behavioral problems including apathy, disinhibition, aggressiveness, and impulse control disorders are reported, and the cognitive impairment that is describe ranges from mild memory and attention deficits to dementia with a frontal-subcortical profile (5, 36, 37).

As evidenced by the neuropsychological evaluations, our patient had findings of cognitive (impaired attention, delayed processing speed, and executive dysfunction), behavioral (apathy and disinhibition) and psychiatric manifestations (depression and irritability). These findings can be attributed to a dysfunction of the frontal-subcortical circuits including the anterior cingulate, the dorsolateral prefrontal, and the lateral orbitofrontal circuits. According to the Rate Model developed in the late 1980s and early 1990s (38, 39), the basal ganglia are responsible for the execution and maintenance of both motor and cognitive functions (40). Impaired executive function, apathy, and impulsivity, all of which were present in our patient, are likely explained by disturbances in the anterior cingulate and dorsolateral prefrontal circuits that are known to regulate these functions (36, 41, 42). Additionally, mood disorders including depression, also present in our patient, can be attributed to dysfunction in the lateral orbitofrontal circuit (36, 41, 42).

This report demonstrates the importance of genetic sequencing in patients with progressive neuropsychiatric disease and extensive basal ganglia calcification that suggests PFBC. Uncovering the full genetic spectrum in patients with PFBC can contribute to further understanding of disease pathogenesis and may be integral in developing targeted molecular and genetic therapies. Without targeted therapies, the treatment remains supportive with the help of a multidisciplinary team including a neurologist, psychiatrist, psychotherapist, physical therapist, and cognitive and speech therapist. The limitations of our study include the inability to perform co-segregation studies and genetic analysis of parents' samples, and the inability to sequence the two autosomal recessive genes *MYORG* and *JAM2*. Future studies are warranted to investigate the variant's functional effect on the tyrosine-kinase activity of PDGFRB protein.

Patient's perspective

We thank the patient and her family for allowing us to discuss her clinical course and genetic findings in this report. Undergoing the multiple panel genetic testing, the patient was hopeful to find a clear genetic cause for her disease; however, the patient remains unsure about the pathogenesis of her disease as the *PDGFRB* variant she carries is of unknown clinical significance, and she hopes that future functional analysis can prove or disprove the disease causality of her variant.

Data availability statement

The original contributions presented in the study are included in the article/Supplementary material, further inquiries can be directed to the corresponding author.

Ethics statement

Written informed consent was obtained from the individual (s) for the publication of any potentially identifiable images or data included in this article.

Author contributions

JA performed data extraction, manuscript writing, and preparation of the figures. JY worked on data extraction, manuscript editing, and preparation of the table. MP worked on data extraction, manuscript editing, and preparation of the table. JF, JM, and KS conceived the study, edited the manuscript, and edited the figures and table. All authors contributed to the article and approved the submitted version.

Acknowledgments

Parts of this manuscript has been released as a meeting abstract by the American Academy of Neurology (43).

Conflict of interest

The authors declare that the research was conducted in the absence of any commercial or financial relationships that could be construed as a potential conflict of interest.

Publisher's note

Supplementary material

The Supplementary material for this article can be found online at: https://www.frontiersin.org/articles/10.3389/fneur.2023.1235909/full#supplementary-material

References

1. Ellie E, Julien J, Ferrer X. Familial idiopathic striopallidodentate calcifications. *Neurol Int*. (1989) 39:381–5. doi: 10.1212/WNL.39.3.381

2. Manyam BV, Bhatt MH, Moore WD, Devleschoward AB, Anderson DR, Calne DB. Bilateral striopallidodentate calcinosis: cerebrospinal fluid, imaging, and electrophysiological studies. *Ann Neurol*. (1992) 31:379–84. doi: 10.1002/ana.410310406

3. Ramos EM, Oliveira J, Sobrido MJ, Coppola G. Primary familial brain calcification. GeneReviews®. (2017) Available at: https://www.ncbi.nlm.nih.gov/books/NBK1421/ (Accessed 25 July 2022).

4. Benke T, Karner E, Seppi K, Delazer M, Marksteiner J, Donnemiller E. Subacute dementia and imaging correlates in a case of Fahr's disease. *J Neurol Neurosurg Psychiatry*. (2004) 75:1163–5. doi: 10.1136/jnnp.2003.019547

5. Carbone MG, Della Rocca F. Neuropsychiatric manifestations of Fahr's disease, diagnostic and therapeutic challenge: A case report and a literature review. *Clin Neuropsychiatry*. (2022) 19:121–31. doi: 10.36131/cnfioritieditore20220206

6. Geschwind DH, Loginov M, Stern JM. Identification of a locus on chromosome 14q for idiopathic basal ganglia calcification (Fahr disease). *Am J Hum Genet*. (1999) 65:764–72. doi: 10.1086/302558

7. Modrego PJ, Mojonero J, Serrano M, Fayed N. Fahr's syndrome presenting with pure and progressive presenile dementia. *Neurol Sci*. (2005) 26:367–9. doi: 10.1007/s10072-005-0493-7

8. Nicolas G, Pottier C, Maltete D, Coutant S, Rovelet-Lecrux A, Legallic S, et al. Mutation of the PDGFRB gene as a cause of idiopathic basal ganglia calcification. *Neurol Int*. (2013) 80:181–7. doi: 10.1212/WNL.0b013e31827ccf34

9. Shakibai SV, Johnson JP, Bourgeois JA. Paranoid delusions and cognitive impairment suggesting Fahr's disease. *Psychosomatics*. (2005) 46:569–72. doi: 10.1176/appi.psy.46.6.569

10. Weisman DC, Yaari R, Hansen LA, Thal LJ. Density of the brain, decline of the mind: an atypical case of Fahr disease. *Arch Neurol*. (2007) 64:756–7. doi: 10.1001/archneur.64.5.756

11. Manyam BV, Walters AS, Narla KR. Bilateral striopallidodentate calcinosis: clinical characteristics of patients seen in a registry. *Mov Disord*. (2001) 16:258–64. doi: 10.1002/mds.1049

12. Balck A, Schaake S, Kuhnke NS, Domingo A, Madoev H, Margolesky J, et al. Genotype-phenotype relations in primary familial brain calcification: Systematic MDSGene Review. *Mov Disord*. (2021) 36:2468–80. doi: 10.1002/mds.28753

13. Guo XX, Zou XH, Wang C, Yao XP, Su HZ, Lai LL, et al. Spectrum of SLC20A2, PDGFRB, PDGFB, and XPR1 mutations in a large cohort of patients with primary familial brain calcification. *Hum Mutat*. (2019) 40:392–403. doi: 10.1002/humu.23703

14. Nicolas G, Richard AC, Pottier C, Verny C, Durif F, Roze E, et al. Overall mutational spectrum of SLC20A2, PDGFB and PDGFRB in idiopathic basal ganglia calcification. *Neurogenetics*. (2014) 15:215–6. doi: 10.1007/s10048-014-0404-2

15. Westenberger A, Klein C. The genetics of primary familial brain calcifications. *Curr Neurol Neurosci Rep*. (2014) 14:490. doi: 10.1007/s11910-014-0490-4

16. Cen Z, Chen Y, Chen S, Wang H, Yang D, Zhang H, et al. Biallelic loss-of-function mutations in JAM2 cause primary familial brain calcification. *Brain*. (2020) 143:491–502. doi: 10.1093/brain/awz392

17. Yao XP, Cheng X, Wang C, Zhao M, Guo XX, Su HZ, et al. Biallelic mutations in MYORG cause autosomal recessive primary familial brain calcification. *Neuron*. (2018) 98:1116–1123.e5. doi: 10.1016/j.neuron.2018.05.037

18. Sherry ST, Ward MH, Kholodov M, Baker J, Phan L, Smigielski EM, et al. dbSNP: the NCBI database of genetic variation. *Nucleic Acids Res*. (2001) 29:308–11. doi: 10.1093/nar/29.1.308

19. Moura DAP, de Oliveira JRM. The master of puppets: pleiotropy of PDGFRB and its relationship to multiple diseases. *J Mol Neurosci*. (2020) 70:2102–6. doi: 10.1007/s12031-020-01618-4

20. Karczewski KJ, Francioli LC, Tiao G, Cummings BB, Alföldi J, Wang Q, et al. The mutational constraint spectrum quantified from variation in 141,456 humans. *Nature*. (2020) 581:434. doi: 10.1038/s41586-020-2308-7

21. Richards S, Aziz N, Bale S, Bick D, das S, Gastier-Foster J, et al. Standards and guidelines for the interpretation of sequence variants: a joint consensus recommendation of the American College of Medical Genetics and Genomics and the Association for Molecular Pathology. *Genet Med*. (2015) 17:405–24. doi: 10.1038/gim.2015.30

22. Winkler EA, Bell RD, Zlokovic BV. Pericyte-specific expression of PDGF beta receptor in mouse models with normal and deficient PDGF beta receptor signaling. *Mol Neurodegener*. (2010) 5:32. doi: 10.1186/1750-1326-5-32

23. DeMeo NN, Burgess JD, Blackburn PR, Gass JM, Richter J, Atwal HK, et al. Co-occurrence of a novel PDGFRB variant and likely pathogenic variant in CASR in an individual with extensive intracranial calcifications and hypocalcaemia. *Clin Case Rep*. 6:8–13. doi: 10.1002/ccr3.1265

24. Ramos EM, Carecchio M, Lemos R, Ferreira J, Ferreira J, Legati A, et al. Primary brain calcification: an international study reporting novel variants and associated phenotypes. *Eur J Hum Genet*. (2018) 26:1462–77. doi: 10.1038/s41431-018-0185-4

25. Nicolas G, Pottier C, Charbonnier C, Guyant-Maréchal L, Le Ber I, Pariente J, et al. Phenotypic spectrum of probable and genetically-confirmed idiopathic basal ganglia calcification. *Brain*. (2013) 136:3395–407. doi: 10.1093/brain/awt255

26. Wang C, Yao XP, Chen HT, Lai JH, Guo XX, Su HZ, et al. Novel mutations of PDGFRB cause primary familial brain calcification in Chinese families. *J Hum Genet*. (2017) 62:697–701. doi: 10.1038/jhg.2017.25

27. Sanchez-Contreras M, Baker MC, Finch NA, Nicholson A, Wojtas A, Wszolek ZK, et al. Genetic screening and functional characterization of PDGFRB mutations associated with basal ganglia calcification of unknown etiology. *Hum Mutat*. (2014) 35:964–71. doi: 10.1002/humu.22582

28. Mathorne SW, Sørensen K, Fagerberg C, Bode M, Hertz JM. A novel PDGFRB sequence variant in a family with a mild form of primary familial brain calcification: a case report and a review of the literature. *BMC Neurol*. (2019) 19:60. doi: 10.1186/s12883-019-1292-8

29. Lenglez S, Sablon A, Fénelon G, Boland A, Deleuze JF, Boutoleau-Bretonnière C, et al. Distinct functional classes of PDGFRB pathogenic variants in primary familial brain calcification. *Hum Mol Genet*. (2022) 31:399–409. doi: 10.1093/hmg/ddab258

30. Arts FA, Velghe EI, Stevens M, Renauld JC, Essaghir A, Demoulin JB. Idiopathic basal ganglia calcification-associated PDGFRB mutations impair the receptor signalling. *J Cell Mol Med*. (2015) 19:239–48. doi: 10.1111/jcmm.12443

31. Vanlandewijck M, Lebouvier T, Andaloussi Mäe M, Nahar K, Hornemann S, Kenkel D, et al. Functional characterization of germline mutations in PDGFB and PDGFRB in primary familial brain calcification. *PLoS One*. (2015) 10:e0143407. doi: 10.1371/journal.pone.0143407

32. Sarwar S, Mohamed AS, Rogers S, Sarmast ST, Kataria S, Mohamed KH, et al. Neuropsychiatric systemic lupus erythematosus: a 2021 update on diagnosis, management, and current challenges. *Cureus*. (2021) 13:11. doi: 10.7759/cureus.17969

33. CalabrÒ RS, Spadaro L, Marra A, Bramanti P. Fahr's disease presenting with dementia at onset: a case report and literature review. *Behav Neurol*. (2014) 2014:1–3. doi: 10.1155/2014/750975

34. Ghogare AS, Nemade S. Fahr's syndrome presenting as pre-senile dementia with Behavioral abnormalities: a rare case report. *Cureus*. (2021) 13:e20680. doi: 10.7759/cureus.20680

35. Zangrandi A, Gasparini F, Marti A, Ivanovski I, Napoli M, Barletta-Rodolfi C, et al. Imaging and neuropsychological profile of four patients with Fahr's disease. *Psychol Neurosci*. (2018) 11:68–79. doi: 10.1037/pne0000114

36. Benke T, Delazer M, Bartha L, Auer A. Basal ganglia lesions and the theory of fronto-subcortical loops: neuropsychological findings in two patients with left caudate lesions. *Neurocase*. (2003) 9:70–85. doi: 10.1076/neur.9.1.70.14374

37. Donzuso G, Mostile G, Nicoletti A, Zappia M. Basal ganglia calcifications (Fahr's syndrome): related conditions and clinical features. *Neurol Sci*. (2019) 40:2251–63. doi: 10.1007/s10072-019-03998-x

38. Albin RL, Young AB, Penney JB. The functional anatomy of basal ganglia disorders. *Trends Neurosci*. (1989) 12:366–75. doi: 10.1016/0166-2236(89)90074-X

39. DeLong MR. Primate models of movement disorders of basal ganglia origin. *Trends Neurosci*. (1990) 13:281–5. doi: 10.1016/0166-2236(90)90110-V

40. Nelson AB, Kreitzer AC. Reassessing models of basal ganglia function and dysfunction. *Annu Rev Neurosci*. (2014) 37:117:–135. doi: 10.1146/annurev-neuro-071013-013916

41. Mega MS, Cummings JL. Frontal-subcortical circuits and neuropsychiatric disorders. *J Neuropsychiatry Clin Neurosci*. (1994) 6:358–70. doi: 10.1176/jnp.6.4.358

42. Bonelli RM, Cummings JL. Frontal-subcortical circuitry and behavior. *Dialogues Clin Neurosci*. (2007) 9:141–51. doi: 10.31887/DCNS.2007.9.2/rbonelli

43. Ali AL, Yang J, Phillips MS, Fink J, Mastrianni J, Seibert K. A novel mutation in pdgfrb in a patient with primary familial brain calcification: Case Report (P2-12.005). In Proceedings of the 75th Annual American Academy of Neurology conference. AAN: 2023 Apr 22-27; Boston (MA). Neurology [Internet]. 2023 Apr 25 [cited 2023 Aug 29];100(17 Supplement 2):1584. Available at: https://n.neurology.org/content/100/17_Supplement_2/1584

frontiers | Frontiers in Neurology

TYPE Case Report
PUBLISHED 22 September 2023
DOI 10.3389/fneur.2023.1255128

OPEN ACCESS

EDITED BY
Huifang Shang,
Sichuan University, China

REVIEWED BY
Chao Yuan,
Southern Medical University, China
Arushi Gahlot Saini,
Post Graduate Institute of Medical Education and Research (PGIMER), India

*CORRESPONDENCE
Lixia Qin
✉ qinlixia1027@csu.edu.cn

RECEIVED 08 July 2023
ACCEPTED 28 August 2023
PUBLISHED 22 September 2023

CITATION
Chen Q, Tang J, Zhang H and Qin L (2023) Case report: Desquamating dermatitis, bilateral cerebellar lesions in a late-onset methylmalonic acidemia patient. *Front. Neurol.* 14:1255128. doi: 10.3389/fneur.2023.1255128

Case report: Desquamating dermatitis, bilateral cerebellar lesions in a late-onset methylmalonic acidemia patient

Qihua Chen, Jianguang Tang, Hainan Zhang and Lixia Qin*

Department of Neurology, The Second Xiangya Hospital, Central South University, Changsha, Hunan, China

Introduction: Cobalamin C (cblC) deficiency is a rare hereditary disorder affecting intracellular cobalamin metabolism, primarily caused by mutations in *MMACHC*. This condition is characterized by combined methylmalonic acidemia and hyperhomocysteinemia, displaying a wide range of clinical manifestations involving multiple organs. Owing to its uncommon occurrence and diverse clinical phenotypes, diagnosing cblC deficiency is challenging and often leads to delayed or missed diagnoses.

Case description: In this report, we present a case of late-onset cblC deficiency with brown desquamating dermatitis on the buttocks. Magnetic resonance imaging (MRI) of the brain revealed bilateral cerebellar abnormalities. The suspicion of an inherited metabolic disorder was raised by abnormal serum amino acid and acylcarnitine levels, along with increased urine methylmalonic acid and serum homocysteine levels. Whole-exome sequencing helped identify a homozygous variant (c.482G>A) in *MMACHC*, confirming the diagnosis of cblC deficiency. However, despite receiving treatment with hydroxocobalamin and betaine, the patient did not experience clinical improvement, which may be attributed to the delayed diagnosis as indicated by the declining homocysteine and methylmalonic acid levels.

Conclusion: Collectively, we emphasize the significance of recognizing the skin lesions and observing serial MRI changes in patients with cblC deficiency. Our case underscores the importance of early diagnosis and timely therapeutic intervention for this severe yet frequently manageable condition.

KEYWORDS

desquamating dermatitis, cerebellum, genes, cobalamin C deficiency, skin lesions

Introduction

Combined with methylmalonic acidemia and homocystinuria, cobalamin C (cblC) is the most common inborn error in cobalamin metabolism. Newborn genetic screening studies for metabolic errors revealed that the estimated incidence of CblC deficiency is 1/3,920 in Shandong Province, China (1), and 1/100,000 in New York, United States (2). In 2006, Lerner-Ellis et al. (3) cloned the disease-causing *MMACHC* gene. To date, over 50 mutations have been identified in patients with *MMACHC*. Mutations in *MMACHC* disrupt the intracellular metabolism of cobalamin, causing the accumulation of methylmalonic acid and homocysteine and a lack of methionine. However, the underlying pathophysiological mechanisms are not well understood.

cblC deficiency is associated with systemic involvement and complex clinical manifestations, including progressive encephalopathy, subacute combined degeneration of the spinal cord, maculopathy, anemia, thromboembolic complications, pulmonary arterial hypertension, and kidney injury (4, 5). Skin manifestations, although rare, are often overlooked (6). Brain magnetic resonance imaging (MRI) findings commonly include hydrocephalus, progressive white matter abnormalities, and atypical lesions in the basal ganglia and cerebellum (4, 7). Late-onset cblC deficiency, which occurs in approximately 10% of affected individuals aged above 12 months, generally presents with milder symptoms, more evident clinical presentations and improvement, and a more favorable prognosis than that observed in the early-onset form. However, some patients do not respond well to treatment, particularly those with severe complications or delayed or insufficient initiation of therapy. In this case report, we describe a 21-year-old man who presented with psychiatric symptoms, skin lesions, and bilateral cerebellar abnormalities on brain MRI. The diagnosis of cblC deficiency was confirmed using whole-exome sequencing.

Case description

A 21-year-old man with no significant family history presented with a two-year history of weakness, numbness, and painful sensations in his lower limbs. Over the course of 1 month, he also experienced psychiatric disturbances. Figure 1 provides a timeline of the events. The patient reported additional symptoms, including urinary and bowel incontinence, as well as intellectual and motor developmental delays. He exhibited a motionless posture with a distressed facial expression, occasionally crying out loudly. Seborrheic dermatitis was observed on his face and trunk, and the buttocks had prominent brown hyperpigmentation with desquamating dermatitis (Figure 2A). Tendon reflexes were normal, with no signs of pyramidal neurological deficits. However, the patient's impaired consciousness hindered further examination. Laboratory tests revealed hypochromic microcytic anemia (hemoglobin level: 91 g/L), elevated transaminase levels (glutamic-pyruvic transaminase: 168.7 U/L; aspartate aminotransferase: 84.1 U/L), and significantly increased serum homocysteine levels (258.4 μmol/L, normal range, 5–15.0 μmol/L). Urine organic acid analysis and serum amino acid and acylcarnitine analysis showed substantially elevated urine methylmalonic acid levels (24.8 μmol/L, normal range, <4.0 μmol/L) and serum propionyl carnitine/acetylcarnitine ratio (0.33, normal range, 0.02–0.2) (Figures 2B,C). No signs of infection, inflammation, or toxicity were present, and serum and cerebrospinal fluid (CSF) anti-cerebellitis antibodies were negative. Spinal cord MRI scan results were normal. Electromyogram (EMG) findings indicated widespread motor and sensory demyelination with accompanying axonal injuries in the limbs, particularly affecting the lower limbs. The first MRI, obtained 2 months after symptom onset, revealed diffuse cerebral atrophy (Figures 3A–C). Subsequent MRI performed at this visit (2 years after symptom onset) revealed bilateral symmetrical lesions in the cerebellum, characterized by hyperintensity on T2-weighted images, restricted diffusion on diffusion-weighted imaging (DWI), and no enhancement (Figures 3D–F). Based on the abnormal serum amino acid and acylcarnitine levels, elevated urine methylmalonic acid level, and increased serum homocysteine level, inherited metabolic diseases were strongly suspected. The diagnosis of late-onset cblC deficiency was further supported by whole-exome genetic sequencing, revealing a homozygous variant (c.482 G > A) in *MMACHC* (Figure 2D). Further genetic analysis proved that the patient in our case was maternal uniparental disomy (mUPD). Following treatment with adequate betaine (9 g/day, administered intragastrically), cobamamide (1.5 mg/day, administered via intramuscular injection), mecobalamin (1 mg/day, administered via intramuscular injection), and B vitamins, the patient's serum homocysteine levels substantially decreased (60.9 μmol/L), as did urine methylmalonic acid levels (12.5 μmol/L). At discharge, the patient did not experience significant clinical improvement, as well as observed changes on brain MRI (Figures 3G–I). Within 1.5 years of follow-up, he relieved slightly but relapsed after treatment discontinuation.

Discussion

cblC deficiency is the most prevalent disorder associated with cobalamin metabolism (5) and is a rare autosomal recessive disease induced by homozygous recessive or compound heterozygous mutations in *MMACHC* (3, 8). These mutations disrupt cobalamin

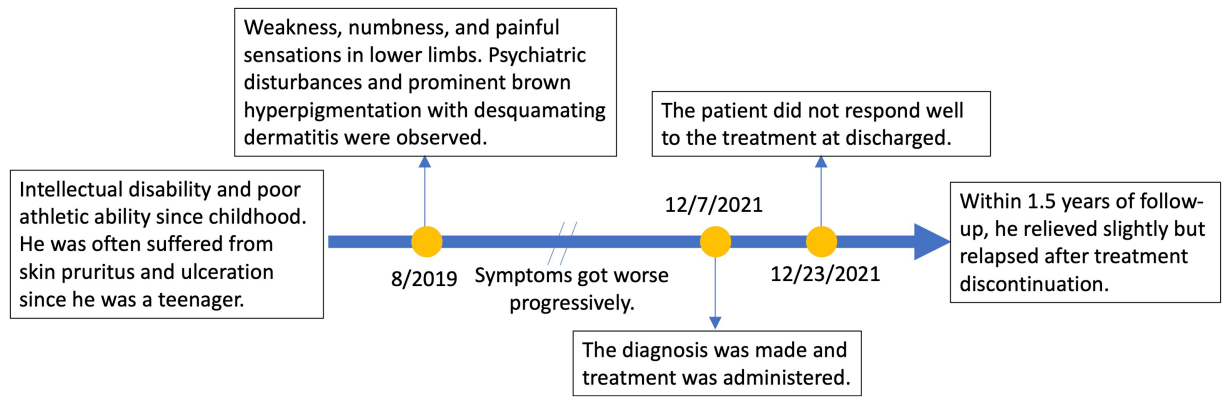

FIGURE 1
A timeline of events.

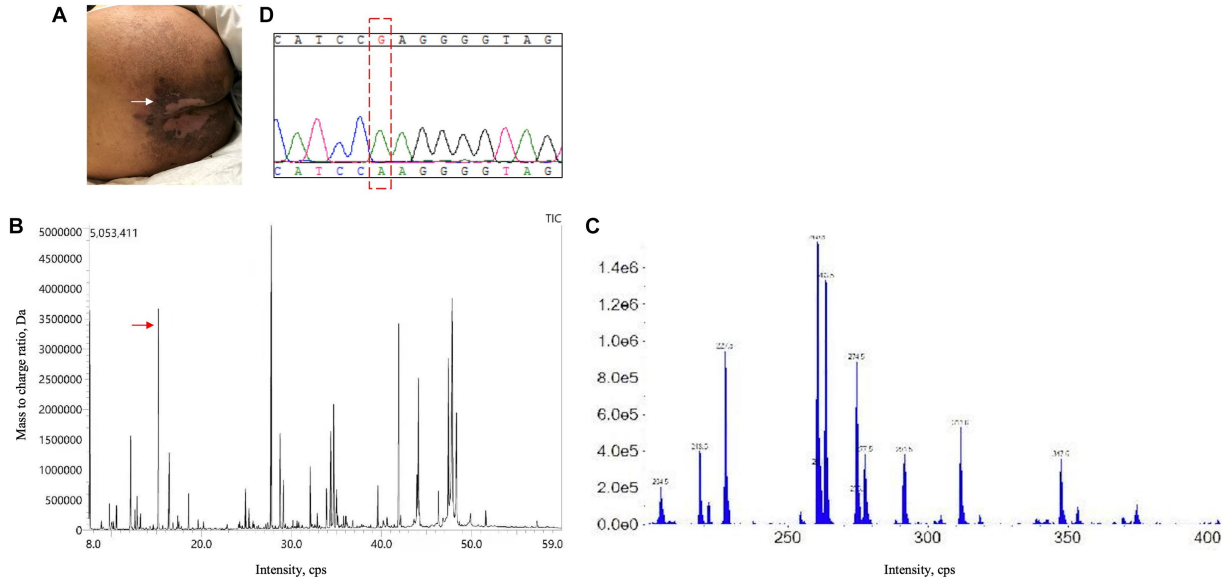

FIGURE 2
Skin lesion, urine organic acid analysis, serum amino acid and acylcarnitine analysis, and genetic testing results. **(A)** Superficial, erosive desquamating dermatitis on the buttocks of the present patient. **(B)** Urine organic acid analysis revealed an evident increase in methylmalonic acid levels (24.8 μmol/L; normal range: <4.0 μmol/L). **(C)** Serum amino acid and acylcarnitine analysis exhibited an increased propionyl carnitine/acetylcarnitine ratio (0.33; normal range: 0.02–0.2). **(D)** Next-generation sequencing identified a homozygous variant (c.482 G > A) in *MMACHC*, which was further validated by sanger sequencing.

metabolism, leading to the accumulation of toxic levels of metabolites, homocysteine and methylmalonic acid, which cause oxidative injury. While the central and peripheral nervous system are commonly affected, cblC deficiency can also involve more organs and tissues, including the kidneys (9), lung (10), micrangium (11), retina (12), and skin (6). Early-onset cblC deficiency, with an age of onset <12 months, is more prevalent and typically manifests with feeding difficulties, somnolence, developmental delays, seizures, muscular hypotonia, hydrocephalus, and microcephaly (1, 4, 8, 13). Late-onset cblC deficiency is characterized by neuropsychiatric symptoms, cognitive dysfunction, myelopathy, rental function abnormality, and pulmonary arterial hypertension (14, 15). The present case exhibited psychiatric symptoms, cognitive decline, peripheral neuropathy, dermatitis, anemia, and hepatic dysfunction were found.

Diffuse cerebral atrophy and bilateral hyperintensity in the deep white matter and cerebellum are common brain MRI findings in patients with late-onset cblC deficiency (15, 16). The patient presented with symmetrical bilateral cerebellar lesions. The differential diagnoses of cerebellar lesions are broad and include vascular causes (occlusion of lateral posterior inferior cerebellar artery), infectious agents (such as bacteria, viruses, and mycoplasma), autoimmune factors (such as anti-glutamate decarboxylase 65 antibody-associated cerebellitis, paraneoplastic), hereditary conditions (hereditary spinocerebellar ataxia, fragile X–associated tremor ataxia syndrome), as well as metabolic and toxic factors (such as alcohol, cytotoxicity drugs, organic solvent) (17–20). The clinical history and laboratory analyzes narrowed the diagnostic possibilities, and genetic testing confirmed the final diagnosis.

Skin lesions owing to nutritional deficiency are rare manifestations of extra-nervous system involvement in cblC deficiency. They can present as cheilitis, diffuse erythema with erosions and desquamation, and superficial erosive desquamating dermatitis, which may be attributed to enzymatic deficiency or nutritional restriction (6, 21, 22). Researchers have suggested that erosive desquamating dermatitis with histopathological characteristics resembling acrodermatitis enteropathica may be an initial systemic sign of cblC deficiency. The presence of brown desquamation dermatitis should prompt clinicians to consider this diagnosis when nutritional deficiency is suspected. Renal examination was normal, but screening for optic neuropathy and retina was not performed for the patient's poor psychiatric status.

CblC deficiency is often curable. Most patients with late-onset cblC deficiency respond well to hydroxocobalamin and betaine treatment. The goals of treatment are to improve clinical presentation, normalize serum methionine levels, reduce urine methylmalonic acid levels, and lower homocysteine levels by promoting homocysteine-to-methionine conversion, facilitating re-methylation, and accelerating acylcarnitine clearance (5, 23). The patient in our case only received betaine, cobamamide, and mecobalamin, not hydroxycobalamin, because hydroxycobalamin injection was not available in many provinces of China. Delayed diagnosis and therapeutic intervention, low compliance to maintenance treatment, and no hydroxycobalamin was given contributed to the poor outcomes in this case. Constant and aggressive treatment seems to be required.

In conclusion, we reported a rare case of late-onset cblC deficiency with a delayed diagnosis, presenting with brown desquamation dermatitis and bilateral cerebellar MRI abnormalities. Owing to its rarity and heterogeneous clinical presentation, the diagnosis of cblC deficiency poses challenges and is often delayed or missed. Our case highlights the importance of early diagnosis and timely therapeutic intervention for this severe but often treatable disease. Otherwise, irreversible damage to multiple organs,

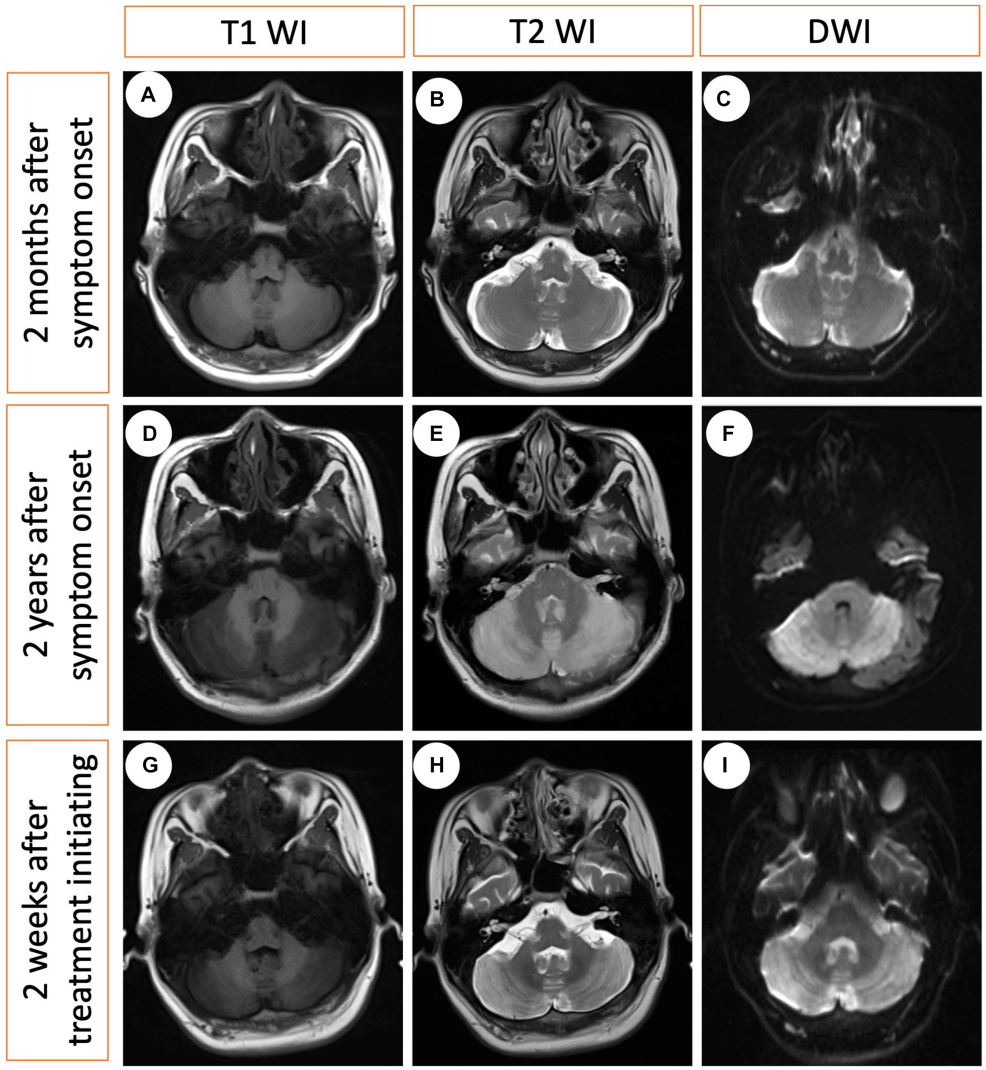

FIGURE 3
Serial MRI changes at three different time points. **(A–C)** The first MRI obtained 2 months after symptom onset (no treatment), indicating modest cerebral atrophy. **(D–F)** The second MRI obtained 2 years after symptom onset (no treatment), revealing bilateral hyperintensity in the cerebellum on the T2-weighted image and diffusion-weighted imaging (DWI), with hypointensity on the T1-weighted image. **(G–I)** The third MRI obtained 2 weeks after treatment initiation indicating minimal changes.

particularly neurological complications, is unavoidable, ultimately resulting in poor outcomes.

Data availability statement

The datasets presented in this article are not readily available because of ethical and privacy restrictions. Requests to access the datasets should be directed to the corresponding author.

Ethics statement

The studies involving human participants were reviewed and approved by the Ethics Committee of the Second Xiangya Hospital, Central South University. The patients/participants provided their written informed consent to participate in this study. Written informed consent was obtained from the individual(s) for the publication of any potentially identifiable images or data included in this article.

Author contributions

QC: Writing – original draft, Writing – review & editing. JT: Writing – original draft, Writing – review & editing. HZ: Writing – original draft, Writing – review & editing. LQ: Writing – original draft, Writing – review & editing.

Funding

This work was supported by grant from the National Natural Science Foundation of China (No. 82101342 to LQ), the Provincial Natural Science Foundation (No. 2022JJ30833 to LQ), and Scientific

Research Launch Project for new employees of the Second Xiangya Hospital of Central South University.

Conflict of interest

The authors declare that the research was conducted in the absence of any commercial or financial relationships that could be construed as a potential conflict of interest.

Publisher's note

References

1. Han B, Cao Z, Tian L, Zou H, Yang L, Zhu W, et al. Clinical presentation, gene analysis and outcomes in young patients with early-treated combined methylmalonic Acidemia and Homocysteinemia (Cblc type) in Shandong Province. *China Brain Dev*. (2016) 38:491–7. doi: 10.1016/j.braindev.2015.10.016

2. Weisfeld-Adams JD, Morrissey MA, Kirmse BM, Salveson BR, Wasserstein MP, McGuire PJ, et al. Newborn screening and early biochemical follow-up in combined methylmalonic aciduria and homocystinuria, Cblc type, and utility of methionine as a secondary screening analyte. *Mol Genet Metab*. (2010) 99:116–23. doi: 10.1016/j.ymgme.2009.09.008

3. Lerner-Ellis JP, Tirone JC, Pawelek PD, Doré C, Atkinson JL, Watkins D, et al. Identification of the gene responsible for methylmalonic aciduria and homocystinuria. *Nat Genet*. (2006) 38:93–100. doi: 10.1038/ng1683

4. Carrillo-Carrasco N, Venditti CP. Combined methylmalonic Acidemia and homocystinuria, Cblc type. Ii. Complications, pathophysiology, and outcomes. *J Inherit Metab Dis*. (2012) 35:103–14. doi: 10.1007/s10545-011-9365-x

5. Carrillo-Carrasco N, Chandler RJ, Venditti CP. Combined methylmalonic Acidemia and homocystinuria, Cblc type. I. Clinical presentations, diagnosis and management. *J Inherit Metab Dis*. (2012) 35:91–102. doi: 10.1007/s10545-011-9364-y

6. Gilson RC, Wallis L, Yeh J, Gilson RT. Dementia, Diarrhea, desquamating shellac-like dermatitis revealing late-onset Cobalamin C deficiency. *JAAD Case Rep*. (2018) 4:91–4. doi: 10.1016/j.jdcr.2017.09.016

7. Longo D, Fariello G, Dionisi-Vici C, Cannatà V, Boenzi S, Genovese E, et al. Mri and 1h-Mrs findings in early-onset Cobalamin C/D defect. *Neuropediatrics*. (2005) 36:366–72. doi: 10.1055/s-2005-873057

8. Wang F, Han L, Yang Y, Gu X, Ye J, Qiu W, et al. Clinical, biochemical, and molecular analysis of combined methylmalonic Acidemia and Hyperhomocysteinemia (Cblc type) in China. *J Inherit Metab Dis*. (2010) 33:435–42. doi: 10.1007/s10545-010-9217-0

9. Lemoine M, Grangé S, Guerrot D. Kidney disease in Cobalamin C deficiency. *Nephrol Ther*. (2019) 15:201–14. doi: 10.1016/j.nephro.2019.03.011

10. Liu J, Tang X, Zhou C, Xu H, Yang H, He R, et al. Cobalamin C deficiency presenting with diffuse alveolar Hemorrhage and pulmonary microangiopathy. *Pediatr Pulmonol*. (2020) 55:1481–6. Epub 2020/04/16. doi: 10.1002/ppul.24781

11. George JN, Cobalamin C. Deficiency-associated thrombotic microangiopathy: uncommon or unrecognised? *Lancet*. (2015) 386:1012. doi: 10.1016/s0140-6736(15)00077-x

12. Garcia-Gonzalez JM, Neiweem AE, Grassi MA. Cobalamin C deficiency-associated pigmentary retinopathy. *JAMA Ophthalmol*. (2015) 133:e152161. doi: 10.1001/jamaophthalmol.2015.2161

13. Rosenblatt DS, Aspler AL, Shevell MI, Pletcher BA, Fenton WA, Seashore MR. Clinical heterogeneity and prognosis in combined methylmalonic aciduria and homocystinuria (Cblc). *J Inherit Metab Dis*. (1997) 20:528–38. doi: 10.1023/a:1005353530303

14. Thauvin-Robinet C, Roze E, Couvreur G, Horellou MH, Sedel F, Grabli D, et al. The adolescent and adult form of Cobalamin C disease: clinical and molecular Spectrum. *J Neurol Neurosurg Psychiatry*. (2008) 79:725–8. doi: 10.1136/jnnp.2007.133025

15. Huemer M, Scholl-Bürgi S, Hadaya K, Kern I, Beer R, Seppi K, et al. Three new cases of late-onset Cblc defect and review of the literature illustrating when to consider inborn errors of metabolism beyond infancy. *Orphanet J Rare Dis*. (2014) 9:161. doi: 10.1186/s13023-014-0161-1

16. Wang SJ, Zhao YY, Yan CZ. Reversible encephalopathy caused by an inborn error of Cobalamin metabolism. *Lancet*. (2019) 393:e29. doi: 10.1016/s0140-6736(19)30043-1

17. Baizabal-Carvallo JF, Jankovic J. Autoimmune and paraneoplastic movement disorders: an update. *J Neurol Sci*. (2018) 385:175–84. doi: 10.1016/j.jns.2017.12.035

18. de Silva RN, Vallortigara J, Greenfield J, Hunt B, Giunti P, Hadjivassiliou M. Diagnosis and Management of Progressive Ataxia in adults. *Pract Neurol*. (2019) 19:196–207. doi: 10.1136/practneurol-2018-002096

19. Mitoma H, Manto M, Hampe CS. Immune-mediated cerebellar ataxias: practical guidelines and therapeutic challenges. *Curr Neuropharmacol*. (2019) 17:33–58. doi: 10.2174/1570159x16666180917105033

20. Klockgether T. Sporadic ataxia with adult onset: classification and diagnostic criteria. *Lancet Neurol*. (2010) 9:94–104. doi: 10.1016/s1474-4422(09)70305-9

21. Howard R, Frieden IJ, Crawford D, McCalmont T, Levy ML, Rosenblatt DS, et al. Methylmalonic Acidemia, Cobalamin C type, presenting with cutaneous manifestations. *Arch Dermatol*. (1997) 133:1563–6. doi: 10.1001/archderm.1997.03890480083012

22. Karamifar H, Shakibazad N, Saki F, Saki N, Kardeh S. Skin manifestation of methylmalonic Acidemia: case report and review of the literature. *G Ital Dermatol Venereol*. (2015) 150:741–4.

23. Gurkas E, Kartal A, Aydin K, Kucukçongar A, Dilber C, Ceylaner S. Reversible clinical and magnetic resonance imaging findings in late-onset Cobalamin C defect. *Genet Couns*. (2015) 26:425–30. Epub 2016/02/09.

frontiers | Frontiers in Neurology

TYPE Case Report
PUBLISHED 20 October 2023
DOI 10.3389/fneur.2023.1253398

OPEN ACCESS

EDITED BY
Huifang Shang,
Department of Neurology,
Sichuan University, China

REVIEWED BY
Alessandro Simonati,
University of Verona, Italy
Alessandro Capuano,
Azienda Sanitaria Locale di Viterbo, Italy

*CORRESPONDENCE
Xuemei Zhang
✉ xuemeizh001@163.com

RECEIVED 05 July 2023
ACCEPTED 18 September 2023
PUBLISHED 20 October 2023

CITATION
Chen X, Qu HB, Yao Q, Cai XT, He TT and Zhang XM (2023) Case report: Analysis of a gene variant and prenatal diagnosis in a family with megalencephalic leukoencephalopathy with subcortical cysts.
Front. Neurol. 14:1253398.
doi: 10.3389/fneur.2023.1253398

Case report: Analysis of a gene variant and prenatal diagnosis in a family with megalencephalic leukoencephalopathy with subcortical cysts

Xi Chen[1,2,3], Haibo Qu[3,4], Qiang Yao[2,3], Xiaotang Cai[3,5], Tiantian He[1,2,3] and Xuemei Zhang[1,2,3]*

[1]Department of Medical Genetics and Prenatal Diagnosis Center, West China Second University Hospital, Sichuan University, Chengdu, China, [2]Department of Obstetrics and Gynecology, West China Second University Hospital, Sichuan University, Chengdu, China, [3]Key Laboratory of Birth Defects and Related Diseases of Women and Children (Sichuan University), Ministry of Education, Chengdu, China, [4]Department of Radiology, West China Second University Hospital, Sichuan University, Chengdu, China, [5]Department of Rehabilitation, West China Second University Hospital, Sichuan University, Chengdu, China

Megalencephalic leukoencephalopathy with subcortical cysts (MLC) is a rare inherited cerebral white matter disorder in children. Pathogenic variations in the causative gene *MLC1* are found in approximately 76% of patients and are inherited in an autosomal recessive manner. In this study, we identified an IVS2 + 1delG variant in *MLC1* in the firstborn girl of a pregnant woman who has the clinical features of MLC, including macrocephaly, motor development delay, progressive functional deterioration, and myelinopathy, whereas no obvious subcortical cysts were observed by magnetic resonance imaging of the brain. The proband is homozygous for the IVS2 + 1delG mutation, which was inherited from the parents. This variant disrupts the donor splice site, causing an abnormal transcript that results in a premature termination codon and produces a truncated protein, which was confirmed to affect splicing by *MLC1* cDNA analysis. This variant was also detected in family members, and a prenatal diagnosis for the fetus was undertaken. Eventually, the couple gave birth to an unaffected baby. Furthermore, we conducted a long-term follow-up of the proband's clinical course. This report improves our understanding of the genetic and phenotypic characteristics of MLC and provides a new genetic basis for prenatal diagnosis and genetic counseling.

KEYWORDS

MLC, *MLC1*, leukodystrophy, splice mutation, clinical phenotype, prenatal diagnosis, genetic counseling

1. Introduction

Megalencephalic leukoencephalopathy with subcortical cysts (MLC) is a rare inherited cerebral white matter disorder characterized by early-onset macrocephaly and delayed-onset neurological deterioration, including cerebellar ataxia, spasticity, epilepsy, and mild cognitive decline (1, 2). Magnetic resonance imaging (MRI) of the brain shows evidence of severe white matter involvement and cysts in the tips of the temporal lobes, as well as in the frontoparietal

subcortical area (3). The disease is progressive and results in the regression of motor and cognitive functions.

Two genes are associated with three types of MLC. Type 1 (OMIM 604004) is caused by a recessive mutation in *MLC1* (OMIM 605908), type 2A (OMIM 613925) is caused by a recessive mutation in *HEPACAM* (OMIM 611642), and type 2B (OMIM 613926) is caused by a dominant mutation in *HEPACAM*. Biallelic pathogenic variants in *MLC1* are observed in approximately 76% of individuals with MLC, whereas pathogenic variants in *HEPACAM* are found in approximately 22% (1). This suggests there may be other related genes not yet discovered.

The *MLC1* gene has been mapped to chromosome 22q13.33 (4, 5), which contains 12 exons, encodes 377 amino acids, and contains 8 transmembrane domains (6, 7). Over 100 mutations in *MLC1* have been reported globally (HGMD® Professional 2023.4), most of which occur throughout the coding and non-coding regions. All types of mutations are included: missense and nonsense mutations (51%), splice mutations (19%), deletions (14%), and insertions (6%) (HGMD).

In this study, we recruited a woman in early pregnancy whose firstborn girl was clinically diagnosed with leukoencephalopathy based on symptoms and brain MRI findings. In this family, a splicing mutation was identified in *MLC1*, which induces protein truncation with a premature stop codon. A prenatal diagnosis was made for this family, and clinical follow-up was performed for the proband and second child.

2. Materials and methods

2.1. Clinical materials and participants

Patients and family members were recruited at the West China Second University Hospital, and blood samples were obtained from all participants. Genomic DNA was extracted from peripheral blood according to the manufacturer's instructions (CWBIO, Beijing, China), and total RNA was isolated using the RNA Pure Blood Kit (CWBIO). Clinical data were collected and evaluated by a multidisciplinary team of geneticists, radiologists, obstetricians, and pediatricians. The phenotypes of the individuals were longitudinally and systematically evaluated. Studies involving human participants were reviewed and approved by the Medical Ethics Committee of the West China Second University Hospital, Sichuan University. Written informed consent to participate in this study was obtained from participants or their legal guardians.

2.2. Mutation identification and analysis

Exome sequencing of the target gene panel associated with leukoencephalopathy was performed on the proband's DNA sample at Beijing Mygenostics Inc. (Beijing, P.R. China) using an Illumina NextSeq 500 (Illumina, San Diego, CA, USA). The mutation was confirmed by Sanger sequencing. All family members and 100 Chinese control samples were screened for this mutation. The primers for Sanger sequencing can be provided upon request.

The mRNA transcription of *MLC1* was examined using reverse transcription-polymerase chain reaction (RT-PCR) (PrimeScript™ RT reagent Kit, TaKaRa). The following were the primers used: forward (5′-AAC TGG TGA CAC GTG GCT GT-3′), reverse (5′-TTG CTG ATG GGT TCA GGA CT-3′), or reverse (5′-ACT TCG TCC AGA ATG TTG GC-3′). Both PCR and RT-PCR were performed in a 25-μL reaction, containing a 50 ng template, 12.5 μL Gold Taq Green Master Mix (Promega, Madison, Wisconsin, USA), and 10 pmol/L of each primer. The reactions were performed under the following conditions: 95°C for 1.5 min, 35 cycles at 94°C for 40 s, 60°C for 40 s, and 72°C for 40 s, followed by a final extension at 72°C for 5 min. The amplifiers were purified using the Wizard SV Gel and PCR Clean-Up System (Promega), followed by direct sequencing on an ABI 3500 Genetic Analyzer (Applied Biosystems, Waltham, MA, USA), and the data was evaluated using Chromas software (2.6.5). Alphafold 2[1] was used to predict and analyze protein structure.

2.3. Prenatal diagnosis

Amniocentesis was performed at 19 weeks of gestation, according to standard clinical operating procedures (8). Amniotic fluid was extracted from the gravida for prenatal diagnosis to identify whether the second fetus shared the mutation found in the proband. After high-speed centrifugation (900 rcf, 8 min) of the amniotic fluid, the supernatant was discarded and the bottom cell precipitate was retained. DNA was extracted and sequenced, as described above. The mother's blood sample was collected in an EDTA vacutainer to identify maternal cell contamination during prenatal diagnosis.

3. Results

3.1. Case presentation

A 29-year-old pregnant woman, gravida 2, para 1, was referred to the Department of Medical Genetics and Prenatal Diagnosis Center of West China Second University Hospital because her firstborn was clinically suspected of having leukoencephalopathy. She and her spouse were non-consanguineous, with no notable medical conditions, and denied a family history of genetic diseases or a known history of neurological disorders (Figure 1A). She was in her second pregnancy at 12 weeks with no complications and had no notable history in her first pregnancy.

The proband (firstborn), a 2-year-old girl, was born naturally at full term and had a normal occipitofrontal circumference (OFC) (33.5 cm) and weight (3.2 kg) at birth. Macrocephaly was observed during her first year of life when she appeared with a large head circumference (HC) (46 cm, > +3 SD) at 6 months of age [according to the median HC (MHC) in Chinese girls (9)] and presented an HC of 48.5 cm (> +3 SD, MHC: 43.5 cm) at 8 months of age. At the age of 1 year and 3 months, her HC increased to 53.5 cm (> +3 SD, MHC: 45.9 cm; Figures 1B,C), whereas her height (75 cm) and weight (10 kg) were normal. Brain MRI at 13 months revealed swelling in the bilateral cerebral cortex and diffuse signal abnormalities in the cerebral white matter, showing a low signal on T1-weighted images and a high signal on T2-weighted images, as well as fluid-attenuated inversion recovery

1 https://github.com/deepmind/alphafold

FIGURE 1
Family pedigree and clinical features of the proband. **(A)** Family pedigree. The proband was noted to have a homozygous variant. Parents and grandparents carried the heterozygous variant. The fetus carried the wild-type form of *MLC1*. **(B)** The appearance of the proband's head at 2 years of age. **(C)** The curve of the HC of the proband. Macrocephaly was observed during her first year of life and her HC at 15 months was 53.5 cm, > +3SD. The early rapid growth of the head, crossing +3 SD at approximately 6 months, was followed only a few months later (at approximately 1 year of age) by a slow growth that parallels the median curve.

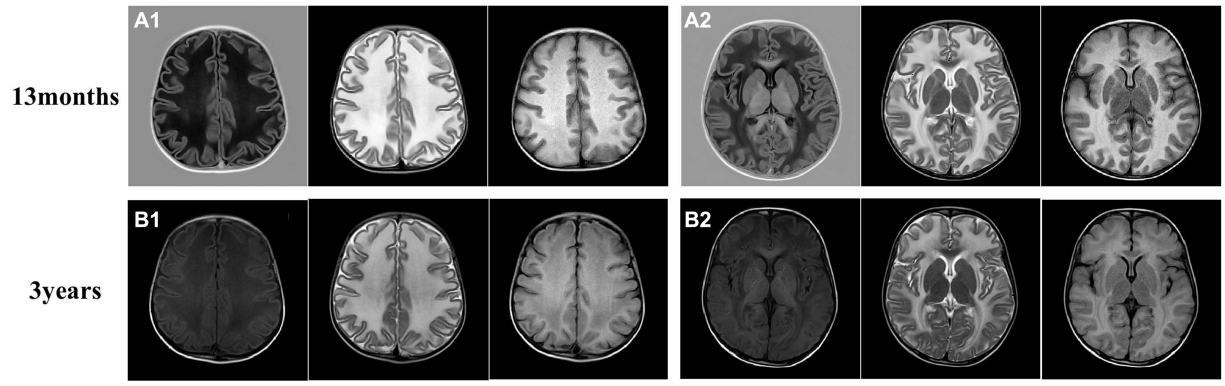

FIGURE 2
Brain magnetic resonance imaging (MRI) of the proband. **(A)** The brain MRI of the proband at 13 months. **(B)** Another image was taken at 3 years old. The MRI revealed swelling in the bilateral cerebral cortex and diffuse signal abnormalities in cerebral white matter, showing a low signal on T1-weighted images and a high signal on T2-weighted images, as well as in fluid-attenuated inversion recovery images. Subcortical cysts were not observed in any section.

images; however, subcortical cysts were not seen in all sections (Figure 2A).

The proband also presented with severe motor developmental delay and low muscle tone. She could not roll over at 6 months, stand until she was 1 year and 6 months of age, or crawl and independently sit and walk until she was 2 years old. She often walked unsteadily and exhibited poor motor coordination. She had no early-onset seizures, epilepsy, or spasticity before 2 years of age, and her vision and hearing functions were normal. Her cognitive functions were delayed; she could say a few enunciated words but often spoke to herself unconsciously and could not understand the meaning of words, follow instructions, express her intentions, or otherwise verbally communicate. She had a motor developmental index of less than 50 on the Bayley Scales of Infant Development (BSID-II) at 19 months of age and a cognitive developmental index of 52, which, respectively, equaled those of 10- and 12-month-old infants. These results indicated that the patient had substantial deficits in her motor, cognitive, and language development levels outside the normal range. Detailed information is provided in Table 1; Figure 3.

3.2. Clinical follow-up of the proband

We also followed the proband's clinical course after she turned 2 years-old. After becoming 2 ½ years-old, the patient began to experience convulsions and epilepsy, accompanied by strabismus and loss of consciousness, lasting 1 to 2 min, which occurred after a collision on the top of her head. She has been taking valproate (depakin) since then, bringing her seizures under control with an average of 1–2 minor epileptic events per year. At 3 years of age, an MRI of the brain showed no obvious changes in brain lesions (Figure 2B); however, she began to experience deterioration in motor function; she could not walk unaided, although unsteadily, until she was 4 years old. After that, her motor functions progressively regressed, and she relied on a wheelchair after 5 years of age. Her language skills also did not improve, and her speech became slurred at 3 years old. From the age of 6 years, her cognitive function appeared worse than before; she began to have hypomnesia, forgetting songs she used to remember. She developed psychiatric problems at 3 years old and gradually began crying frequently and exhibiting more severe signs, including screaming, poor sleep, and difficulty regulating her

TABLE 1 The Comparison of clinical findings in MLC.

Clinical findings of MLC1 reported previously	Clinical findings of the present patient (age of onset)	Clinical findings of the case with the same variant* (age of onset)
Macrocephaly/increasing HC	+(6 month)	+(3 month)
Brain MRI		
Subcortical cysts	–	+
Leukodystrophy	+	/
Cortical atrophy	–	/
Developmental delay	+	/
Motor function		
Independent walking	+(2 year)	+(2 year)
Ataxic gait	+	/
Motor deterioration	+(4 year)	+
Loss of ambulation	+(5 year)	+(5 year)
Speech		
First words	(1 year)	(1 year)
Speech deterioration	+(6 year)	/
Dysarthria	+(6 year)	/
Neurologic injuries		
Hypotonia/dystonia	+(6 month)	/
Pyramidal findings	+	/
Neuroregression	+	/
Seizures after head trauma(Focal epilepsy)	+(2.5 year)	+
Tremor	–	/
Choreoathetosis	–	/
Cognitive deterioration	+(6 year)	/
Emotional and behavioral problems	+(3 year)	+(4–5 year)
Hearing disorder	–	/
Visual impairment	–	/
Dysphagia	–	/
Absence of bladder control	–	/

"/", not available; *Patrono et al. (10).

emotions. She was prescribed olanzapine at 3 years of age, which reduced her crying to some extent. The parents also found ways to calm her, so they continued olanzapine treatment under the guidance of a psychiatrist. She had been undergoing regular rehabilitation training at a local rehabilitation center since the age of 5 years but to little avail. Electroencephalogram analysis at 8 years of age showed diffuse mixed slow-wave activity in the bilateral prefrontal, frontal, central, parietal, occipital, and temporal regions during awakening. Regrettably, as the child was emotional and unable to cooperate, valuable electroencephalogram data have not yet been collected, and she could not undergo a brain MRI again. Detailed information is provided in Figure 3; Table 1.

3.3. Analysis of the splice mutation in this family

A cerebral white matter disorder was suspected based on clinical features and MRI findings. To confirm the diagnosis of the proband, we screened for genetic mutations using a monogenic disorder panel associated with leukoencephalopathy.

A homozygous splice variant, NM_015166.4: [IVS2 + 1 delG], of *MLC1,* was identified in the proband (Figures 1A, 4A). These results were confirmed by Sanger sequencing, and the patient was verified to be homozygous for a mutation passed down from her parents and grandmothers (Figure 1A). None of the 100 Chinese normal controls harbored this mutation. This mutation was not found in the ClinVar database or reported in the literature, nor was it included in the healthy population (gnomAD, the 1,000 Genomes Project), local, or SNP databases. No other plausible candidate variants were consistent with the clinical phenotype of the patient.

"Deletion G" is in a classical splice recognition site, which can influence mRNA splicing, so the possibility of the disease being caused by a homozygous mutation cannot be ruled out, and no functional studies have confirmed the reliability of its pathogenicity. Therefore, we conducted further functional analyses by examining mRNA reverse transcription and predicting the protein structure. The cDNA of nuclear family members (parents and the proband) was obtained using RT-PCR. The cDNA amplicon sequence indicated that the mutation was responsible for the protein truncation of the *MLC1* gene after exon 2 (Figure 4B). The homozygous single-base deletion disrupts the normal donor splice site of intron 2, which inhibits splicing and causes an aberrant transcript that retains intron 2. A reading frame shift occurs at the codon from GGG to GGA, and the translation continues for five amino acids; finally, it is terminated early after reaching a premature stop codon (TGA; Figure 4B). The wild-type protein structures and of this mutation were predicted using Alphafold2, indicating that the mutation prematurely terminates the synthesis of the *MLC1* protein, preventing the formation of a normal three-dimensional protein structure as illustrated in Figure 4C. Consequently, this variant likely leads to a loss of function of *MLC1*.

3.4. Genetic counseling and prenatal diagnosis

Molecular genetic tests and functional analysis confirmed the pathogenicity of the *MLC1* variant IVS2 + 1 delG(PVS1 + PS3 + PM2) (11), and genetic counseling was performed to assess the risk of recurrence and provide guidance on fertility. We informed the couple that they had a 25% risk of having another child with abnormalities. The gravida received a molecular prenatal diagnosis by amniocentesis of DNA extracted in the 19th week of pregnancy, confirming that the fetus possessed the wild type of this site (Figure 5A). Therefore, we recommended the gravida continue the pregnancy. The following year, a healthy baby was born at full term (Figure 5B). The second child never showed similar symptoms and signs as his older sister, and all of his physical indicators were normal, including HC.

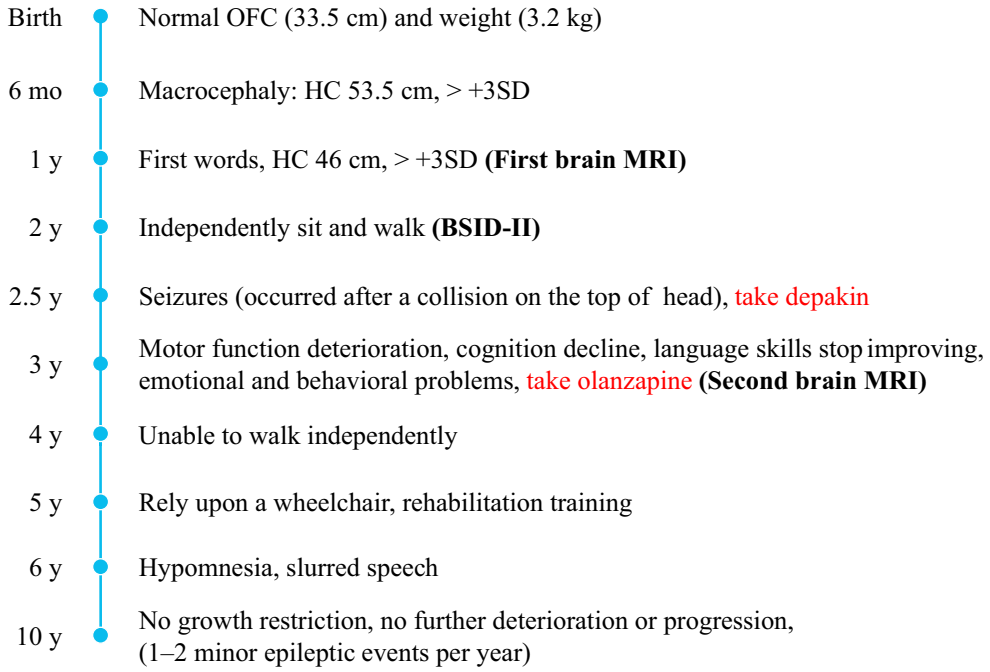

FIGURE 3
Timeline of clinical manifestations. Macrocephaly, spasticity, motor and cognitive regression, and psychiatric symptoms are the main clinical manifestations of the proband.

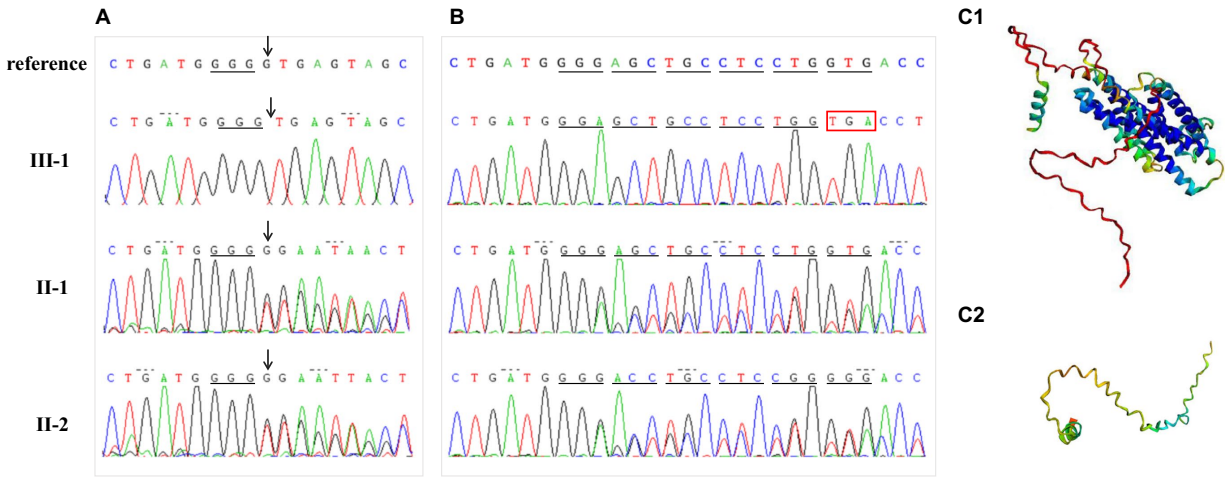

FIGURE 4
Mutation analysis. **(A)** Proband DNA sequencing (III-1) with an arrow pointing to the homozygous deletion (IVS2 + 1delG) of *MLC1*. Sequences of this mutation region in other family members (II-1, II-2) with an arrow pointing to heterozygous deletion. **(B)** Results of cDNA sequencing for the proband and her parents. Compared to normal protein translation, the homozygous single-base deletion (IVS2 + 1delG) changed the donor splice site, disrupted normal splicing, and caused a premature stop codon. **(C)** The protein structure was modeled by Alphafold2 in wild (C1) and mutant (C2) types, respectively.

4. Discussion

An increasing number of patients have been diagnosed with MLC globally, although the clinical manifestations of MLC vary greatly. Leukoencephalopathy is distinguished by the inconsistency between mild neurological findings and severe white matter abnormalities (3, 12–14). The patient exhibited typical clinical manifestations, such as a substantially increased HC, severely delayed motor development, and diffuse symmetrical white matter lesions according to brain MRI scans, which are summarized in Table 1.

The hallmark of MLC is the presence of subcortical cysts in the anterior temporal, frontal, or parietal regions (2, 15). Brain biopsies from a patient with MLC showed vacuolization of myelin (16), and the vacuoles were lined with myelin, representing intramyelinic

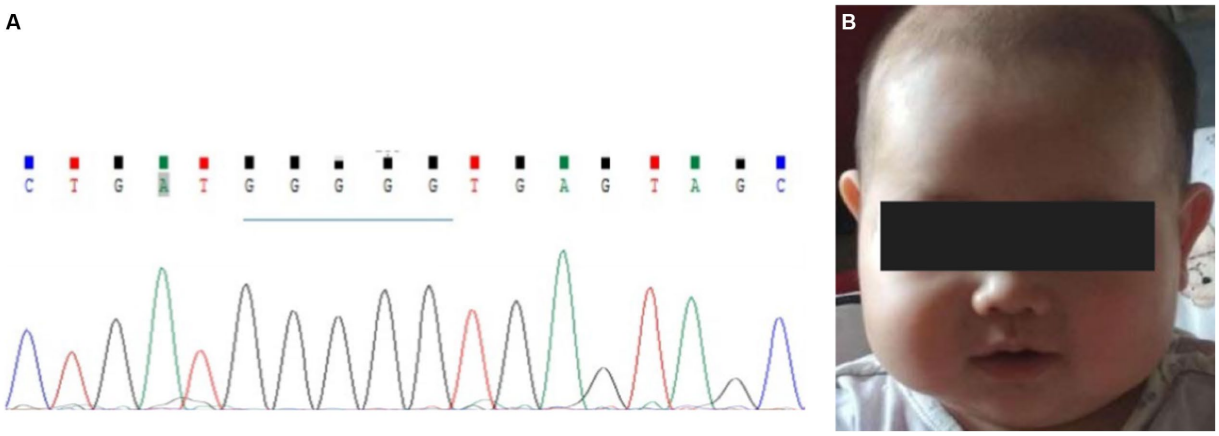

FIGURE 5
Prenatal diagnosis for the second child. **(A)** gDNA sequence of amniotic fluid cells. The arrow shows the position of the normal site, IVS2 + 1. **(B)** No abnormalities were found when the baby was approximately 10 months old.

edema, and no loss of myelin (17). Duarri et al. (18) established an *in vitro* MLC model in which *MLC1* was knocked down in primary astrocytes; reduced expression of *MLC1* resulted in the appearance of intracellular vacuoles, proposing that this vacuolization is associated with the loss of *MLC1*'s role in maintaining integrity. Interestingly, previously reported patients with *MLC1* mutations showed more subcortical cysts outside the temporal region than those with *HEPACAM* mutations (2, 19). However, the brain MRI of this proband was not entirely similar to those previously reported, as subcortical cysts were not found at the ages of 2 and 3 years. A previous study reported two sisters with compound heterozygous mutations (c. 393C > T and c. 823C > A) in *MLC1*, and subcortical cysts were not found in all sections (axial, coronal, sagittal image) of the brain MRI of the older sister (20), similar to the MRI findings of this patient. Mahmoud et al. reported manifold brain MRI findings, including mild cerebellar vermis hypoplasia and mild ventriculomegaly. Furthermore, inter and intrafamilial variability has been observed (19, 21), revealing that some unknown modifying factors can influence the phenotype. Thus, more studies are necessary on the specific functions of *MLC1* to verify the link between *MLC1* and subcortical cysts.

Macrocephaly is the most consistent and prominent feature observed in patients with MLC. The proband had a large HC (53.5 cm, > + 3SD) from 6 to 15 months of age. As seen in the HC curve of this proband (Figure 1C), the rapid early growth of the head, crossing the +3SD at approximately 6 months, was only followed a few months later (at approximately 1 year of age) by slow growth, which parallels the median curve. The change trend of the HC curve in the early stage was roughly consistent with that previously reported (12). Motor impairment is also one of the most common manifestations of MLC. The proband showed progressive deterioration of gait by her 4th year, and she finally had to rely on a wheelchair after the age of 5 years, although Patrono et al. observed a stationary course in patients who could not walk and showed no signs of deterioration (10, 21).

Epilepsy is a common feature in patients with MLC. Research has shown that the regulatory disorder of astrocytes in the homeostasis of ions and water leads to overexcitation of neural networks and seizures (22). The onset of epilepsy does not appear to depend on the number of cysts or the causative gene (21). This proband began to have generalized tonic–clonic seizures after 2 years of age, accompanied by strabismus and loss of consciousness, which were provoked by minor head trauma, as reported in the literature (23). She responded well to antiepileptic drugs and her seizures were controlled and reduced to an average of one to two minor epileptic episodes per year. Furthermore, mild-to-moderate developmental delays have been reported in patients with MLC of various ethnic backgrounds (3, 10, 12, 19, 24, 25). This proband experienced an obvious stagnation period in the development of her language skills and cognitive function, after which they retrogressed. The proband is currently 10 years old, her height and weight are within the normal range, and she has no growth restriction. However, it is unknown whether this situation will change after she enters puberty.

The non-specific clinical manifestations and imaging features of the proband suggested the possibility of leukodystrophy, which led to a bottleneck in her clinical diagnosis. It is a challenge to provide pregnant women with effective genetic counseling and an accurate risk assessment. Advances in molecular diagnostic tools have allowed us to identify the detailed underlying etiology of leukodystrophy and to increase the diagnostic yield (26). Therefore, we performed exome sequencing for the target gene panel associated with leukoencephalopathy. The *MLC1* mutation IVS2 + 1delG identified in this study is a homozygous mutation found in both parents with no consanguinity and is not a uniparental diploid. Although this mutation was recorded in the HGMD database as c.177 + 1delG (10, 27), the description of this mutation was indistinct in these two studies, and the effect of changes in RNA splicing was not confirmed by transcriptional studies. Therefore, in this study, for an accurate prenatal diagnosis, we analyzed the family cDNA of the mutant gene by RT-PCR and confirmed that the mutation caused changes in mRNA splicing. Splicing mutations can cause the retention of introns, complete skipping of exons, or the introduction of a new splice site within an exon or intron (28). This variant disrupted the donor splice site of intron 2, inhibited splicing, resulted in the retention of intron 2, and produced an aberrant transcript (Figure 4B). This variation in *MLC1* may produce a truncated protein without the normal eight transmembrane domains (6, 7) or induce degradation of mRNAs by nonsense-mediated mRNA decay, which was also indicated by the

protein structure predicted by Alphafold2. Having elucidated the function of this genetic variation, we performed a prenatal diagnosis of the fetus.

There is no cure for MLC, and treatment is primarily symptomatic. Bosch et al. injected an adeno-associated virus (AAV), encoding human *MLC1* under the control of a glial fibrillary acid protein promoter into the subarachnoid space of the cerebellum of *Mlc1* knockout mice (29). The expression of *MLC1* in the cerebellum significantly reduced myelin vacuolation at all ages in a dose-dependent manner. This study may provide patients with MLC with a potential therapeutic approach in the future.

In conclusion, we analyzed a variant of *MLC1* and confirmed that it is pathogenic, probably causing MLC. In addition, the clinical course of the patient and the findings of the brain MRI are detailed. Furthermore, we made a prenatal diagnosis for this family on the explicit basis of the proband. Our study provides additional information on the genotype and atypical phenotype of MLC1 and the prenatal diagnosis process, which is important for physicians providing genetic counseling and conducting prenatal diagnosis or preimplantation genetic tests for families. The information and clinical experience in this study could contribute to the field, and help other families with MLC make informed decisions about their reproductive options.

Data availability statement

The datasets presented in this article are not readily available because of ethical and privacy restrictions. Requests to access the datasets should be directed to the corresponding author.

Ethics statement

The studies involving human participants were reviewed and approved by the Medical Ethical Committees of the West China Second University Hospital, Sichuan University. Written informed consent to participate in this study was provided by the participants' legal guardian/next of kin. Written informed consent was obtained from the individual(s), and minor(s)' legal guardian/next of kin, for the publication of any potentially identifiable images or data included in this article.

Author contributions

XCh: Writing – original draft. HQ: Writing – review & editing. QY: Writing – review & editing. XCa: Writing – review & editing. TH: Writing – review & editing. XZ: Writing – review & editing.

Funding

This work was supported by a grant from the Sichuan Science and Technology Program (2022NSFSC0658).

Acknowledgments

We thank the family for their participation, which made this research possible.

Conflict of interest

The authors declare that the research was conducted in the absence of any commercial or financial relationships that could be construed as a potential conflict of interest.

The handling editor HS declared a shared affiliation with the authors at the time of review.

Publisher's note

References

1. López-Hernández T, Sirisi S, Capdevila-Nortes X, Montolio M, Fernández-Dueñas V, Scheper GC, et al. Molecular mechanisms of MLC1 and GLIALCAM mutations in megalencephalic leukoencephalopathy with subcortical cysts. *Hum Mol Genet*. (2011) 20:3266–77. doi: 10.1093/hmg/ddr238

2. van der Knaap MS, Boor I, Estevez R. Megalencephalic leukoencephalopathy with subcortical cysts: chronic white matter oedema due to a defect in brain ion and water homoeostasis. *Lancet Neurol*. (2012) 11:973–85. doi: 10.1016/S1474-4422(12)70192-8

3. van der Knaap MS, Barth PG, Stroink H, van Nieuwenhuizen O, Arts WFM, Hoogenraad F, et al. Leukoencephalopathy with swelling and a discrepantly mild clinical course in eight children. *Ann Neurol*. (1995) 37:324–34. doi: 10.1002/ana.410370308

4. Durand CM, Betancur C, Boeckers TM, Bockmann J, Chaste P, Fauchereau F, et al. Mutations in the gene encoding the synaptic scaffolding protein SHANK3 are associated with autism spectrum disorders. *Nat Genet*. (2007) 39:25–7. doi: 10.1038/ng1933

5. Nomura N, Miyajima N, Sazuka T, Tanaka A, Kawarabayasi Y, Sato S, et al. Prediction of the coding sequences of unidentified human genes. I. the coding sequences of 40 new genes (KIAA0001-KIAA0040) deduced by analysis of randomly sampled cDNA clones from human immature myeloid cell line KG-1. *DNA Res*. (1994) 1:27–35. doi: 10.1093/dnares/1.1.27

6. Lanciotti A, Brignone MS, Molinari P, Visentin S, de Nuccio C, Macchia G, et al. Megalencephalic leukoencephalopathy with subcortical cysts protein 1 functionally cooperates with the TRPV4 cation channel to activate the response of astrocytes to osmotic stress: dysregulation by pathological mutations. *Hum Mol Genet*. (2012) 21:2166–80. doi: 10.1093/hmg/dds032

7. Leegwater PA, Yuan BQ, van der Steen J, Mulders J, Könst AAM, Boor PKI, et al. Mutations of MLC1 (KIAA0027), encoding a putative membrane protein, cause megalencephalic leukoencephalopathy with subcortical cysts. *Am J Hum Genet*. (2001) 68:831–8. doi: 10.1086/319519

8. Liu J, Gao J, Jiang Y, et al. *Invasive prenatal diagnostic techniques: From theory to practice. 1st* ed. Beijing: People's Military Medical Press (2012). 9 p.

9. National Health Commission of the People's Republic of China. Growth standard for children under 7 years of age. (2022).

10. Patrono C, di Giacinto G, Eymard-Pierre E, Santorelli FM, Rodriguez D, de Stefano N, et al. Genetic heterogeneity of megalencephalic leukoencephalopathy and subcortical cysts. *Neurology*. (2003) 61:534–7. doi: 10.1212/01.WNL.0000076184.21183.CA

11. Richards S, Aziz N, Bale S, Bick D, das S, Gastier-Foster J, et al. Standards and guidelines for the interpretation of sequence variants: a joint consensus

recommendation of the American College of Medical Genetics and Genomics and the Association for Molecular Pathology. *Genet Med*. (2015) 17:405–24. doi: 10.1038/gim.2015.30

12. Cao B, Yan H, Guo M, Xie H, Wu Y, Gu Q, et al. Ten novel mutations in Chinese patients with megalencephalic leukoencephalopathy with subcortical cysts and a long-term follow-up research. *PLoS One*. (2016) 11:e0157258. doi: 10.1371/journal.pone.0157258

13. van der Knaap MS, Lai V, Köhler W, Salih MA, Fonseca MJ, Benke TA, et al. Megalencephalic leukoencephalopathy with cysts without MLC1 defect. *Ann Neurol*. (2010) 67:NA–7. doi: 10.1002/ana.21980

14. van der Knaap MS, Valk J, Barth PG, Smit LME, van Engelen BGM, Donati PT. Leukoencephalopathy with swelling in children and adolescents: MRI patterns and differential diagnosis. *Neuroradiology*. (1995) 37:679–86. doi: 10.1007/BF00593394

15. van der Knaap MS, Bugiani M. Leukodystrophies: a proposed classification system based on pathological changes and pathogenetic mechanisms. *Acta Neuropathol*. (2017) 134:351–82. doi: 10.1007/s00401-017-1739-1

16. van der Knaap MS, Barth PG, Vrensen GF, Valk J. Histopathology of an infantile-onset spongiform leukoencephalopathy with a discrepantly mild clinical course. *Acta Neuropathol*. (1996) 92:206–12. doi: 10.1007/s004010050510

17. van der Knaap MS, Bugiani M. Leukodystrophies - much more than just diseases of myelin. *Nat Rev Neurol*. (2018) 14:747–8. doi: 10.1038/s41582-018-0093-9

18. Duarri A, Lopez de Heredia M, Capdevila-Nortes X, Ridder MC, Montolio M, López-Hernández T, et al. Knockdown of MLC1 in primary astrocytes causes cell vacuolation: a MLC disease cell model. *Neurobiol Dis*. (2011) 43:228–38. doi: 10.1016/j.nbd.2011.03.015

19. Mahmoud IG, Mahmoud M, Refaat M, Girgis M, Waked N, el Badawy A, et al. Clinical, neuroimaging, and genetic characteristics of megalencephalic leukoencephalopathy with subcortical cysts in Egyptian patients. *Pediatr Neurol*. (2014) 50:140–8. doi: 10.1016/j.pediatrneurol.2013.10.008

20. Masuda T, Ueda M, Ueyama H, Shimada S, Ishizaki M, Imamura S, et al. Megalencephalic leukoencephalopathy with subcortical cysts caused by compound heterozygous mutations in MLC1, in patients with and without subcortical cysts in the brain. *J Neurol Sci*. (2015) 351:211–3. doi: 10.1016/j.jns.2015.03.010

21. Abdel-Salam GM, Abdel-Hamid MS, Ismail SI, Hosny H, Omar T, Effat L, et al. Megalencephalic leukoencephalopathy with cysts in twelve Egyptian patients: novel mutations in MLC1 and HEPACAM and a founder effect. *Metab Brain Dis*. (2016) 31:1171–9. doi: 10.1007/s11011-016-9861-7

22. Dubey M, Brouwers E, Hamilton EMC, Stiedl O, Bugiani M, Koch H, et al. Seizures and disturbed brain potassium dynamics in the leukodystrophy megalencephalic leukoencephalopathy with subcortical cysts. *Ann Neurol*. (2018) 83:636–49. doi: 10.1002/ana.25190

23. Pascual-Castroviejo I, van der Knaap MS, Pronk JC, García-Segura JM, Gutiérrez-Molina M, Pascual-Pascual SI. Vacuolating megalencephalic leukoencephalopathy: 24 year follow-up of two siblings. *Neurologia*. (2005) 20:33–40.

24. Gorospe JR, Singhal BS, Kainu T, Wu F, Stephan D, Trent J, et al. Indian Agarwal megalencephalic leukodystrophy with cysts is caused by a common MLC1 mutation. *Neurology*. (2004) 62:878–82. doi: 10.1212/01.WNL.0000115106.88813.5B

25. Tinsa F, Farid O, Douira W, Rodriguez D, Burglen L, Boussetta K, et al. Megalencephalic leukoencephalopathy with subcortical cysts in a Tunisian boy. *J Child Neurol*. (2009) 24:87–9. doi: 10.1177/0883073808324021

26. Ashrafi MR, Amanat M, Garshasbi M, Kameli R, Nilipour Y, Heidari M, et al. An update on clinical, pathological, diagnostic, and therapeutic perspectives of childhood leukodystrophies. *Expert Rev Neurother*. (2020) 20:65–84. doi: 10.1080/14737175.2020.1699060

27. Chen X, Qu H, Yu T, Luo R. Identification of a novel MLC1 mutation in a Chinese patient affected with megalencephalic leukoencephalopathy with subcortical cysts. *Zhonghua Yi Xue Yi Chuan Xue Za Zhi*. (2016) 33:316–9. doi: 10.3760/cma.j.issn.1003-9406.2016.03.008

28. Baralle D, Baralle M. Splicing in action: assessing disease causing sequence changes. *J Med Genet*. (2005) 42:737–48. doi: 10.1136/jmg.2004.029538

29. Bosch A, Estevez R. Megalencephalic leukoencephalopathy: insights into pathophysiology and perspectives for therapy. *Front Cell Neurosci*. (2020) 14:627887. doi: 10.3389/fncel.2020.627887

frontiers | Frontiers in Neurology

TYPE Case Report
PUBLISHED 01 December 2023
DOI 10.3389/fneur.2023.1292320

OPEN ACCESS

EDITED BY
Ryan Davis,
Kolling Institute, Australia

REVIEWED BY
Laura Mauring,
Tartu University Hospital, Estonia
Valerio Carelli,
University of Bologna, Italy

*CORRESPONDENCE
Rita Horvath
✉ rh732@medschl.cam.ac.uk

†These authors have contributed equally to this work

RECEIVED 11 September 2023
ACCEPTED 03 November 2023
PUBLISHED 01 December 2023

CITATION
Major TC, Arany ES, Schon K, Simo M, Karcagi V, van den Ameele J, Yu Wai Man P, Chinnery PF, Olimpio C and Horvath R (2023) Case report: Mutations in *DNAJC30* causing autosomal recessive Leber hereditary optic neuropathy are common amongst Eastern European individuals. *Front. Neurol.* 14:1292320. doi: 10.3389/fneur.2023.1292320

Case report: Mutations in *DNAJC30* causing autosomal recessive Leber hereditary optic neuropathy are common amongst Eastern European individuals

Toby Charles Major[1†], Eszter Sara Arany[1†], Katherine Schon[2,3], Magdolna Simo[4], Veronika Karcagi[5], Jelle van den Ameele[2], Patrick Yu Wai Man[2,6,7], Patrick F. Chinnery[2], Catarina Olimpio[2,3] and Rita Horvath[2*]

[1]School of Clinical Medicine, University of Cambridge, Cambridge, United Kingdom, [2]Department of Clinical Neurosciences, School of Clinical Medicine, University of Cambridge, Cambridge, United Kingdom, [3]Department of Clinical Genetics, East Anglian Medical Genetics Service, Addenbrooke's Hospital, Cambridge, United Kingdom, [4]University Clinic of Neurology, Semmelweis University, Budapest, Hungary, [5]Istenhegyi Genetic Diagnostic Center, Budapest, Hungary, [6]NIHR Biomedical Research Centre, Moorfields Eye Hospital & UCL Institute of Ophthalmology, London, United Kingdom, [7]Cambridge Eye Unit, Addenbrooke's Hospital, Cambridge University Hospitals, Cambridge, United Kingdom

Background: Leber Hereditary Optic Neuropathy (LHON) is the most common inherited mitochondrial disease characterized by bilateral, painless, subacute visual loss with a peak age of onset in the second to third decade. Historically, LHON was thought to be exclusively maternally inherited due to mutations in mitochondrial DNA (mtDNA); however, recent studies have identified an autosomal recessive form of LHON (arLHON) caused by point mutations in the nuclear gene, *DNAJC30*.

Case Presentations: In this study, we report the cases of three Eastern European individuals presenting with bilateral painless visual loss, one of whom was also exhibiting motor symptoms. After a several-year-long diagnostic journey, all three patients were found to carry the homozygous c.152A>G (p.Tyr51Cys) mutation in *DNAJC30*. This has been identified as the most common arLHON pathogenic variant and has been shown to exhibit a significant founder effect amongst Eastern European individuals.

Conclusion: This finding adds to the growing cohort of patients with arLHON and demonstrates the importance of *DNAJC30* screening in patients with molecularly undiagnosed LHON, particularly in Eastern European individuals. It is of heightened translational significance as patients diagnosed with arLHON exhibit a better prognosis and response to therapeutic treatment with the co-enzyme Q10 analog idebenone.

KEYWORDS

Leber hereditary optic neuropathy (LHON), mitochondrial LHON (mtLHON), autosomal recessive LHON (arLHON), DNA-J heat shock protein family (Hsp40) member C30 (DNAJC30), c.152A>G (p.Tyr51Cys), recessive optic neuropathy, idebenone

Introduction

Leber hereditary optic neuropathy

Leber Hereditary Optic Neuropathy (LHON) is the most common disease caused by mutations in mitochondrial DNA (mtDNA) and typically manifests in the second or third decade of life (1). LHON is characterized by acute or subacute bilateral painless visual loss, often accompanied by dyschromatopsia and central or centrocecal scotomas (1, 2). The penetrance of LHON does not appear to be related to the mitochondrial mutation load; however, the incidence of LHON manifestation is 3–5 times higher in male individuals (3, 4), which may be attributable to lifestyle and hormonal factors (3–6).

Mitochondrial LHON

The majority of LHON cases, approximately 90–95%, are caused by mutations in mtDNA that are maternally inherited. This mitochondrial form of LHON (mtLHON) is most commonly associated with one of three mutations, in order of frequency: m.11778G>A (p.Arg340His) in MT-ND4, m.14484T>C (p.Met64Val) in MT-ND6, and m.3460G>A (p.Ala52Thr) in MT-ND1 (1, 7). In addition to these, 30 other rare variants in mtDNA are known to be associated with the disease (8).

mtLHON is thought to occur due to dysfunction in complex I (CI) of the mitochondrial electron transport chain, which leads to decreased adenosine triphosphate (ATP) synthesis and the increased production of reactive oxygen species (ROS). Damage to cellular components caused by ROS generation as well as the increased energy demands of the retinal ganglion cells (RGCs) renders them particularly vulnerable to declining levels of ATP, which is then thought to culminate in cellular death and axonal degeneration (1, 7).

The prognosis of mtLHON can be improved by treatment with the coenzyme Q10 analog idebenone, which has recently been approved for use in patients with LHON in the United Kingdom (9). Idebenone facilitates the bypass of dysfunctional CI, thereby restoring ATP synthesis and increasing energy availability to the RGCs, thus improving visual symptoms (10–13). For reasons not yet understood, spontaneous visual recovery can also occur in some patients (14, 15).

Autosomal recessive LHON

More recently, a growing cohort of patients have been identified with an autosomal recessive form of LHON (arLHON). These patients present with similar visual symptoms as are seen in mtLHON (16) and show the same male predominance pattern (8.5:1 male:female ratio) (17). The majority of arLHON cases can be attributed to point mutations in the nuclear gene *DNAJC30* (16), but a number of other nuclear genes, including *NDUFS2* (18), *NDUFA12* (19), *MCAT* (20), and MECR (21), have also been implicated.

To date, there have been six reported pathogenic variants in *DNAJC30* associated with arLHON. These include three missense variants c.152A>G (p.Tyr51Cys), c.232C>T (p.Pro78Ser) (16), and c.302T>A (p.Leu101Gln) (16), a nonsense variant c.610G>T (p.Glu204*), a 3 bp in-frame deletion c.230_232del (p.His77del), and a frameshift variant c.130_131del (p.Ser44ValfsTer8) (22). Accounting for ≥90% of these cases is the c.152A>G (p.Tyr51Cys) point mutation. This specific mutation has been shown to exhibit a strong founder effect amongst individuals of Eastern European descent (16, 23) and is thought to have arisen from a common ancestor around 85 generations ago. In addition to this, more recent data have suggested that this mutation is also more prevalent than predicted in other European populations, including Central Europeans (24) and Estonians (25).

Although arLHON-causing mutations are less common than the mitochondrial variants as a whole, the individual prevalence of the c.152A>G (p.Tyr51Cys) variant in *DNAJC30* is not far below that of the m.14484T>C (p.Met64Val) in the MT-ND6 mutation causing mtLHON (24). In addition, a retrospective study has suggested that variants in *DNAJC30* can account for up to 7.7% of clinically apparent LHON (24). Aside from arLHON, mutations in *DNAJC30* have also been found in patients with Leigh syndrome (26) and in one family who were exhibiting a movement disorder phenotype (22).

The largest cohort of investigated patients and published case studies suggest that arLHON may have subtle but distinct clinical features compared to mtLHON. arLHON is likely to present at a younger age (24, 27), with a shorter interval between the onset of symptoms in both eyes (24) compared to mtLHON. Furthermore, arLHON patients may have a more favorable prognosis (24, 27) and have been shown to exhibit a better response to idebenone (17, 28).

The *DNAJC30* gene encodes a chaperone protein mainly expressed in neurons, which has been shown to interact with multiple components of the electron transport chain. The protein is thought to be involved in the regulation of CI by promoting the exchange of CI subunits, which have been exposed to higher levels of oxidative damage in order to maintain a high-functioning state of CI (16). In addition, it has been shown to interact with the H^+-loading component of complex V (29). Whilst there is still some discussion about the prevalent function of *DNAJC30*, the impaired assembly, maintenance, and turnover of CI are all thought to contribute to the observed arLHON phenotype (16) in patients with *DNAJC30* mutations.

Here, we present a case report of three patients from Eastern Europe who were found to have homozygous pathogenic variants in *DNAJC30*. All patients exhibited symptoms of LHON, and one of them also displayed a movement disorder phenotype.

Case presentations

Patient 1

A 35-year-old male Polish patient presented with bilateral painless visual loss that had developed over a 1-month period 2 years prior. He had also developed diplopia and gait disturbances. He was born in Poland to non-consanguineous parents before

moving to the United Kingdom. There was no family history of similar symptoms, and he had one younger, healthy female sibling.

On examination, he was found to have reduced bilateral visual acuity, ophthalmoparesis, diplopia on the side gaze, and a right-sided nystagmus. He was also noted to exhibit mild sensorineural hearing loss. A peripheral neurological examination found mild gait ataxia and mild muscle weakness in the upper and lower limbs that were worse proximally. Deep tendon reflexes were present but mildly reduced with normal ankle jerks and down-going plantar reflexes. Tandem gait was difficult, and the patient exhibited a mildly positive Romberg sign. There was no evidence of dysarthria, dysmetria, or dysdiadochokinesia.

Prior investigations had concluded that the patient had severe bilateral optic atrophy with an almost total absence of retinal ganglion cells in the macula of both eyes (Figure 1). A contrast-enhanced brain MRI revealed symmetrical enhancements of the posterior basal ganglia, which raised the suspicion of mitochondrial disease (Figure 2A).

Ischemic vascular, compressive, and acquired nutritional causes of bilateral visual loss were thoroughly investigated and ruled out based on brain imaging, blood work, and thorough history-taking and examination. The patient was negative for both aquaporin 4 (AQP-4) antibodies and myelin oligodendrocyte glycoprotein (MOG) antibodies. CSF analysis was unremarkable with normal lactate levels, and no demyelinating lesions were identified. The patient was also negative for anti-treponemal antibodies.

Carbon monoxide poisoning was also investigated, as this is a known cause of visual disturbance and increased T2-weighted MRI signal intensity in the posterior basal ganglia. However, this was ruled out after the patient's boiler was assessed by a gas service engineer, who found no carbon monoxide or other toxic fume production.

Hereditary causes of optic atrophy were also investigated. The patient was negative for the three most common mtLHON-causing mutations as well as for another 63 known hereditary optic atrophy-causing mutations across mitochondrial and autosomal genes, which were assessed using the NHS National Genomic Test Directory R41 Gene Panel. At the time, *DNAJC30* was not included in this panel. Given our patient's demographics, we decided to sequence a locus of his DNAJC30 gene known to contain the site of the c.152A>G (p.Tyr51Cys) mutation. Sequencing using the Sanger method revealed that the patient was homozygous for this pathogenic variant, confirming the diagnosis of arLHON.

At follow-up in the neurogenetics clinic, his symptoms had largely remained the same, with some minor improvement noted in his diplopia and tandem gait. Importantly, for this patient, the confirmation of his diagnosis allowed us to recommend treatment with idebenone. We were also able to offer genetic counseling to both the patient and his sister, as well as additional screening for her and her children to investigate further at-risk relatives.

Although idebenone (Raxone) was approved by the European Medicines Agency for the treatment of LHON, it has not been approved for reimbursement by NHS England (9). Therefore, it was not possible to commence the patient on idebenone, and he was unable to self-fund the treatment. At the last follow-up, the patient's visual acuity had improved spontaneously to 6/18 in his right eye and 6/60 in his left eye. His motor symptoms had not changed.

Patient 2

A 49-year-old Hungarian woman presented to the clinic with bilateral painless visual loss that had begun 3 years prior. Her symptoms developed over a 3-month period, starting with involvement of the right eye before progressing to involve the left eye 2 months later. She had no other neurological symptoms, and there was no relevant family history.

On examination, she had bilaterally reduced visual acuity of 0.01 and 0.02 in the right and left eye, respectively. Her pupils were reactive, and there was no ophthalmoparesis or nystagmus. A full neurological examination found no additional neurological deficits.

Goldmann perimetry and visual evoked potentials testing concluded that the patient was suffering from severe bilateral optic atrophy with a large centrocecal scotoma extending upwards, temporally, and downwards beyond the blind spot and center in the right eye and a scotoma affecting the lower center and extending downward from it in the left eye.

Multiple contrast-enhanced MRIs indicated T2 signal enhancement with contrast accumulation in the right optic nerve and a similar but smaller signal enhancement on the left side, consistent with inflammation. On repeated imaging, contrast material accumulation resolved, but signal enhancement along the right optic nerve and tracts became more marked (Figure 2B). There were also some small, non-specific, hyper-enhancing lesions present in subcortical, intracerebral locations (multiple in the corona radiata and one in the cerebellum), reported as small ischemic lesions, probably not contributing to the patient's symptoms (Figure 2C). CSF protein levels were normal, as were the cell counts. CSF immunological tests were also normal, including AQP-4 and MOG antibodies. Treponema, HIV, Borrellia, HCV serology, and sACE levels were normal, and a thrombophilia panel was unremarkable.

Although no antibodies were identified in her case, inflammatory causes remained one of the top differential diagnoses, given the MRI findings and the initial clinical progression that were consistent with neuromyelitis optica (NMO). Initially, she was started on steroid treatment, which did not cause any change in her symptoms. She was commenced on a regular rituximab infusion, which did not cause any immediate improvement; however, she reported improved visual acuity after 2 years. The significant delay in symptom improvement after prolonged immunosuppressive therapy with steroids and rituximab made an inflammatory cause very unlikely.

This led to the consideration of hereditary causes of optic atrophy. The patient's mitochondrial DNA sample was negative for m.11778G>A (p.Arg340His) in MT-ND4, m.3460G>A (p.Ala52Thr) in MT-ND1, and m.14484T>C (p.Met64Val) in MT-ND6.

Prior to confirmation of the genetic diagnosis, this patient received genetic counseling, and her treatment was commenced by the clinical team in Hungary. Akin to the situation in the United Kingdom, there is currently no reimbursement offered by the national health insurance system in Hungary for idebenone therapy in LHON. She was however able to self-fund the treatment comprising 200 mg of coenzyme Q10 and 450 mg of idebenone. At the last follow-up appointment, the patient's disease was stable with

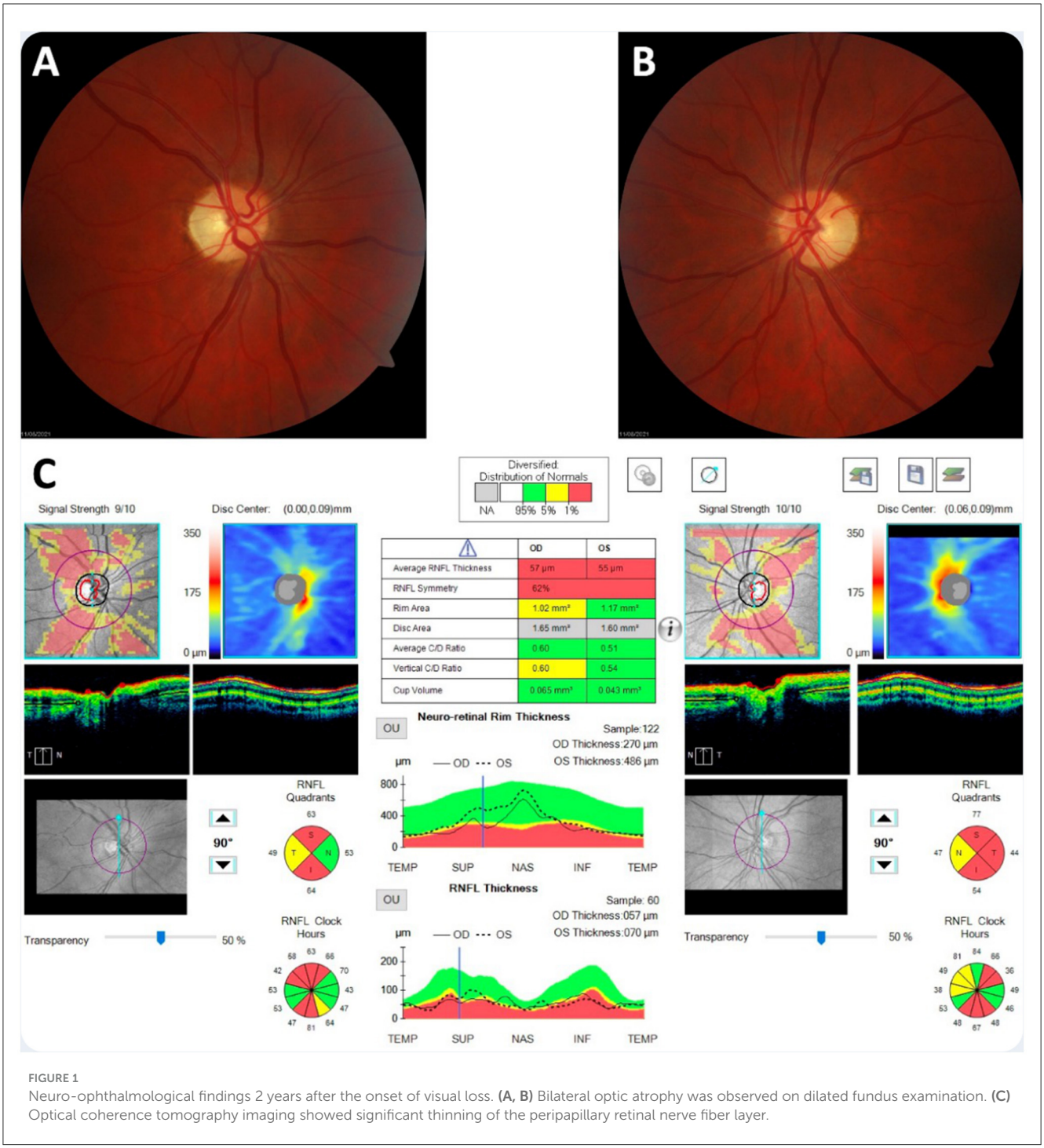

FIGURE 1
Neuro-ophthalmological findings 2 years after the onset of visual loss. **(A, B)** Bilateral optic atrophy was observed on dilated fundus examination. **(C)** Optical coherence tomography imaging showed significant thinning of the peripapillary retinal nerve fiber layer.

no evidence of progression. Her visual acuity was slightly improved in the right eye (0.05) and significantly improved in the left eye (0.8). Sanger sequencing in our lab later confirmed that the patient is homozygous for the c.152A>G (p.Tyr51Cys) pathogenic variant.

Patient 3

A 45-year-old Polish man, living in the United Kingdom, presented with sequential painless visual loss at the age of 31. His symptoms developed over a 4-month period, starting with involvement of the left eye, followed by involvement of the right eye 3 months later. He had a history of migraines but no other neurological symptoms. There was no relevant family history, and his parents were non-consanguineous. He smoked cigarettes from the age of 17 to 31 (1 packet a day) and drank beer at the weekend. He had a near-complete loss of central and color vision and was severely sight impaired. Routine investigation, including brain MRI, testing for common LHON mutations, POLG sequencing, and OPA1 sequencing, did not reveal a cause. A quadriceps muscle

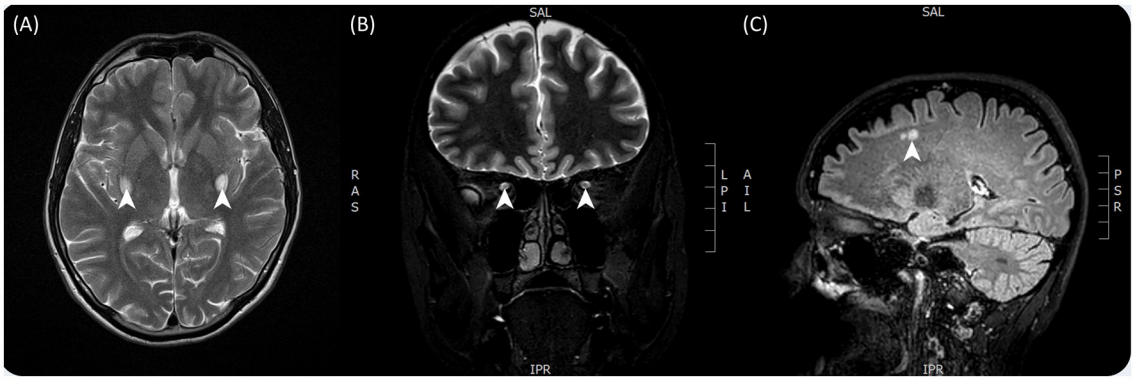

FIGURE 2
T2-weighted contrast-enhanced brain MRI images taken from both patients. **(A)** Taken from patient 1 and showing bilateral enhancements of the posterior basal ganglia in particular the putamen. **(B)** Taken from patient 2 and showing hyperintensity of the optic tracts bilaterally. **(C)** Taken from patient 2 and showing hyperintense lesions in the subcortical layer of the cerebrum.

biopsy showed one COX-deficient fiber and no ragged red fibers. Whole mtDNA genome sequencing was normal. He was recruited for the 100,000 Genomes Project. The optic neuropathy panel applied did not include *DNAJC30*, so he did not initially receive a diagnosis through the Genomic Medicine Centre. However, his homozygous pathogenic variant was discovered by researchers in the research environment and fed back to his clinical team.

Examination at the age of 45 showed severe visual impairment, with him being able to see only hand motions. He had bilateral afferent pupillary defects and scored 0/15 bilaterally on the Ishihara testing. He had pale optic disks bilaterally. Repeated optical coherence tomography examinations showed stable optic atrophy. He was taking Coenzyme Q10 400 mg BD. He was aware of idebenone but was unable to self-fund the treatment.

Materials and methods

DNAJC30 sequencing

For Patients 1 and 2, DNA was extracted from stored blood samples. The locus known to contain the site of the c.152A>G (p.Tyr51Cys) mutation was amplified using the polymerase chain reaction. The sequences of the forward and reverse primers used for amplification were 5′-GCTGTTACCTTGGAGGTTGC-3′ and 5′-AAGTTGAACATCGTGCGGTTG-3′, respectively. Sanger sequencing was then used to sequence the amplified fragment and interrogate the sequence for the presence of the c.152A>G mutation.

100,000 genomes project

Patient 3 was identified based on data collected as part of the 100,000 Genomes Project. This project recruited participants with genetically undiagnosed rare diseases between 2015 and 2018 through Genomic Medicine Centres in the United Kingdom (30). Patient 3 was recruited under the category of inherited optic neuropathies. DNA extraction, sequencing, alignment, and variant calling were performed as previously described (31, 32). A virtual gene panel for inherited optic neuropathies was applied (33). Variants were classified into four "tier" groups according to the probability of being causative (31, 32). We analyzed tier 1–3 variants in the *DNAJC30* gene and identified that Patient 3 had a homozygous pathogenic variant. We contacted his clinician about the diagnosis and offered to see the patient in the context of mitochondrial clinical research studies.

Results

All three patients were identified as homozygotes for the c.152A>G mutation in *DNAJC30*. The region of the *DNAJC30* gene harboring the mutation is shown in Figure 3.

Discussion

In this study, we report the cases of three Eastern European individuals with arLHON associated with the c.152A>G (p.Tyr51Cys) pathogenic variant in *DNAJC30*. This adds to the growing cohort of patients with arLHON and provides further evidence for the hypothesis of a significant founder effect associated with this variant. Interestingly, we find additional clinical evidence of motor involvement associated with the disease, with one of our patients exhibiting gait ataxia and proximal muscle weakness characteristic of Leigh syndrome. This may in future form part of the spectrum of clinical features that distinguish arLHON from mtLHON, alongside its apparent earlier age of onset and greater therapeutic response to idebenone. The main clinical symptom exhibited by Patient 1 was optic neuropathy; however, neurological examination detected some other subtle signs. The recent literature on potential genetic modifiers in nuclear-encoded complex I-related genes in patients with more severe and complex LHON raises the possibility of such an additional modifier in this patient. We could not detect any additional variant on the optic neuropathy panel containing NDUFA12, but we cannot exclude variants in other nuclear complex I genes (23). Identification of

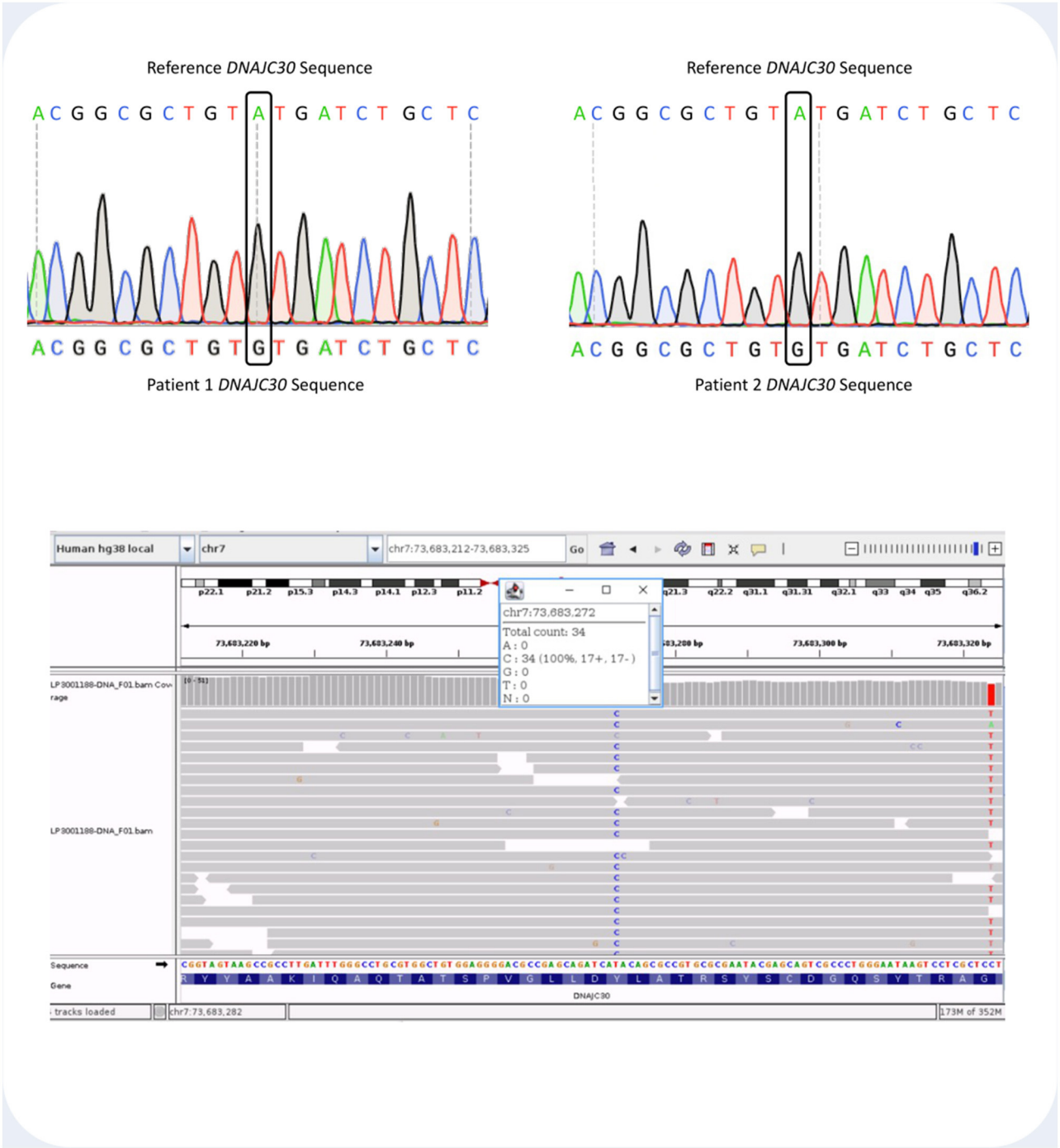

FIGURE 3
(Top) Sanger sequencing histogram readout showing the DNAJC30 loci containing the site of the c.152A>G (p.Tyr51Cys) mutation in Patient 1 and 2. Above each histogram there is the DNAJC30 reference sequence. **(Bottom)** Integrative Genome Viewer (IGV) screenshot showing the aligned sequencing reads and the count details for Patient 3. The homozygous T>C variant at genomic coordinates GRCh38 chr7-73,683,272 represents the c.152A>G DNAJC30 pathogenic variant.

the DNAJC30 pathogenic variant in further patients may elucidate if these symptoms form part of the spectrum of clinical features in arLHON.

Recognizing arLHON remains a challenge, as the male predominance and low penetrance of the disease reduce the likelihood of symptom manifestation. This could mean that families harboring arLHON-associated *DNAJC30* mutations may go undetected for several generations. In addition, with the differential diagnosis of optic atrophy remaining wide, there are several different etiologies to consider, such as neuromyelitis optica, carbon monoxide poisoning, and infectious or vascular causes. These cases emphasize the importance of considering arLHON in

patients with features of LHON but for whom genetic testing is not possible or has so far proved inconclusive. This is of heightened significance in individuals of Eastern European descent presenting with subacute, bilateral painless visual loss.

Similarly, the cases reported here strengthen the argument to include *DNAJC30* testing as part of the diagnostic work-up in patients presenting with bilateral optic atrophy/neuropathy. Until recently (March 2023), the NHS National Genomic Test Directory did not include testing of *DNAJC30* as part of its R41 (Optic Neuropathy) Gene Panel. Furthermore, despite this recent progress in testing, it still appears difficult for patients in the United Kingdom with arLHON to access idebenone treatment on the NHS as funding is not currently in place for the drug. Given the good responsiveness of arLHON to idebenone therapy compared with mtLHON, combined with the potential for timely intervention to prevent significant visual loss, action should be taken to make this treatment available. Similarly, *DNAJC30* genetic testing should be adopted wherever possible, especially in Europe and the United States, which have a large population of patients of Eastern European descent.

Further research may clarify the significance of the other nuclear genes (*NDUFS2, NDUFA12, MCAT*, and *MECR*) involved in CI assembly, stability, and fatty acid biosynthesis in the pathogenesis and prognosis of painless visual loss.

Data availability statement

The datasets presented in this article are not readily available because of ethical and privacy restrictions. Requests to access the datasets should be directed to the corresponding author.

Ethics statement

Ethical review and approval was not required for the study on human participants in accordance with the local legislation and institutional requirements. The human samples used in this study were acquired from a by- product of routine care or industry. All patients gave written informed consent for the publication of this study.

Author contributions

TM: Data curation, Formal analysis, Investigation, Methodology, Writing—original draft, Writing—review & editing. EA: Investigation, Writing—original draft, Writing—review & editing. KS: Data curation, Investigation, Methodology, Writing—review & editing. MS: Data curation, Writing—review & editing. VK: Data curation, Writing—review & editing. JA: Writing—review & editing. PY: Data curation, Resources, Writing—review & editing. PC: Supervision, Writing - review & editing. CO: Writing—review & editing. RH: Conceptualization, Data curation, Funding acquisition, Investigation, Methodology, Resources, Supervision, Writing—review & editing.

Funding

The author(s) declare financial support was received for the research, authorship, and/or publication of this article. RH was a Wellcome Trust Investigator (109915/Z/15/Z), who receives support from the Medical Research Council (UK) (MR/V009346/1), the Addenbrookes Charitable Trust (G100142), the Evelyn Trust, the Stoneygate Trust, the Lily Foundation, Action for AT, and an MRC strategic award to establish an International Centre for Genomic Medicine in Neuromuscular Diseases (ICGNMD) MR/S005021/1. This research was supported by the NIHR Cambridge Biomedical Research Centre (BRC-1215-20014). The National Genomic Research Library was funded by the National Institute for Health Research and NHS England. The Wellcome Trust, Cancer Research UK, and the Medical Research Council have also funded the research infrastructure. JA is supported by a Wellcome Clinical Research Career Development Fellowship (219615/Z/19/Z).

Acknowledgments

This research was made possible through access to data in the National Genomic Research Library, which is managed by Genomics England Limited (a wholly-owned company of the Department of Health and Social Care). The National Genomic Research Library holds data provided by patients and collected by the NHS as part of their care and data collected as part of their participation in research.

Conflict of interest

The authors declare that the research was conducted in the absence of any commercial or financial relationships that could be construed as a potential conflict of interest.

Publisher's note

Author disclaimer

The views expressed are those of the authors and not necessarily those of the NIHR or the Department of Health and Social Care. RH was part of the PROSPAX consortium under the frame of EJP RD, the European Joint Programme on Rare Diseases, under the EJP RD COFUND-EJP N°825575.

References

1. Amore G, Romagnoli M, Carbonelli M, Barboni P, Carelli V, La Morgia C. Therapeutic options in hereditary optic neuropathies. *Drugs.* (2021) 81:57–86. doi: 10.1007/s40265-020-01428-3

2. La Morgia C, Carbonelli M, Barboni P, Sadun AA, Carelli V. Medical management of hereditary optic neuropathies. *Front Neurol.* (2014) 5:141. doi: 10.3389/fneur.2014.00141

3. Carelli V, d'Adamo P, Valentino MC, La Morgia C, Ross-Cisneros FN, Caporali L, et al. Parsing the differences in affected with LHON: genetic versus environmental triggers of disease conversion. *Brain.* (2016) 139:e17. doi: 10.1093/brain/awv339

4. Giordano C, Montopoli M, Perli E, Orlandi M, Fantin M, Ross-Cisneros FN, et al. Oestrogens ameliorate mitochondrial dysfunction in Leber's hereditary optic neuropathy. *Brain.* (2011) 134:220–234. doi: 10.1093/brain/awq276

5. Shankar SP, Fingert JH, Carelli V, Valentino ML, King TM, Daiger SP, et al. Evidence for a novel X-linked modifier locus for leber hereditary optic neuropathy. *Ophthal Genet.* (2008) 29:17–24. doi: 10.1080/13816810701867607

6. Yu J, Liang X, Ji Y, Ai C, Liu J, Zhu L, et al. PRICKLE3 linked to ATPase biogenesis manifested Leber's hereditary optic neuropathy. *J Clin Invest.* (2020) 130:4935–46. doi: 10.1172/JCI134965

7. Yu-Wai-Man P, Votruba M, Burté F, La Morgia C, Barboni P, Carelli V. A neurodegenerative perspective on mitochondrial optic neuropathies. *Acta Neuropathol.* (2016) 132:789–806. doi: 10.1007/s00401-016-1625-2

8. Yu-Wai-Man P, Griffiths PG, Chinnery PF. Mitochondrial optic neuropathies – Disease mechanisms and therapeutic strategies. *Prog Retin Eye Res.* (2011) 30:81–114. doi: 10.1016/j.preteyeres.2010.11.002

9. National Health Service England (NHSE). *Clinical Commissioning Policy: Idebenone for Treating People Over 12 Years of Age With Leber's Hereditary Optic Neuropathy NHS England Reference: 200401P 2 Prepared by the National Institute for Health and Care Excellence (NICE) Commissioning Support Programme*. National Health Service England (NHSE) (2020).

10. Catarino CB, von Livonius B, Priglinger C, Banik R, Matloob S, Tamhankar MA, et al. Real-world clinical experience with idebenone in the treatment of leber hereditary optic neuropathy. *J Neuro-Ophthalmol.* (2020) 40:558–65. doi: 10.1097/WNO.0000000000001023

11. Zhao X, Zhang Y, Lu L, Yang H. Therapeutic effects of idebenone on leber hereditary optic neuropathy. *Curr Eye Res.* (2020) 45:1315–23. doi: 10.1080/02713683.2020.1736307

12. Klopstock T, Yu-Wai-Man P, Dimitriadis K, Rouleau J, Heck S, Bailie M, et al. A randomized placebo-controlled trial of idebenone in Leber's hereditary optic neuropathy. *Brain.* (2011) 134:2677–86. doi: 10.1093/brain/awr170

13. Suno M, Nagaoka A. Inhibition of lipid peroxidation by idebenone in brain mitochondria in the presence of succinate. *Arch Gerontol Geriatr.* (1989) 8:291–7. doi: 10.1016/0167-4943(89)90010-1

14. Johns, DR. Leber's hereditary optic neuropathy. *Arch Ophthalmol.* (1992) 110:1577. doi: 10.1001/archopht.1992.01080230077025

15. Moon Y, Kim US, Han J, Ahn H, Lim HT. Clinical and optic disc characteristics of patients showing visual recovery in leber hereditary optic neuropathy. *J Neuro-Ophthalmol.* (2020) 40:15–21. doi: 10.1097/WNO.0000000000000830

16. Stenton SL, Sheremet NL, Catarino CB, Andreeva NA, Assouline Z, Barboni P, et al. Impaired complex I repair causes recessive Leber's hereditary optic neuropathy. *J Clin Invest.* (2021) 131: e138267. doi: 10.1172/JCI138267

17. Lenaers G, Beaulieu C, Charif M, Gerber S, Kaplan J, Rozet J-M. Autosomal recessive Leber hereditary optic neuropathy, a new neuro-ophthalmo-genetic paradigm. *Brain.* (2023) 146:3156–61. doi: 10.1093/brain/awad131

18. Gerber S, Ding MG, Gérard X, Zwicker K, Zanlonghi X, Rio M, et al. Compound heterozygosity for severe and hypomorphic NDUFS2 mutations cause non-syndromic LHON-like optic neuropathy. *J Med Genet.* (2017) 54:346–56. doi: 10.1136/jmedgenet-2016-104212

19. Magrinelli F, Cali E, Braga VL, Yis U, Tomoum H, Shamseldin H, et al. Biallelic loss-of-function NDUFA12 variants cause a wide phenotypic spectrum from leigh/leigh-like syndrome to isolated optic atrophy. *Mov Disord Clin Pract.* (2022) 9:218–28. doi: 10.1002/mdc3.13398

20. Gerber S, Orssaud C, Kaplan J, Johansson C, Rozet JM. MCAT mutations cause nuclear LHON-like optic neuropathy. *Genes.* (2021) 12:521. doi: 10.3390/genes12040521

21. Fiorini C, Degiorgi A, Cascavilla ML, Tropeano CV, Morgia CL, Battista M, et al. Recessive MECR pathogenic variants cause an LHON-like optic neuropathy. *J Med Genet.* (2023) 2023:109340. doi: 10.1136/jmg-2023-109340

22. Zawadzka M, Krygier M, Pawłowicz M, Wilke MVMB, Rutkowska K, Gueguen N, et al. Expanding the phenotype of DNAJC30 associated Leigh syndrome. *Clin Genet.* (2022) 102:438–43. doi: 10.1111/cge.14196

23. Stenton SL, Tesarova M, Sheremet NL, Catarino CB, Carelli V, Ciara E, et al. DNAJC30 defect: a frequent cause of recessive Leber hereditary optic neuropathy and Leigh syndrome. *Brain.* (2022) 145:1624–31. doi: 10.1093/brain/awac052

24. Kieninger S, Xiao T, Weisschuh N, Kohl S, Rüther K, Kroisel PM, et al. DNAJC30 disease-causing gene variants in a large Central European cohort of patients with suspected Leber's hereditary optic neuropathy and optic atrophy. *J Med Genet.* (2022) 59:1027–34. doi: 10.1136/jmedgenet-2021-108235

25. Mauring L, Puusepp S, Parik M, Roomets E, Teek R, Reimand T, et al. Autosomal recessive Leber's hereditary optic neuropathy caused by a homozygous variant in DNAJC30 gene. *Eur J Med Genet.* (2023) 66:104821. doi: 10.1016/j.ejmg.2023.104821

26. Nesti C, Ticci C, Rubegni A, Doccini S, Scaturro G, Vetro A, et al. Additive effect of DNAJC30 and NDUFA9 mutations causing Leigh syndrome. *J Neurol.* (2023) 270:3266–9. doi: 10.1007/s00415-023-11673-7

27. Pojda-Wilczek D, Wójcik J, Kmak B, Krawczyński MR. Phenotypic variation of autosomal recessive leber hereditary optic neuropathy (arLHON) in one family. *Diagnostics.* (2022) 12:2701. doi: 10.3390/diagnostics12112701

28. Wiggs JL. DNAJC30 biallelic mutations extend mitochondrial complex I–deficient phenotypes to include recessive Leber's hereditary optic neuropathy. *J Clin Invest.* (2021) 131:e147734. doi: 10.1172/JCI147734

29. Tebbenkamp ATN, Varela L, Choi J, Paredes MI, Giani AM, Song JE, et al. The 7q11.23 protein DNAJC30 interacts with ATP synthase and links mitochondria to brain development. *Cell.* (2018) 175:1088–104.e23. doi: 10.1016/j.cell.2018.09.014

30. Turnbull C, Scott RH, Thomas E, Jones L, Murugaesu N, Pretty FB, et al. The 100,000 Genomes Project: bringing whole genome sequencing to the NHS. *BMJ.* (2018) 361:k1687. doi: 10.1136/bmj.k1687

31. Schon KR, Horvath R, Wei W, Calabrese C, Tucci A, Ibañez K, et al. Use of whole genome sequencing to determine genetic basis of suspected mitochondrial disorders: cohort study. *BMJ.* (2021) 375:e066288. doi: 10.1136/bmj-2021-066288

32. Genomes Project Pilot Investigators. 100,000 genomes pilot on rare-disease diagnosis in health care - preliminary report. *N Engl J Med.* (2021) 385:1868–80. doi: 10.1056/NEJMoa2035790

33. Martin AR, Williams E, Foulger RE, Leigh S, Daugherty LC, Niblock O, et al. PanelApp crowdsources expert knowledge to establish consensus diagnostic gene panels. *Nat Genet.* (2019) 51:1560–5. doi: 10.1038/s41588-019-0528-2

frontiers | Frontiers in Neurology

TYPE Case Report
PUBLISHED 05 December 2023
DOI 10.3389/fneur.2023.1284339

OPEN ACCESS

EDITED BY
Nahid Tayebi,
Genetics and Molecular Biology Branch (NHGRI), United States

REVIEWED BY
Grisel Lopez,
National Human Genome Research Institute (NIH), United States
Samantha Nishimura,
National Institutes of Health (NIH), United States
Santasree Banerjee,
Jilin University, China

*CORRESPONDENCE
Carla Marini
✉ carla.marini@ospedaliriuniti.marche.it

RECEIVED 28 August 2023
ACCEPTED 31 October 2023
PUBLISHED 05 December 2023

CITATION
Cursio I, Siliquini S, Carducci C, Bisello G, Mastrangelo M, Leuzzi V, Bertoldi M and Marini C (2023) Case report: Childhood epilepsy and borderline intellectual functioning hiding an AADC deficiency disorder associated with compound heterozygous *DDC* gene pathogenic variants.
Front. Neurol. 14:1284339.
doi: 10.3389/fneur.2023.1284339

Case report: Childhood epilepsy and borderline intellectual functioning hiding an AADC deficiency disorder associated with compound heterozygous *DDC* gene pathogenic variants

Ida Cursio[1], Sabrina Siliquini[1], Claudia Carducci[2], Giovanni Bisello[3], Mario Mastrangelo[4], Vincenzo Leuzzi[5], Mariarita Bertoldi[3] and Carla Marini[1]*

[1]Child Neurology and Psychiatric Unit, Pediatric Hospital G. Salesi, Azienda Ospedaliero Universitaria delle Marche, Ancona, Italy, [2]Department of Experimental Medicine, Sapienza - Università di Roma, Rome, Italy, [3]Department of Neuroscience, Biomedicine and Movement Sciences, University of Verona, Verona, Italy, [4]Department of Women/Child Health and Urological Science, Sapienza - Università di Roma, Rome, Italy, [5]Department of Human Neuroscience, Sapienza - Università di Roma, Rome, Italy

Aromatic L-amino acid decarboxylase (AADC) deficiency is a rare autosomal recessive neurometabolic disorder leading to severe combined serotonin, dopamine, norepinephrine, and epinephrine deficiency. We report on a female patient with borderline functioning and sporadic clear-cut focal to bilateral seizures from age 10years. A neuropsychological assessment highlighted a mild impairment in executive functions, affecting attention span and visual–spatial abilities. Following the diagnosis of epilepsy with a presumed genetic etiology, we applied a diagnostic approach inclusive of a next-generation sequencing (NGS) gene panel, which uncovered two variants *in trans* in the DOPA decarboxylase (*DDC*) gene underlying an AADC deficiency. This compound heterozygous genotype was associated with a mild reduction of homovanillic acid, a low level of the norepinephrine catabolite, and a significant reduction of 5-hydroxyindoleacetic acid in cerebrospinal fluid. Remarkably, 3-O-methyldopa (3-OMD) and 5-hydroxytryptophan were instead increased. During the genetically guided re-evaluation process, some mild signs of dysautonomic dysfunction (nasal congestion, abnormal sweating, hypotension and fainting, excessive sleepiness, small hands and feet, and increased levels of prolactin, tiredness, and fatigue), more typical of AADC deficiency, were evaluated with new insight. Of the two AADC variants, the R347Q has already been characterized as a loss-of-function with severe catalytic impairments, while the novel L391P variant has been predicted to have a less severe impact. Bioinformatic analyses suggest that the amino acid substitution may affect affinity for the PLP coenzyme. Thus, the genotype corresponds to a phenotype with mild and late-onset symptoms, of which seizures were the clinical sign, leading to medical attention. This case report expands the spectrum of AADC deficiency phenotypes to encompass a less-disabling clinical condition including borderline cognitive functioning, drug-responsive epilepsy, and mild autonomic dysfunction.

KEYWORDS

epilepsy, focal seizures, AADC deficiency, *DDC* gene, compound heterozygous variants, autonomic dysfunction

Introduction

Aromatic L-amino acid decarboxylase (AADC) deficiency (OMIM 608643) is a rare, autosomal recessive, inborn error of neurotransmitter biosynthesis resulting in a combined deficiency of serotonin, dopamine, and the metabolic derivatives norepinephrine and epinephrine (1).

AADC deficiency is caused by biallelic pathogenic variants in the *DDC* gene, and most identified genotypes are compound heterozygous (73%) (2). In the last few years, there has been a marked increase in the number of identified variants, yet no clear genotype–phenotype correlation has been identified.

The DDC gene, located on chromosome 7p12.2-p12.1, is a protein-coding gene encoding the AADC enzyme that is implicated in two important metabolic pathways of neurotransmitter synthesis. It enables 5-hydroxy-L-tryptophan decarboxylase activity to form serotonin from 5-OH tryptophan and L-DOPA decarboxylase activity, giving rise to dopamine from L-dihydroxyphenylalanine (L-DOPA) (3). AADC deficiency presents with an infantile encephalopathy resulting in severe neurological and neurodevelopmental impairment, leading to a permanent, severe disabling condition in approximately 80% of patients (4).

Presenting symptoms of AADC deficiency include movement disorders (oculogyric crisis, dystonia, and hypokinesia), hypotonia, developmental delay, pseudo-myasthenic features (ptosis and fatigability), and autonomic dysfunction (nasal congestion, abnormal sweating, excessive drooling, orthostatic hypotension, bradycardia, and temperature instability). Less common symptoms are episodes of hypoglycemia, prematurity, failure to thrive, behavioral and sleep disorders, and gastrointestinal symptoms (gastroesophageal reflux, diarrhea, and constipation) (5–7). Epilepsy associated with AADC deficiency is a rare finding described only in 4–7% of published patients (5, 6).

Clinical diagnosis is based on the genetic analysis of *DDC* confirmed by assessing dopamine and serotonin metabolites in CSF. Blood and CSF levels of 3-*O*-methyldopa (3-OMD) and blood prolactin may be useful surrogate diagnostic biomarkers (5, 6).

Treatment options include oral pyridoxine, dopamine-mimetic drugs, and inhibitors of dopamine catabolism (5). Intracerebral gene therapy has been recently developed as an alternative treatment for severely affected patients (8–14).

In this study, we describe a 13-year-old girl with late-onset, mild, and atypical AADC deficiency diagnosed 'by chance' with a next-generation sequencing (NGS) multigene panel, which included the *DDC* gene.

Case report

Clinical history

A 13-year-old female of Caucasian ethnic origin originated from a small town in the north-west area of Sicily. The father had epilepsy in childhood (responsive to carbamazepine, discontinued after a few years), and the mother had migraine; two siblings were healthy.

Psychomotor developmental milestones were reached at the correct age; past medical history was uneventful but for sporadic migraine episodes since childhood and sleep apnea with snoring.

At the age of 10 years, during wakefulness, she presented an episode of loss of awareness, head and eye deviation to the right, and gestural automatisms lasting a few minutes, followed by gradual, spontaneous recovery. The second episode occurred 4 months later, during sleep, when she was found unconscious with bilateral clonic jerking. EEG recording, performed soon after the seizure, reported multifocal spikes and sharp waves. She was treated with levetiracetam at a dose of 750 mg/daily. After 2 years without seizures, levetiracetam was gradually stopped. Yet, 3 months after discontinuing the medication, seizures relapsed, and treatment was restarted. On clinical examination, she showed hands and feet smaller than expected, mild bilateral ptosis, mild bradykinesia, and clumsiness in gross motor tasks. Deep tendon reflexes were normal. No psychiatric comorbidities emerged from clinical observation and anamnestic interview with the girl However, her parents described her as shy and avoidant of social interaction with peers. Cognitive assessment (*Wechsler Intelligence Scale for Children - IV*) revealed low normal performances (total IQ score 78) with a disharmonic profile for prevalent perceptual reasoning index impairment (score: 76) with respect to working memory (score: 88), verbal comprehension (score: 86), and processing speed (score: 82). Overall, the neuropsychological assessment highlighted a mild impairment in executive functions, mainly affecting attention span and visual–spatial abilities.

Brain CT and MRI scans were normal. Current, interictal video-EEG monitoring showed sporadic sharp waves in the occipital bilateral regions during sleep (Figure 1). The clinical history of the patient, evolution over time, and applied diagnostic procedures are summarized in Figure 2.

We then applied a NGS approach used in many gene identification procedures (15–18) by exploiting a commercial gene panel. In detail, a saliva sample was collected and sent to Blueprint Genetics Oy (Keilaranta 16 A-B, 02150 Espoo, Finland) for NGS analysis. Blueprint Genetics FLEX Comprehensive Epilepsy Panel Plus (covering 668 genes and 9,999 exons, version 1, May 17, 2022) was used. The test was developed, approved, and certified as reported in the Manufacturer's Report (ISO 15189 accreditation). Details of the process and quality control systems for identifying the candidate variants are provided in Supplementary methods from the Manufacturer Datasheet.

The sequence analysis detected two missense variants on the *DDC* gene of paternal (NM000790.4, c.1040G > A, p. Arg347Gln) and maternal (NM000790.4, c.1172T > C, p. Leu391Pro) origin. The Arg347Gln amino acid transition was reported as pathogenic by ClinVar and has already been reported in many patients with AADC deficiency (2, 4). The Leu391Pro substitution is novel and classified as a variant of uncertain significance.

Bioinformatic analysis of the AADC

The human AADC structure predicted by AlphaFold2 (AF2) (19) was used to determine the position of Leu391, and the absence of cofactors in the AF2 predicted proteins has been overcome by the algorithm AlphaFill (20). Since AADC is an obligate functional dimer, we determined the impact of amino acid substitution on the AADC protein population that theoretically can be synthesized by the compound heterozygous patient. Three different types of AADC dimers protein could indeed be present: the homodimers of Arg347Gln and Leu391Pro variants and the Arg347Gln/Leu391Pro heterodimer (21–23). The Arg347Gln homodimeric variant has

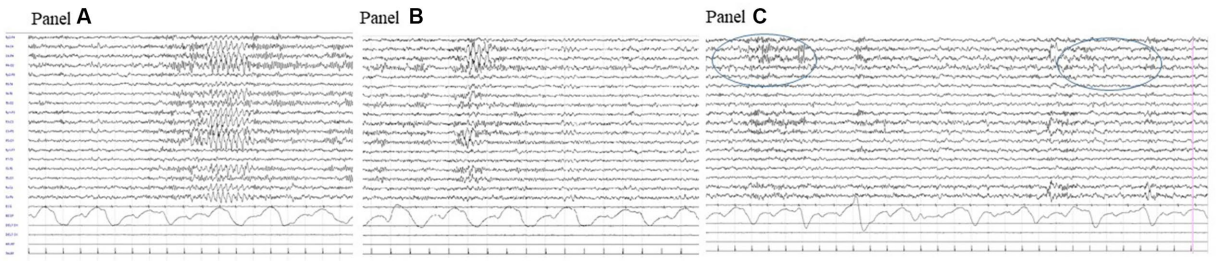

FIGURE 1
Interictal video-EEG recording at age 11 years: polygraphic recording during drowsiness showing a bilateral discharge of rhythmic sharply contoured delta waves **(A)**; a similar activity but with right predominance **(B)** and right occipital spikes during sleep (circled area, **C**).

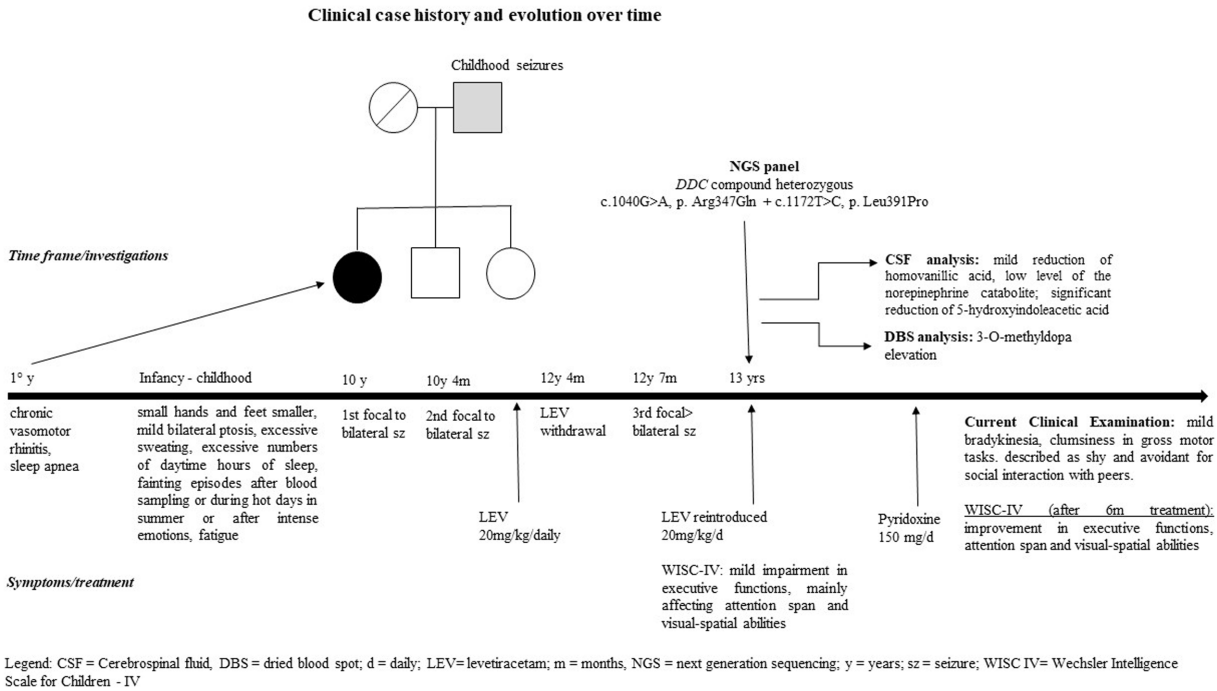

FIGURE 2
Clinical case history and evolution over time, including diagnostic procedures.

already been characterized as loss-of-function with severe catalytic impairments and classified as pathogenic (2).

Instead, the Leu391Pro variant is a novel and never-characterized substitution. *In silico* inspection of the AADC crystal structure shows that Leu391 is located on a surface alpha-helix of the C-terminal domain distant from the active site (Figure 3A), possibly involved in hydrophobic cluster stabilization important for folding and pyridoxal 5′-phosphate (PLP) binding (Figure 3B), since other pathogenic variants (Glu283Ala, Cys410Gly, Arg447His, Arg453Cys, and Arg462Gln) mapping in this protein region affect affinity for the coenzyme (24–26). Its substitution for Pro may destabilize the helix, leading to the exposure of hydrophobic residues and somewhat influencing PLP binding. Interestingly, it can be predicted (2) that the AADC heterodimer maintains one active site fully functional while the other is affected by both Arg347Gln and Leu391Pro substitutions.

Clinical reassessment following genetic or metabolic diagnosis

Following the genetic result, we interviewed the father, focusing on all signs/symptoms associated with AADC deficiency. He reported that the daughter tended to sleep several hours during the day; she also easily fainted after blood sampling, during hot days in the summer, or after intense emotions. She has suffered from excessive sweating and chronic vasomotor rhinitis since her first years of life. Finally, she complained of lower limb pain after prolonged inactivity. Table 1 highlights clinical findings in our patient compared with a typical AADC presentation.

CSF examination showed a mild reduction of homovanillic acid (101 nmol/L; r.v. 148–434), an incongruently low level of the norepinephrine catabolite 3-methoxy-4-hydroxyphenylglycol (11 nmol/L; r.v. 28–60), and a more remarkable reduction of 5-hydroxyindoleacetic acid (7 nmol/L; r.v. 68–115). As expected,

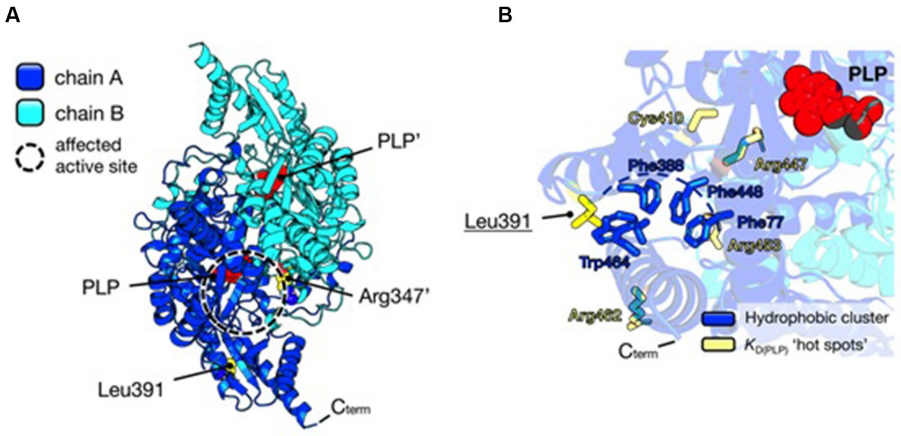

FIGURE 3
Structural analysis of AADC protein and localization of substituted amino acids. **(A)** AADC dimeric structure is represented as a cartoon. Chain A is blue and Chain B is cyan. PLP molecule for each active site is represented as red spheres. Leu391 and Arg347' in the heterodimeric protein are shown as yellow spheres. The prime indicates the residue and cofactor molecules belonging to subunit B. The active site where both variants may exert their effect is highlighted as a dashed circle. **(B)** Localization of Leu391. The cluster of hydrophobic residues (Phe77, Phe388, Phe448, and Trp464) shielded from the solvent is shown as blue sticks, while yellow sticks represent residues whose pathogenic substitutions lead to decreased affinity for the PLP molecule (red spheres). Protein visualization, measurement, dimer building, and rotamer analysis were performed using PyMOL 2.2.3, The PyMOL Molecular Graphics 50 System, Version 2.0 Schrödinger, LLC, New York, NY, 2021.

TABLE 1 **Laboratory analysis of liquor neurotransmitters metabolites.**

Liquor neurotransmitters metabolites		
Neurotransmitter	Result (nmol/L)	Reference values (nmol/L)
Homovanillic acid	101	148–434
5-hydrosyindoleacidic acid	7	68–115
3-O-metildopa	542	<50
5-hydroxytryptophan	45	<10

3-OMD (542 nmol/L (r.v. < 50)) and 5-hydroxytryptophan (45 nmol/L (r.v. <10)) were increased (Table 2). 3-OMD elevation was also found in dried blood spot (DBS) (2,820 nmol/L;r.v. <1,000 nmol/L) (Table 1) (15), while prolactin was marginally increased (27.2 ng/mL, r.v. 27 ng/mL).

The patient is currently being treated with pyridoxine 150 mg/daily and levetiracetam 1,500 mg/daily. Since she started treatment, she no longer fainted, while sleep disturbances and abnormal sweating remained unchanged. Neuropsychological re-evaluation after 6 months of pyridoxine supplementation showed an improvement in executive functions and overall cognitive performance at WISC-IV.

Discussion

We report on a 13-year-old patient reaching a diagnosis of AADC deficiency. Childhood epilepsy with recurring focal to bilateral seizures and borderline intellectual functioning with mild impairment of the executive functions affecting attention span and visual–spatial abilities were the clinical signs leading the girl to medical attention, thus uncovering a phenotype that is not typically related to AADC deficiency.

The current diagnostic approach to patients with unexplained epilepsy and variable degrees of intellectual disability includes the application of NGS gene panels, which in our patient led to the unexpected result of compound heterozygous variants of the *DDC* gene. A subsequent targeted clinical interview uncovered some features attributable to AADC deficiency. We regarded with new insight some clinical aspects, including nasal congestion, sleep apnea, frequent faints, abnormal sweating, a slow and awkward bradykinetic attitude, small hands and feet, and emotional lability. We also noticed that many of the Italian patients affected by AADC deficiency come from Sicily (4, 27), a populated island in the Mediterranean; differently from what was reported in Taiwan (28), a founder effect could not be identified.

Most signs and symptoms described in patients with AADC deficiency can be attributed to dopamine, norepinephrine, epinephrine, and serotonin deficiencies. Disturbance in serotonin biosynthesis affects appetite, sleep, memory, learning, body temperature, mood, cardiovascular function, and endocrine functions. In our patient, the prevalence of dysautonomic symptoms is consistent with a prevalent deficiency of norepinephrine and serotonin and a relatively preserved dopamine synthesis. Indeed, the mild reduction of HVA (the surrogate marker of dopamine) and the low concentration of CSF MHPG (the surrogate marker of norepinephrine) cannot be attributed to enzyme-substrate depletion. The high frequency in the general population of polymorphic variants on the dopamine beta-hydroxylase gene associated with variable reductions in enzymatic activity might contribute to this discrepancy (29). We could also speculate that the mild motor symptoms observed in our patients might be related to a progressive autoregulation of the dopaminergic (but not serotoninergic) network occurring with age and resulting in a progressive increase of brain dopamine levels via pre- and postsynaptic adaptive mechanisms, as observed in murine models (4, 30).

Epilepsy is a rare finding in AADC patients, reported in only 7.6% (9 of 117 patients) examined for the development of AADC guidelines (5) and in none of the 64 patients reported by Pearson et al. (7). EEG abnormalities, including slowing, fast activity, and poly-spikes, have been reported in some patients (6, 31). We can argue that the decreased cerebral serotoninergic system might contribute to the epilepsy that was our patient's presenting and more relevant clinical signs. Indeed, it is known that depletion of brain 5-HT lowers the threshold for audiogenically, chemically,

TABLE 2 Clinical findings in our patient compared with typical AADC presentation.

Clinical findings	
Sign / symptoms of AADC deficiency	Patient
Common	
Early onset hypotonia	
Developmental delay	x
Oculogyric crisis	
Dystonia	
Hypokinesia	
Nasal congestion	x
Abnormal sweating	x
Excessive drooling	
Hypotension	x
Bradycardia	
Temperature instability	
Pseudo-myasthenic features (ptosis and fatigue)	x
Less common	
Infantile episodes of hypoglycemia	
Behavioral disorders	
Insomnia	
Excessive sleepiness	x
Gastrointestinal symptoms	
Epilepsy	x
Other findings	
Hyperreflexia	
Small hands and feet	x
Sleep apnea	x

and electrically evoked convulsions (32). There is also ample preclinical and clinical evidence suggesting the importance of serotonergic neurotransmission in human epilepsy. Current research highlights the potential of modulating serotonergic transmission and targeting distinct serotonin (5-HT) receptors in treating epilepsy (33).

Our proband carries compound heterozygous pathogenic variants combining a known splice site catalytic variant with severe functional impact with a novel missense change with minor functional consequences. A positive or negative complementation has been proposed in compound heterozygotes based on the number of affected active sites in heterodimeric AADC proteins (2, 21). In this case, the milder mutation in the heterodimer could positively complement the most severe one, since only one active site is negatively affected while the other can properly function. These data agree with the patient's mild phenotype. Indeed, bioinformatic analysis suggests that the Leu391Pro variant may affect affinity for the coenzyme (PLP), which is confirmed by the improvement the patients experienced after 6 months of B6 treatment. Yet, since the Arg347Gln variant is catalytically affected, treatment with vitamin B6 cannot fully rescue the phenotype. As a result of systematic clinical observation, non-ergot dopamine agonists, such as rotigotine and pramipexole, inhibitors of MAO and/or COMT, might be considered as potential treatments (4, 34, 35). The patient showed a good response to monotherapy with B6 supplementation; thus, further therapeutic decisions will be based on a clinical follow-up and, possibly, a new CSF dosage of biogenic amine metabolites.

AADC has been the first genetic disease for which effective intracerebral gene therapy has been developed. This treatment has dramatically improved the neurological defect related to dopamine depletion (8–13). *DDC* gene therapy is currently a valid option for patients unresponsive to pharmacological therapy. It is approved in the European Union and United Kingdom for patients older than 18 months with severe motor and developmental impairment (14).

In conclusion, the present case enlarges the phenotypic spectrum of AADC deficiency, encompassing less-disabling conditions, such as borderline cognitive functioning, drug-responsive epilepsy, and prevalent autonomic dysfunction. This case report also highlights how heterogeneous this condition is, thus underlying the probability that it might still be underdiagnosed.

Data availability statement

The datasets presented in this study can be found in online repositories. The names of the repository/repositories and accession number(s) can be found in the article/Supplementary material.

Ethics statement

The studies involving humans were approved by Comitato etico territoriale delle marche; azienda ospedaliera universitaria (AOU) marche, Ancona, Italy. The studies were conducted in accordance with the local legislation and institutional requirements. Written informed consent for participation in this study was provided by the participants' legal guardians/next of kin. Written informed consent was obtained from the individual(s) for the publication of any potentially identifiable images or data included in this article.

Author contributions

IC: Conceptualization, Investigation, Data curation, Methodology, Writing – original draft, Writing – review & editing. SS: Conceptualization, Investigation, Writing – original draft, Writing – review & editing, Data curation, Methodology. CC: Data curation, Investigation, Methodology, Writing – review & editing. GB: Data curation, Methodology, Writing – review & editing, Investigation. MM: Data curation, Methodology, Writing – review & editing, Conceptualization. VL: Conceptualization, Data curation, Methodology, Writing – review & editing, Supervision. MB: Data curation, Methodology, Supervision, Investigation, Writing – original draft, Writing – review & editing. CM: Investigation, Data curation, Methodology, Supervision, Writing – original draft, Conceptualization, Writing – review & editing.

Funding

The author(s) declare financial support was received for the research, authorship, and/or publication of this article. Unconditional support for medical writing received by Medical Affairs PTC Italy.

Conflict of interest

The authors declare that the research was conducted in the absence of any commercial or financial relationships that could be construed as a potential conflict of interest.

Publisher's note

All claims expressed in this article are solely those of the authors and do not necessarily represent those of their affiliated organizations, or those of the publisher, the editors and the reviewers. Any product that may be evaluated in this article, or claim that may be made by its manufacturer, is not guaranteed or endorsed by the publisher.

Supplementary material

The Supplementary material for this article can be found online at: https://www.frontiersin.org/articles/10.3389/fneur.2023.1284339/full#supplementary-material

References

1. Hyland K, Clayton PT. Aromatic amino acid decarboxylase deficiency in twins. *J Inherit Metab Dis*. (1990) 13:301–4. doi: 10.1007/BF01799380

2. Himmelreich N, Bertoldi M, Alfadhel M, Alghamdi MA, Anikster Y, Bao X, et al. Prevalence of DDC genotypes in patients with aromatic L-amino acid decarboxylase (AADC) deficiency and in silico prediction of structural protein changes. *Mol Genet Metab*. (2023) 139:107624. doi: 10.1016/j.ymgme.2023.107624

3. Christenson JG, Dairman W, Udenfriend S. On the identity of DOPA decarboxylase and 5-hydroxytryptophan decarboxylase (immunological titration-aromatic L-amino acid decarboxylase-serotonin-dopamine-norepinephrine). *Proc Nat Acad Sci U S A*. (1972) 69:343–7. doi: 10.1073/pnas.69.2.343

4. Leuzzi V, Mastrangelo M, Polizzi A, Artiola C, van Kuilenburg A, Carducci C, et al. Report of two never treated adult sisters with aromatic L-amino acid decarboxylase deficiency: a portrait of the natural history of the disease or an expanding phenotype? *JIMD Rep*. (2015) 15:39–45. doi: 10.1007/8904_2014_295

5. Wassenberg T, Molero-Luis M, Jeltsch K, Hoffmann GF, Assmann B, Blau N, et al. Consensus guideline for the diagnosis and treatment of aromatic lamino acid decarboxylase (AADC) deficiency. *Orphanet J Rare Dis*. (2017) 12:12. doi: 10.1186/s13023-016-0522-z

6. Rizzi S, Spagnoli C, Frattini D, Pisani F, Fusco C. Clinical features in aromatic L-amino acid decarboxylase (AADC) deficiency: a systematic review. *Behav Neurol*. (2022) 2022:1–7. doi: 10.1155/2022/2210555

7. Pearson TS, Gilbert L, Opladen T, Garcia-Cazorla A, Mastrangelo M, Leuzzi V, et al. AADC deficiency from infancy to adulthood: symptoms and developmental outcome in an international cohort of 63 patients. *J Inherit Metab Dis*. (2020) 43:1121–30. doi: 10.1002/jimd.12247

8. Chien YH, Lee NC, Tseng SH, Tai CH, Muramatsu SI, Byrne BJ, et al. Efficacy and safety of AAV2 gene therapy in children with aromatic L-amino acid decarboxylase deficiency: an open-label, phase 1/2 trial. *Lancet Child Adolesc Health*. (2017) 1:265–73. doi: 10.1016/S2352-4642(17)30125-6

9. Tai CH, Lee NC, Chien YH, Byrne BJ, Muramatsu SI, Tseng SH, et al. Long-term efficacy and safety of eladocagene exuparvovec in patients with AADC deficiency. *Mol Ther*. (2022) 30:509–18. doi: 10.1016/j.ymthe.2021.11.005

10. Tseng CH, Chien YH, Lee NC, Hsu YC, Peng SF, Tseng WYI, et al. Gene therapy improves brain white matter in aromatic l-amino acid decarboxylase deficiency. *Ann Neurol*. (2019) 85:644–52. doi: 10.1002/ana.25467

11. Hwu WL, Muramatsu S, Tseng SH, Tzen KY, Lee NC, Chien YH, et al. Gene therapy for aromatic L-amino acid decarboxylase deficiency. *Sci Transl Med*. (2012) 4:134ra61. doi: 10.1126/scitranslmed.3003640

12. Kojima K, Nakajima T, Taga N, Miyauchi A, Kato M, Matsumoto A, et al. Gene therapy improves motor and mental function of aromatic l-amino acid decarboxylase deficiency. *Brain*. (2019) 142:322–33. doi: 10.1093/brain/awy331

13. Pearson TS, Gupta N, San Sebastian W, Imamura-Ching J, Viehoever A, Grijalvo-Perez A, et al. Gene therapy for aromatic L-amino acid decarboxylase deficiency by MR-guided direct delivery of AAV2-AADC to midbrain dopaminergic neurons. *Nat Commun*. (2021) 12:4251. doi: 10.1038/s41467-021-24524-8

14. Roubertie A, Opladen T, Brennenstuhl H, Kuseyri Hübschmann O, Flint L, Willemsen MA, et al. Gene therapy for aromatic L-amino acid decarboxylase deficiency: requirements for safe application and knowledge-generating follow-up. *J Inherit Metab Dis*. (2023). doi: 10.1002/jimd.12649

15. Han P, Wei G, Cai K, Xiang X, Deng WP, Li YB, et al. Identification and functional characterization of mutations in LPL gene causing severe hypertriglyceridaemia and acute pancreatitis. *J Cell Mol Med*. (2020) 24:1286–99. doi: 10.1111/jcmm.14768

16. Zhang R, Chen S, Han P, Chen F, Kuang S, Meng Z, et al. Whole exome sequencing identified a homozygous novel variant in CEP290 gene causes Meckel syndrome. *J Cell Mol Med*. (2020) 24:1906–16. doi: 10.1111/jcmm.14887

17. Dai Y, Liang S, Dong X, Zhao Y, Ren H, Guan Y, et al. Whole exome sequencing identified a novel DAG1 mutation in a patient with rare, mild and late age of onset muscular dystrophy-dystroglycanopathy. *J Cell Mol Med*. (2019) 23:811–8. doi: 10.1111/jcmm.13979

18. Zheng Y, Xu J, Liang S, Lin D, Banerjee S. Whole exome sequencing identified a novel heterozygous mutation in HMBS gene in a Chinese patient with acute intermittent Porphyria with rare type of mild Anemia. *Front Genet*. (2018) 9:129. doi: 10.3389/fgene.2018.00129

19. Jumper J, Evans R, Pritzel A, Green T, Figurnov M, Ronneberger O, et al. Highly accurate protein structure prediction with AlphaFold. *Nature*. (2021) 596:583–9. doi: 10.1038/s41586-021-03819-2

20. Hekkelman ML, de Vries I, Joosten RP, Perrakis A. AlphaFill: enriching AlphaFold models with ligands and cofactors. *Nat Methods*. (2023) 20:205–13. doi: 10.1038/s41592-022-01685-y

21. Bisello G, Bertoldi M. Compound heterozygosis in AADC deficiency and its complex phenotype in terms of AADC protein population. *Int J Mol Sci*. (2022) 23:11238. doi: 10.3390/ijms231911238

22. Montioli R, Dindo M, Giorgetti A, Piccoli S, Cellini B, Voltattorni CB. A comprehensive picture of the mutations associated with aromatic amino acid decarboxylase deficiency: from molecular mechanisms to therapy implications. *Hum Mol Genet*. (2014) 23:5429–40. doi: 10.1093/hmg/ddu266

23. Montioli R, Paiardini A, Kurian MA, Dindo M, Rossignoli G, Heales SJR, et al. The novel R347G pathogenic mutation of aromatic amino acid decarboxylase provides additional molecular insights into enzyme catalysis and deficiency. *Biochim Biophys Acta*. (2016) 1864:676–82. doi: 10.1016/j.bbapap.2016.03.011

24. Montioli R, Battini R, Paiardini A, Tolve M, Bertoldi M, Carducci C, et al. A novel compound heterozygous genotype associated with aromatic amino acid decarboxylase deficiency: clinical aspects and biochemical studies. *Mol Genet Metab*. (2019) 127:132–7. doi: 10.1016/j.ymgme.2019.05.004

25. Montioli R, Bisello G, Dindo M, Rossignoli G, Voltattorni CB, Bertoldi M. New variants of AADC deficiency expand the knowledge of enzymatic phenotypes. *Arch Biochem Biophys*. (2020) 682:108263. doi: 10.1016/j.abb.2020.108263

26. Riva A, Iacomino M, Piccardo C, Franceschetti L, Franchini R, Baroni A, et al. Exome sequencing data screening to identify undiagnosed Aromatic l-amimno acid decarboxylase deficiency in neurodevelopmental disorders. *Biochem Biophys Res Commun*. (2023) 673:131–6. doi: 10.1016/j.bbrc.2023.06.065

27. Burlina A, Giuliani A, Polo G, Gueraldi D, Gragnaniello V, Cazzorla C, et al. Detection of 3-O-methyldopa in dried blood spots for neonatal diagnosis of aromatic L-amino-acid decarboxylase deficiency: the northeastern Italian experience. *Mol Genet Metab*. (2021) 133:56–62. doi: 10.1016/j.ymgme.2021.03.009

28. Lee H-F, Tsai CR, Chi CS, Chang TM, Lee HJ. Aromatic L-amino acid decarboxylase deficiency in Taiwan. *Eur J Paediatr Neurol*. (2009) 13:135–40. doi: 10.1016/j.ejpn.2008.03.008

29. Gonzalez-Lopez E, Vrana KE. Dopamine beta-hydroxylase and its genetic variants in human health and disease. *J Neurochem*. (2020) 152:157–81. doi: 10.1111/jnc.14893

30. Lee NC, Shieh YD, Chien YH, Tzen KY, Yu IS, Chen PW, et al. Regulation of the dopaminergic system in a murine model of aromatic Lamino acid decarboxylase deficiency. *Neurobiol Dis*. (2013) 52:177–90. doi: 10.1016/j.nbd.2012.12.005

31. Brun L, Ngu LH, Keng WT, Ch'ng GS, Choy YS, Hwu WL, et al. Clinical and biochemical features of aromatic L-amino acid decarboxylase deficiency. *Neurology*. (2010) 75:64–71. doi: 10.1212/WNL.0b013e3181e620ae

32. Bagdy G, Kecskemeti V, Riba P, Jakus R. Serotonin and epilepsy. *J Neurochem*. (2007) 100:857–73. doi: 10.1111/j.1471-4159.2006.04277.x

33. Sourbron J, Lagae L. Serotonin receptors in epilepsy: novel treatment targets? *Epilepsia Open*. (2022) 7:231–46. doi: 10.1002/epi4.12580

34. Mastrangelo M, Manti F, Patanè L, Ferrari S, Carducci C, Carducci C, et al. Successful pregnancy in a patient with L-amino acid decarboxylase deficiency: therapeutic management and clinical outcome. *Mov Disord Clin Pract*. (2018) 5:446–7. doi: 10.1002/mdc3.12622

35. Manti F, Mastrangelo M, Battini R, Carducci C, Spagnoli C, Fusco C, et al. Al long-term neurological and psychiatric outcomes in patients with aromatic l-amino acid decarboxylase deficiency. *Parkinsonism Relat Disord*. (2022) 103:105–11. doi: 10.1016/j.parkreldis.2022.08.033

frontiers | Frontiers in Neurology

TYPE Case Report
PUBLISHED 12 December 2023
DOI 10.3389/fneur.2023.1308289

OPEN ACCESS

EDITED BY
Huifang Shang,
Sichuan University, China

REVIEWED BY
Wen-Xiong Chen,
Guangzhou Medical University, China
Chao Yuan,
Southern Medical University, China
Xu Wang,
First Affiliated Hospital of Jilin University, China

*CORRESPONDENCE
Yingjie Dai
✉ 15009888333@163.com

RECEIVED 06 October 2023
ACCEPTED 21 November 2023
PUBLISHED 12 December 2023

CITATION
Sun M and Dai Y (2023) Late-onset cobalamin C deficiency type in adult with cognitive and behavioral disturbances and significant cortical atrophy and cerebellar damage in the MRI: a case report.
Front. Neurol. 14:1308289.
doi: 10.3389/fneur.2023.1308289

Late-onset cobalamin C deficiency type in adult with cognitive and behavioral disturbances and significant cortical atrophy and cerebellar damage in the MRI: a case report

Miao Sun and Yingjie Dai*

Department of Neurology, General Hospital of Northern Theater Command, Shenyang, China

Background: Late-onset cobalamin C (cblC) deficiency is associated with a wide range of neurological and psychiatric symptoms, hematological manifestations, anorexia, renal failure, ocular abnormalities, dermatitis, and pancreatitis. However, the neuroimaging characteristics of late-onset cblC deficiency remain insufficiently documented. Common findings include diffuse white matter swelling, varying degrees of severe leukoaraiosis, hydrocephalus, corpus callosum atrophy, and symmetric bilateral basal ganglia lesions. In this report, we present a case of late-onset cblC deficiency in adults presenting with cerebellar ataxia as the primary symptom. The MRI findings revealed bilateral lateral cerebellar hemispheres exhibiting symmetric hyperintensity, primarily observed in diffusion-weighted imaging (DWI), which is a rarely reported imaging change in this context.

Case presentation: Our patient was a male who experienced symptoms starting at the age of 30 years, including unsteady walking, apparent cerebellar ataxia, and cognitive impairment upon nervous system examination. Brain magnetic resonance imaging (MRI) exhibited symmetric hyperintensity in the bilateral lateral cerebellar hemispheres, predominantly manifested in DWI, without any enhancement. Subsequently, significantly elevated blood total homocysteine and urinary methylmalonic acid levels were observed. Genetic analysis confirmed the presence of MMACHC compound heterozygous mutants c.482G > A and c.609G > A, thus confirming the diagnosis of cblC deficiency. These variants were classified as likely pathogenic following the guidelines of the American College of Medical Genetics and Genomics (ACMG) and were verified using Sanger sequencing. Following treatment, the patient experienced improvements in walking ability and cognition, a significant decrease in blood total homocysteine levels, and reversal of the imaging lesions.

In conclusion: Late-onset cblC deficiency presents with diverse clinical and imaging manifestations. Early diagnosis and treatment are crucial in achieving a favorable prognosis. This case serves as a reminder to clinicians not to overlook genetic metabolic disorders, particularly those causing multisite damage, in adult patients with undiagnosed neurological disorders, especially those affecting the cerebellum. Notably, methylmalonic acidemia should be considered within the spectrum of bilateral cerebellar lesions.

KEYWORDS

methylmalonic acidemia, bilateral cerebellar lesions, reversible DWI change, cblC, MMACHC

1 Background

Methylmalonic acidemia (MMA) is a rare autosomal recessive genetic metabolic disorder characterized by defects in methylmalonyl-CoA mutase or cobalamin metabolism within the mitochondria. Consequently, methylmalonic acid, an intermediate product, accumulates in the body, resulting in multisystem damage. While primarily observed in infants and young children, CblC deficiency, a subtype of MMA, is less common in adults. Clinical and imaging manifestations of CblC deficiency exhibit significant heterogeneity (1). Infrequently, cerebellar ataxia manifests as the primary symptom, accompanied by bilateral lateral cerebellar hemispheres showing symmetric hyperintensity on DWI. This case report describes an adult patient with CblC deficiency presenting with bilateral cerebellar damage as the main clinical manifestation.

2 Case presentation

A 30-year-old male presented with a 7-day history of slow response and unsteady walking, as reported by his family. Clinical features included impaired calculation skills, limited language expression, unresponsiveness, difficulty climbing stairs, inability to walk in a straight line, and irritability. No other symptoms such as weakness, numbness, fever, cough, diarrhea, headache, nausea, vomiting, altered consciousness, or convulsions were observed. Skin manifestations, such as resembling staphylococcal scalded skin syndrome or a diffuse erythema with superficial erosions, desquamation, and cheilitis resembling acrodermatitis enteropathica, were not found in our patient. The patient had an unremarkable medical and developmental history, and his relatives did not exhibit similar symptoms. However, his scholastic performance was notably poor compared to his peers, having completed only the 8th grade. Neurological examination revealed delayed reaction times, impaired calculation ability, significant dysmetria on heel–knee–shin testing, and a positive Romberg test. Plasma total homocysteine 296.90 μmol/L (normal value 0.0 ~ 15.0 μmol/L) and D-dimer 9.38 ng/mL (normal value 0.0 ~ 0.55 ng/mL) are elevated.

Auxiliary examinations, including blood routine, biochemistry, thyroid function, rheumatic immune-related antibodies, folic acid, vitamin B12 concentrations, cerebrospinal fluid analysis, and autoimmune encephalitis antibody examination, all yielded normal results. Neuropsychological examination results indicated a Mini-Mental State Examination (MMSE) score of 20, a Montreal Cognitive Assessment (MoCA) score of 18, an International Cooperative Ataxia Rating Scale (ICARS) score of 41, and a Barthel Index (BI) score of 55. MRI revealed cortical atrophy and symmetric hyperintensities in the bilateral lateral cerebellar hemispheres, primarily observed on DWI (Figure 1). Liquid chromatography tandem mass spectrometry-based blood amino acid and acylcarnitine spectroscopy demonstrated significantly elevated levels of propionylcarnitine (10.53 μmol/L, normal range: 0.30–5.00 μmol/L), the propionylcarnitine to acetylcarnitine ratio (0.50, normal range: 0.02–0.20), and the propionylcarnitine to methionine ratio (0.90, normal range: 0.02–0.30). Gas chromatography mass spectrometry-based urine organic acid analysis showed a significant increase in methylmalonic acid (76.9 nmol/L, reference value, 0.00–4.00 nmol/L). These biochemical findings were consistent with a diagnosis of methylmalonic acidemia and homocysteinemia. Whole-exome sequencing, followed by Sanger sequencing for verification, identified compound heterozygous variant in the MMACHC gene: c.609G > A (p.Trp203*), a nonsense variant inherited from the patient's mother, and c.482G > A (p.Arg161Gln), a missense variant inherited from the patient's father (Figure 2). According to the guidelines established by the American College of Medical Genetics and Genomics (ACMG), these variants were classified as likely pathogenic. Treatment for late-onset CblC deficiency in adulthood included intramuscular injection of methylcobalamin (0.5 mg/d), oral supplementation of vitamin B6 (30 mg/d), betaine (9 g/d), folic acid (5 mg/d), levkanitine (3 g/d), and subcutaneous injection of dalteparin (5,000 IU/d). After 1 month of treatment, the patient exhibited decreased plasma total homocysteine levels (78.1 μmol/L) and D-dimer levels (0.36), improved irritability, response times, and walking stability. Neuropsychological examination scores changed as follows: MMSE scale (24 points), MoCA Scale (20 points), ICARS Scale (10 points), and BI Scale (95 points). Additionally, the DWI imaging revealed a reversal of cerebellar signal changes. Follow up with the patient for one year. Currently, the patient's ataxia and intelligence has further improved and he can work normally, but he is still taking medication for supplementation of methylcobalamin (1.5 mg/d), vitamin B6 (30 mg/d), betaine (9 g/d), folic acid (5 mg/d), levkanitine (3 g/d).

3 Discussion and conclusion

We present a case report of a 30-year-old male patient who presented with symptoms of cerebellar ataxia and cognitive impairment. Imaging studies revealed bilateral symmetric hyperintensity in the lateral cerebellar hemispheres, primarily observed on DWI. Various potential disorders were considered based on the presence of bilateral cerebellar symmetric lesions on imaging, including cerebral infarction, cerebellitis (autoimmune or infection-related), and toxic encephalopathy (metronidazole, heroin), among

Abbreviations: cblC, cobalamin C; MMA, Methylmalonic acidemia; MRI, Magnetic Resonance Imaging; DWI, Diffusion Weighted Imaging; MMSE, Mini-Mental State Examination; MoCA, Montreal Cognitive Assessment; ICARS, International Cooperative Ataxia Rating Scale; BI, Barthel index; EMG, electromyography; NMDA, N-methyl-D-day aspartate; NMDAR, N-methyl-D-day aspartate receptor.

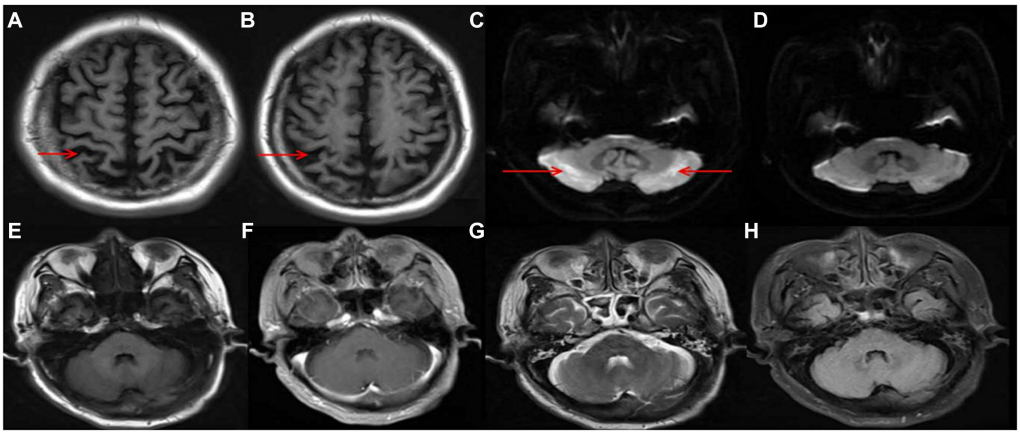

FIGURE 1
Cortical atrophy in T1 **(A,B)**; symmetric hyperintensity in the bilateral lateral cerebellar hemispheres, predominantly manifested in DWI **(C)**; reversal of the of cerebellar lesions after treatment **(D)**; T1/ enhancement/ T2/ FLAIR image no significant changes in cerebellar **(E–H)**.

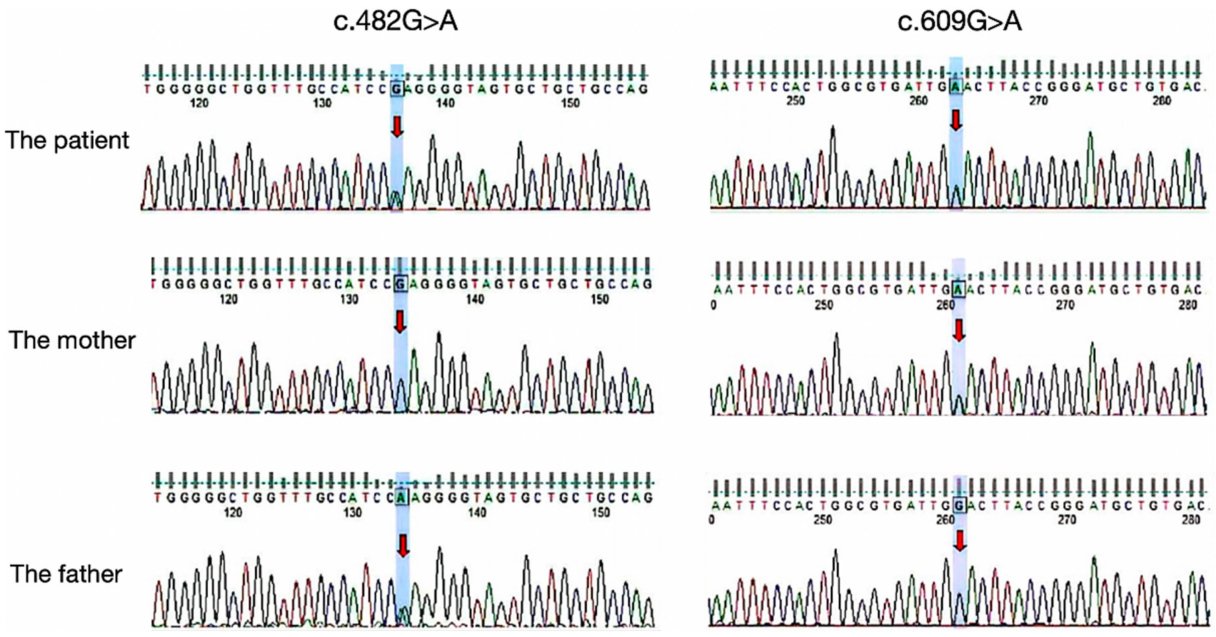

FIGURE 2
Results of the MMACHC gene test. Gene variant in c.482G > A and c.609G > A (red arrows). c.609G > A (p.Trp203*) was a nonsense mutation from his mother and c.482G > A (p.Arg161Gln) is a missense mutation derived from the patient's father.

others (2–5). Through appropriate investigations, these differential diagnoses were ruled out. The patient's blood tests revealed apparent abnormalities in total homocysteine levels, which have been associated with more than 100 diseases or conditions. In adults, values of 10 mmol/L or less are generally considered safe, while values of ≥11 mmol/L warrant intervention (6). Considering the impact of elevated plasma total homocysteine on the nervous system, additional investigations were conducted, including MRI of the cervicothoracic and lumbar spine and screening for organic acids in the urine. The results showed no abnormalities in the spinal MRI, while the elevation of methylmalonic acid indicated a metabolic disease. The diagnosis of late-onset cblC deficiency in adults was confirmed through genetic testing.

MMA, also known as methylmalonic aciduria, is a congenital organic acid metabolic disease with multifactorial autosomal recessive inheritance (7). Various genetic defects in methylmalonic acidemia and homocysteinemia, involving cobalamin metabolism, have been identified, including cblC, cblD, cblF, cblJ, and cblX, with cblC-deficient disease being the most prevalent (8). In 2006, the protein encoded by MMACHC was identified as the cause of cblC deficiency disease, with the MMACHC gene located at 1p34.1 (9). Early-onset cblC disease typically manifests during infancy or within the first year

of life. However, late-onset cblC disease, which appears in adolescence or adulthood, is less common and was first reported in 1980 (10).Only around 100 cases have been reported in the literature (11), often exhibiting atypical clinical symptoms without a family history. Prompt treatment improves prognosis, but late-onset cases are highly heterogeneous and prone to misdiagnosis. On average, there is a delay of 32.1 months from the initial symptoms to diagnosis (12).

Clinical manifestations of late-onset cblC disease may include neurologic symptoms (cognitive dysfunction, myelopathy, gait abnormalities, seizures, pyramidal signs, peripheral neuropathy, and thromboembolic seizures), psychiatric symptoms (progressive cognitive deterioration, degeneration, behavioral and personality changes, social withdrawal, psychosis, confusion), hematologic manifestations, anorexia, renal failure, ocular abnormalities, dermatitis, and pancreatitis, etc. (13–15). Among the various gait abnormalities observed, the predominant manifestations include spastic paraplegia gait, sensory ataxia gait, and stride gait (16). Notably, cerebellar ataxia as a clinical or imaging manifestation is rare in cblC disease.

Neuroimaging findings in late-onset cblC disease are not extensively documented. Diffuse white matter swelling, severe leukoaraiosis of varying degrees, hydrocephalus, corpus callosum atrophy, and symmetric bilateral lesions of the basal ganglia are frequent and distinctive imaging findings in early-onset cblC disease. However, late-onset cases often exhibit cerebral atrophy and patchy lesions in the deep white matter (17–19). Cerebellar involvement is uncommon in cblC disease, and literature review reveals only seven reported cases with cerebellar symptoms or imaging changes (12, 16, 18, 20–23). We summarize the clinical symptoms or MRI differential presentation of the previously reported involving cerebellar related cases with late-onset CblC deficiency in Table 1. The age of onset of the studied cohort was approximately 20 years, and there was a balanced ratio of men to women. Only one patient had a positive family history, and the majority of patients received a diagnosis several years after the initial onset of symptoms. Notably, cognitive deterioration and psychiatric symptoms were the prominent clinical manifestations observed, with only 2 patients developing cerebellar ataxia. Imaging examinations revealed cerebellar lesions in six patients, of which two exhibited concurrent cerebral atrophy and exclusively impacted the cerebellum. One patient demonstrated bilateral cerebellar hemisphere lesions in the T2 sequence, while another patient exhibited T1 low intensity, T2, and DWI hyperintensity in both the cerebellar hemispheres and vermis, with mild enhancement of the lesions. Importantly, the maximum innovation of this article lies in imaging that we present a rare case characterized by cerebellar ataxia and cognitive impairment as the primary disturbances, bilateral lateral cerebellar hemisphere symmetric hyperintensity on DWI without change on T1WI, T2WI, T2FLAIR, and significant cortical atrophy. Among the cohort, three patients exhibited electromyography (EMG) abnormalities, primarily manifesting as sensorimotor polyneuropathy. Unfortunately, complete EMG examination was not conducted for the patients included in this report due to objective reasons, which represents a limitation of this study. Regarding genetic diagnosis, five patients carried the MMACHC gene 482G > A variant. The clinical symptoms of all seven patients improved following treatment with adenosylcobalamin, hydrocobalamin, cyanocobalamin, folic acid, and betaine. Notably, hydrocobalamin drugs, although characterized by long half-lives and easy absorption, are not readily available in the domestic market. In this particular case, the patient received intramuscular injections of methylcobalamin, which led to enhanced clinical symptoms and improved imaging findings.

The pathogenesis of methylmalonic acidemia involves a complex interplay of various mechanisms that contribute to its effects on the nervous system. The cause of cerebellar cytotoxic damage in this patient is unknown, but several potential causes of cerebellar involvement can be considered. Firstly, the cerebellum requires lower levels of methylcobalamin due to its low activity requirements for protein carboxymethylation. As a result, the supply of methylcobalamin to the cerebellar hemispheres is comparatively lower. However, prolonged cobalamin deficiency in the cerebellar hemispheres may render them more vulnerable (24). Secondly, the accumulation of homocysteine stimulates the N-methyl-D-aspartate receptor (NMDAR), leading to increased production of anti-NMDAR antibodies. While cerebellar Purkinje fibers lack NMDAR expression, the binding of anti-NMDAR antibodies to the cerebellar molecular layer and granular layer can cause cytotoxic effects (25, 26). Thirdly, the cerebellar hemisphere has a higher demand for blood, oxygen, and energy metabolism compared to the white matter. Consequently, in metabolic diseases, the cerebellar hemisphere is more susceptible to damage than the white matter. Additionally, the cerebellum is also susceptible to drug and toxin-induced damage, further increasing the likelihood of cerebellar involvement in patients with methylmalonic acidemia (27) (Figure 3). Cerebellar ataxia is commonly seen in neurological practice. There is a wide array of causes of cerebellar ataxia, including vascular, neoplastic, nutritional, metabolic, immune-mediated, infectious, toxic, paraneoplastic and hereditary. MRI is occasionally helpful in making a diagnosis. Most commonly, brain stem and/or cerebellum lesions with reduced diffusivity with ataxia suggest an acquired and acute (usually vascular, inflammatory, or toxic) cause. Despite the utility of neuroimaging in diagnosing cbIC and in identifying the loci and extent of damage, MRI examination often post-dates the acute phase marked by edema affected brain tissue. Therefore, in more cases, atrophy or abnormal signal is the most common manifestation on T2/Flair sequence, less on DWI.

To date, nearly 80 variants in the MMACHC gene have been reported, with 30 of these variants documented in China. The most frequent variant in Europe and the United States is c.271dupA, whereas the most common early-onset variant in China is c.609G > A (28). In the present case, the patient's genetic testing revealed a compound heterozygous variant of the MMACHC genes, specifically c.482G > A and c.609G > A, which are the most commonly reported mutations in cases of late-onset cblC deficiency disease in China. Notably, among cases involving cerebellar manifestations, the c.482G > A variant is the most frequently observed. However, the precise relationship between specific gene variant sites and phenotypes remains unclear.

In conclusion, MMA is a small molecular genetic metabolic disease characterized by acute onset, recurrent courses, nonspecific physical appearance, and imaging features, with remarkable treatment effects. Our case emphasizes the importance of considering genetic metabolic diseases, especially those involving the cerebellum, in adult patients with undiagnosed neurological disorders. Methylmalonic acidemia should be considered as part of the differential diagnosis when bilateral cerebellar lesions are present. In addition, specially

TABLE 1 The clinical symptoms or MRI differential presentation involving cerebellar related cases with late-onset CblC deficiency.

Patient no. [Reference]	Diagnose age	Sex	Clinical symptoms	MRI results	Urine MMA (μM/L)	Serum Hcy (μM/L)	Gene mutations	Gene sites	Outcome
1 (our patient)	30	Male	Cognitive impairment, cerebellar ataxia	Cortical atrophy and symmetric hyperintensities in the bilateral lateral cerebellar hemispheres just on DWI	76.9	296.90	MMACHC	c.609G > A c.482G > A	Improved
2 (12)	14	Female	Cognitive impairment	Hyperintensity in the bilateral cerebellar on T2WI	185.8	110	MMACHC	c.482G > A c.445-446del	Improved
3 (16)	21	Female	Spastic paraplegic gait, lower limb muscle strength decreased	Hyperintensity in the bilateral cerebellar, impaired myelination and periventricular hyperintensity on T2WI	332.9	154.5	MMACHC	c.482G > A c.658-660del	Improved
4 (18)	10	Male	Ataxia gait	Cerebellum, cervical and thoracic cord atrophy	102	89.2	MMACHC	c.217C > T c.615C > A	Improved
5 (20)	29	Female	Cognitive impairment	Abnormal signals in the vermis and in the bilateral cerebellar hemispheres with low signal on T1-weighted image, high signal on T2-weighted image and high signal on DWI sequence with Gd enhancement	306.4	178.41	MMACHC	c.484G > A c.658-660del	Improved
6 (21)	15	Male	Cognitive impairment	Cortical and bilateral cerebellum atrophy	58.42	102.6	MMACHC	c.482G > A c.658-660del	Improved
7 (22)	22	Male	Dysarthria, imbalance walking, weakness of lower limbs, generalized seizure	Bilateral cerebellar on T2/FLAIR hyperintensities, intramedullary T2 hyperintensity at C5–6 with cord atrophy at C7–D7	144	234.4	MMACHC	c.374 T > C c.394C > T	Improved
8 (23)	16	Male	Unsteady gait	MRI of the cervical spine and brain were all normal	149	185.1	MMACHC	c.567dupT c.482 G > A	Improved

10.3389/fneur.2023.1308289

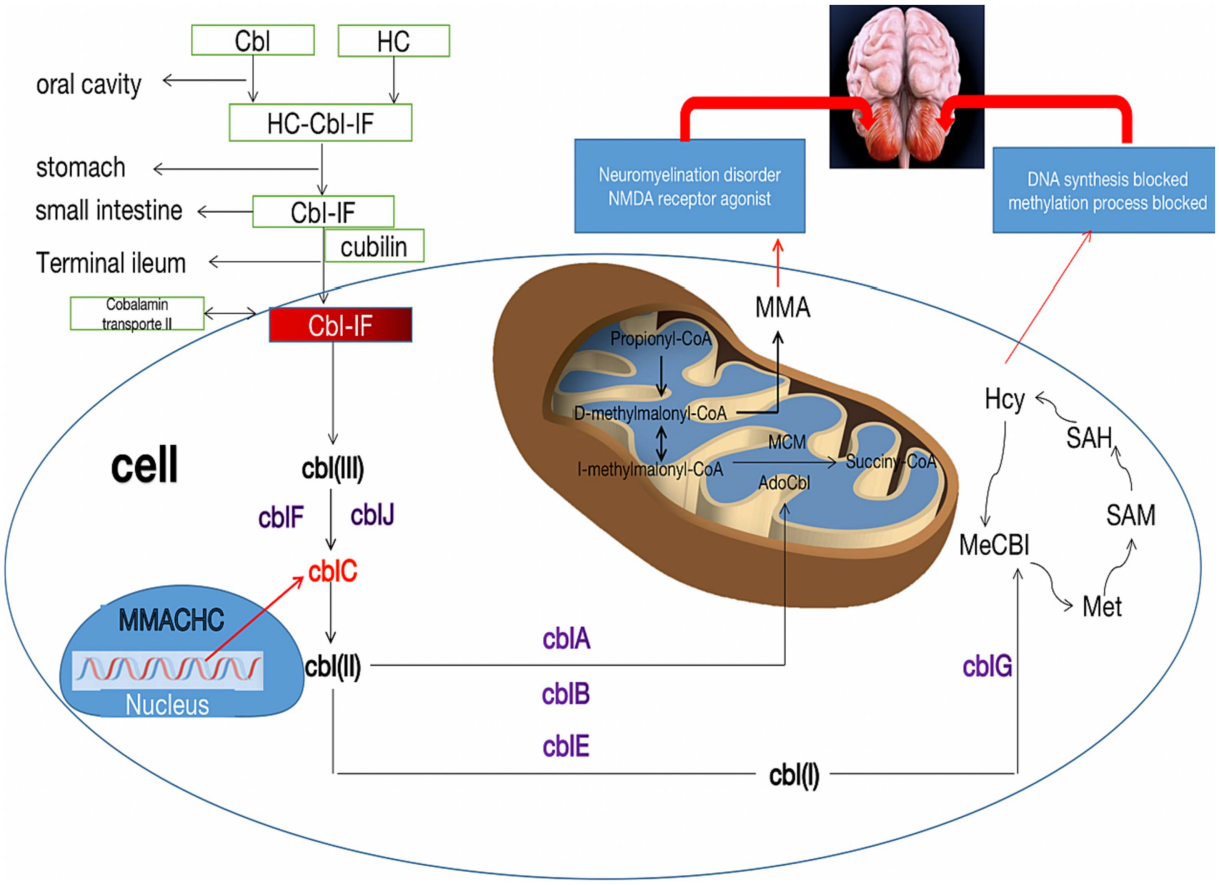

FIGURE 3
Metabolic pathways of cblC defects and its relationship with cerebellar damage. The neurotoxicity of MMA and Hcy due to the cblC defect is described for their importance in the pathophysiology of cerebellar damage. Cbl, cobalamin; HC, haptocorrin; IF, Internalfactor; cblA-G, cblJ, cbl complementation; MMA, methylmalonic acid; Hcy, homocysteine; Met, methionine; SAM, S-adenosyl-methionine; SAH, S-adenosyl-homocysteine; MMACHC, gene responsible for methylmalonic acidemia and homocysteinemia; NMDA, N-methyl-D-day aspartate.

when preliminary investigations exclude most acquired ataxia. Coexistent clinical or subclinical neurological presentations, may support this diagnosis. Further screening for abnormal intracellular vitamin B12 metabolism, biochemical factors, or genetic mutations, may help to confirm the diagnosis and initiate timely treatment.

Data availability statement

The datasets presented in this article are not readily available because of ethical and privacy restrictions. Requests to access the datasets should be directed to the corresponding author.

Ethics statement

The studies involving humans were approved by the Medical Ethical Research Committee of the General Hospital of Northern Theater Command. The studies were conducted in accordance with the local legislation and institutional requirements. Written informed consent for participation in this study was provided by the participants' legal guardians/next of kin. Written informed consent was obtained from the individual(s), and minor(s)' legal guardian/next of kin, for the publication of any potentially identifiable images or data included in this article.

Author contributions

MS: Writing – original draft, Writing – review & editing. YD: Writing – review & editing.

Funding

The author(s) declare that no financial support was received for the research, authorship, and/or publication of this article.

Conflict of interest

The authors declare that the research was conducted in the absence of any commercial or financial relationships that could be construed as a potential conflict of interest.

Publisher's note

References

1. Bourque DK, Mellin-Sanchez LE, Bullivant G, Cruz V, Feigenbaum A, Hewson S, et al. Outcomes of patients with cobalamin C deficiency: a single center experience. *JIMD Rep*. (2021) 57:102–14. doi: 10.1002/jmd2.12179

2. Zhou C, Fan H, Chen H, Wang H, Li Z, Xu N, et al. Evaluation of clinical features and stroke etiology in patients with bilateral middle cerebellar peduncle infarction. *Eur Neurol*. (2020) 83:271–8. doi: 10.1159/000508835

3. Yildirim M, Gocmen R, Konuskan B, Parlak S, Yalnizoglu D, Anlar B. Acute Cerebellitis or Postinfectious cerebellar Ataxia? Clinical and imaging features in acute Cerebellitis. *J Child Neurol*. (2020) 35:380–8. doi: 10.1177/0883073820901407

4. Jiang J, Wang J, Lin M, Wang X, Zhao J, Shang X. Bilateral middle cerebellar peduncle lesions: neuroimaging features and differential diagnoses. *Brain Behav*. (2020) 10:e01778. doi: 10.1002/brb3.1778

5. Emekli AS, Parlak A, Göcen NY, Kürtüncü M. Anti-GAD associated post-infectious cerebellitis after COVID-19 infection. *Neurol Sci*. (2021) 42:3995–4002. doi: 10.1007/s10072-021-05506-6

6. Smith AD, Refsum H. Homocysteine – from disease biomarker to disease prevention. *J Intern Med*. (2021) 290:826–54. doi: 10.1111/joim.13279

7. Lee N, Kim D. Toxic metabolites and inborn errors of amino acid metabolism: what one informs about the other. *Meta*. (2022) 12:527. doi: 10.3390/metabo12060527

8. Kalantari S, Brezzi B, Bracciamà V, Barreca A, Nozza P, Vaisitti T, et al. Adult-onset CblC deficiency: a challenging diagnosis involving different adult clinical specialists. *Orphanet J Rare Dis*. (2022) 17:33. doi: 10.1186/s13023-022-02179-y

9. Lerner-Ellis JP, Tirone JC, Pawelek PD, Doré C, Atkinson JL, Watkins D, et al. Identification of the gene responsible for methylmalonic aciduria and homocystinuria, cblC type. *Nat Genet*. (2006) 38:93–100. doi: 10.1038/ng1683

10. Shinnar S, Singer HS. Cobalamin C mutation (methylmalonic aciduria and homocystinuria) in adolescence. A treatable cause of dementia and myelopathy. *N Engl J Med*. (1984) 311:451–4. doi: 10.1056/NEJM198408163110707

11. Huemer M, Diodato D, Schwahn B, Schiff M, Bandeira A, Benoist JF, et al. Guidelines for diagnosis and management of the cobalamin-related remethylation disorders cblC, cblD, cblE, cblF, cblG, cblJ and MTHFR deficiency. *J Inherit Metab Dis*. (2017) 40:21–48. doi: 10.1007/s10545-016-9991-4

12. Wang SJ, Yan CZ, Liu YM, Zhao YY. Late-onset cobalamin C deficiency Chinese sibling patients with neuropsychiatric presentations. *Metab Brain Dis*. (2018) 33:829–35. doi: 10.1007/s11011-018-0189-3

13. Chen Z, Dong H, Liu Y, He R, Song J, Jin Y, et al. Late-onset cblC deficiency around puberty: a retrospective study of the clinical characteristics, diagnosis, and treatment. *Orphanet J Rare Dis*. (2022) 17:330. doi: 10.1186/s13023-022-02471-x

14. Socha DS, DeSouza SI, Flagg A, Sekeres M, Rogers HJ. Severe megaloblastic anemia: vitamin deficiency and other causes. *Cleve Clin J Med*. (2020) 87:153–64. doi: 10.3949/ccjm.87a.19072

15. Wiedemann A, Oussalah A, Lamireau N, Théron M, Julien M, Mergnac JP, et al. Clinical, phenotypic and genetic landscape of case reports with genetically proven inherited disorders of vitamin B(12) metabolism: a meta-analysis. *Cell Rep Med*. (2022) 3:100670. doi: 10.1016/j.xcrm.2022.100670

16. Chang KJ, Zhao Z, Shen HR, Bing Q, Li N, Guo X, et al. Adolescent/adult-onset homocysteine remethylation disorders characterized by gait disturbance with/without psychiatric symptoms and cognitive decline: a series of seven cases. *Neurol Sci*. (2021) 42:1987–93. doi: 10.1007/s10072-020-04756-0

17. Chen T, Sui C, Lin S, Guo B, Wang Y, Yang L. Follow-up study of neuropsychological scores of infant patients with cobalamin C defects and influencing factors of cerebral magnetic resonance imaging characteristics. *Front Neurosci*. (2022) 16:1093850. doi: 10.3389/fnins.2022.1093850

18. Wang SJ, Yan CZ, Wen B, Zhao YY. Clinical feature and outcome of late-onset cobalamin C disease patients with neuropsychiatric presentations: a Chinese case series. *Neuropsychiatr Dis Treat*. (2019) 15:549–55. doi: 10.2147/NDT.S196924

19. Chen T, Gao Y, Zhang S, Wang Y, Sui C, Yang L. Methylmalonic acidemia: neurodevelopment and neuroimaging. *Front Neurosci*. (2023) 17:1110942. doi: 10.3389/fnins.2023.1110942

20. Wang S, Wang X, Xi J, Yang W, Zhu M. Case report: a case of adult Methylmalonic Acidemia with bilateral cerebellar lesions caused by a new mutation in MMACHC gene. *Front Neurol*. (2022) 13:935604. doi: 10.3389/fneur.2022.935604

21. Wang X, Yang Y, Li X, Li C, Wang C. Distinct clinical, neuroimaging and genetic profiles of late-onset cobalamin C defects (cb1C): a report of 16 Chinese cases. *Orphanet J Rare Dis*. (2019) 14:109. doi: 10.1186/s13023-019-1058-9

22. Aliyar A, Endrakanti M, Singh RK, Elavarasi A, Gupta N, Vibha D, et al. Late-onset cobalamin C disease: rare but treatable. *Pract Neurol*. (2022) 22:418–21. doi: 10.1136/practneurol-2022-003447

23. Wei Y, Hao H. Late-onset cobalamin C disease presenting with acute cerebellar ataxia. *Neurol Sci*. (2021) 42:4839–42. doi: 10.1007/s10072-021-05541-3

24. Pavlov CS, Damulin IV, Shulpekova YO, Andreev EA. Neurological disorders in vitamin B12 deficiency. *Ter Arkh*. (2019) 91:122–9. doi: 10.26442/00403660.2019.04.000116

25. Okada K, Tanaka H, Temporin K, Okamoto M, Kuroda Y, Moritomo H, et al. Akt/mammalian target of rapamycin signaling pathway regulates neurite outgrowth in cerebellar granule neurons stimulated by methylcobalamin. *Neurosci Lett*. (2011) 495:201–4. doi: 10.1016/j.neulet.2011.03.065

26. Yeshokumar AK, Sun LR, Klein JL, Baranano KW, Pardo CA. Gait disturbance as the presenting symptom in young children with anti-NMDA receptor encephalitis. *Pediatrics*. (2016) 138:e20160901. doi: 10.1542/peds.2016-0901

27. Pedroso JL, Vale TC, Braga-Neto P, Dutra LA, França MC Jr, Teive HAG, et al. Acute cerebellar ataxia: differential diagnosis and clinical approach. *Arq Neuropsiquiatr*. (2019) 77:184–93. doi: 10.1590/0004-282x20190020

28. Wang C, Li D, Cai F, Zhang X, Xu X, Liu X, et al. Mutation spectrum of MMACHC in Chinese pediatric patients with cobalamin C disease: a case series and literature review. *Eur J Med Genet*. (2019) 62:103713. doi: 10.1016/j.ejmg.2019.103713

frontiers | Frontiers in Neurology

TYPE Case Report
PUBLISHED 24 January 2024
DOI 10.3389/fneur.2024.1343025

OPEN ACCESS

EDITED BY
Huifang Shang,
Sichuan University, China

REVIEWED BY
Siyi He,
General Hospital of Western Theater Command, China
Lufei Wang,
College of Stomatology, Guangxi Medical University, China

*CORRESPONDENCE
Yimin Hua
✉ nathan_hua@163.com
Jinrong Li
✉ lijinrong224@163.com
Yifei Li
✉ liyfwcsh@scu.edu.cn

†These authors have contributed equally to this work

RECEIVED 24 November 2023
ACCEPTED 11 January 2024
PUBLISHED 24 January 2024

CITATION
Jing S, Peng M, He Y, Hua Y, Li J and Li Y (2024) A novel compound heterozygous variant of *ECEL1* induced joint dysfunction and cartilage degradation: a case report and literature review.
Front. Neurol. 15:1343025.
doi: 10.3389/fneur.2024.1343025

A novel compound heterozygous variant of *ECEL1* induced joint dysfunction and cartilage degradation: a case report and literature review

Siyuan Jing[1†], Mou Peng[1†], Yuping He[1,2†], Yimin Hua[1*], Jinrong Li[1*] and Yifei Li[1*]

[1]Key Laboratory of Birth Defects and Related Diseases of Women and Children of MOE, Department of Pediatrics, West China Second University Hospital, Sichuan University, Chengdu, China, [2]Department of Nursing, West China Second University Hospital, Sichuan University, Chengdu, China

Background: Distal arthrogryposis type 5D (DA5D) represents a subtype of distal arthrogryposis (DA) characterized by congenital joint contractures in the distal extremities. DA5D is inherited in a rare autosomal recessive manner and is associated with the *ECEL1* gene. In this report, we describe a case of an infant with bilateral knee contractures and ptosis, caused by a novel compound heterozygous mutation of *ECEL1*.

Case presentation: We conducted DNA extraction, whole-exome sequencing analysis, and mutation analysis of *ECEL1* to obtain genetic data on the patient. We subsequently analyzed the patient's clinical and genetic data. The proband was a 6 months-old male infant who presented with significant bilateral knee contracture disorders and bilateral ptosis. MRI demonstrated cartilage degradation in knee joint. Whole-exome sequencing of the patient's DNA revealed a compound heterozygous mutation of c.2152-15C>A and c.110_155del in *ECEL1*. Analysis with the MutationTaster application indicated that c.110_155del was pathogenic (probability = 1), causing frameshift mutations affecting 151 amino acids (p.F37Cfs*151). The truncated protein lost the substructure of a transmembranous site based on the predicted protein crystal structure AF-O95672-F1. The variant of c.2152-15C>A of *ECEL1* was also predicted to be disease-causing (probability = 0.98) as it impaired the methylation of *ECEL1* serving as an H3K27me3 modification site, which led to the dysfunction of the second topological domain. Therefore, we concluded that the compound heterozygous mutation caused the pathogenic phenotype of this proband.

Conclusion: The present case highlights the usefulness of molecular genetic screening in diagnosing unexpected joint disorder. Identification of novel mutations in the *ECEL1* gene broadens the mutation spectrum of this gene and adds to the genotype-phenotype map of DA5D. Furthermore, rapid whole-exome sequencing analysis enabled timely diagnosis of this rare disease, facilitating appropriate treatment and scheduled follow-up to improve clinical outcomes.

KEYWORDS

***ECEL1*, joint disorder, WES, case report, literature review**

1 Introduction

Distal arthrogryposis is a congenital contracture disorder that is inheritable. The disorder mainly affects the flexion and extension of distal joints and is not associated with neurological and/or muscle diseases. Since it was introduced by Hall et al. (1), several clinical manifestations have been described, including contractures of distal joints, scoliosis, sensorineural hearing loss, ophthalmoplegia, multiple pterygium, and camptodactyly. The contractures of distal joints, such as those in the ankle, knee, hip, hand, wrist, elbow, and shoulder, typically contribute to the significant morbidity of all subtypes of distal arthrogryposis. Based on the typical clinical presentations, distal arthrogryposis can be divided into several subtypes (2). Distal arthrogryposis type 5D (DA5D) is a rare genetic disorder that primarily affects the hands and feet, resulting in multiple joint contractures, muscle weakness, and bone abnormalities. In addition, DA5D reveals a unique feature due to its specific extraocular muscle involvement, leading to ophthalmoplegia and ptosis (3). About 50% of distal arthrogryposis cases are caused by genetic variants that encode skeletal myofibers' contractile proteins, including *TPM2*, *TNNI2*, *TNNT3*, *MYH3*, *MYBPC1*, *MYH8*, *FBN2*, *PIEZO2* and *ECEL1* (3). Currently, there is insufficient research to fully elucidate the genetic-related molecular function of the reported gene, while most of the diseases demonstrate autosomal recessive inheritance. Genome sequencing has been used to identify a missense mutation in the *MYH3* gene in a family with DA5D. *MYH3* encodes a myosin protein involved in muscle contraction, and the mutation was found to disrupt the protein's function, leading to abnormal muscle development and contractures (4). Similarly, a study identified a *de novo* missense mutation in the *PIEZO2* gene, which encodes a mechanosensitive ion channel involved in touch and proprioception. The mutation was found to affect the function of the channel, leading to abnormal sensory feedback and joint contractures (5). In addition, a mutation was identified in the *GPR126* gene in a family with DA5D. *GPR126* encodes a transmembrane protein involved in myelination and nerve function, and the mutation was found to affect the protein's function, leading to abnormal development of the peripheral nervous system and joint contractures (6). Identifying these additional mutations may also provide new insights into the pathogenesis of the disease and potential therapeutic targets.

Endothelin-converting enzyme-like 1 (*ECEL1*) is a transmembrane zinc metalloprotease primarily localized in the endoplasmic reticulum. It is known to be involved in developing neuromuscular junctions and bone development during the prenatal phase (7, 8). *ECEL1* had been confirmed to be involved in the bone development and chondrocyte homeostasis. Through a pan-genomic approach, Dieterich et al. confirmed that homozygous or compounded heterozygous variants in the *ECEL1* gene on chromosome 2q37 were associated with DA5D. The disorder is caused by mutations impairing the function of ECEL1, resulting in abnormal development of the neuromuscular junctions and synapses, leading to cartilage degradation. However, there are only a few reported cases of DA5D associated with ECEL1 variants, which highlights the need for further understanding of ECEL1's molecular function.

In the present study, we reported a six-month-old male infant who suffered DA5D, and a compound heterozygous mutations of *ECEL1* (NM_004826: c.2152-15C>A, c.110_155del p.F37Cfs*151) had been identified in the proband. Furthermore, the allele of c.2152-15C>A was maternally inherited, and the allele of c.110_155del was paternally inherited, a novel pathogenic variant of *ECEL1*. This report expanded the understanding of *ECEL1* in DA5D and emphasized the importance of assessment of ECEL1 compound heterozygous variants in patients with joint disorder. Also, the timely WES detection promoted early intervention for DA5D which help to improve the prognosis.

2 Methods

The study was approved by the ethics committee of the West China Second Hospital of Sichuan University (approval number 2014-034). In addition, we obtained written, informed consent from the patient's parents prior to performing WES and for the inclusion of the patient's clinical and imaging details in publications.

The genetic test had been performed at 8 months-old. The peripheral blood sample was obtained from the patient in an ethylenediaminetetraacetic acid (EDTA) anticoagulant blood sample tube that stored at 4°C for less than 6 h. DNA was extracted using the Blood Genome Column Medium Extraction Kit (Tiangen Biotech, Beijing, China) according to the manufacturer's instructions. WES was performed using the NovaSeq 6000 platform (Illumina, San Diego, CA, United States), and the raw data were processed using FastP to remove adapters and filter low-quality reads. Paired-end reads were aligned to the Ensembl GRCh37/hg19 reference genome using the Burrows–Wheeler Aligner. Variant annotation was performed in accordance with database-sourced minor allele frequencies (MAFs) and practical guidelines on pathogenicity issued by the American College of Medical Genetics. The annotation of MAFs was performed based on the 1,000 Genomes, dbSNP, ESP, ExAC, and Chigene inhouse MAF database, Provean, Sift, Polypen2_hdiv, and Polypen2_hvar databases using R software (R Foundation for Statistical Computing, Vienna, Austria).

3 Case presentation

3.1 Clinical presentation and physical examination

The proband was a male infant admitted to our hospital at 6 months of age. However, the patient had received several medical consultations starting from 1 month of age due to severe and worsening symptoms of bilateral knee flexion and extension disorders and bilateral ptosis. In addition to the two primary symptoms, both thumbs showed adduction. and the facial abnormalities were arched eye brows, micrognathia, broad frontotemporal and high palatine arches. The parents provided gestational information that the routine fetal assessment ultrasound had identified the patient's standard position of major joints, while femur lengths were within the normal range at different gestational stages. In addition, cranial screening and echocardiography found no impairments or abnormalities. No fetal genetic tests related to low risk of Down syndrome were conducted. The proband was delivered by cesarean section at 38 + 6 gestational weeks, with a birth weight of 2,600 g (P3.6), height of 50 cm (P41.6), and head circumference of 34 cm (P33). Initial physical examination

after birth showed fully extended joint movement and normal muscle tone. Furthermore, this was the first child of the couple, and they denied any positive family history of chromosomal abnormalities, birth defects, autoimmune disease, rheumatoid arthritis, epilepsy, and neurological developmental disorder. Additionally, they denied any potential exposure to teratogens during pregnancy. All onset time points of major symptoms are presented in a timeline diagram in Figure 1.

According to the patient's parents, bilateral ptosis was first observed at 2 weeks of age (Figure 2A). The ophthalmological evaluation revealed myogenic ptosis with levator palpebrae dysfunction. Lagophthalmos and refractive errors were not detected at such a young age. Additionally, the patient's parents reported that bilateral knee flexion disorders began at 3 months of age (Figures 2A′–A′′). At this age, the patient's weight, length, and head circumference percentiles remained between P20 and P50.

No other birth defects were detected based on the physical examination performed when the patient was 6 months old. The skull shape was within normal limits, and visual and hearing evaluations were normal. Physical examination of the chest, heart, and abdomen did not reveal any abnormalities, except for the absence of scoliosis or hyperlordosis. The patient's motor development was assessed and found to be expected for neck, upper limb, and foot movements, with the ability to maintain balance while sitting. However, both knees showed impairments in both flexion and extension. Specifically, the left knee could only be passively flexed at an angle of 50°, while the right knee could be passively flexed to a degree of 55°, and neither joint could be placed in an extended position. In addition, external rotation of the hip joint was slightly impaired, which limited the movements of the lower extremities. The spine was normal without any scoliosis or curvature.

At the age of 8 months, the patient exhibited aggressive and severe ptosis. Furthermore, at 8 months old, he was unable to sit independently and failed to handle grasp building blocks by 12 months of age. The Gesell evaluation conducted at 12 months revealed a moderate delay in gross and fine motor development. Consequently, the proband underwent regular daily rehabilitation training, including head control, rolling over, crawling training, assisted standing, bilateral hand grasping, and sitting balance, as part of the training program.

3.2 Laboratory and imaging evaluation

Blood gas analysis, blood cell counts, and hepatic and renal function yielded no significant findings. The essential metabolic screening did not identify any impairment. The echocardiography demonstrated a normal heart function and structure (Figure 2B). The Hip ultrasonography showed a Graf type I structure on his left hip joint and a Graf type IIa structure on his right hip joint (Figure 2C). X-ray examination of the hip and knee joint showed no definite abnormality in the anterior-posterior view. In contrast, the lateral view demonstrated an over-extensive positive of the knee joint (Figures 2D,D′). In addition, the joint MRI presented normal signaling in muscles, bones, and ligaments associated with his knee joints while it still presented an over-extensive position with a decreased volume of cartilage, indicating degradation of chondrocyte, while the tail vertebras were normal (Figures 2E,E′). The cerebral MRI revealed a typical structure and signaling in T1 and T2 (Figures 2F,F′). Moreover, electromyography was involved, which presented a normal muscle response.

3.3 Molecular results

According to the analysis result of WES, a novel compound heterozygous variant had been identified as c.2152-15C>A and c.110_155del (p.F37Cfs*151) of *ECEL1* gene. The Sanger validation demonstrated that the c.2152-15C>A allele was maternal inherited and the c.110_155del allele was paternal inherited (Figure 3A). The variant of *ECEL1* c.110_155del had never reported in database (Figure 3B), while two cases reported the variant of *ECEL1* c.110_155del. However, this should be the first report of a patients with the compound variants with c.2152-15C>A and c.110_155del together. The Sanger sequencing had been presented in Figure 3C. Besides, we had excluded all the potential variants

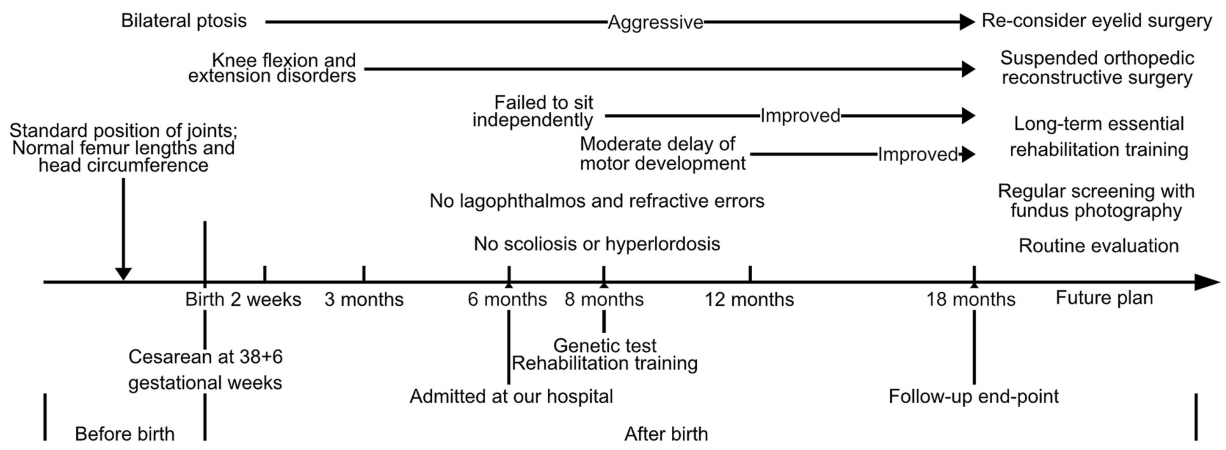

FIGURE 1
Time-line diagram presented the onset timepoints of major symptoms and further therapeutic plan for this DA5D patient with a compound heterozygous variant of *ECEL1* (c.2152-15C>A and c.110_155del).

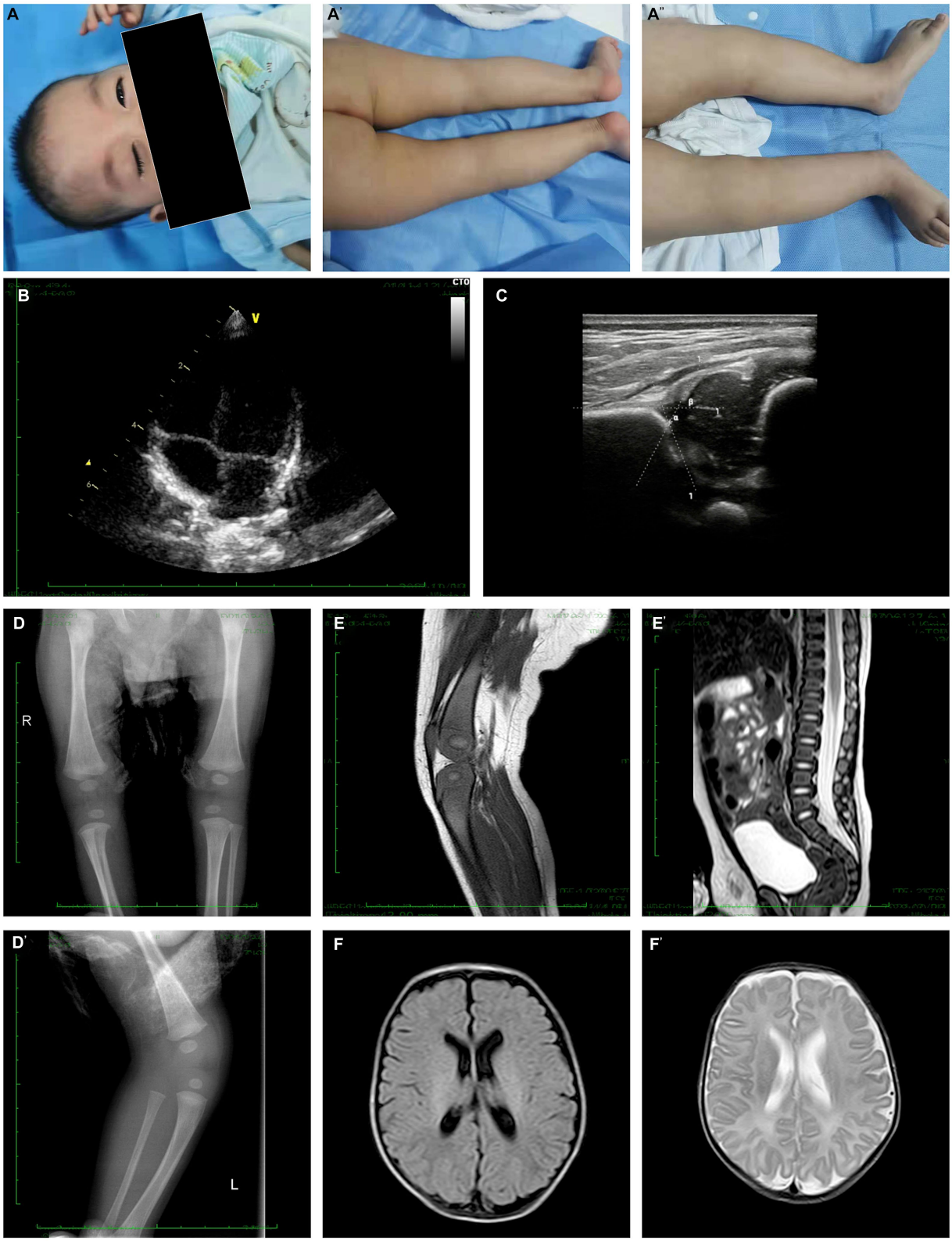

FIGURE 2
Clinical and radiology manifestation in the current proband. **(A)** The proband presented bilateral ptosis and impaired flexion of bilateral knees. **(B)** Echocardiography demonstrated a normal heart function and structure. **(C)** Hip ultrasonography showed Graf type I structure on his left hip joint. **(D)** X-ray examination of hip joint and knee joint showed that there was no definite abnormality in anterior-posterior view, while the lateral view demonstrated an over-extensive positive of knee joint. **(E)** The joint MRI presented a normal signaling in muscles, bones and ligaments associated to his knee joints while it still presented an over-extensive position, and the tail vertebras were normal. **(F)** The cerebral MRI revealed a normal structure and signaling both in T1 and T2.

10.3389/fneur.2024.1343025

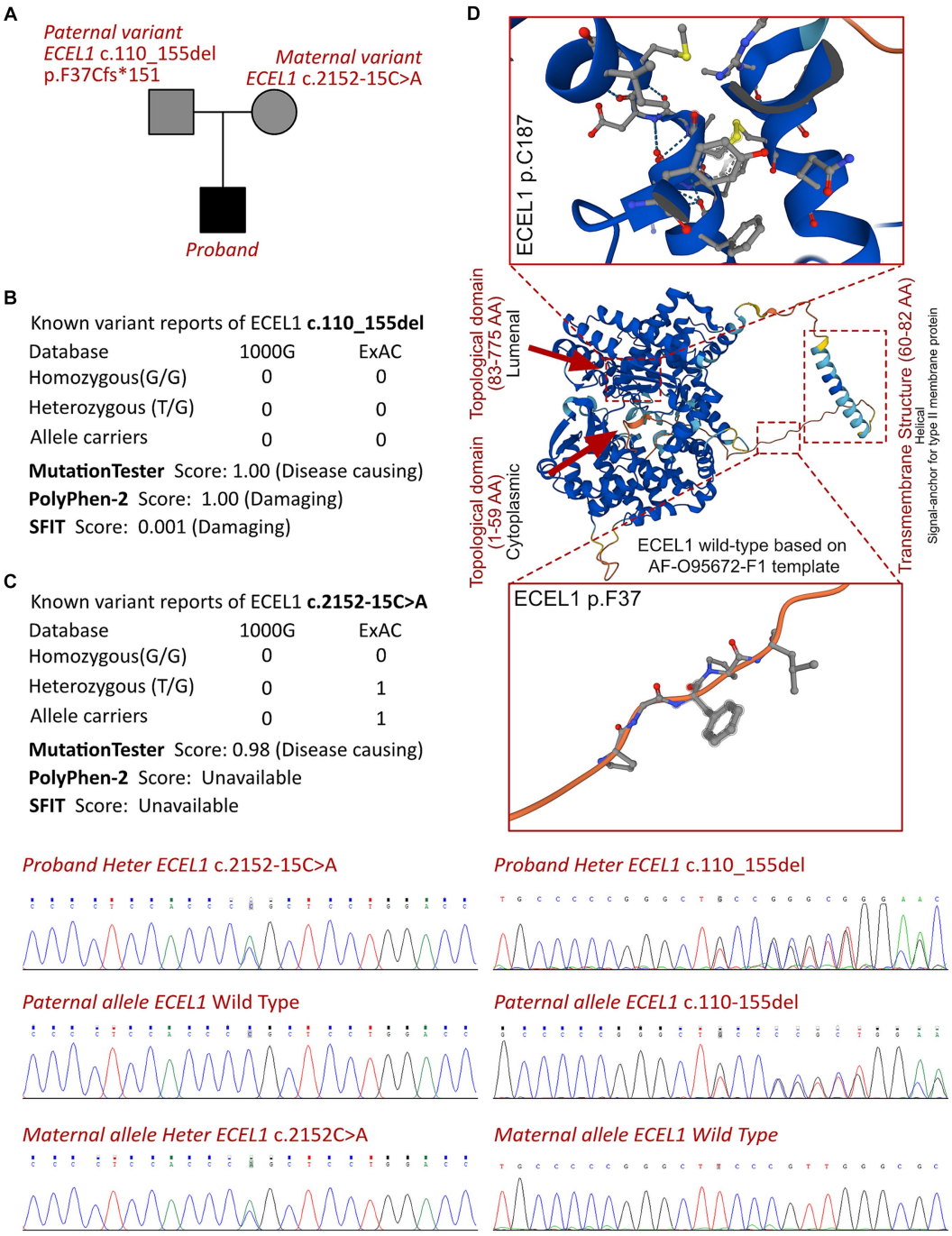

FIGURE 3
The ECEL1 molecular analysis. **(A)** The proband exhibited a compound heterozygous variant of ECEL1 (c.2152-15C>A and c.110_155del, p.F37Cfs*151). **(B)** The variant of ECEL1 c.110_155del had never reported in 1000G and ExAC, it has predicted protein damaging by PolyPhen-2 and SFIT, while only one report had been retrieved of the ECEL1 c.2152-15C>A variant. **(C)** Sanger sequence validation. **(D)** Protein structure predicted by AlphaFold (AF-O95672-F1), two topological domains and one transmembrane structure had been revealed with analyzed crystal structure. The variant of c.110_155del leads to the truncated protein locating in the substructure of transmembranous site.

involved in neurological development and muscle disordered. Then we reviewed all the other variants which were reported as pathogenic or likely pathogenic ones, and none of them was confirmed to be associated with the phenotype of the proband. So that, we suspected the compound heterozygous variant of ECEL1 contributed to the pathogenic phenotype of this proband. To elucidate the molecular architecture of the human *ECEL1* gene, we used MutationTaster with R software to predict the pathogenicity of *ECEL1* c.2152-15C>A and c.110_155del (p.F37Cfs*151), and assess the impact of these mutations on protein structure. As there was no available full-length protein crystal structure for ECEL1 which had been analyzed by X-ray or cryo-EM, AlphaFold protein

structure software[1] tool had been used to predicted protein crystal structure. The protein structure of ECEL1 has been built and named AF-O95672-F1 (9, 10). Within the structure, two important domains (topological domain) had been revealed with analyzed crystal structure. Then we performed modeling analysis using the SWISS-MODEL[2] for the domain in wild type with the AF-O95672-F1.A template. We estimated the capability of the protein structure using Ramachandran plots. According to the American College of Medical Genetics, the mutation c.110_155del has certain pathogenicity (PVS1 + PM3 + PM2_Supporting), while the mutation c.2152-15C>A has not been reported in any populations and has uncertain pathogenicity (PM2_Supporting+PM3). The analyses from MutationTaster revealed the variant of c.110_155del impaired the transcription of *ECEL1* leading to amino acid sequence changes, frameshift, protein features affected, and truncated proteins and the variant was predicted as disease causing. The truncated protein lost the substructure of transmembranous site (Figure 3D). Although the variant of c.2152-15C>A of *ECEL1* would not alter the amino acid sequence in prior of exon 16, but this variant impaired the methylation of *ECEL1* serving as a H3K27me3 modification site, which was also predicted as disease causing due to the potential dysfunction of second Topological domain. DA5D is caused by homozygous or compound heterozygous variants, especially for *ECEL1*, which contributes as an autosomal recessive manner. So that, the newly identified variants of *ECEL1* need to be addressed their pathogenicities in specific cases. Although the variants of *ECEL1* c.2152-15C>A and c.110_155del had been retrieved in databases, there was no reported diagnosed cases could be analyzed for each variant. It means, such variants had been observed in population sequencing screening, and there was no convinced evidence to make an association between the mutations of *ECEL1* c.2125-15C>A and c.110_155del. Thus, this is the very first case to present a certain diagnosed case of DA5D with compound heterozygous variants, indicating and verifying the pathogenicities of the two variants, and draw an association between the novel genotype and clinical phenotype. So that, we concluded that the compound variant of *ECEL1* would be responsible for the pathogenic phenotype of this proband.

3.4 Final diagnosis and treatment

Upon analyzing the clinical manifestations, conducting imaging assessments, and genetic screening, the patient has been diagnosed with DA5D. A long-term follow-up plan has been devised for the proband, which includes ophthalmological, orthopedic, neurological, and developmental evaluations. The ophthalmologists have suggested regular screenings with fundus photography for the proband and re-evaluating eyelid surgical treatment based on the examination. Although there were no lagophthalmos and refractive errors, previous studies have shown that such complications are age-dependent, and regular evaluation is helpful for early detection. Tarsorrhaphy would be considered during follow-up to minimize corneal exposure, which is the most adverse ophthalmic complication leading to corneal perforation and blindness. Treatment for ptosis should be provided when the visual axis is blocked.

Orthopedic assessments are critical in managing DA5D, and at 18 months of age, the degree of joint contractures of hip joints is not significantly severe. Therefore, orthopedic reconstructive surgery has not been performed. The general structure of the spine is typical, and other joints do not show any contractures. However, due to fibrosis proliferation, the contracture phenotypes are expected to limit the function of major joints more extensively, and the indication for surgical therapy should be reconsidered. The parents have been informed that such surgeries may not be avoidable to relieve joint contractures and scoliosis. Rehabilitation treatment of the hip joint has been performed to maintain its development. Long-term essential rehabilitation training has improved muscular function, enabling the proband to sit and walk independently, which was the perspective of the patient's parents. Rehabilitation training includes three aspects: movement, language and environment adaptation training. The important exercise training for this patient includes exercises such as pinching objects with fingers, turning over, crawling, and walking with railings. However, the proband experiences significant difficulty in completing squatting. A re-examined Gesell assessment at 18 months old revealed only slight delays in gross and major motor movements, significantly improving compared to the situation before rehabilitation therapy. And the maximal passive flexibility degree of hip-joint would up to 120 degree. Therefore, regular and long-term rehabilitation therapy is still considered helpful and should be administered as early as possible, which would benefit the prognosis of this disease.

4 Discussion

Distal arthrogryposis is a specific type of arthrogryposis, and its symptoms typically involve restricted movement of the distal joint, which cannot be fully flexed or extended. These impairments can affect various body parts, such as the feet, ankles, knees, hands, wrists, elbows, hips, and shoulders. In some severe cases, impairments in temporomandibular and atlantoaxial joints may also be present since birth. The rapid development of genetic, molecular, and radiological imaging techniques has provided essential insights into distal arthrogryposis. Clinical features and genetic associations have contributed to the subtype's identification. However, since distal arthrogryposis is a rare disorder, there is limited cohort research on this condition. Nevertheless, case reports have illustrated the essential clinical characteristics of distal arthrogryposis. During fetal development, reduced intrauterine movement may accumulate connective tissue around the distal joints, resulting in a pathogenic phenotype postnatally (11). With the increased identification of genetic variants in this condition, 10 gene variants have been associated with distal arthrogryposis, including *TPM2*, *TNNI2*, *TNNT3*, *MYH3*, *MYBPC1*, *MYH8*, *FBN2*, *PIEZO2*, and *ECEL1* (3). These genes play crucial roles in cartilage development, myofibroblast differentiation, and proliferation. At present, this disease is considered to be a congenital non-progressive disease. For children with early detection and diagnosis, rehabilitation training can significantly improve related joint symptoms in the critical period of their development, and later surgical treatment is more of a supplementary

1 https://alphafold.ebi.ac.uk/

2 https://swissmodel.expasy.org/

treatment for patients with severe related symptoms and who can accept surgery.

Previous literature reviews have shown that ptosis is the most commonly observed clinical manifestation in patients with DA5D, with 43 out of 57 reported cases experiencing ptosis (3, 8, 12–26). This characteristic is considered congenital and myogenic and results from the lack of an eyelid crease and dysfunction of the levator muscle (27). Fibrosis of the muscle can also cause significant ocular complications, including lagophthalmos and corneal injuries. Aggressive contractures, including scoliosis, can also result from joint fibrosis. While motor function development is often delayed in younger patients, most of them exhibit nearly regular motor function (20, 22). Therefore, early diagnosis, careful follow-up to manage related complications, and administering rehabilitation therapy are crucial to treating this disease. However, ptosis or limited hip abduction may not be specific symptoms in children, which can lead to delayed diagnosis of DA5D. Additionally, the molecular mechanisms of DA5D remain unclear, which hinders the development of precise medications. With the rapid application of WES in diagnosing rare diseases, DA5D can be identified more definitively in a shorter time, providing more molecular information about the etiology of these diseases. Foe this proband, the variant of *ECEL1* c.110_155del could cause the truncated protein which lead to the transcriptional and translational impairments. Given that, it was critical to identify the impact of *ECEL1* c.2125-15C>A on protein structure and function. Indeed, the variant hind in splice site might not result in protein structural formation. Otherwise, it would significantly reduce the expression of *ECEL1*, as DA5D was associated with autosomal recessive manner which indicated the bi-alleles dysfunction. According to the analysis and the convinced clinical manifestation and targeted variants, we assumed that the variant of ECEL1 c.2125-15C>A in splice site would impair the translation of ECEL1.

DA5D is a specific type of distal arthrogryposis inherited in an autosomal recessive manner and is characterized by the involvement of the extraocular muscles and cartilage. In this review, we examined case reports of DA5D from the past few decades and summarized all the genetic mutation sites. Their corresponding changed amino acid sequences and all the clinical features demonstrated by genetic manners (see Table 1). Dieterich et al. (8) conducted a genome-wide single-nucleotide polymorphism (SNP) genotyping association study and identified a relationship between DA5D and the *ECEL1* gene. The *ECEL1* gene contains 18 exons that encode UTRs and protein-coding-sequence domains, as well as three Zn^{2+} binding sites and two active sites called topological domains. ECEL1 cleaves neuropeptides at a specific site within the C-terminal region, and this cleavage is regulated by zinc binding to the protein. This study provides insight into the substrate specificity and regulation of ECEL1 (24). Dysfunction of the ECEL1 molecule can be caused by impairments in each domain and transmembranous part. The mutation disrupts the splicing of the *ECEL1* gene, resulting in a truncated protein that lacks key functional domains, leading to DA5D. Several studies have investigated the molecular role of ECEL1 in the nervous system. This study highlights the genetic and clinical heterogeneity of DA5D and expands the known spectrum of ECEL1 mutations associated with the disorder. *ECEL1* is also involved in processing the neuropeptide substance P, a crucial modulator of pain perception. Researchers have found that ECEL1 cleaves substance P at a specific site, producing a shorter, biologically active form of the neuropeptide (28). The researchers also found that ECEL1 cleaves these precursors at specific sites, producing a range of biologically active neuropeptides. In addition, several studies have implicated ECEL1 in regulating synaptic transmission and neuronal plasticity. For example, a study showed that ECEL1 regulates glutamatergic transmission in the hippocampus, a brain region involved in learning and memory (29). Furthermore, the researchers found that ECEL1 is involved in processing the neuropeptide somatostatin, which modulates the release of glutamate from presynaptic terminals. *ECEL1* mutations have been associated with the rare genetic disorder DA5D, characterized by multiple joint contractures and muscle weakness in the hands and feet. Interestingly, according to the reported cases, most patients presented with significant symptoms since birth, and the onset time did not differ between heterozygous variants and bi-allelic or homozygous variants. However, the difference between single-allelic and bi-allelic variants would determine the therapeutic strategy and the age at which surgery is performed. Unlike other subtypes of DA, which are inherited through autosomal dominance, DA5D is a rare disease that is inherited in an autosomal recessive manner. After the studies on the relationship between *ECEL1* and DA5D reported by McMillin (3) and Dieterich (8), almost all the subsequent studies on this disease have been related to *ECEL1*. Due to its rarity, no population-specific or race-specific associations have been reported. From the reported cases, there have been no reports of fetal death, but there are significant developmental disorders. Meanwhile, some patients who were not diagnosed and intervened in time after birth will die due to complications caused by related malformations, such as death caused by the influence of breathing related muscles and chest malformations. We believe that this disease is a birth defect, and the reported patients almost all showed corresponding typical symptoms after birth. The difference in mutation sites is more likely to lead to the difference in severity of symptoms. The influence of other exposure factors is still unclear.

According to previous researches, abnormal biological force loading to chondrocyte would induce the degradation of cartilage, including RAP2/YAP signaling (30). Moreover, integrins, TGFBR1/2, TRPV4, PIEZO1/2 channels also mediating the mechontransduction in chondrocyte (31). The overtime exceeding pressure loading impaired the normal metabolic hemostasis and cartilage development, resulting in decreased volume of cartilage in particular joints. Importantly, the degradation of cartilage had been considered as non-reversible pathophysiological process (31). Thus, the early relief abnormal pressure loading was critical in managing such diseases. According to this issue, the essential timely surgical treatment would be much benefit to maintain cartilage development and functional performance among the disorders of joint, especially for such muscular dysfunctions and arthrogryposis. In this case, the positive joint treatment would be much helpful to improve his prognosis by efficient clinical and molecular diagnosis via MRI screening and WES analysis.

In the current case, the proband exhibited a typical clinical presentation, including bilateral contractures of knee flexion and ptosis, strongly suggesting the diagnosis of DA5D. To confirm the diagnosis, a WES was performed, which identified a specific ECEL1 pathogenic variant allele from the patient's father and an uncertain pathogenic variant allele from his mother, enabling a diagnosis of DA5D based on mutation site and protein structure assessments. None of the proband's parents exhibited disease manifestations related

TABLE 1 Summary of reported *ECEL1* mutations and clinical features.

Reference	Nucleotide (cDNA)	Protein alteration	Distal arthrogryposis	Ocular phenotype	Other manifestation
McMillin et al., Am J Hum Genet. 2013	c.716dupA (exon2)	p.Tyr239* ($n = 2$)	Onset age: 1 year Contractures of foot, ankle, knee (flexion), hip, hand, wrist, elbow and shoulder	Right ptosis	Bulbous nose Scoliosis Mild micrognathia
	c.716dupA c.344_355 del (exon2)	p.Tyr239* ($n = 1$)	Contractures of ankle, knee (flexion), hip, hand, wrist, elbow, shoulder and neck	Right ptosis	Bulbous nose Reduced facial expression Slightly crouched gait Pterygia in neck and axillae Micrognathia
	c.869A>G (exon4) c.797_801delins GCT (exon3)	p.Tyr290Cys p.Asp266Glyfs*15 ($n = 2$)	Contractures of foot, ankle, knee (extension), hip, hand and wrist	One is right ptosis; another one is mild bilateral ptosis	Bulbous nose Mild micrognathia Short neck Glabellar hemangioma Posteriorly rotated ears
	c.1252C>A (exon7) c.1184-3A>T (exon6)	p.Arg418Ser ($n = 2$)	Contractures of foot, ankle, knee(extension), hip, hand and wrist	One is right ptosis Another one is normal	Bulbous nose Micrognathia
	c.1184G>A (exon6)	p.Arg395Gln ($n = 1$)	Contractures of foot, ankle, knee (extension), hip, hand, wrist, elbow, shoulder and neck	Right ptosis	Bulbous nose Pterygia in elbows, axillae and neck Dislocated hips Reduced fetal movements
	c.590G>A (exon2) c.1252C>T (exon7)	p.Gly197Asp p.Arg418Cys ($n = 1$)	Contractures of foot, ankle, hip, hand, wrist, elbow, shoulder and neck	Severe bilateral ptosis	Bulbous nose Micrognathia Short neck Cupped ears
Dieterich et al., Hum Mol Genet. 2013	c.1649C>G (exon10)	p.Ser550* ($n = 2$)	Flexed fifingers III–V Congenital hip dislocation and/or limited hip movement Limited knee flexion Talus or talus valgus deformity of feet	Ptosis Pseudoexophthalmos and lagophthalmos	Reduced facial expression Tongue atrophy Speech difficulties Short neck Scoliosis Hyperlordosis
	c.1470G>A (exon8) c.997C>T (exon5)	p.Try490* p.Arg333* ($n = 1$)	Flexed fifingers III–V Distal interphalangeal joint hyperlaxity Congenital hip dislocation and/or limited hip movement Limited knee flexion Talus or talus valgus deformity of feet	—	Tongue atrophy Short neck Scoliosis Hyperlordosis
	c.874delG (exon4)	p.Val292Cysfs*51 ($n = 1$)	Flexed fifingers III–V Congenital hip dislocation and/or limited hip movement Limited knee flexion	Ptosis	Small mouth Short neck
	c.1685+1G>T (intron)	p.Lys552AlafsX33 ($n = 2$)	Flexed fifingers III–V Distal interphalangeal joint hyperlaxity Congenital hip dislocation and/or limited hip movement Limited knee flexion Talus or talus valgus deformity of feet	Ptosis	Short neck Hyperlordosis

(Continued)

TABLE 1 (Continued)

Reference	Nucleotide (cDNA)	Protein alteration	Distal arthrogryposis	Ocular phenotype	Other manifestation
	c.966+1G>A (intron)	p.Asp559AlafsX33 ($n = 1$)	Flexed fifingers III–V Limited knee flexion Talus or talus valgus deformity of feet	Ptosis	Mouth held open Short neck Sucking and swallowing difficulties Scoliosis Hyperlordosis
	c.2278C>T (exon18)	p.Cys760Arg ($n = 3$)	Flexed fifingers III–V Congenital hip dislocation and/or limited hip movement Limited knee flexion Talus or talus valgus deformity of feet	Only one with ptosis	Tongue atrophy Short neck Scoliosis Hyperlordosis
Khan et al., J AAPOS. 2014	c.1221_1223dup (exon7)	— ($n = 4$)	Contractures of the hands and feet	Three of 4 have strabismus with abnormal synkinesis and ptosis (one is bilateral and other two are unilateral)	—
Shaheen et al., Clin Genet. 2014	c.1221_1223dup (exon7)	— ($n = 4$)	Camptodactyly	Three with ptosis and Strabismus	Two with scoliosis Short stature
	c.1057dupC (exon5)	— ($n = 2$)	Camptodactyly Hip dislocation	Ptosis	—
	c.1210C>T (exon7)	p.Arg404Cys ($n = 3$)	Camptodactyly Club foot Hip dislocation	One with ptosis	—
	c.1819G>A (exon13)	p.Ser607Gly ($n = 2$)	Contractures of hand, knee (flexion), wrist and shoulder	Ophthalmoplegia One with ptosis	Arched eye brows Small mouth Short neck Reduced facial expression Bulbous nose Micrognathia Scoliosis One with hyperlordosis
Barnett et al., Am J Med Genet A. 2014	c.1531G>A (exon9) c.1797-1G>A (intron 12/exon 13 boundary)	p.Gly511Ser ($n = 2$)	Contractures of foot, ankle, knee, hip, hand, wrist and elbow One with neck Contractures	Ptosis	Micrognathia Pterygia Central tongue atrophy/grooved tongue
Patil et al., Am J Med Genet A. 2014	c.2023G>A (exon15)	p.Ala675Thr ($n = 1$)	Limitated in knee flexion and elbow movement Hands with camptodactyly and/or ulnar deviation of fingers Congenital dislocation of hips	Ptosis Refractive errors Light pigmented fundus	Bulbous nose Micrognathia Small mouth Cleft palate Furrowed tongue Pterygia Short neck Hypoplastic labia majora Scoliosis
Bayram et al., J Clin Invest. 2016	c.1147C>T (exon6)	p.Gln383X ($n = 2$)	One with severe flexion contracture of knees, camptodactyly, hip dislocation The other one with contractures of hands, hip-joint dysplasia	—	The other one with a mask-like whistling appearance, and short neck
Stattin et al., Am J Med Genet A. 2018	c.1163 T>C (exon6)	p.Leu388Pro	Contractures of wrist, shoulder, ankle, knee, metacarpophalangeal joints(extension); hip-joint dysplasia	Unilateral ptosis	Reduced facial expression Lacrimal duct stenosis Bulbous nose Small mouth

(Continued)

TABLE 1 (Continued)

Reference	Nucleotide (cDNA)	Protein alteration	Distal arthrogryposis	Ocular phenotype	Other manifestation
Ullmann et al., Neuromuscul Disord. 2018	c.589G>A (exon 2)	p.Gly197Ser ($n = 1$)	Contractures of finger, shoulder, elbow, wrist, hip, ankle and knee	—	Reduced foetal movements Breech presentation Cleft palate Central groove in tongue Micrognathia
	c.2005_2006delAC (exon 15)	p.Thr669fs ($n = 1$)	Contractures of finger, shoulder, hip and knee	Bilateral ptosis	Reduced foetal movements Breech presentation Central groove in tongue Neck webbing Scoliosis
	c.1470G>A (exon8)	p.Trp490Ter ($n = 2$)	Contractures of finger, ankle and knee	One with bilateral ptosis	Breech presentation One with micrognathia
Umair et al., Front Pediatr. 2019	c.158C>A (exon 2)	p.Pro53Leu ($n = 2$)	Contractures of finger, elbow, ankle and knee Camptodactyly	Ptosis Strabismus	Facial dysmorphism
Jin et al., Biomed Res Int. 2020	c.69C>A (exon 2) c.1810G>A (exon 13)	p.Cys23Ter p.Gly604Arg	Bilateral contractures of the fingers, wrist, elbow, and knees	Left ptosis	Webbing of the bilateral fingers and elbows Arched eyebrows, strabismus, protruding ears, and cleft palate
Alesi et al., Int J Mol Sci. 2021	c.1507-9G>A (intron)	— ($n = 2$)	Contractures of elbow and knee	Unilateral ptosis	Decreased fetal movements Congenital hip dislocation
Huddar et al., Children. 2021	c.602 T>C (exon2)	p.Met201Thr ($n = 1$)	Multiple joint contractures	Asymmetric ptosis	Motor developmental delay Pes planus, kyphoscoliosis, undescended testis Distal lower limb weakness
	c.83C>T (exon2)	p.Ala28Val ($n = 2$)	Multiple contractures, pes cavus, prominent hyperextensibility at the knee, hypotonia of lower limbs, wasting and weakness of all limbs (distal > proximal)	Unconjugated eye movements, and primary optic atrophy	White hairlock Tented upper lip Bulbous nose Tongue furrowing Small low set ears
Zhang et al., Taiwan J Obstet Gynecol. 2021	c.110_155del46 (exon2) c.633G>C (enon2)	p.Phe37Cysfs*151 p.Trp211Cys	Prenatal ultrasound examination demonstrated reduced fetal movements, clenched hands, fixated extended knees; Rocker bottom feet and scoliosis	—	—
Gowda et al., Clin Dysmorphol 2021	c.493_517del (enon2)	p.Leu165Alafs*30 ($n = 3$)	Contractures of hip, hand, finger, elbow, ankle, wrist, shoulder, neck, foot and knee Talus valgus/Varus, abnormal foot curvature, short toes	Ptosis Pulled lower palpebra	Short stature Limited facial expression Facial asymmetry Arched eyebrows Bulbous nose Scoliotic spine
Cohen et al., Ophthalmic Genet 2023	c.110_155del (enon2)	p.Phe37Cysfs*151 ($n = 3$)	The upper and lower limbs in various degrees; camptodactyly and adducted thumbs	Down-slanting palpebral fissures Ptosis; inferior scleral show	Scoliosis Arched eyebrows Small mouth and furrowed tongue
Ahangari et al., Mol Genet Genomic Med 2023	c.535A>G (exon2)	p. Lys179Glu ($n = 2$)	Limited shoulder movement and elbow movement; severe contracture of fingers II–V; talus valgus, deformity of feet and difficulty in walking	Mild ptosis Limitation of ocular motility in the vertical direction	Decreased facial movements; speech difficulties

to distal arthrogryposis, thus indicating that the novel compound heterozygous variant was responsible for the disease manifestation. A case report by Zhang et al. (25) has reported a compound mutation of *ECEL1*, however, prenatal ultrasound examination demonstrated reduced fetal movements, clenched hands, fixated extended knees and rocker bottom feet and scoliosis, and the pregnant chose to terminate the pregnancy. But in our report, ultrasound during pregnancy showed no abnormalities. Cohen has reported a case only with c.110_155del mutation in *ECEL1* (12). Compared with our patient, both cases presented ptosis, thumb adduction, arched eyebrows and scoliosis. However, our patient only had lower extremity knee contracture, while the other one presented with abnormalities in both upper and lower joints. Moreover, our patients received rehabilitation treatment for joint related symptoms and achieved better symptom improvement due to the early intervention time. Unfortunately, the two patients reported by Cohen were diagnosed in middle age and focused on the description and treatment of eye muscle related symptoms. Mutations in multiple exons and introns of the ECEL1 gene have been reported to induce DA5D, while mutations in exon 2, such as c.716dupA, c.344_355 del, c.590G>A, c.589G>A, c.158C>A, c.69C>A, c.602 T>C, c.83C>T, c.633G>C, and c.110_155del, were primarily recorded in DA5D patients, suggesting that impairment of exon 2 transcription significantly contributes to DA5D (3, 19–21, 24, 25).

5 Conclusion

In summary, a comprehensive evaluation of early-onset distal arthrogryposis is crucial, and WES can provide valuable genetic information to help diagnose specific types of distal arthrogryposis. DA5D is associated with ECEL1 variants that exhibit autosomal recessive inheritance, and mutations in exon 2 are essential in the context of ECEL1-related DA5D. This study expands the spectrum of ECEL1 mutations and provides essential information for the genotype-phenotype map of DA5D. Furthermore, the prompt diagnosis of this rare disease through rapid WES analysis can facilitate appropriate treatment by inhibition degradation of cartilage, thereby improving clinical outcomes.

Data availability statement

The datasets presented in this article are not readily available because of ethical and privacy restrictions. Requests to access the datasets should be directed to the corresponding authors.

Ethics statement

The studies involving humans were approved by West China Second Hospital of Sichuan University (approval number 2014-034). The studies were conducted in accordance with the local legislation and institutional requirements. Written informed consent for participation in this study was provided by the participants' legal guardians/next of kin. Written informed consent was obtained from the individual(s), and minor(s)' legal guardian/next of kin, for the publication of any potentially identifiable images or data included in this article.

Author contributions

SJ: Conceptualization, Data curation, Formal analysis, Investigation, Methodology, Software, Visualization, Writing – original draft. MP: Investigation, Methodology, Software, Supervision, Validation, Writing – original draft. YHe: Data curation, Formal analysis, Investigation, Methodology, Writing – original draft. YHu: Methodology, Project administration, Supervision, Validation, Writing – review & editing. JL: Conceptualization, Investigation, Methodology, Project administration, Resources, Software, Supervision, Validation, Writing – review & editing. YL: Conceptualization, Formal analysis, Funding acquisition, Investigation, Methodology, Project administration, Software, Supervision, Validation, Visualization, Writing – review & editing.

Funding

The author(s) declare financial support was received for the research, authorship, and/or publication of this article. This work was supported by grants from Technology Project of Sichuan Province of China (2021YFQ0061) and the National Natural Science Foundation of China (82270249). The funder was not involved in the study design, collection, analysis, interpretation of data, the writing of this article, or the decision to submit it for publication.

Conflict of interest

The authors declare that the research was conducted in the absence of any commercial or financial relationships that could be construed as a potential conflict of interest.

The handling editor HS declared a shared parent affiliation with the authors at the time of review.

Publisher's note

References

1. Hall JG, Reed SD, Greene G. The distal arthrogryposes: delineation of new entities—review and nosologic discussion. *Am J Med Genet*. (1982) 11:185–239. doi: 10.1002/ajmg.1320110208

2. Bamshad M, Jorde LB, Carey JC. A revised and extended classification of the distal arthrogryposes. *Am J Med Genet*. (1996) 65:277–81. doi: 10.1002/(sici)1096-8628(19961111)65:4<277::Aid-ajmg6>3.0.Co;2-m

3. McMillin MJ, Below JE, Shively KM, Beck AE, Gildersleeve HI, Pinner J, et al. University of Washington Center for Mendelian G. Mutations in ECEL1 cause distal arthrogryposis type 5D. *Am J Hum Genet*. (2013) 92:150–6. doi: 10.1016/j.ajhg.2012.11.014

4. Megarbane A, Bizzari S, Deepthi A, Sabbagh S, Mansour H, Chouery E, et al. A 20-year clinical and genetic neuromuscular cohort analysis in Lebanon: an international effort. *J Neuromuscul Dis*. (2022) 9:193–210. doi: 10.3233/jnd-210652

5. Abdel-Salam GMH, Afifi HH, Saleem SN, Gadelhak MI, El-Serafy MA, Sayed ISM, et al. Further evidence of a continuum in the clinical spectrum of dominant PIEZO2-related disorders and implications in cerebellar anomalies. *Mol Syndromol*. (2022) 13:389–96. doi: 10.1159/000523956

6. Mitgau J, Franke J, Schinner C, Stephan G, Berndt S, Placantonakis DG, et al. The N terminus of adhesion G protein-coupled receptor GPR126/ADGRG6 as allosteric force integrator. *Front Cell Dev Biol*. (2022) 10:873278. doi: 10.3389/fcell.2022.873278

7. Benoit A, Vargas MA, Desgroseillers L, Boileau G. Endothelin-converting enzyme-like 1 (ECEL1) is present both in the plasma membrane and in the endoplasmic reticulum. *Biochem J*. (2004) 380:881–8. doi: 10.1042/bj20040215

8. Dieterich K, Quijano-Roy S, Monnier N, Zhou J, Fauré J, Smirnow DA, et al. The neuronal endopeptidase ECEL1 is associated with a distinct form of recessive distal arthrogryposis. *Hum Mol Genet*. (2013) 22:1483–92. doi: 10.1093/hmg/dds514

9. Varadi M, Anyango S, Deshpande M, Nair S, Natassia C, Yordanova G, et al. AlphaFold protein structure database: massively expanding the structural coverage of protein-sequence space with high-accuracy models. *Nucleic Acids Res*. (2022) 50:D439–d444. doi: 10.1093/nar/gkab1061

10. Jumper J, Evans R, Pritzel A, Green T, Figurnov M, Ronneberger O, et al. Highly accurate protein structure prediction with AlphaFold. *Nature*. (2021) 596:583–9. doi: 10.1038/s41586-021-03819-2

11. Hall JG. Arthrogryposis (multiple congenital contractures): diagnostic approach to etiology, classification, genetics, and general principles. *Eur J Med Genet*. (2014) 57:464–72. doi: 10.1016/j.ejmg.2014.03.008

12. Cohen D, Sloma R, Pizem H, Fedida A, Kalfon L, Ovadia R, et al. Long term ophthalmic complications of distal arthrogryposis type 5D. *Ophthalmic Genet*. (2023) 44:28–34. doi: 10.1080/13816810.2022.2141791

13. Barnett CP, Todd EJ, Ong R, Davis MR, Atkinson V, Allcock R, et al. Distal arthrogryposis type 5D with novel clinical features and compound heterozygous mutations in ECEL1. *Am J Med Genet A*. (2014) 164:1846–9. doi: 10.1002/ajmg.a.36342

14. Khan AO, Shaheen R, Alkuraya FS. The ECEL1-related strabismus phenotype is consistent with congenital cranial dysinnervation disorder. *J AAPOS*. (2014) 18:362–7. doi: 10.1016/j.jaapos.2014.03.005

15. Patil SJ, Rai GK, Bhat V, Ramesh VA, Nagarajaram HA, Matalia J, et al. Distal arthrogryposis type 5D with a novel ECEL1 gene mutation. *Am J Med Genet A*. (2014) 164A:2857–62. doi: 10.1002/ajmg.a.36702

16. Shaheen R, Al-Owain M, Khan AO, Zaki MS, Hossni HA, Al-Tassan R, et al. Identification of three novel ECEL1 mutations in three families with distal arthrogryposis type 5D. *Clin Genet*. (2014) 85:568–72. doi: 10.1111/cge.12226

17. Bayram Y, Karaca E, Coban Akdemir Z, Yilmaz EO, Tayfun GA, Aydin H, et al. Molecular etiology of arthrogryposis in multiple families of mostly Turkish origin. *J Clin Invest*. (2016) 126:762–78. doi: 10.1172/jci84457

18. Stattin EL, Johansson J, Gudmundsson S, Ameur A, Lundberg S, Bondeson ML, et al. A novel ECEL1 mutation expands the phenotype of distal arthrogryposis multiplex congenita type 5D to include pretibial vertical skin creases. *Am J Med Genet A*. (2018) 176:1405–10. doi: 10.1002/ajmg.a.38691

19. Ullmann U, D'Argenzio L, Mathur S, Whyte T, Quinlivan R, Longman C, et al. ECEL1 gene related contractural syndrome: long-term follow-up and update on clinical and pathological aspects. *Neuromuscul Disord*. (2018) 28:741–9. doi: 10.1016/j.nmd.2018.05.012

20. Umair M, Khan A, Hayat A, Abbas S, Asiri A, Younus M, et al. Biallelic missense mutation in the ECEL1 underlies distal arthrogryposis type 5 (DA5D). *Front Pediatr*. (2019) 7:343. doi: 10.3389/fped.2019.00343

21. Jin JY, Liu DY, Jiao ZJ, Dong Y, Li J, Xiang R. The novel compound heterozygous mutations of ECEL1 identified in a family with distal arthrogryposis type 5D. *Biomed Res Int*. (2020) 2020:2149342. doi: 10.1155/2020/2149342

22. Alesi V, Sessini F, Genovese S, Calvieri G, Sallicandro E, Ciocca L, et al. A new Intronic variant in ECEL1 in two patients with distal arthrogryposis type 5D. *Int J Mol Sci*. (2021) 22:2106. doi: 10.3390/ijms22042106

23. Gowda M, Mohan S, Ramesh D, Chinta N. Distal arthrogryposis type 5D in a south Indian family caused by novel deletion in ECEL1 gene. *Clin Dysmorphol*. (2021) 30:100–3. doi: 10.1097/mcd.0000000000000364

24. Huddar A, Polavarapu K, Preethish-Kumar V, Bardhan M, Unnikrishnan G, Nashi S, et al. Expanding the phenotypic spectrum of ECEL1-associated distal arthrogryposis. *Children*. (2021) 8:909. doi: 10.3390/children8100909

25. Zhang YL, Zhen L, Xu LL, Li DZ. Fetal akinesia: the need for clinical vigilance in first trimester with decreased fetal movements. *Taiwan J Obstet Gynecol*. (2021) 60:559–62. doi: 10.1016/j.tjog.2021.03.032

26. Ahangari N, Gholampour-Faroji N, Doosti M, Ghayour Mobarhan M, Shahrokhzadeh S, Karimiani EG, et al. ECEL1 novel mutation in arthrogryposis type 5D: a molecular dynamic simulation study. *Mol Genet Genomic Med*. (2023) 11:e2153. doi: 10.1002/mgg3.2153

27. Pollazzon M, Caraffi SG, Faccioli S, Rosato S, Fodstad H, Campos-Xavier B, et al. Clinical and genetic findings in a series of eight families with arthrogryposis. *Genes*. (2021) 13:29. doi: 10.3390/genes13010029

28. Fossella J, Fan J, Liu X, Guise K, Brocki K, Hof PR, et al. Provisional hypotheses for the molecular genetics of cognitive development: imaging genetic pathways in the anterior cingulate cortex. *Biol Psychol*. (2008) 79:23–9. doi: 10.1016/j.biopsycho.2007.12.006

29. Ortuño-Sahagún D, Rivera-Cervantes MC, Gudiño-Cabrera G, Junyent F, Verdaguer E, Auladell C, et al. Microarray analysis of rat hippocampus exposed to excitotoxicity: reversal Na^+/Ca^{2+} exchanger NCX3 is overexpressed in glial cells. *Hippocampus*. (2012) 22:128–40. doi: 10.1002/hipo.20869

30. Qi H, Zhang Y, Xu L, Zheng X, Li Y, Wei Q, et al. Loss of RAP2A aggravates cartilage degradation in TMJOA via YAP signaling. *J Dent Res*. (2023) 102:302–12. doi: 10.1177/00220345221132213

31. Zhao Z, Li Y, Wang M, Zhao S, Zhao Z, Fang J. Mechanotransduction pathways in the regulation of cartilage chondrocyte homoeostasis. *J Cell Mol Med*. (2020) 24:5408–19. doi: 10.1111/jcmm.15204

frontiers | Frontiers in Neurology

TYPE Case Report
PUBLISHED 24 January 2024
DOI 10.3389/fneur.2024.1272802

OPEN ACCESS

EDITED BY
Huifang Shang,
Sichuan University, China

REVIEWED BY
Stuart Fraser,
University of Texas Health Science Center at Houston, United States
Zhigang Liang,
Yantai Yuhuangding Hospital, China

*CORRESPONDENCE
Yang Liu
✉ a.liu@mx.uni-saarland.de
Feng Wang
✉ wangfengtzyy@163.com

RECEIVED 07 August 2023
ACCEPTED 05 January 2024
PUBLISHED 24 January 2024

CITATION
Ying A, Zhou Y, Wang C, Wang T, Zhang X, Wang S, Ke S, Bao Y, Liu Y and Wang F (2024) The *FGG* c.952G>A variant causes congenital dysfibrinogenemia characterized by recurrent cerebral infarction: a case report. *Front. Neurol.* 15:1272802. doi: 10.3389/fneur.2024.1272802

The *FGG* c.952G>A variant causes congenital dysfibrinogenemia characterized by recurrent cerebral infarction: a case report

Anna Ying[1], Yuanlin Zhou[1], Chunyue Wang[2], Tao Wang[2], Xuan Zhang[2], Shanshan Wang[1], Shaofa Ke[1], Yuyan Bao[1], Yang Liu[1,3]* and Feng Wang[1]*

[1]Department of Neurology, Taizhou Hospital of Zhejiang Province Affiliated to Wenzhou Medical University, Linhai, China, [2]Key Laboratory of Digital Technology in Medical Diagnostics of Zhejiang Province, Dian Diagnostics Group Co., Ltd., Hangzhou, China, [3]Department of Neurology, Saarland University, Homburg, Germany

Background: Congenital dysfibrinogenemia (CD) is a rare hereditary coagulation disorder resulting from mutations in fibrinogen genes. CD primarily presents with bleeding symptoms, but it can also lead to thrombotic events, including ischemic stroke.

Case presentation: This report describes the case of a 52-year-old Chinese man who was admitted to the hospital twice due to recurrent cerebral infarction, characterized by sudden speech impairment and weakness in the right upper extremity. Brain MRI revealed multiple ischemic changes, predominantly in the left frontal and parietal lobes. Coagulation tests demonstrated reduced plasma fibrinogen (Clauss method), prolonged prothrombin time and thrombin time, and an elevated international normalized ratio. However, the ELISA assay indicated elevated levels of fibrinogen γ-chain protein. Despite a 2-month-old treatment regimen with aspirin, clopidogrel, and atorvastatin after the first hospitalization, the patient experienced a second ischemic stroke. Genetic analysis using whole-exome sequencing (WES) and Sanger sequencing identified a rare heterozygous missense variation, *FGG* c.952G>A (rs267606810), in both the stroke patient and his asymptomatic sister. Both individuals exhibited the same alterations in fibrinogen, characterized by reduced functional levels but increased antigenic protein. Subsequently, the patient was diagnosed with ischemic stroke associated with congenital dysfibrinogenemia.

Conclusion: This case report expands the clinical phenotype spectrum associated with *FGG* c.952G>A (rs267606810) and underscores the significance of considering CD as a potential etiology for unexplained ischemic stroke, particularly in patients with a family history of coagulation disorders.

KEYWORDS

***FGG* gene, c.952G>A, congenital dysfibrinogenemia, cerebral infarction, fibrinogen**

Introduction

Congenital dysfibrinogenemia [CD; Online Mendelian Inheritance in Man® (OMIM): #616004] is a rare hereditary coagulation disease, usually caused by mutation(s) in one of the genes *FGA*, *FGB*, or *FGG*, which jointly encode fibrinogen (Fib), a protein that plays a crucial role in coagulation (1, 2). Mutation(s) in the Fib gene may lead to changes in the structure or functional properties of Fib and further impair its ability to form stable blood clots. In CD patients, the synthesis of abnormal Fib generates a wide spectrum of clinical manifestations, ranging from asymptomatic forms to bleeding and/or thrombosis (1, 3). While bleeding tendency due to impaired clot formation is often associated with CD, a small proportion of CD patients may paradoxically have an increased risk of thrombotic events. Nevertheless, due to the variability of clinical presentation and the rarity of CD, clinicians are less likely to immediately consider CD as a cause of thrombotic events without further investigation. Several common coagulation function tests, such as Fib protein level and activity tests, active partial plasma prothrombin time (APTT), prothrombin time (PT), and thrombin time (TT), are the preferred methods for the diagnosis of coagulation disorders. However, these tests are of limited value in the etiological diagnosis of CD. In addition, interpretation of laboratory results for coagulation disorders can be complex, and misinterpretation of results often causes misdiagnosis or delayed diagnosis of CD, ultimately resulting in unnecessary or inappropriate treatments and an increased risk of fatal complications such as excessive bleeding, recurrent thrombotic events, and multiple organ failure (3–6). As CD is a genetic disease, genetic testing is often necessary for the definitive diagnosis and appropriate management of CD, especially when there is a suspected underlying genetic predisposition to unexplained thrombosis.

We report here the case of a 52-year-old male CD patient with abnormal coagulation function and recurrent cerebral infarcts. Through whole-exome sequencing (WES) analysis, we identified a heterozygous missense variant c.952G>A in the *FGG* gene as a potential genetic causative factor.

Case presentation

Case overview

The patient was a 52-year-old Chinese man who was admitted to the hospital due to two cerebral infarctions. Initially, a sudden speech disorder was the main cause of hospitalization. Physical examination at that time revealed only Broca's aphasia-like symptoms. Coagulation tests indicated a coagulation disorder, which was characterized by a decrease in the plasma level of Fib as determined by the Clauss method, an increase in Fib plasma concentration as detected by ELISA, and prolongation of PT and TT. In addition, brain imaging examinations revealed ischemic changes in multiple brain regions. As a result, the patient was diagnosed with unexplained multiple cerebral infarction and was treated with aspirin, clopidogrel, and atorvastatin. Although the short-term treatment alleviated his speech disorder, it failed to prevent the recurrence of the cerebral infarction. A second ischemic stroke manifested itself in the form of mild aphasia and weakness of the right upper extremity. Through family screening and genetic testing, we identified a rare heterozygous missense variant *FGG* c.952G>A (rs267606810) in the patient and his asymptomatic sister, both of whom exhibited the same alterations in Fib, characterized by reduced functional levels (Clauss method) but increased antigenic protein (ELISA assay). Taking the findings together, the patient was definitively diagnosed with CD. Finally, the patient underwent long-term therapy with clopidogrel and atorvastatin, which has so far brought about a satisfactory recovery from cerebral infarction and the associated neurological symptoms.

Initial hospitalization

A 52-year-old man was admitted to our hospital on 30 April 2022 due to a sudden speech disorder that had persisted for 17 h. On admission, his blood pressure was 118/69 mmHg, and his heart rate was 58 beats per min. He was conscious and had normal facial expressions. The bilateral pupils were equal in size, round (diameter approximately 3.0 mm), and reacted to light. Notably, he exhibited Broca's aphasia-like symptoms with repetition of words or simple phrases, but not fluent grammatical sentences, and he was aware of his own speech impairment. Nevertheless, the ability to understand was not impaired. Physical examinations showed normal systemic motor and sensory functions and normal muscle strength (grade V) in four limbs, and neither pyramidal signs nor meningeal irritation signs were observed. The National Institutes of Health Stroke Scale (NIHSS) score was 4, which indicated minor to moderate stroke. Brain computed tomography angiography (CTA) showed patchy hypointense signals in the left frontal lobe. The distal branches of the left anterior cerebral artery were sparser than those of the contralateral artery (Figure 1A). Diffusion-weighted magnetic resonance imaging (DW-MRI) further revealed ischemic changes in multiple brain regions, including the left frontal lobe, the parietal lobe, the occipital lobe, the basal ganglia, and the corona radiata (Figure 1B). Vascular ultrasound showed intima–media thickening of the right carotid artery and bilateral lower limb arteries. A complete blood count showed a high platelet count (366×10^9/L), leucocyte count (12.5×10^9/L), and absolute neutrophil count (9.0×10^9/L), and a low erythrocyte count (4.23×10^{12}/L). Importantly, laboratory tests showed reduced activity of plasma Fib (0.6 g/L, Clauss method), prolonged PT (16.1 s) and TT (26.6 s), and an elevated international normalized ratio (INR; 1.34), although APTT (32.7 s) and D-dimer (0.19 mg/L) were within normal reference ranges (Table 1). Moreover, plasma anticardiolipin antibody, antithrombin antibody, homocysteine, glycated hemoglobin, triglyceride, and cholesterol were normal. Electrocardiogram and cardiac ultrasound revealed normal cardiac function. Echocardiography with agitated saline contrast, also known as a bubble study, showed no bubbles within the left heart (Figure 1C). As a positive control, bubbles were visualized in the left heart within 3–5 beats in a patient with a patent foramen ovale (PFO) (Figure 1D). Abdominal ultrasound also showed no obvious abnormalities. Kidney and liver function were normal.

The patient was diagnosed with unexplained multiple cerebral infarction. As there was no indication for interventional therapy, he was treated with dual antiplatelet and hypolipidemic therapy for 10 days, including aspirin (100 mg, q.d.), clopidogrel (75 mg, q.d.), and atorvastatin (20 mg, q.d.). He was subsequently discharged with significant relief from Broca's aphasia-like symptoms. After discharge, clopidogrel was continued for a further 11 days, and aspirin and atorvastatin were taken regularly.

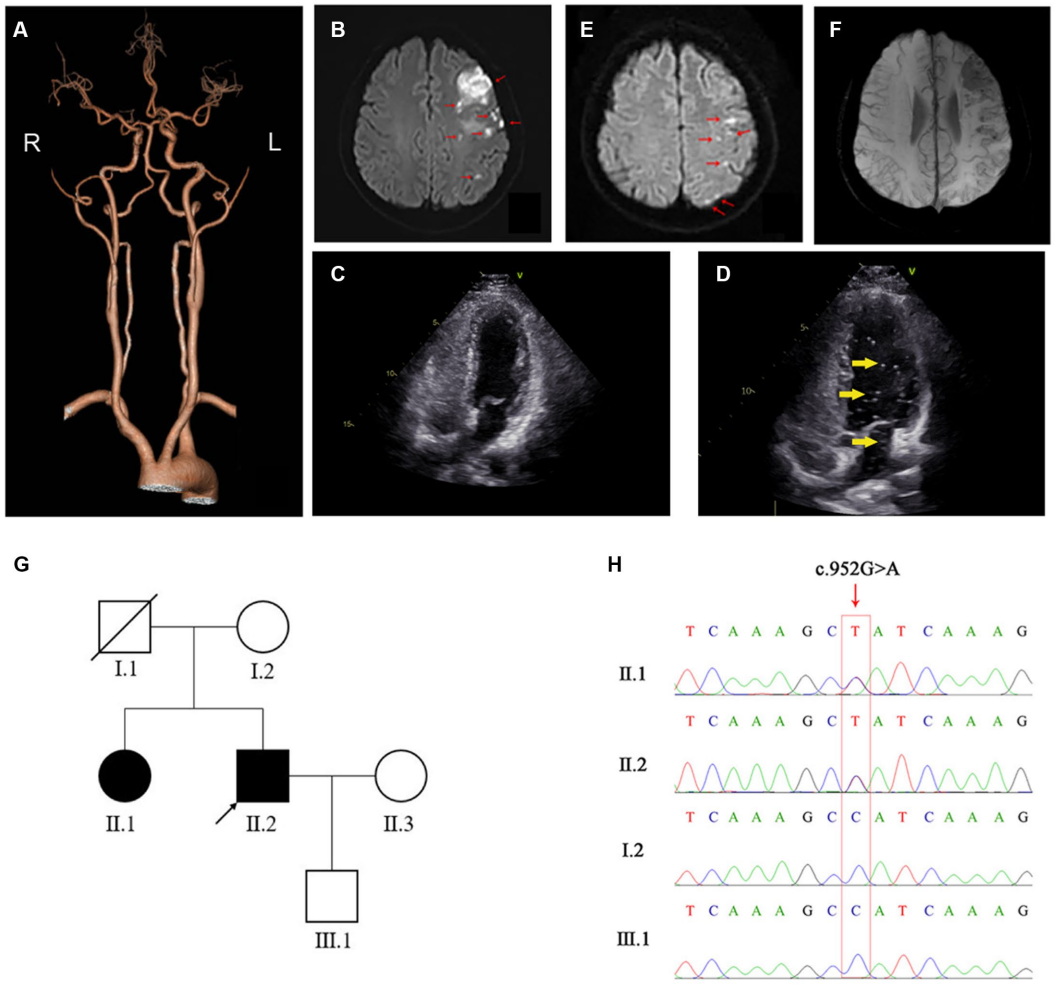

FIGURE 1
Imaging and genetic results for the patient. **(A)** Representative CTA image of the patient's brain. **(B)** On first admission, DW-MRI of the brain shows high signal in the left frontal lobe, the parietal lobe, the occipital lobe, the basal ganglia, and corona radiate, as indicated with red arrows. **(C,D)** Agitated-saline-contrast echocardiography of the reported patient **(C)** and a positive control patient with patent foramen ovale (PFO) **(D)** show bubbles (indicated by yellow arrows) in the left ventricle of the PFO patient but not in the stroke patient (our case). **(E)** On second admission, DW-MRI of the brain shows high signal in the left frontal and parietal lobes, as indicated by red arrows. **(F)** SWI-MRI of the brain shows low signal in the left frontal lobes, the parietal lobes, and the left basal ganglia, where the lesions were located on first admission. **(G)** Pedigree analysis of the patient's family. The patient and his older sister, who both carried *FGG* c.952G>A, are shown in solid black. Healthy family members are shown in hollow white. The patient, i.e., the proband, is marked with an arrow and his deceased father with a diagonal slash. **(H)** Sanger sequencing confirms the presence of *FGG* c.952G>A in the patient and his older sister, and the absence of *FGG* c.952G>A in his mother and son.

TABLE 1 **Results of coagulation function tests in the patient and his older sister.**

Member	Date	PT (s)	INR	APTT (s)	TT (s)	D-dimers (mg/L)	Fibrinogen (g/L)	
							Clauss	PT
Normal range	/	11.0–14.5	0.8–1.2	28.0–42.0	14.0–21.0	0–0.5	2.0–4.0	2.0–4.0
II.2	2022.04.30	16.1	1.34	32.7	26.0	0.19	0.60	/
	2022.06.17	16.1	1.33	34.2	25.3	0.10	0.45	3.02
II.1	2022.10.24	15.4	1.24	34.7	28.1	/	0.60	/

Readmission to hospital

On 16 June 2022, the patient was readmitted to the hospital due to mild aphasia and persistent weakness of the right upper limb for 29 h. On the second recording, his consciousness, pupils, blood pressure, and heart rate were normal, but he showed mild symptoms of aphasia. Strikingly, his right nasolabial sulcus was flat, and his mouth was tilted to the left. The muscle strength of his right arm was grade IV, and the other limbs were grade V. DW-MRI of the brain showed new ischemic lesions located mainly in the left frontal and

TABLE 2 Plasma levels of Fib γ-chain.

Member	Fibrinogen γ-chain (pg/mL)
II.2	3.37
II.1	2.72
II.3	0.91
Control ($n = 5$)	2.02 ± 0.43

parietal lobes, while encephalomalacia of previous ischemic areas was observed (Figure 1E). Susceptibility-weighted imaging (SWI) further revealed cerebral microbleeds and remote hemorrhage in the left frontal and parietal lobes and in the left basal ganglia (Figure 1F). Again, routine blood tests showed a high platelet count (385×10^9/L) and low erythrocyte count (4.19×10^{12}/L). Importantly, the PT-derived method detected a normal concentration of plasma Fib (3.02 g/L; Table 1), which was dramatically higher than the concentration detected by the Clauss method. The PT-derived/Clauss ratio of plasma Fib was 6.71. In addition to the previously observed abnormalities of common coagulation markers, we found an increased plasma level of von Willebrand factor (vWF) antigen (182%; normal range: 77.9%–137.1%), while plasma levels of protein S, protein C, antithrombin III, lupus anticoagulant, and fibrin/Fib degradation products (FDPs) were normal. Moreover, the activity of coagulation factor VIII was increased, while plasminogen (PLG) activity was normal. As the antiplatelet agents had been unable to prevent the recurrence of cerebral infarction, the patient was treated with atorvastatin and the anticoagulant rivaroxaban (15 mg, q.d.). However, the 2 days course of treatment with rivaroxaban led to nosebleeds, so rivaroxaban was discontinued. The patient then took clopidogrel and atorvastatin for a further 10 days, which gradually improved his aphasia, abnormal facial expression, and right arm weakness. After discharge, clopidogrel and atorvastatin were taken regularly, and strict follow-up was required. No further neurological symptoms had occurred at the time of writing of this article.

Cascade genetic testing

The patient stated that he had no family history of neurological, hemorrhagic, and/or thrombotic diseases. Nevertheless, his asymptomatic older sister (55 years old) underwent the usual coagulation function tests, which also revealed a reduced plasma level of Fib (Clauss method), prolonged PT and TT, and an increased INR (Table 1). Other family members refused coagulation function tests. To determine the genetic etiology, we collected peripheral blood genomic DNA from the patient and performed WES analysis using standard protocols. After filtering common variants and variants that were irrelevant to neurological and coagulation disorders, we identified a rare heterozygous missense variant in exon 8 of the *FGG* gene, i.e., *FGG* c.952G>A (rs267606810). By Sanger sequencing, we further confirmed the presence of this *FGG* variant in the patient and his sister, but not in his healthy mother or son (Figures 1G,H).

FGG c.952G>A (rs267606810) leads to the replacement of non-polar and aliphatic glycine with polar and uncharged serine at position 318 in the C-terminal of the Fib γ-chain, which plays a crucial role in binding to the N-terminal of the Fib α-chain. *FGG* c.952G>A was predicted by REVEAL, ClinPred, SIFT, and PolyPhen2 to be highly detrimental to the function of the encoded protein. This missense variant has been reported in a patient associated with thrombotic disease (7). In the ClinVar database, *FGG* c.952G>A is defined as a variant of undetermined significance.[1]

Notably, ELISA assay using a human Fib γ-chain ELISA kit (Cat No.: JL19902, Jianglai Biological, China) further revealed that the patient and his sister had similar plasma levels of Fib γ-chain, which were higher than those of the patient's healthy wife and five healthy control subjects (Table 2), suggesting that *FGG* c.952G>A may cause a compensatory increase in abnormal Fib γ-chain. Considering these genetic results, we speculate that *FGG* c.952G>A may contribute to the pathogenesis of the patient's coagulopathy and recurrent cerebral infarction. Finally, a definitive diagnosis of CD was made for this patient.

Discussion

CD is a clinically heterogeneous hereditary disease that is primarily associated with bleeding tendency rather than thrombotic events. In a large cohort study with 102 Chinese CD patients, thrombotic events occurred in only 4/102 (3.9%), and the remaining patients either were either asymptomatic (68.6%) or showed bleeding tendency (27.5%) (8). CD-related thrombosis occurs in all blood vessels, but cerebral vessels are less frequently affected than vessels in the legs or lungs (8, 9). Cerebral thrombosis can lead to cerebral infarction, resulting in symptoms that are not specific to CD, such as severe headaches, seizures, visual and speech disorders, and other neurological deficits. Because of these overlapping symptoms and its rarity, a cerebral infarction caused by CD is difficult to distinguish from one with other causes.

Clinical manifestations of CD largely depend on the specific location(s) of Fib gene variant(s). However, the genotype–phenotype correlation of many variants remains unexplored. To date, several variants have been found to be clearly associated with CD-related thrombotic events, such as the p.Arg16Cys variant (Nanning), p.Ser532Cys (Caracas V), and p.Arg554Cys (Dusart) in Fib α-chain; p.Ala68Thr (Naples) in β-chain; and p.Asp364Val (Melun) in γ-chain (1, 10). Compared with heterozygous variants, homozygous and compound heterozygous variants in the Fib gene are more likely to cause bleeding/thrombotic symptoms (1, 2). However, it is important to note that the clinical presentation of CD can vary among individuals carrying the same variant, even within the same family.

In this study, we identified a heterozygous *FGG* c.952G>A (p.Gly318Ser; rs267606810) variant in the patient and his asymptomatic older sister. This variant occurs in the C-terminal of Fib γ-chain, which plays an important role in the structure and function of Fib. Fib proteins undergo a complex process called polymerization to form fibrin (11, 12). The C-terminal region of Fib γ-chain participates in polymerization by facilitating the proper alignment, association, and stabilization of Fib molecules (11, 12). In addition, the C-terminal region of the γ-chain contains binding sites for various proteins involved in coagulation and fibrinolysis processes, including factor XIIIa, thrombin,

1 https://www.ncbi.nlm.nih.gov/clinvar/RCV000851954

plasminogen, and tissue-type plasminogen activator (tPA) (11, 12). Therefore, it stands to reason that the p.Gly318Ser variant we have reported impairs the stability and functionality of the fibrin clot and the subsequent activation of fibrinolysis. *FGG* c.952G>A has been identified as a mutation associated with thrombotic diseases; however, a clear clinical phenotype remains to be defined (7). The ClinVar database lists p.Gly318Ser as a variant of uncertain significance. Here, we provide evidence that recurrent cerebral infarcts are clinical manifestations of this variant. However, further research is needed to evaluate the pathogenicity of *FGG* c.952G>A and investigate the underlying mechanism.

The Clauss method is commonly used to quantify the Fib concentration in plasma based on calculation of the conversion rate of Fib to fibrin (3). Due to abnormal Fib structure or function, the Clauss method often detects reduced plasma Fib levels in CD patients (6). However, in the same patients, plasma Fib may be determined to be normal or even increased when tested using the PT-derived method, which calculates Fib concentrations indirectly by measuring plasma turbidity during the PT clotting process (6). CD patients may be misdiagnosed as having hypofibrinogenemia when tested using the Clauss method or overlooked when diagnosed by the PT-derived method. Many studies have emphasized the combined use of these two laboratory tests to determine plasma Fib levels in CD patients (6, 13). It has been reported that the PT-derived/Clauss ratio of Fib (>1.43) has excellent sensitivity and specificity for the diagnosis of CD (6). In this study, we carefully measured the patient's plasma Fib levels using both the Clauss method and the PT-derived method, and the PT-derived/Clauss ratio was 6.71, which is consistent with the characteristics of CD. However, it should be noted that both the Clauss method and the PT-derived method depend on the function of Fib. Immunologic detection of Fib antigens is still required to distinguish dysfibrinogenemia from hypofibrinogenemia. In our study, we found that the levels of Fib γ-chain in the plasma of our patient and his sister, who both carried the p.Gly318Ser variant, were higher than those of healthy controls.

Therapy for CD patients who undergo thrombotic events can be determined according to the specific clinical scenario. In general, anticoagulation therapy and/or antiplatelet therapy may be used initially to treat acute thrombotic events (1). These therapies may help to prevent further thromboembolism and allow the anticoagulants to dissolve the existing thrombus, even if this increases the risk of bleeding. In fact, anticoagulant therapy with rivaroxaban, a specific factor Xa inhibitor, showed an obvious side effect in the form of bleeding in our patient. Fortunately, dual antiplatelet therapy with aspirin and clopidogrel showed satisfactory long-term efficacy in the treatment of cerebral thrombosis, but aspirin alone did not seem to be able to control the recurrence of cerebral infarction. However, further extensive studies are needed to understand the efficacy and safety of antiplatelet agents in people with Fib gene variants.

In summary, we report a CD patient characterized by recurrent ischemic stroke, an uncommon clinical entity in CD. Family screening and genetic testing identified a heterozygous *FGG* c.952G>A (rs267606810) variant in this patient and his asymptomatic older sister with coagulation disorder. Our report expands the clinical phenotype spectrum of the *FGG* c.952G>A variant and underscores the importance of considering CD as a potential cause of unexplained ischemic stroke, especially for those with a family history of coagulation disorder.

Data availability statement

The datasets presented in this article are not readily available because of ethical and privacy restrictions. Requests to access the datasets should be directed to the corresponding authors.

Ethics statement

The studies involving humans were approved by the Ethics Committee of Taizhou Hospital, Zhejiang Province. The studies were conducted in accordance with the local legislation and institutional requirements. Written informed consent for participation in this study was provided by the participants' legal guardians/next of kin. Written informed consent was obtained from the individual(s) for the publication of any potentially identifiable images or data included in this article.

Author contributions

AY: Writing – original draft. YZ: Data curation, Writing – original draft. CW: Methodology, Writing – original draft. TW: Software, Writing – original draft. XZ: Formal analysis, Writing – review & editing. SW: Formal analysis, Writing – review & editing. SK: Data curation, Writing – review & editing. YB: Data curation, Writing – review & editing. YL: Writing – original draft. FW: Writing – original draft.

Funding

The author(s) declare financial support was received for the research, authorship, and/or publication of this article. This work was supported by grants from the Zhejiang Provincial Basic and Public Welfare Research Program (grant number: GF21H020023) and the Zhejiang Provincial Medicine and Health Research Foundation (grant number: 2021RC141).

Acknowledgments

The authors would like to thank the patient and his family for participating in our study.

Conflict of interest

CW, TW, and XZ are employed by Dian Diagnostics Group Co., Ltd., Hangzhou, Zhejiang Province.

The remaining authors declare that the research was conducted in the absence of any commercial or financial relationships that could be construed as a potential conflict of interest.

Publisher's note

References

1. Casini A, Neerman-Arbez M, Ariens RA, de Moerloose P. Dysfibrinogenemia: from molecular anomalies to clinical manifestations and management. *J Thromb Haemost*. (2015) 13:909–19. doi: 10.1111/jth.12916

2. Tiscia GL, Margaglione M. Human fibrinogen: molecular and genetic aspects of congenital disorders. *Int J Mol Sci*. (2018) 19:1597. doi: 10.3390/ijms19061597

3. Lebreton A, Casini A. Diagnosis of congenital fibrinogen disorders. *Ann Biol Clin*. (2016) 74:405–12. doi: 10.1684/abc.2016.1167

4. Chen X, Yan J, Xiang L, Lin F. Misdiagnosis of a patient with congenital dysfibrinogenemia: a case report and literature review. *J Clin Lab Anal*. (2022) 36:e24624. doi: 10.1002/jcla.24624

5. Jia Y, Zhang XW, Wu YS, Wang QY, Yang SL. Congenital dysfibrinogenemia misdiagnosed and inappropriately treated as acute fatty liver in pregnancy: a case report and review of literature. *World J Clin Cases*. (2022) 10:12996–3005. doi: 10.12998/wjcc.v10.i35.12996

6. Xiang L, Luo M, Yan J, Liao L, Zhou W, Deng X, et al. Combined use of Clauss and prothrombin time-derived methods for determining fibrinogen concentrations: screening for congenital dysfibrinogenemia. *J Clin Lab Anal*. (2018) 32:e22322. doi: 10.1002/jcla.22322

7. Downes K, Megy K, Duarte D, Vries M, Gebhart J, Hofer S, et al. Diagnostic high-throughput sequencing of 2396 patients with bleeding, thrombotic, and platelet disorders. *Blood*. (2019) 134:2082–91. doi: 10.1182/blood.2018891192

8. Zhou J, Ding Q, Chen Y, Ouyang Q, Jiang L, Dai J, et al. Clinical features and molecular basis of 102 Chinese patients with congenital dysfibrinogenemia. *Blood Cells Mol Dis*. (2015) 55:308–15. doi: 10.1016/j.bcmd.2015.06.002

9. Casini A, Blondon M, Lebreton A, Koegel J, Tintillier V, de Maistre E, et al. Natural history of patients with congenital dysfibrinogenemia. *Blood*. (2015) 125:553–61. doi: 10.1182/blood-2014-06-582866

10. Bor MV, Feddersen S, Pedersen IS, Sidelmann JJ, Kristensen SR. Dysfibrinogenemia-potential impact of genotype on thrombosis or bleeding. *Semin Thromb Hemost*. (2022) 48:161–73. doi: 10.1055/s-0041-1730358

11. Pieters M, Wolberg AS. Fibrinogen and fibrin: an illustrated review. *Res Pract Thromb Haemost*. (2019) 3:161–72. doi: 10.1002/rth2.12191

12. Weisel JW, Litvinov RI. Fibrin formation, structure and properties. *Subcell Biochem*. (2017) 82:405–56. doi: 10.1007/978-3-319-49674-0_13

13. Miesbach W, Schenk J, Alesci S, Lindhoff-Last E. Comparison of the fibrinogen Clauss assay and the fibrinogen PT derived method in patients with dysfibrinogenemia. *Thromb Res*. (2010) 126:e428–33. doi: 10.1016/j.thromres.2010.09.004

frontiers | Frontiers in Neurology

TYPE Case Report
PUBLISHED 01 February 2024
DOI 10.3389/fneur.2024.1258831

OPEN ACCESS

EDITED BY
Huifang Shang,
Sichuan University, China

REVIEWED BY
Wanjin Chen,
First Affiliated Hospital of Fujian Medical University, China
Jun Mitsui,
The University of Tokyo, Japan

*CORRESPONDENCE
Xuemei Zhang
xuemeizh001@163.com

RECEIVED 14 July 2023
ACCEPTED 05 January 2024
PUBLISHED 01 February 2024

CITATION
Jiang J, Cai X, Qu H, Yao Q, He T, Yang M, Zhou H and Zhang X (2024) Case report: Identification of facioscapulohumeral muscular dystrophy 1 in two siblings with normal phenotypic parents using optical genome mapping. *Front. Neurol.* 15:1258831. doi: 10.3389/fneur.2024.1258831

Case report: Identification of facioscapulohumeral muscular dystrophy 1 in two siblings with normal phenotypic parents using optical genome mapping

Jieni Jiang[1,2,3], Xiaotang Cai[3,4], Haibo Qu[3,5], Qiang Yao[2,3], Tiantian He[1,2,3], Mei Yang[1,2,3], Hui Zhou[3,4] and Xuemei Zhang[1,2,3]*

[1]Department of Medical Genetics and Prenatal Diagnosis Center, West China Second University Hospital, Sichuan University, Chengdu, China, [2]Department of Obstetrics and Gynecology, West China Second University Hospital, Sichuan University, Chengdu, China, [3]Key Laboratory of Birth Defects and Related Diseases of Women and Children (Sichuan University), Ministry of Education, Chengdu, China, [4]Department of Rehabilitation, West China Second University Hospital, Sichuan University, Chengdu, China, [5]Department of Radiology, West China Second University Hospital, Sichuan University, Chengdu, China

Objective: Facioscapulohumeral muscular dystrophy type 1 (FSHD1) is one of the most common forms of autosomal-dominant muscular dystrophies characterized by variable disease penetrance due to shortened D4Z4 repeat units on 4q35. The molecular diagnosis of FSHD1 is usually made by Southern blotting, which is complex, time-consuming, and lacks clinical practicality. Therefore, in this study, optical genome mapping (OGM) is employed for the genetic diagnosis of FSHD1. Furthermore, epigenetic heterogeneity is determined from methylation analysis.

Methods: Genomic DNA samples from four members of the same family were subjected to whole-exome sequencing. OGM was used to identify structural variations in D4Z4, while sodium bisulfite sequencing helped identify the methylation levels of CpG sites in a region located distally to the D4Z4 array. A multidisciplinary team collected the clinical data, and comprehensive family analyses aided in the assessment of phenotypes and genotypes.

Results: Whole-exome sequencing did not reveal variants related to clinical phenotypes in the patients. OGM showed that the proband was a compound heterozygote for the 4qA allele with four and eight D4Z4 repeat units, whereas the affected younger brother had only one 4qA allele with four D4Z4 repeat units. Both the proband and her younger brother were found to display asymmetric weakness predominantly involving the facial, shoulder girdle, and upper arm muscles, whereas the younger brother had more severe clinical symptoms. The proband's father, who was found to be normal after a neurological examination, also carried the 4qA allele with eight D4Z4 repeat units. The unaffected mother exhibited 49 D4Z4 repeat units of the 4qA allele and a minor mosaic pattern with four D4Z4 repeat units of the 4qA allele. Consequently, the presence of the 4qA allele in the four D4Z4 repeat units strongly pointed to the occurrence of maternal germline mosaicism. The CpG6 methylation levels were lower in symptomatic patients compared to those in the asymptomatic parents. The older sister had lower clinical scores and ACSS and higher CpG6 methylation levels than that of her younger brother.

Conclusions: In this study, two siblings with FSHD1 with phenotypically normal parents were identified by OGM. Our findings suggest that the 4qA allele of four D4Z4 repeats was inherited through maternal germline mosaicism. The clinical phenotype heterogeneity is influenced by the CpG6 methylation levels. The results of this study greatly aid in the molecular diagnosis of FSHD1 and in also understanding the clinical phenotypic variability underlying the disease.

KEYWORDS

facioscapulohumeral muscular dystrophy 1, optical genome mapping, sibling patient, low-level mosaicism, germline mosaicism, disease penetrance, molecular diagnosis, methylation analysis

Introduction

Facioscapulohumeral muscular dystrophy (FSHD; OMIM 158900), which is one of the most common hereditary myopathies, is predominantly characterized by progressive asymmetrical weakness of the facial and shoulder girdle muscles. The severity of the disease varies with age and sex. Thus, the degree of muscle damage shows a vast difference at the clinical level, ranging from almost asymptomatic weakness related to eye closure to significant disability with weakness of the shoulder and pelvic girdle and bilateral leg drop (1, 2). These clinical manifestations are characteristic of the highly heterogeneous nature of the FSHD phenotype.

The genetic changes associated with FSHD are highly complicated, and the disease's origin is considered to be commonly linked to the disruption of epigenetic silencing mechanisms, which leads to the abnormal expression of the distal double homeobox protein 4 (*DUX4*) gene. Type I FSHD is characterized by a macrosatellite array of tandem D4Z4 repeat units at the distal end of chromosomal region 4q35 (3), as well as a permissive type-A haplotype after the distal repeat that maintains stable *DUX4* transcription (4). FSHD1, the most common form of FSHD, is the most frequent finding as it is diagnosed in 95% of all clinical cases presented and is found to be caused by an autosomal-dominant route. The 1–10 D4Z4 units are repeated in individuals with a pathogenic form of FSHD1, whereas 11–150 repeat units are present in unaffected individuals (5). Another pathogenic form, FSHD2, is caused by mutated epigenetic modifiers, such as *SMCHD1* or *DNMT3B* (6, 7), as a result of digenic inheritance.

The molecular diagnosis of FSHD1 is made based on the number of D4Z4 repeat units at the chromosome 4q35 locus in the presence of a permissive 4q35A haplotype. But this diagnosis is complicated by the size of the repeat units, which have an approximate length of 3.3 kb, and their variable number. In addition, homologous polymorphic repeat arrays are present on chromosomes 4 and 10, and there is a possible exchange between these chromosomal regions. These factors enable the molecular diagnosis of FSHD. The traditional genetic methods employed for diagnosing FSHD are pulsed-field gel electrophoresis and Southern blotting (8). However, both these techniques are complex and time-consuming, require a large amount of high-quality DNA, and they cannot be used to accurately determine critical lengths (9, 10). A simple and uniform method of diagnosis that enables easy interpretation replication by laboratories worldwide would be beneficial. Optical genome mapping (OGM) offers an accurate and highly reproducible method for identifying FSHD-associated chromosomal abnormalities (11). This method overcomes some of the important problems encountered in conventional analytical techniques, such as distinguishing 4q35-D4Z4 repeats from the highly homologous 10q26 array, measuring the number of repeats at 4q35, and differentiating between the 4qA and 4qB alleles (12).

Previous studies have suggested that reduced DNA methylation levels in potentially pathogenic alleles could be used as a reliable marker for diagnosing FSHD (13). Furthermore, various clinical features observed in FSHD, such as penetrance variability, gender bias in severity, and asymmetric muscle wasting, can be explained by reduced methylation.

In this study, we employed OGM for the diagnosis of FSHD by identifying D4Z4 repeat units within permissive 4qA haplotypes. We complemented this diagnosis by examining the CpG methylation levels within the furthest D4Z4 arrays, which is used as a particularly critical approach for diagnosing, predicting, and providing genetic counseling to individuals carrying D4Z4 alleles of borderline size and their relatives with the same reduced D4Z4 allele.

Patients and methods

Subjects

Two siblings (the proband and her younger brother) and their unaffected parents were recruited from the West China Second University Hospital (Sichuan University). Their clinical data was recorded by a multidisciplinary team. This study was approved by the Medical Ethics Committee of West China Second University Hospital (Sichuan University). Informed consent was obtained from all study participants.

Clinical assessments

Clinical data, such as patient history, systemic features, and physical and auxiliary examinations, were collected prospectively.

FSHD clinical score (CS) was employed to assess muscle strength. The clinical severity score (CSS) was used to determine the disease severity. The CSSs ranged from 0 to 5, with 10 levels. A score of 0 represented no symptoms of muscle weakness and a score of 5 represented wheelchair-dependent patients with a severe disease. The score increased in increments of 0.5 with a concomitant progress in disease severity. The CSS was adjusted according to patient age at examination to derive the age-corrected clinical severity score (ACSS), which was used to determine disease severity and was calculated as described previously (14, 15):

$$ACSS = ([CSS \times 2]/age\ at\ examination) \times 1,000$$

The clinical features and assessments of the siblings are presented in Table 1.

Genetic analysis

Whole-exome sequencing analysis

Blood samples (2–3 mL) were collected in ethylenediaminetetraacetic acid (EDTA) tubes. Genomic DNA was extracted from all samples using a QIAamp DNA Blood Mini Kit (Qiagen, Valencia, CA, USA), following the manufacturer's guidelines. A whole-exome sequencing (WES) library was done using the NanoWES Human Exome V1Kit (Berry Genomics, Beijing). Sequencing was performed using the NovaSeq6000 platform with 150-base pair (bp) paired-end reads. The mean depth of coverage of the sequenced sample was 100×. The Burrows–Wheeler aligner software tool was used for aligning the sequencing reads with hg38/GRCh38, and local alignment and recalibration of the base quality of the aligned reads was performed using the GATK Indel Realigner and the GATK Base Recalibrator, respectively (broadinstitute.org/). Single-nucleotide variants (SNVs) and small insertions or deletions were identified using the GATK Unified Genotyper (broadinstitute.org/), and functional annotation was performed using ANNOVAR and the Enliven Variants Annotation Interpretation System (Berry genomics, Beijing). Several public databases were accessed for genome filtering, including gnomAD (http://gnomad.broadinstitute.org/) and the 1000 Genomes Project (http://browser.1000genomes.org). The pathogenicity of the detected SNVs was evaluated based on scientific and medical literature and disease databases, including OMIM (http://www.omim.org), PubMed (https://www.ncbi.nlm.nih.gov/pubmed/), ClinVar (http://www.ncbi.nlm.nih.gov/clinvar), and the Human Gene Mutation Database (http://www.hgmd.org). Variants were classified according to the American College of Medical Genetics and Genomics guidelines. The potential pathogenic variants were validated using Sanger sequencing on an ABI 3500 Genetic Analyzer (Applied Biosystems, Waltham, MA, USA), and the data were evaluated using Chromas software (2.6.5).

OGM analysis

Blood samples (2–3 mL) were collected in EDTA tubes, and ultra-high molecular weight (UHMW) DNA was extracted, labeled, and processed for use on the Bionano Genomics Saphyr Platform (Bionano Genomics; San Diego, CA), according to the manufacturer's protocol. UHMW DNA was extracted using the Bionano Prep SP Blood and Cell DNA Isolation Kit (Bionano Genomics). Briefly, cells were treated with a lysis-and-binding buffer to extract gDNA, which was subsequently bound to a nanobind disk. The disk was then washed and eluted in the provided elution buffer. The integrity and size of the isolated DNA were validated using pulsed-field gel electrophoresis. HMW DNA quantification was performed with Qubit dsDNA assay BR kits using a Qubit 2.0 Fluorometer (Thermo Fisher Scientific); the final UHMW DNA concentration was 36–150 ng/μL. To generate the Saphyr data, 750 ng of UHMW DNA was labeled with DLE-green fluorophores at a specific six-base sequence (CTTAAG motif) using the Bionano Prep DLS (Direct Label and Stain) Kit (Bionano) following the manufacturer's protocol. Subsequently, the direct labeling enzyme was digested with Proteinase K (Qiagen), and unbound DL-Green fluorophores were washed using the membrane-adsorption procedure. Then, the UHMW DNA samples were stained blue using DNA stain and quantified using the Qubit® HS (High Sensitivity) dsDNA Assay Kit (Thermo Fisher). The samples were placed in the Saphyr system to capture the images of the labeled DNA molecules. Following the conversion of the images into digital representations of the molecules accompanied by labels, the resulting digital data was transferred to the Bionano Access software. This software functioned as a central data hub, enabling data visualization and facilitating the initiation of secondary analysis. Data generated by Saphyr is automatically assembled in the software Bionano Solve 3.7 and visual analysis is performed using Bionano Access 1.7.

The Bionano EnFocus™ FSHD Analysis pipeline was used to identify the FSHD haplotype and the number of D4Z4 repeat units in patients suspected of FSHD. The pipeline first distinguished the D4Z4 region of chromosome 4 from that of chromosome 10 based on the fluorescent pattern of markers proximal to the D4Z4 repeat region. Then the selected molecules that aligned with these regions were identified so as to create a local assembly of the D4Z4 regions of chromosomes 4 and 10. Subsequently, the resulting genome maps were analyzed to determine the size of the repeat units and assign haplotypes to the alleles. While the DLE-1 enzyme did not directly mark individual D4Z4 units, the FSHD pipeline could estimate the lengths of repeat arrays by analyzing the intervals between labels that bordered the D4Z4 arrays. The pipeline also identified other structural variants and copy-number gains or losses near the D4Z4 repeat unit on chromosome 4 and the SMCHD1 gene on chromosome 18. Additionally, the OGM *de novo* pipeline was employed to assemble comprehensive maps to manually determine the number of large repeat units and haplotypes. To evaluate the quality of the assembled map, the pipeline was used to examine genomic regions that were considered stable according to the hg38 reference genome. To ensure that the molecular quality was good enough for downstream analyses, the quality control criteria were set to an N50 value of ≥200 kbp, a mapping rate of ≥70%, an average label density of 14–17, an effective coverage of ≥75×, a positive label variance of 3–10%, and a negative label variance of 6–15% (16).

10.3389/fneur.2024.1258831

TABLE 1 Clinical features and assessments of the siblings.

Subjects	III-9	III-10	II-7	II-8
Sex	F	M	M	F
Relationship	Daughter (proband)	Son	Father	Mother
Age at onset (years)	17	13	/	/
Age at examination(years)	17	15	/	/
Age at diagnosis(years)	27	25	50	47
Age at reported(years)	28	26	51	48
Genetic/epigenetic				
4q haplotype and D4Z4 repeats units	4qA with 4 D4Z4 repeats, 4qA with 8 D4Z4 repeats	4qA with 4 D4Z4 repeats, 4qB with 28 D4Z4 repeats	4qA with 8 D4Z4 repeats, 4qB with 28 D4Z4 repeats	4qA with 49 D4Z4 repeats and low-level mosaicism of 4 D4Z4 repeats
10q haplotype and D4Z4 repeats units	10qA with 17 D4Z4 repeats/ 10qB with 9 D4Z4 repeats	10qA with 17 D4Z4 repeats	10qA with 17 D4Z4 repeats/ 10qB with 9 D4Z4 repeats	10qA with 7 and 17 D4Z4 repeats
CpG6 methylation values, %	60	20	90	90
Clinical phenotype				
Hearing loss	No	No	No	No
Vision loss	No	No	No	No
Dysphagia	No	No	No	No
Impaired intellectual development	No	No	No	No
Facial muscle weakness and atrophy	Severe	Severe	No	No
Shoulder girdle muscle weakness and atrophy	Moderate	Severe	No	No
Upper arm muscle weakness and atrophy	Moderate	Severe	No	No
Abdominal wall muscle weakness and atrophy	No	Severe	No	No
Lower limb and pelvic muscle weakness and atrophy	Mild	Severe	No	No
Foot extensor muscle weakness	No	Severe	No	No
Scapular winging	Yes	Yes	No	No
Spine deformities	Mild	Severe	No	No
Stand up from a chair	Yes, without support	Yes, with support	Yes, without support	Yes, without support
Wheelchair dependency	No	No	No	No
Assessments, range				
FSHD clinical score(0-15)	8	9	0	0
Clinical severity score (0–5)	3	4	0	0
Age-corrected clinical severity score (0–10000)	353	533	0	0
Auxiliary examination				
Serum creatine kinase(normal range:24-194IU/L)	840 IU/L (in 2012)	1153 IU/L (in 2012)	ND	ND
Electromyography	Myogenic changes (in 2012)	Myogenic changes (in 2012)	ND	ND
Biopsy of skeletal muscle	ND	Myogenic changes (in 2012)	ND	ND
Echocardiography	No abnormality (in 2022)	No abnormality (in 2022)	ND	ND

(Continued)

TABLE 1 (Continued)

Subjects	III-9	III-10	II-7	II-8
X-ray	Slightly scoliotic spine and a straightened cervical spine (in 2022)	Increased physiological curvature of the lumbar spine, and an upturned sacrum. Slight curvature of the spine, a straight cervical spine (in 2022)	ND	ND
MRI	Myogenic changes in the bilateral buttocks and thighs, as well as the right upper arm and paravertebral muscles (in 2022)	ND	ND	ND
Pulmonary function test	Slight decrease in pulmonary ventilation reserve function and mild restrictive ventilatory dysfunction (pulmonary ventilation reserve was 88.1%) (in 2023)	ND	ND	ND
DMD test	Negative (in 2015)	Negative (in 2015)	ND	ND
WES	Negative (in 2021 and 2022)	Negative (in 2018 and 2022)	Negative	Negative

ND, not done.

Sodium bisulfite sequencing and CpG methylation analysis

To analyze the methylation levels in CpGs in a region distal to the D4Z4 array in this family, sodium bisulfite sequencing (conducted by Tsingke Biotechnologies, China) was performed with a 4qA allele-specific FasPAS primer, and 10 CpGs were analyzed according to the previously described protocols (17).

Results

Clinical presentation

Patient 1

The proband (patient III-9, Figure 1A), a 27-year-old married woman with undiagnosed myopathy, was referred to our hospital for the confirmation of facioscapulohumeral muscular dystrophy type 1 and an assessment of pregnancy risk. She was the first child born to non-consanguineous parents. Neither of the parents presented with any relevant medical history or neuromuscular symptoms (Supplementary Figure 1). At the age of 17, when her younger brother (aged 15) visited a hospital for a possible diagnosis of muscular atrophy after experiencing muscle weakness in his bilateral upper limbs for 2 years, she realized that she also had symptoms similar to those of her younger brother, which presented in her right upper arm, with slightly limited lifting activities. Her creatine kinase level was 840 IU/L (normal range: 24–194 IU/L). Electromyographic analysis revealed myogenic changes in both the lower limbs and a physician at a local hospital suspected the condition to be muscular dystrophy. The symptoms did not improve significantly after the rehabilitation treatment. Three years later (at the age of 20), the symptoms of muscle atrophy in her upper arms were significantly aggravated, and she had difficulty in climbling stairs, running, and jumping. By the time she was 27, she obviously had limited lifting ability in her upper arms. Though she could take care of herself, she had difficulty in combing her hair. She was still able to live independently but could not perform activities that demanded heavy physical work. Her FSHD CS (8) and ACSS (353) are shown in Table 1.

Upon physical examination (in 2022), the patient displayed limited facial expression and could not close her eyes at all (Figure 1B). Her lips were thickened and slightly distorted with false hypertrophy of the orbicularis oris, which made it difficult for her to purse her lips, and she could not puff her cheeks or whistle. She had asymmetric muscle weakness in the upper arm, a clear "winged scapula" presentation (Figure 1B) when her arms were extended forward, and demonstrated a "duck stance" when running. She exhibited a limited range of motion when extending both arms to the sides or front but had no involuntary movements, and her deep tendon reflexes were normal. Her sensation, coordination, and cognitive functions were normal, and she had no hearing loss or significant visual impairment. No scoliosis or apparent abnormalities in squatting or gait were observed.

Radiographic examination (in 2022) of the spine revealed a slight curvature, and the cervical spine was found to be straightened. Limb-muscle magnetic-resonance imaging (MRI) analysis (in 2022) showed changes in the bilateral buttocks and thighs, as well as in the right upper arm and paravertebral muscles (Figure 2A). These changes were consistent with muscular dystrophy. Multiplex ligation-dependent probe amplification (MLPA) did not highlight deletions and duplications in the *DMD* gene (in 2015). WES was performed at another hospital, and the results were also negative (in 2021).

Additional tests were performed to assess risks associated with pregnancy (in 2022). Pulmonary function tests showed a slight decrease in pulmonary ventilation reserve function and mild restrictive ventilatory dysfunction (pulmonary ventilation reserve, 88.1%). A 24-h Holter electrocardiogram revealed sinus arrhythmia. Color Doppler echocardiography showed no abnormalities, whereas cardiac MRI revealed slightly dense muscle trabeculae in the left ventricle. However, the left ventricular systolic function was normal.

10.3389/fneur.2024.1258831

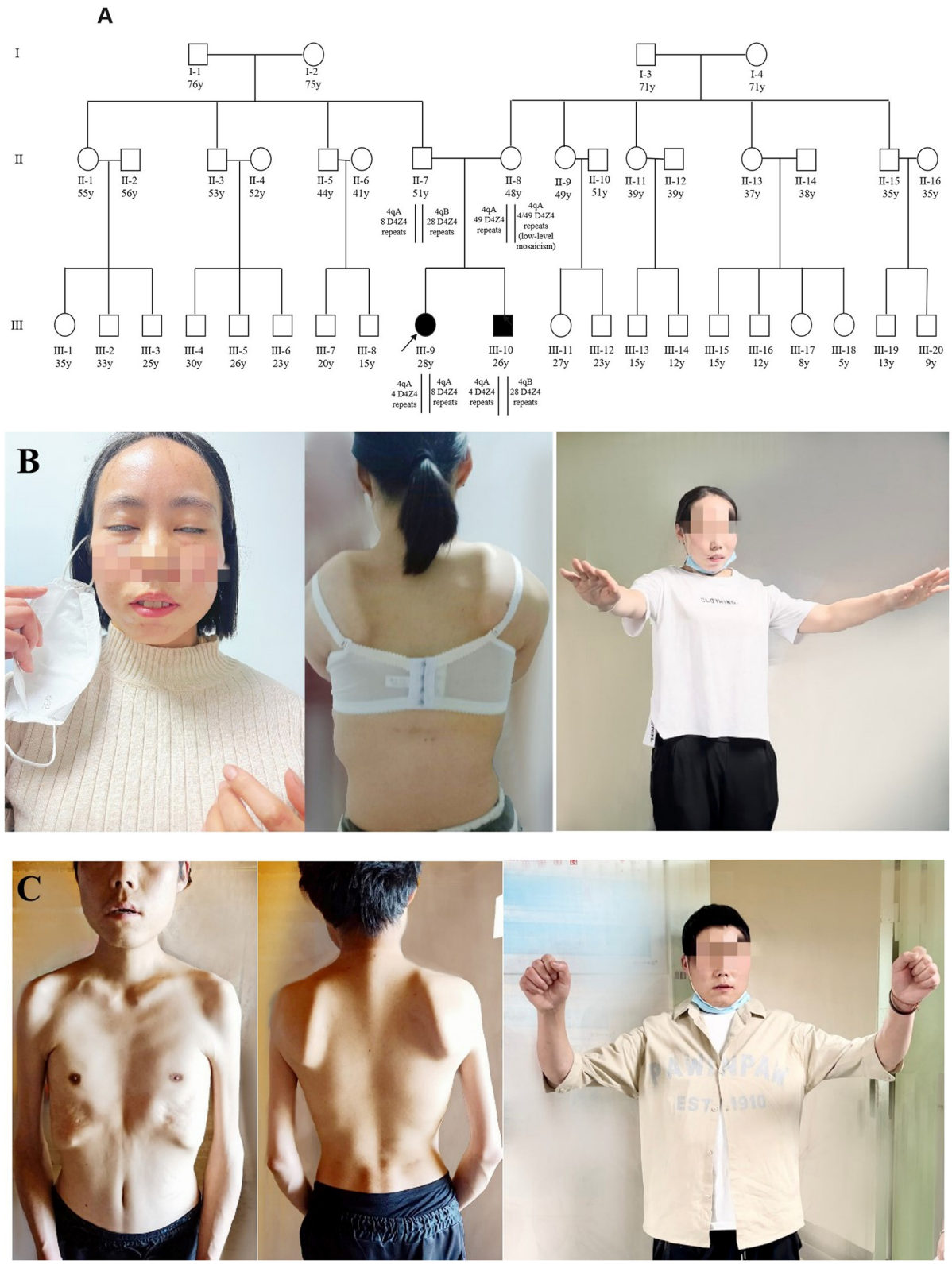

FIGURE 1
Pedigree and clinical features of two patients. **(A)** Pedigree of the family with FSHD1. The age in years, number of D4Z4 repeat units, and haplotype are shown for each subject. Subject III-9 was identified as a compound heterozygote because of a shortened FSHD1 alleles, whereas her affected brother (III-10) carried just one allele. The parents (II-7 and II-8) were asymptomatic; the father was a heterozygote for eight units of D4Z4 with 4qA, while the mother was a low-level mosaic for four units of D4Z4 with 4qA. All other members of this family were asymptomatic. **(B)** The proband (III-9) showed decreased facial expression and an inability to close her eyes completely (left). She showed false hypertrophy of the orbicularis oris, her lips were thickened and slightly distorted (left), and she presented with a winged scapula (middle) and limitations in lifting activities in the bilateral upper limbs (right). **(C)** Patient 2 (III-10) showed atrophy of the facial muscles (middle), shoulder, upper arm, and chest muscles (right). He presented with a winged scapula (middle) and limitations in lifting activities in the bilateral upper limbs (right). The photographs of the proband (III-9) and the proband's younger brother (III-10) were taken at ages 27 and 25, respectively.

FIGURE 2
Imagological examination of two patients. **(A)** X-ray examination of patient 1 (III-9). She had a slightly scoliotic spine and a straightened cervical spine **(left)**. MRI analysis of the limb muscles revealed changes in the bilateral buttocks and thighs and the right upper arm and paravertebral muscles (middle and right). These changes were consistent with the presence of muscular dystrophy. **(B)** X-ray examination of the spine of patient 2 (III-10). The left image shows increased physiological curvature of the lumbar spine and an upturned sacrum. The right image shows a slight curvature of the spine, a straight cervical spine.

Patient 2

The proband's younger brother (patient III-10, Figure 1A), was 25 years old when he began participating in this case study. He first noticed symptoms of muscular atrophy of the bilateral upper arms when he was 13 years old without any apparent cause but did not pay attention to it. At the age of 15 years, the symptoms gradually worsened, with mild limitations in lifting activities, and his creatine kinase level was 1,153 IU/L (normal value: 24–194 IU/L). Electromyographic analysis showed myogenic changes in the bilateral upper and right lower limb muscles. A muscle biopsy in the right upper extremity revealed primary muscular dystrophy. He was suspected of having myotonic dystrophy, but his symptoms did not improve significantly after a rehabilitation treatment. His symptoms worsened with each passing year, and the muscles of both shoulders, upper arms, and chest began to atrophy. At the age of 25 years, he and his older sister visited our hospital for confirmation of the disease. Currently, he has weakness in the muscles of the upper limbs, facial weakness, an abnormal gait when walking, difficulty standing after squatting, and more severe clinical symptoms than those of his sister. His FSHD CS (9) and ACSS (533) were higher than those of his older sister (8 and 353, respectively), as shown in Table 1.

Upon physical examination (in 2022), he displayed no movements in his facial expression and could not close his eyes completely; his lips were thickened and slightly distorted with false hypertrophy of the orbicularis oris, and he could not puff his cheeks or whistle. The patient showed substantially winged scapula and limited shoulder girdle mobility. He was unable to raise his arms above his shoulders (Figure 1C). He struggled to rise from a squatting to a standing position and walked with a waddling gait. He also had significant bilaterally winged scapulae, which were more severe than those of the proband. He exhibited limited extension of both upper limbs to the sides and front with no signs of involuntary movement. His sensation, coordination, and cognitive functions were normal. No hearing loss or visual impairments were observed.

Radiographic analysis (in 2022) revealed a slight curvature of the spine, a straight cervical spine, increased physiological curvature of the lumbar spine, and an upturned sacrum. Hyperlordosis of the lumbar spine was also observed (Figure 2B). Electrocardiographic analysis revealed sinus bradycardia. Cardiac color Doppler ultrasonography showed no abnormalities (in 2022). The MLPA results (in 2015) also pointed to no deletions or duplications in the *DMD* gene. WES (in 2018) performed at another hospital showed negative results.

OGM identified D4Z4 repeats and the 4qA haplotype in the family

WES of genomic DNA samples from all four family members did not reveal any pathogenic or likely pathogenic variations associated with the disease phenotype. But OGM analysis of all four individuals showed a repetition of D4Z4 units for both the 4qA and 4qB alleles, enabling precise determination of their genotypes (Figure 3). The proband (III-9) was a compound heterozygote for the 4qA allele with four and eight separate D4Z4 repeat units (Figure 3A), as confirmed through haplotype analysis, whereas her affected younger brother (III-10) was a heterozygote who inherited only one 4qA allele with four D4Z4 repeat units (Figure 3B). The clinical symptoms in the younger brother were more severe than those of the proband. The proband's father (II-7, aged 50 years), who was found to have a normal phenotype upon neurological examination, also carried the 4qA allele with eight D4Z4 repeat units (Figure 3C). It should be emphasized that the unaffected mother (II-8) had a 4qA allele with 49 D4Z4 repeat units and low-level mosaicism with four D4Z4 repeat units (Figures 3D, F), but the proportion of low-level mosaicism

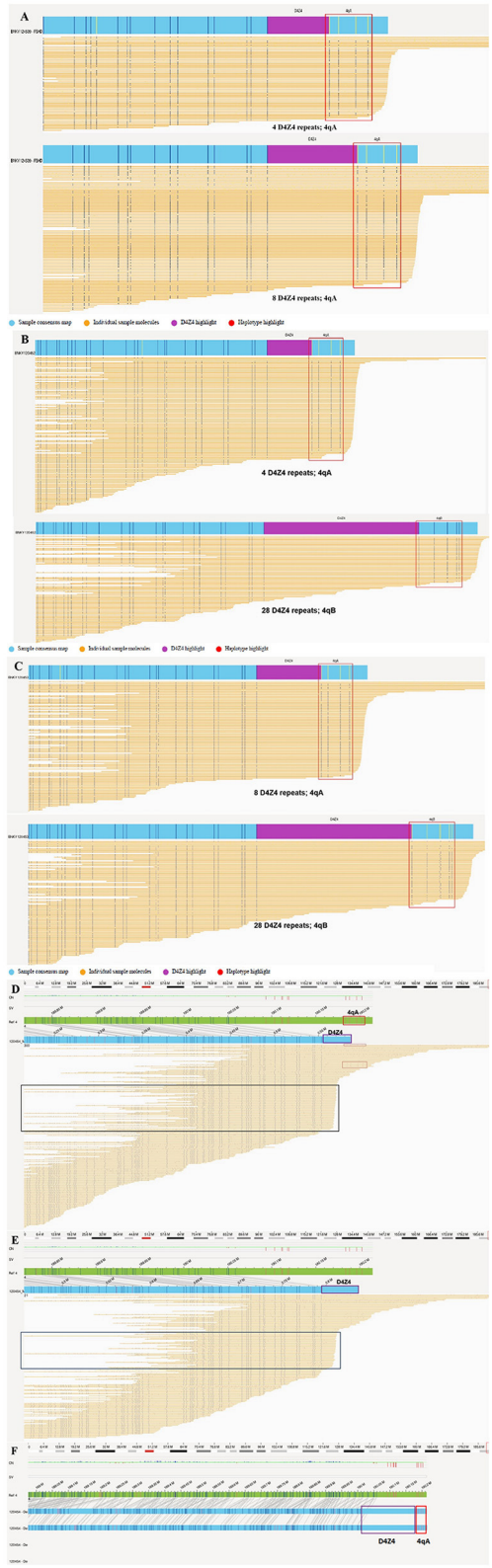

FIGURE 3
OGM results for this family. **(A)** The proband (III-9) was identified as a compound heterozygote for the 4qA allele with four and eight D4Z4 repeat units. **(B)** The younger brother (III-10) was found to only have one 4qA allele with four D4Z4 repeats and a 4qB allele with 28 D4Z4 repeat units. **(C)** The proband's father (II-7) carried the 4qA allele with eight D4Z4 repeats and a 4qB allele with 28 D4Z4 repeat units. *(Continued)*

FIGURE 3 (Continued)
(D–F) The OGM results of the proband's mother (II-8). The green bar is the reference map of chromosome 4, and the blue bar is the assembled map of chromosome 4. **(D)** Chromosome 4 of subject II-8 was found to have a calculated repeat count of ≥5 with an unknown haplotype via FSHD pipeline analysis. A high proportion of consistently truncated sequences (black boxes) might reflect terminal DNA deletions or insufficiently long DNA strands. Several sequences are followed by the 4qA haplotype (red box) with a D4Z4 array length (approximately four repeat units) shorter than that in each map containing five units (purple box). **(E)** Chromosome 4 of a subject whose haplotype was unknown had a calculated repeat count of ≥8, as determined by FSHD pipeline analysis. **(F)** A 4qA allele and 49 D4Z4 repeat units were manually determined based on the consensus maps of the de novo pipeline analysis.

could not be confirmed. The FSHD pipeline was used for an alignment analysis to assess the support for a given map. In the chromosome 4 D4Z4 regions, the map was truncated before the ends of the repeat units, and the haplotype was considered unknown because the sequences did not fully span the repeat units and haplotype-specific labels; thus, the pipeline generated lower-bound estimates of the repeat counts of ≥5 and ≥8 (Figures 3D, E). To determine the exact number of repeats, we prepared a standard *de novo* whole-genome assembly and obtained a fully assembled map of the chromosome 4 D4Z4 region. The similarity between the intervals of the reference haplotype-specific and assembled maps was checked manually, and the homozygous haplotype 4qA was found in the unaffected mother. Repeat unit lengths were estimated based on the interval between the labels flanking the D4Z4 arrays, and the number of D4Z4 repeat units was manually calculated to be 49 for the mother (Figure 3F). Furthermore, when we manually checked the sequences supporting a given map, we found several sequences followed by the 4qA haplotype (Figure 3D [red box]) with a D4Z4 array length to be shorter than that of the given map (Figure 3D [purple box]). In addition, a large fraction of sequences was consistently truncated (Figure 3D [black boxes]), which could have been due to terminal deletion or an insufficient DNA sequence length. In addition, OGM accurately identified the D4Z4 repeat units in both the 10qA and 10qB alleles in all family members, as shown in Supplementary Figure 2.

CpG methylation analysis

We analyzed 10 CpG sequences and used CpG6 methylation values <73% as the threshold for FSHD according to previous literature (17). Methylation analysis showed that CpG6 methylation levels in four subjects (III-9, III-10, II-7 and II-8) were 60%, 20%, 90%, and 90%, respectively (Supplementary Table 1, Supplementary Figure 3).

Methylation levels of all the 10 CpG sequences were lower in symptomatic patients (III-9 and III-10) compared to those in asymptomatic parents (II-7 and II-8). The CpG6 methylation levels in both father (asymptomatic carrier) and mother (mosaic carrier) was greater than 73%. However, the younger brother who carried only one D4Z4 reduced allele had lower methylation levels of CpG6

(20% vs. 60%), higher CS (9 vs. 8), and higher ACCS scores (533 vs. 353) compared to the older sister who carried two D4Z4 reduced alleles (Supplementary Table 1).

Discussion

The molecular diagnosis of FSHD is difficult because of the relatively large size of the repeat units (3.3 kb), the variable number of repeat units, the existence of homologous polymorphic repeat arrays on chromosomes 4 and 10, and potential exchanges between these chromosomal regions (18). FSHD is traditionally diagnosed by Southern blotting (8), molecular combing (19, 20), Pacific Biosciences (PacBio) sequencing (21), and Nanopore sequencing (22). The most commonly used technique for diagnosing FSHD1 is Southern blotting, which is time-consuming (because it involves multiple enzymatic reactions) and only results in an estimate of the number of D4Z4 repeat units based on the band size. In recent years, OGM has emerged as an effective method for a precise determination of the number of repeat units and differentiating DNA fragments from 4q35 and 10q26 (11, 18).

In this study, we applied OGM for the genetic diagnosis of FSHD1 in a family with two siblings who presented the classical FSHD phenotype. We found that suspected mosaicism in maternal germ cells and phenotype heterogeneity were prominent features in the family. The proband was a compound heterozygote carrying two D4Z4 alleles with four and eight 4qA-D4Z4 repeat units, and the younger brother carried a single shortened D4Z4 allele with four 4qA repeat units. The younger brother had an earlier onset of the disease at the age of 13 and higher ACCS scores than the older sister, although the proband had two D4Z4 alleles with four and eight 4qA repeats. Thus, a further methylation analysis is required to explain clinical heterogeneity in this family.

The existence of an inverse relationship between the number of D4Z4 repeats and disease severity has been confirmed in several FSHD genotype–phenotype correlation studies. In general, shortened D4Z4 alleles with 1–3 units cause more severe disease symptoms, whereas D4Z4 alleles with 4–8 units point to the classic form of FSHD (23, 24). The phenotypic expression of individuals who carried one reduced D4Z4 allele with 7–8 units was quite similar to those with 9–10 units (25). Even within families, individuals carrying the same fragment size of the repeat units have presented significant clinical variations, ranging from seriously impacted to asymptomatic individuals. Comprehending the clinical diversity of FSHD continues to be challenging. In this study, both siblings carried fragments of the same size, that is, four D4Z4 units; however, the clinical phenotype of the younger brother was more severe than that of the proband.

Wohlgemuth et al. (26) proposed that the dosage effect caused by contraction of the D4Z4 repeat array on both 4q35 chromosomes results in the compound heterozygote phenotype in probands and that disease penetrance appears to be associated with the residual repeat size. However, we observed that the clinical severity of the compound heterozygote proband carrying a paternally inherited D4Z4 allele (eight repeat units) and a maternally inherited D4Z4 allele (four repeat units) was milder than that of her younger brother, who carried a single D4Z4 allele with four repeat units from his mother. Methylation analysis showed that the compound heterozygous sister had a higher methylation level of CpG6 than the heterozygous brother, which is consistent with the conclusion of previous studies that, besides the size of the D4Z4 repeats, the level of CpG6 methylation can be used as an indicator of the severity of the disease (27).

Recent genetic data indicate that the disease penetrance remains incomplete even in older individuals, with non-penetrance rates ranging from 32% to 53%. Both the number of repeats and the extent of kinship contribute to this variation in disease penetrance (28–31). For carriers possessing eight repeat units, there exists a 20% likelihood of experiencing symptoms by the age of 70, with only a 24% probability of the disease onset later being identified through clinical examination at 30 years of age (30). However, Ruggiero et al. reported that most individuals (52.8%) carrying D4Z4 with seven to eight repeat units presented with no muscle weakness (25). The clinical phenotypic variation in FSHD is extensive, including incomplete penetrance and significant heterogeneity between individuals and within families. Interestingly, the father, who carried a D4Z4 allele with eight 4qA repeat units, did not show FSHD symptoms at 50 years (when the disease usually manifests). These conditions differ from the typical clinical manifestations of FSHD. Other studies have previously proposed that the degree of hypomethylation at distal D4Z4 arrays determines disease penetrance, and our data show the father, despite possessing hypermethylated state, with the D4Z4 methylation levels at 90%, there was no disease penetrance. Therefore, we consider the D4Z4 allele of the father as a non-penetrant allele. This not only explains why the father carried the contracted D4Z4 allele without phenotype but also why the two contracted D4Z4 repeats did not result in a more severe phenotype in our proband, which could be because the dosage effect of a "non-penetrant" 4qA allele and a "normal penetrant" 4qA allele was not increased.

Women commonly experience a later FSHD onset and exhibit atypical or milder phenotypes, the reasons for which are currently unclear (32). However, male-specific hormones such as testosterone (a powerful anabolic agent that promotes muscle protein synthesis) and muscle regeneration likely render males significantly more sensitive to the pathogenic mechanisms of FSHD (33). Additionally, because of differences in hormonal profiles, men and women may react to catabolic conditions in various ways (34, 35). Other studies showed that the different degrees of methylation levels between asymptomatic carriers and patients with FSHD1 might be caused by sex of the individuals (36). However, these hypotheses need to be confirmed in future studies.

Interestingly, among 107 individuals evaluated by Padberg (37), the proportion of asymptomatic females (21/48, 44%) was twice as high as that of males (13/59, 22%). Ricci et al. (14) noted that six of seven non-penetrant carriers in their series were female. In addition, Van der Maarel et al. (38) noted a sex difference in the presence of mosaicism and found in a review of 35 de novo FSHD families that somatic mosaicism was present in 40% of the cases, either in the patient or the asymptomatic parent. Interestingly, while mosaic males often had symptoms, mosaic females did not. According to Goto et al., the clinical symptoms of parents with mosaicism were not significantly different between the males and

females despite the fact that asymptomatic female carriers with mosaicism have been reported to be more common (28, 39, 40).

This case study presents an intriguing example where post-zygotic mosaicism was inferred in the proband's mother, who was suspected of having germline mosaicism. Of all reported sporadic cases, 19% having a mosaic germline are a phenotypically normal parent, and mothers of sporadic cases may be at a higher risk of being mosaicism carriers with a higher recurrence risk for further affected children (28). In the family in our case study, the mother carried a 4qA-D4Z4 allele of normal size (49 D4Z4 units) and a low-level mosaic (in the peripheral blood) with a 4qA-D4Z4 allele (four D4Z4 units). The two siblings each carried a 4qA-D4Z4 allele of four units as well as a paternal 4qA-D4Z4 allele with eight and 28 repeat units, respectively. Given the fact that both siblings carry the 4qA allele with four D4Z4 repeat units, we speculate that the mother has a mosaic germline and that a low proportion of mosaic variants with four D4Z4 repeats and the 4qA haplotype are present in her peripheral blood cells. Therefore, we infer the absence of symptoms in the mother to be associated with low-level mosaicism and D4Z4 hypermethylation.

These findings support a previously reported observation that many parents with germline mosaicism during oogenesis may have been overlooked (40). Additionally, 15–20% of healthy parents of patients with FSHD had somatic mosaicism in the 4q35 region (38, 40–42). Lemmers et al. (43) demonstrated that the standard diagnostic techniques failed to detect somatic mosaicism in patients with FSHD. A thorough investigation of somatic and germline mosaicism in families with de novo FSHD needs to be undertaken to generate more accurate data so as to give genetic counseling to them. In this study, we manually checked the sequences that supported the OGM map.

We extended our surveys to the grandparents, the siblings of the parents, as well as their sons and daughters. None of these individuals we studied displayed any clinical phenotypes, despite many being older than the typical age of onset (over forty years old) (Figure 1A). Unfortunately, we did not collect samples from them and therefore are unable to determine whether they carry FSHD-sized alleles and possess specific methylation levels.

However, we acknowledge some limitations in our approach. The mother's 4qA-D4Z4 allele with 49 repeat units was not conducive to accurate automated analysis, and manual analysis was necessary in this case. We could not accurately determine the proportion of low-level mosaic variants with four D4Z4 repeats with the 4qA haplotype. Thus, establishing the diagnosis necessitates close exchange between clinicians and molecular geneticists regarding the genotypes and phenotypes of the subjects, as well as the exploitation of all OGM data and interpretation strategies to avoid missed diagnoses. Although the current price of OGM is relatively high, it is expected to gradually become affordable, given the ongoing commercial development and promotion of OGM technology. Despite its high cost, we believe that OGM presents a viable approach for the fast and accurate analysis of FSHD1 and also for the detection of somatic mosaicism.

Conclusion

In conclusion, we employed the OGM approach to accurately diagnose FSHD1 in two siblings in a family, thus pointing the usefulness of OGM in the accurate genetic diagnosis of FSHD1 and to effectively exclude interference by 10q26 repeat elements. OGM also revealed low-level mosaicism in the mother's peripheral blood sample; thus, we highly suspected maternal germline mosaicism in this family. The results of this study emphasize the complexity of the genetics underlying FSHD1; high clinical variability was observed among patients carrying the same alleles, even within the same family, which could be attributed to the CpG6 methylation levels. An accurate diagnosis can aid in the genetic counseling for cases falling within the borderline range of 8–10 D4Z4 repeat units. Clinicians must also acknowledge the limitations associated with genetic testing within this borderline range. Solely relying on the number of D4Z4 repeat units is insufficient to ascertain the severity of FSHD or to determine whether these repeat units are pathogenic. Additional markers are necessary to confirm the diagnosis of FSHD.

Data availability statement

The datasets presented in this article are not readily available because of ethical and privacy restrictions. Requests to access the datasets should be directed to the corresponding author.

Ethics statement

The studies involving human participants were reviewed and approved by the Medical Ethics Committee of West China Second University Hospital, Sichuan University. The patients/participants provided their written informed consent to participate in this study. Written informed consent was obtained from the individual(s) for the publication of any potentially identifiable images or data included in this article.

Author contributions

JJ: Data curation, Formal analysis, Investigation, Methodology, Writing – original draft. XC: Data curation, Formal analysis, Investigation, Writing – review & editing. HQ: Formal analysis, Investigation, Writing – review & editing. QY: Formal analysis, Investigation, Writing – review & editing. TH: Methodology, Resources, Writing – review & editing. MY: Formal analysis, Writing – review & editing. HZ: Formal analysis, Writing – review & editing. XZ: Conceptualization, Funding acquisition, Investigation, Supervision, Writing – review & editing, Writing – original draft.

Funding

The author(s) declare financial support was received for the research, authorship, and/or publication of this article. This research was supported by the Sichuan Science and Technology Program (2022NSFSC0658).

Acknowledgments

The authors thank the patients and their families for their involvement in the study. We thank Prof. Silvere Van der Maarel Leiden University Medical Center for the information on the 4qA allele-specific FasPAS primers. We appreciate Peicong Fan for his valuable review of the clinical score.

Conflict of interest

The authors declare that the research was conducted in the absence of any commercial or financial relationships that could be construed as a potential conflict of interest.

The handling editor declared a shared parent affiliation with the authors at the time of review.

Publisher's note

Supplementary material

The Supplementary Material for this article can be found online at: https://www.frontiersin.org/articles/10.3389/fneur.2024.1258831/full#supplementary-material

References

1. Deenen JC, Arnts H, van der Maarel SM, Pedberg GW, Verschuuren J, Bakker E, et al. Population-based incidence and prevalence of facioscapulohumeral dystrophy. *Neurology*. (2014). 83:1056-9. doi: 10.1212/WNL.0000000000000797

2. DeSimone AM, Pakula A, Lek A, Emerson CP. Facioscapulohumeral muscular dystrophy. *Compr Physiol*. (2017) 7:1229–79. doi: 10.1002/cphy.c160039

3. Wijmenga C, Hewitt JE, Sandkuijl LA, Clark LN, Wright J, Dauwerse HG, et al. Chromosome 4q DNA rearrangements associated with facioscapulohumeral muscular dystrophy. *Nat Genet*. (1992) 2:26–30. doi: 10.1038/ng0992-26

4. Lemmers RJ, van der Vliet PJ, Klooster R, Sacconi S, Camani P, Dauwerse JG, et al. A unifying genetic model for facioscapulohumeral muscular dystrophy. *Science*. (2010) 329:1650–3. doi: 10.1126/science.1189044

5. Wijmenga C, Frants RR, Hewitt JE, van Deutekom JC, van Geel M, Wright TJ, et al. Molecular genetics of facioscapulohumeral muscular dystrophy. *Neuromuscul Disord*. (1993) 3:487–91. doi: 10.1016/0960-8966(93)90102-P

6. Lemmers RJLF, Tawil R, Petek LM, Balog J, Block GJ, Santen GWE, et al. Digenic inheritance of an SMCHD1 mutation and an FSHD-permissive D4Z4 allele causes facioscapulohumeral muscular dystrophy type 2. *Nat Genet*. (2012) 44:1370–4. doi: 10.1038/ng.2454

7. van den Boogaard ML, Lemmers RJLF, Balog J, Wohlgemuth M, Auranen M, Mitsuhashi S, et al. Mutations in DNMT3B modify epigenetic repression of the d4z4 repeat and the penetrance of facioscapulohumeral dystrophy. *Am J Hum Genet*. (2016) 98:1020–9. doi: 10.1016/j.ajhg.2016.03.013

8. L RJL, de Kievit P, van Geel M, van der Wielen MJ, Bakker E, Padberg GW, et al. Complete allele information in the diagnosis of facioscapulohumeral muscular dystrophy by triple DNA analysis. *Ann Neurol*. (2001) 50:816–9. doi: 10.1002/ana.10057

9. Zampatti S, Colantoni L, Strafella C, Galota RM, Caputo V, Campoli G, et al. Facioscapulohumeral muscular dystrophy (FSHD) molecular diagnosis: from traditional technology to the NGS era. *Neurogenetics*. (2019) 20:57–64. doi: 10.1007/s10048-019-00575-4

10. Montagnese F, de Valle K, Lemmers RJLF. 268th ENMC workshop participants. 268th ENMC workshop - Genetic diagnosis, clinical classification, outcome measures, and biomarkers in Facioscapulohumeral Muscular Dystrophy (FSHD): Relevance for clinical trials. *Neuromuscul Disord*. (2023) 33:447–62. doi: 10.1016/j.nmd.2023.04.005

11. Koppikar P, Shenoy S, Guruju N, Hegde M. Testing for facioscapulohumeral muscular dystrophy with optical genome mapping. *Curr Protoc*. (2023) 3:e629. doi: 10.1002/cpz1.629

12. Stence AA, Thomason JG, Pruessner JA, Sompallae RR, Snow A, Ma D, et al. Validation of optical genome mapping for the molecular diagnosis of facioscapulohumeral muscular dystrophy. *J Mol Diagn*. (2021) 23:1506–14. doi: 10.1016/j.jmoldx.2021.07.021

13. de Greef JC, Wohlgemuth M, Chan OA, Hansson KB, Frants S, Weemaes CM, et al. Hypomethylation is restricted to theD4Z4 repeat array in phenotypic FSHD. *Neurology*. (2007) 69:1018–26. doi: 10.1212/01.wnl.0000271391.44352.fe

14. Ricci E, Galluzzi G, Deidda G, Cacurri S, Colantoni L, Merico B, et al. Progress in the molecular diagnosis of facioscapulohumeral muscular dystrophy and correlation between the number of KpnI repeats at the 4q35 locus and clinical phenotype. *Ann Neurol*. (1999) 45:751–7.

15. van Overveld PG, Enthoven L, Ricci E, Rossi M, Felicetti L, Jeanpierre M, et al. Variable hypomethylation of D4Z4 in facioscapulohumeral muscular dystrophy. *Ann Neurol*. (2005) 58:569–76. doi: 10.1002/ana.20625

16. Bionano Genomics. *Bionano Solve Theory of Operation: Bionano EnFocusTM FSHD Analysis*. San Diego, CA: Bionano Genomics. (2021).

17. Calandra P, Cascino I, Lemmers RJ, Galluzzi G, Teveroni E, Monoforte M, et al. Allele-specific DNA hypomethylation characterises FSHD1 and FSHD2. *J Med Genet*. (2016) 53:348–55. doi: 10.1136/jmedgenet-2015-103436

18. Dai Y, Li P, Wang Z, Liang F, Yang F, Fang L, et al. Single-molecule optical mapping enables quantitative measurement of D4Z4 repeats in facioscapulohumeral muscular dystrophy (FSHD). *J Med Genet*. (2020) 57:109–20. doi: 10.1136/jmedgenet-2019-106078

19. Nguyen K, Puppo F, Roche S, Gaillard M, Chaix C, Lagarde A, et al. Molecular combing reveals complex 4q35 rearrangements in Facioscapulohumeral dystrophy. *Hum Mutat*. (2017) 38:1432–41. doi: 10.1002/humu.23304

20. Vasale J, Boyar F, Jocson M, Sulcova V, Chan P, Liaquat K, et al. Molecular combing compared to Southern blot for measuring D4Z4 contractions in FSHD. *Neuromuscul Disord*. (2015) 25:945–51. doi: 10.1016/j.nmd.2015.08.008

21. Morioka MS, Kitazume M, Osaki K, Wood J, Tanaka Y. Filling in the gap of human chromosome 4: single molecule real time sequencing of macrosatellite repeats in the facioscapulohumeral muscular dystrophy locus. *PLoS ONE*. (2016) 11:e0151963. doi: 10.1371/journal.pone.0151963

22. Mitsuhashi S, Nakagawa S, Takahashi Ueda M, Imanishe T, Frith M, Mitsuhashi H, et al. Nanopore-based single molecule sequencing of the D4Z4 array responsible for facioscapulohumeral muscular dystrophy. *Sci Rep*. (2017) 7:14789. doi: 10.1038/s41598-017-13712-6

23. Nikolic A, Ricci G, Sera F, Bucci E, Govi M, Mele F, et al. Clinical expression of facioscapulohumeral muscular dystrophy in carriers of 1-3 D4Z4 reduced alleles: experience of the FSHD Italian National Registry. *BMJ Open*. (2016) 6:e007798. doi: 10.1136/bmjopen-2015-007798

24. Statland JM, Donlin-Smith CM, Tapscott SJ, Lemmers RJLF, van der Maarel SM, Tawil R. Milder phenotype in facioscapulohumeral dystrophy with 7-10 residual D4Z4 repeats. *Neurology*. (2015) 85:2147–50. doi: 10.1212/WNL.0000000000002217

25. Ruggiero L, Mele F, Manganelli F, Bruzzese D, Ricci G, Vercelli L, et al. Phenotypic variability among patients with d4z4 reduced allele facioscapulohumeral muscular dystrophy. *JAMA Netw Open*. (2020) 3:e204040. doi: 10.1001/jamanetworkopen.2020.4040

26. Wohlgemuth M, Lemmers RJ, van der Kooi EL, Wielen MJv, van Overveld PG, Dauwerse H, et al. Possible phenotypic dosage effect in patients compound heterozygous for FSHD-sized 4q35 alleles. *Neurology*. (2003) 61:909–13. doi: 10.1212/WNL.61.7.909

27. Zheng F, Qiu L, Chen L, Zheng Y, Lin X, He J, et al. Association of 4qA-specific distal D4Z4 hypomethylation with disease severity and progression in facioscapulohumeral muscular dystrophy. *Neurology*. (2023) 101:e225–37. doi: 10.1212/WNL.0000000000207418

28. Goto K, Nishino I, Hayashi YK. Very low penetrance in 85 Japanese families with facioscapulohumeral muscular dystrophy 1A. *J Med Genet*. (2004) 41:e12. doi: 10.1136/jmg.2003.008755

29. Tonini MMO, Passos-Bueno MR, Cerqueira A, Matioli SR, Pavanello R, Zatz M. Asymptomatic carriers and gender differences in facioscapulohumeral muscular dystrophy (FSHD). *Neuromuscul Disord.* (2004) 14:33–8. doi: 10.1016/j.nmd.2003.07.001

30. Ricci G, Scionti I, Sera F, Govi M, D'Amico R, Frambolli I, et al. Large scale genotype–phenotype analyses indicate that novel prognostic tools are required for families with facioscapulohumeral muscular dystrophy. *Brain.* (2013) 136:3408–17. doi: 10.1093/brain/awt226

31. Salort-Campana E, Nguyen K, Bernard R, Jouve E, Solé G, Nadaj-Pakleza A, et al. Low penetrance in facioscapulohumeral muscular dystrophy type 1 with large pathological D4Z4 alleles: a cross-sectional multicenter study. *Orphanet J Rare Dis.* (2015) 10:2. doi: 10.1186/s13023-014-0218-1

32. Zatz M, Marie SK, Cerqueira A, Vainzof M, Pavanello RC, Passos-Bueno MR. The facioscapulohumeral muscular dystrophy (FSHD1) gene affects males more severely and more frequently than females. *Am J Med Genet.* (1998) 77:155-61.

33. Anderson LJ, Liu H, Garcia JM. Sex differences in muscle wasting. *Adv Exp Med Biol.* (2017) 1043:153–97. doi: 10.1007/978-3-319-70178-3_9

34. Bredella MA. Sex differences in body composition. *Adv Exp Med Biol.* (2017) 1043:9–27. doi: 10.1007/978-3-319-70178-3_2

35. Ruggiero L, Manganelli F, Santoro L. Muscle pain syndromes and fibromyalgia: the role of muscle biopsy. *Curr Opin Support Palliat Care.* (2018) 12:382–7. doi: 10.1097/SPC.0000000000000355

36. Gaillard M-C, Roche S, Dion C, Tasmadjian A, Bouget G, Salort-Campana E, et al. Differential DNA methylation of the D4Z4 repeat in patients with FSHD and asymptomatic carriers. *Neurology.* (2014) 83:733–42. doi: 10.1212/WNL.0000000000000708

37. Padberg. *Facioscapulohumeral Disease* (PhD Thesis) The Netherlands: Intercontinental Graphics, (1982) p. 243. Available online at: from https://hdl.handle.net/1887/25818

38. van der Maarel SM, Deidda G, Lemmers RJ, van Overveld PG, van der Wielen M, Hewitt JE, et al. De novo facioscapulohumeral muscular dystrophy: frequent somatic mosaicism, sex-dependent phenotype, and the role of mitotic transchromosomal repeat interaction between chromosomes 4 and 10. *Am J Hum Genet.* (2000) 66:26–35. doi: 10.1086/302730

39. Zatz M, Marie SK, Passos-Bueno MR, Vainzof M, Campiotto S, Cerqueira A, et al. High proportion of new mutations and possible anticipation in Brazilian facioscapulohumeral muscular dystrophy families. *Am J Hum Genet.* (1995) 56:99–105.

40. Köhler J, Rupilius B, Otto M, Bathke K, Koch MC. Germline mosaicism in 4q35 facioscapulohumeral muscular dystrophy (FSHD1A) occurring predominantly in oogenesis. *Hum Genet.* (1996) 98:485–90. doi: 10.1007/s004390050244

41. Padberg GW, Frants RR, Brouwer OF, Wijmenga C, Bakker E, Sandkuiji LA. Facioscapulohumeral muscular dystrophy in the Dutch population. *Muscle Nerve Suppl.* (1995) 2:S81–4. doi: 10.1002/mus.880181315

42. Upadhyaya M, Maynard J, Osborn M, Jardine P, Harper PS, Lunt P. Germinal mosaicism in facioscapulohumeral muscular dystrophy (FSHD). *Muscle Nerve Suppl.* (1995) 2:S45-9. doi: 10.1002/mus.880181310

43. Lemmers RJLF, van der Wielen MJR, Bakker E, Padberg GW, Frants RR, van der Maarel SM. Somatic mosaicism in FSHD often goes undetected. *Ann Neurol.* (2004) 55:845–50. doi: 10.1002/ana.20106

frontiers | Frontiers in Neurology

TYPE Case Report
PUBLISHED 06 February 2024
DOI 10.3389/fneur.2024.1339642

OPEN ACCESS

EDITED BY
Huifang Shang,
Sichuan University, China

REVIEWED BY
Marco Russo,
S. Maria Nuova Hospital, Italy
Takao Takeshima,
Tominaga Hospital, Japan

*CORRESPONDENCE
Sen Yang
✉ 459641483@qq.com

†These authors have contributed equally to this work and share first authorship

RECEIVED 16 November 2023
ACCEPTED 24 January 2024
PUBLISHED 06 February 2024

CITATION
Zhang H, Jiang L, Xian Y and Yang S (2024) Familial hemiplegic migraine type 2: a case report of an adolescent with ATP1A2 mutation.
Front. Neurol. 15:1339642.
doi: 10.3389/fneur.2024.1339642

Familial hemiplegic migraine type 2: a case report of an adolescent with ATP1A2 mutation

Hui Zhang[1,2†], Li Jiang[1,2†], Yuqi Xian[1,2] and Sen Yang[1,2*]

[1]The Fifth People's Hospital of Chengdu, Chengdu, China, [2]The Fifth People's Hospital Affiliated to Chengdu University of Traditional Chinese Medicine, Chengdu, China

This study presents a case report of a male adolescent diagnosed with familial hemiplegic migraine type 2 (FHM2), an autosomal dominant inheritance disorder caused by ATP1A2 mutation. We report the patient who presented with headache, aphasia, and left-sided weakness. Cerebrovascular disease and various infectious agents were unremarkable during the patient's extended hospital stay. Our case revealed that brain hyperperfusion in familial hemiplegic migraine (FHM) persists over an extended duration, and despite the disease being in a state of recovery, enhanced brain magnetic resonance imaging (MRI) continues to exhibit hyperperfusion. A genetic testing was performed which revealed a mutation in the FHM2 gene (c.1133C>T). The patient has been followed for 3years after hospital discharge. The boy suffered four episodes of hemiplegia and multiple episodes of headaches, and gradually developed seizures and cognitive impairment. It is advisable to consider FHM as a potential diagnosis for patients presenting with typical symptoms such as recurrent paroxysmal headaches and limb activity disorders.

KEYWORDS

ATP1A2, familial hemiplegic migraine, adolescent, hemiplegia, case report

Introduction

Migraine is a complex neurological disorder that affects 11% of the adults and 5% of children worldwide (1, 2). FHM is an uncommon autosomal dominant form of migraine characterized by a unique aura (3). The International Classification of Headache Disorders (ICHD-3) diagnostic criteria for FHM are as follows: A. at least two attacks, B. the presence of a reversible motor deficit, C. at least two of the following four characteristics: 1.at least one aura symptom spreads gradually over ≥5 min, and/or two or more symptoms occur in succession, 2. each individual aura symptom lasts 5–60 min, 3. at least one aura symptom is unilateral, 4. the aura is accompanied, or followed within 60 min, by headache, D. similar episodes in relatives, and E. subjects with related diseases were excluded (4). Three specific mutations in causative genes have been identified: CACNA1A (which encodes the subunit of the voltage-gated Ca2+ channel CaV2.1), ATP1A2 (which encodes the α2-subunit of the Na+/K+-ATPase), and SCN1A (which encodes the alpha subunit of a voltage-gated neuronal sodium channel) (5–7). In this report, we present the case of a 13-year-old adolescent patient with an undocumented novel mutation and multiple imaging findings associated with FHM2.

Case report

A 13-year-old male patient presented to our department with symptoms of headache, blurred vision, and left-sided weakness. Prior to his admission, the patient experienced a brief episode of blurred vision, followed by a severe right-sided headache accompanied by vomiting. Eventually, the patient developed difficulty moving his left side. Neurologic examination revealed drowsiness, restlessness upon stimulation, dysphagia, dysarthria, left-sided facial nerve palsy, left visual field defect, and a muscle strength of grade 1 in the left upper limb and grade 2 in the left lower limb. The boy experienced a febrile convulsion at the age of 6 months. Leading to hospitalization for fever, headache, and general convulsion at the ages of 4 and 5, respectively, with a subsequent coma lasting 5 to 6 days. He received a diagnosis of viral encephalitis and epilepsy. However, over the next 5 years, his electroencephalogram (EEG) showed no abnormalities. In his familial history, his grandmother has a history of recurrent headaches but no occurrences of hemiplegia.

Upon admission, the boy's body temperature was within the normal range. Nevertheless, he developed a fever after 10 h, which persisted for 2 days. The highest recorded body temperature was 39.2°C.

Laboratory examinations, encompassing blood routine test, C-reactive protein, and procalcitonin, exhibited no deviations. The cerebrospinal fluid (CSF) analysis and MRI of the cervical and thoracic spine (3 days after symptom onset) yielded negative findings. Computed tomography angiography (CTA) of the head and neck conducted 3 h after symptom onset, as well as brain MRI performed 22 h after symptom onset, revealed no pathological irregularities. Subsequently, an enhanced brain MRI conducted 12 days after symptom onset indicated the presence of a shallow right cerebral hemisphere groove and swelling of the gyrus. A brain MRI performed 45 days post-disease revealed normal results. EEG conducted during the boy's hospitalization and after discharge yielded normal results. Subsequently, a genetic analysis was conducted on the male patient, revealing a heterozygous point mutation (c.1133C>T) in exon 9 of chromosome 1q23. This mutation, located at amino acid 378, results in a threonine to isoleucine (p.Thr378Ile) substitution. The imaging findings are shown in Figure 1.

Treatment and prognosis: upon admission, the boy received empirical treatment consisting of intravenous (IV) ceftriaxone, acyclovir, and intravenous gammaglobulin for acute encephalitis. He experienced a persistent headache for a duration of 14 days. By hospital day 12, the boy exhibited improved mobility, accompanied by gradual muscle strength recovery, enabling him to ambulate independently with the assistance of external objects. On the 13th day of hospitalization, he achieved autonomous ambulation without requiring external aid. Consequently, he was discharged from the hospital on the 16th day of his hospitalization. Following discharge, the boy underwent a follow-up period exceeding 3 years. During this period, he experienced multiple times headaches, the headache locations were not fixed and predominantly throbbing sensation, and persisted for a duration ranging from a few seconds to a few hours, ultimately resolving spontaneously. Additionally, the boy experienced four episodes of hemiparesis, with three instances affecting the left side and one affecting the right side, and each occurrence of hemiparesis was accompanied by concurrent headaches and fever. The hemiplegia resolved spontaneously within a short time frame of minutes to hours. However, one of the hemiplegic episodes lasted 2 days, prompting the patient's admission to the hospital. The patient remained hospitalized for a total of 17 days, during which a brain MRI was conducted and yielded normal results. The patient gradually developed cognitive impairment and seizures, leading to a treatment regimen involving the administration of flunarizine for a period of 2 years, as well as the use of levetiracetam and Chinese traditional medicine for over 1 year.

Discussion

ATP1A2 gene is located on chromosome 1q23 and serves as the genetic unit responsible for encoding the a2 subunit of the Na+, K+ ATPase (a2NKA) (6). The a2 isoform is mainly expressed in skeletal muscle, heart, and brain, especially in astrocytes (8). The missense mutation FHM2 occurs in the ATP1A2 gene, resulting in a complete or partial impairment of a2NKA function (9). This abnormality in astrocytes disrupts the clearance of extracellular K+ and glutamate, leading to a reduction in glutamate clearance and an elevation of K+ levels in the synaptic cleft. Consequently, this cascade of events triggers an augmented susceptibility to inhibitory influences throughout the cortex of the affected hemisphere, ultimately leading

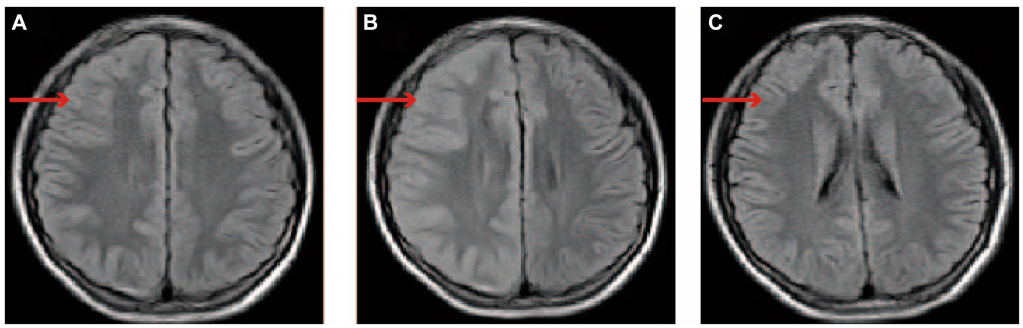

FIGURE 1
The changes of brain MRI images. **(A)** On day 1 following the onset of symptoms, the brain's MRI displayed unremarkable findings. **(B)** On day 12 after symptom onset, the brain enhancement MRI is characterized by thickening of the cerebral cortex in the right cerebral hemisphere, the widening of the gyri, and the disappearance or shallowness of the sulci. **(C)** On day 45 after symptom onset, the MRI of the brain returned to its normal state. The red arrow indicates the right cerebral cortex. MRI: magnetic resonance imaging.

to cortical depolarization and the manifestation of migraine aura (10–12).

The symptoms commonly observed in individuals with FHM include reversible visual, sensory, or language disturbances, as well as varying degrees of limb hemiplegia (13). Some individuals with FHM who possess a mutation in the ATP1A2 gene have experienced severe attacks characterized by recurrent coma, fever, and/or epileptic seizures (13, 14). It is plausible to consider that the viral encephalitis and seizures diagnosed in the boy at the age of 5 may represent a manifestation of the severe acute encephalopathy associated with this disease.

FHM2 brain imaging shows biphasic cerebral blood flow changes during the prolonged aura. After approximately 18–19 h of aura symptom onset of hemiplegic migraine with prolonged aura, there might be a turning point in the transition from hypoperfusion to hyperperfusion (15). Research conducted on FHM2 mutant mice has identified heightened sensitivity of smooth muscle cells in the middle cerebral artery to changes in intracellular calcium levels, resulting in localized cerebral vasoconstriction and subsequent hypoperfusion when subjected to subthreshold stimulation. This is followed by a gradual impairment of calcium channels, opening of the blood–brain barrier, and prolonged depolarization, leading to the diffusion of water from the intracellular to the extracellular space. Following an extended depolarization period, water permeated from the cellular interior to the extracellular space, leading to a delayed occurrence of heightened perfusion (16). Brain enhancement MRI findings in patients with ATP1A2 exhibit two characteristics: (i) normal findings, primarily observed in patients with mild hemiplegic migraine (HM) (17, 18), and (ii) hypoperfusion in the initial stage of the hemisphere opposite to the hemiplegia, followed by widespread diffusion-weighted imaging hyperintense signals in the subsequent stage, often accompanied by cortical swelling in certain patients (15, 17). Regrettably, the brain CTA of the boy conducted 3 hours after the onset of symptoms yielded normal results, with no findings of hypoperfusion. A brain enhanced MRI was not conducted on the boy 22 h following the onset of symptoms, instead, solely a brain MRI was performed, which did not detect any abnormalities. Surprisingly, on the 12th day post-admission, the patient's enhanced brain MRI revealed cortical swelling and increased cortical density, which were suggestive of hyperperfusion. In our study, it was observed that despite the patient's recovery 2 weeks after admission, the brain MRI still exhibited a hyperperfusion image in the affected cerebral hemisphere. This phenomenon can be attributed to the persistent and long-term nature of cortical spreading depression (CSD). The significant alterations in microcirculation and metabolism induced by CSD lead to a decline in blood vessel reactivity, disruption of the neurovascular coupling effect, continuous cerebral vessel edema, and ultimately prolonged high perfusion imaging.

According to the more than three-year follow-up, the patient had several times headache and limb weakness attacks. Significantly, it has been observed that the patient experienced long periods without hemiplegia attacks from the age of 5 to 12, indicating that the duration between episodes in individuals with FHM can extend to multiple years. The occurrence of FHM episodes primarily manifests during childhood, adolescence, and early adulthood, and the presence of early severe acute encephalopathies may be an indicator of poor disease prognosis. Several neuropsychological studies have demonstrated that focal and degenerative cerebellar disorders associated with FHM can result in significant cognitive impairments (19). Furthermore, individuals with FHM2 may exhibit severe forms of intellectual disability (14, 19). Additionally, investigations have revealed that mutations in all three FHM genes have the potential to cause epilepsy, with ATP1A2 mutations being particularly prevalent (19, 20). The occurrence of recurring migraine and hemiparesis in our case during adolescence, along with the progressive emergence of epilepsy and cognitive impairments, indicates the possibility of a severe gene mutation in the boy. This case presents an opportunity to investigate the mechanisms underlying this mutated gene through animal experiments focused on FHM. Additionally, the patient requires long-term antiepileptic treatment, rehabilitation training, and ongoing follow-up.

In recent years, when considering ATP1A2 mutations, it may be necessary to consider FHM and alternating hemiplegia of childhood (AHC), as they may share the same pathological mechanisms (21–23). Diagnostic criteria for AHC include: (1) repeated episodes of hemiplegia of varying severity or duration, involving alternating sides or both sides of the body; (2) onset before 18 months of age; (3) presence of other paroxysmal clinical signs, such as dystonic posturing, choreoathetoid movements, tonic spells, nystagmus, and autonomic features; and (4) progressive cognitive and neurological decline over time (24). In our case, the child experienced predominantly left-sided hemiplegic seizures, with occasional involvement of the right side. The boy also had epilepsy and varying degrees of mental retardation in the later stages of the disease, which needed to be distinguished from ACH. In this case, the boy had a history of febrile convulsions at 6 months old, convulsions and coma at 4–5 years old, and hemiplegic migraines at 13 years old. There were no other neurological abnormalities observed in this boy for over 10 years. Additionally, only the patient's maternal grandmother had a history of headaches, and there were no instances of hemiplegia in the family. Therefore, ATP1A2-induced hemiplegia and migraine should be carefully differentiated.

In summary, it is crucial to explore the familial history of headaches and hemiplegia in patients, even in the absence of conventional brain imaging and examination. Genetic testing is of utmost importance for individuals exhibiting signs of potential hereditary disorders.

Data availability statement

The original contributions presented in the study are included in the article/supplementary material, further inquiries can be directed to the corresponding author.

Ethics statement

The studies involving humans were approved by the Fifth People's Hospital of Chengdu. The studies were conducted in accordance with the local legislation and institutional requirements. Written informed consent for participation in this study was provided by the participants' legal guardians/next of kin. Written informed consent was obtained from the minor(s)' legal guardian/next of kin for the publication of any potentially identifiable images or data included in this article.

Author contributions

HZ: Writing – original draft, Writing – review & editing. LJ: Writing – review & editing, Writing – original draft. YX: Writing

– review & editing. SY: Writing – review & editing, Conceptualization.

Funding

The author(s) declare that no financial support was received for the research, authorship, and/or publication of this article.

Acknowledgments

The authors are grateful to colleagues and radiologist for their close cooperation in image data collection and technical consultation.

Conflict of interest

The authors declare that the research was conducted in the absence of any commercial or financial relationships that could be construed as a potential conflict of interest.

Publisher's note

References

1. Scher AI, Gudmundsson LS, Sigurdsson S, Ghambaryan A, Aspelund T, Eiriksdottir G. Migraine headache in middle age and late-life brain infarcts. *JAMA*. (2009) 301:2563–70. doi: 10.1001/jama.2009.932

2. Amiri P, Kazeminasab S, Nejadghaderi SA, Mohammadinasab R, Pourfathi H, Araj-khodaei M, et al. Migraine: a review on its history, global epidemiology, risk factors, and comorbidities. *Front Neurol*. (2022) 12:800605. doi: 10.3389/fneur.2021.800605

3. Romanos J, Benke D, Pietrobon D, Zeilhofer HU, Santello M. Astrocyte dysfunction increases cortical dendritic excitability and promotes cranial pain in familial migraine. *Sci Adv*. (2020) 6:eaaz1584. doi: 10.1126/sciadv.aaz1584

4. Headache Classification Subcommittee of the International Head-ache Society. The international classification of headache disorders: 3rd edition. *Cephalalgia*. (2013) 33:629–808. doi: 10.1177/0333102413485658

5. Ophoff RA, Terwindt GM, Vergouwe MN, van Eijk R, Oefner PJ, Hoffman SM, et al. Familial hemiplegic migraine and episodic ataxia Type-2 are caused by mutations in the Ca2+ channel gene CACNL1A4. *Cell*. (1996) 87:543–52. doi: 10.1016/S0092-8674(00)81373-2

6. Fusco MD, Marconi R, Silvestri L, Atorino L, Rampoldi L, Morgante L, et al. Haploinsufficiency of ATP1A2 encoding the na+/K+ pump α2 subunit associated with familial hemiplegic migraine type 2. *Nat Genet*. (2003) 33:192–6. doi: 10.1038/ng1081

7. Dichgans M, Freilinger T, Eckstein G, Babini E, Lorenz-Depiereux B, Biskup S, et al. Mutation in the neuronal voltage-gated sodium channel SCN1A in familial hemiplegic migraine. *Lancet*. (2005) 366:371–7. doi: 10.1016/S0140-6736(05)66786-4

8. Smith SE, Chen X, Brier LM, Bumstead JR, Rensing NR, Ringel AE, et al. Astrocyte deletion of α2-na/K ATPase triggers episodic motor paralysis in mice via a metabolic pathway. *Nat Commun*. (2020) 11. doi: 10.1038/s41467-020-19915-2

9. Stoica A, Larsen BR, Assentoft M, Holm R, Holt LM, Vilhardt F, et al. The α2β2 isoform combination dominates the astrocytic na+/K+-ATPase activity and is rendered nonfunctional by the α2.G301R familial hemiplegic migraine type 2-associated mutation. *Glia*. (2017) 65:1777–93. doi: 10.1002/glia.23194

10. Leo L, Gherardini L, Barone V, De Fusco M, Pietrobon D, Pizzorusso T, et al. Increased susceptibility to cortical spreading depression in the mouse model of familial hemiplegic migraine type 2. *PLoS Genet*. (2011) 7:e1002129. doi: 10.1371/journal.pgen.1002129

11. Capuani C, Melone M, Tottene A, Bragina L, Crivellaro G, Santello M, et al. Defective glutamate and K+clearance by cortical astrocytes in familial hemiplegic migraine type 2. *EMBO Mol Med*. (2016) 8:967–86. doi: 10.15252/emmm.201505944

12. Unekawa M, Ikeda K, Tomita Y, Kawakami K, Suzuki N. Enhanced susceptibility to cortical spreading depression in two types of na+,K+-ATPase α2 subunit-deficient mice as a model of familial hemiplegic migraine 2. *Cephalalgia*. (2017) 38:1515–24. doi: 10.1177/0333102417738249

13. Pelzer N, Blom DE, Stam AH, Vijfhuizen LS, Hageman ATM, van Vliet JA, et al. Recurrent coma and fever in familial hemiplegic migraine type 2. A prospective 15-year follow-up of a large family with a novel ATP1A2 mutation. *Cephalalgia*. (2016) 37:735–55. doi: 10.1177/0333102416651284

14. Du Y, Li C, Duan F, Zhao C, Zhang W. Early treatment in acute severe encephalopathy caused by ATP1A2 mutation of familial hemiplegic migraine type 2: case report and literature review. *Neuro pediatrics*. (2019) 51:215–20. doi: 10.1055/s-0039-3400986

15. Iizuka T, Tominaga N, Kaneko J, Sato M, Akutsu T, Hamada J, et al. Biphasic neurovascular changes in prolonged migraine aura in familial hemiplegic migraine type 2. *J Neurol Neurosurg Psychiatry*. (2014) 86:344–53. doi: 10.1136/jnnp-2014-307731

16. Staehr C, Hangaard L, Bouzinova EV, Kim S, Rajanathan R, Boegh Jessen P, et al. Smooth muscle Ca2+ sensitization causes hypercontractility of middle cerebral arteries in mice bearing the familial hemiplegic migraine type 2 associated mutation. *J Cereb Blood Flow Metab*. (2019) 39:1570–87. doi: 10.1177/0271678X18761712

17. Yang GE, Song CL, Yang B, Zhou SZ, Li WH. Clinical features and genetic analysis of two Chinese ATP1A2 gene variants pedigrees of familial hemiplegic migraine. *Jf Neurorestoratol*. (2023) 11. doi: 10.1016/j.jnrt.2023.100053

18. Antonaci F, Ravaglia S, Grieco GS, Gagliardi S, Cereda C, Costa A. Familial hemiplegic migraine type 2 due to a novel missense mutation in ATP1A2. *J Headache Pain*. (2021) 22:12. doi: 10.1186/s10194-021-01221-x

19. Li YJ, Tang WJ, Kang L, Kong SS, Zhao D, Zhao DF, et al. Functional correlation of ATP1A2 mutations with phenotypic spectrum: from pure hemiplegic migraine to its variant forms. *J Headache Pain*. (2021) 22:92. doi: 10.1186/s10194-021-01309-4

20. Hasırcı Bayır BR, Tutkavul K, Eser M, Baykan B. Epilepsy in patients with familial hemiplegic migraine. *Seizure*. (2021) 88:87–94. doi: 10.1016/j.seizure.2021.03.028

21. Pavlidis E, Uldall P, Gøbel Madsen C, Nikanorova M, Fabricius M, Høgenhaven H, et al. Alternating hemiplegia of childhood and a pathogenic variant of ATP1A3: a case report and pathophysiological considerations. *Epileptic Disord*. (2017) 19:226–30. doi: 10.1684/epd.2017.0913

22. Zhang X, Qiu SY, Yang L, Li YF, Xu LY, Xu N, et al. A novel heterozygous ATP1A2 pathogenic variant in a Chinese child with MELAS-like alternating hemiplegia. *Mol Genet Genomic Med*. (2023) 11:e2146. doi: 10.1002/mgg3.2146

23. Kornbluh AB, Chung MG. Teaching NeuroImages: transient cytotoxic edema in a child with a novelATP1A2mutation. *Neurology*. (2020) 95:e1441–2. doi: 10.1212/WNL.0000000000010103

24. Swoboda KJ, Kanavakis E, Xaidara A, Johnson JE, Leppert MF, Schlesinger-Massart MB, et al. Alternating hemiplegia of childhood or familial hemiplegic migraine? A novel ATP1A2 mutation. *Ann Neurol*. (2004) 55:884–7. doi: 10.1002/ana.20134

frontiers | Frontiers in Neurology

TYPE Case Report
PUBLISHED 28 February 2024
DOI 10.3389/fneur.2024.1319962

OPEN ACCESS

EDITED BY
Huifang Shang,
Sichuan University, China

REVIEWED BY
Masayoshi Sakakura,
Yokohama City University, Tsurumi, Japan
Christopher P. Ptak,
The University of Iowa, United States

*CORRESPONDENCE
Yi-Hui Liu
✉ cygl0722@gmail.com
Yao Deng
✉ 619065374@qq.com
Lu-Lu Tang
✉ lltang@csu.edu.cn

†These authors have contributed equally to this work

RECEIVED 11 October 2023
ACCEPTED 07 February 2024
PUBLISHED 28 February 2024

CITATION
Cao G-H, Zhao M-F, Dong Y, Fan L-L, Liu Y-H, Deng Y and Tang L-L (2024) Case report: A novel variant (H49N) in *Myelin Protein Zero* gene is responsible for a patient with Charcot–Marie–Tooth disease. *Front. Neurol.* 15:1319962. doi: 10.3389/fneur.2024.1319962

Case report: A novel variant (H49N) in *Myelin Protein Zero* gene is responsible for a patient with Charcot–Marie–Tooth disease

Gao-Hui Cao[1†], Mei-Fang Zhao[1†], Yi Dong[1], Liang-Liang Fan[1], Yi-Hui Liu[2*], Yao Deng[3*] and Lu-Lu Tang[1*]

[1]Department of Cell Biology, School of Life Sciences, Central South University, Changsha, China, [2]Department of Neurology, Affiliated Hospital of Yangzhou University, Yangzhou, China, [3]Department of Cardiovascular Surgery, National Clinical Research Center for Geriatric Disorders, Xiangya Hospital, Central South University, Changsha, China

This report presents a case of Charcot–Marie–Tooth dominant intermediate D (CMTDID), a rare subtype of Charcot–Marie–Tooth disease, in a 52 years-old male patient. The patient exhibited mobility impairment, foot abnormalities (pes cavus), and calf muscle atrophy. Whole exome sequencing and Sanger sequencing suggested that a novel variant (NM_000530.8, c.145C>A/p.His49Asn) of *MPZ* may be the genetic lesion in the patient. The bioinformatic program predicted that the new variant (p.His49Asn), located at an evolutionarily conserved site of *MPZ*, was neutral. Our study expands the variant spectrum of *MPZ* and the number of identified CMTDID patients, contributing to a better understanding of the relationship between *MPZ* and CMTDID.

KEYWORDS

***Myelin Protein Zero*, Charcot–Marie–Tooth disease, CMT dominant intermediate D, missense variant, whole exome sequencing**

1 Introduction

Charcot–Marie–Tooth disease (CMTD) encompasses a genetically heterogeneous group of disorders called hereditary sensory and motor neuropathies that damage the peripheral nerves (1, 2). The typical symptoms of CMTD include muscle atrophy in the feet, pes cavus, and decreased sensitivity to touch, heat, and cold in the feet and lower legs (3). Other symptoms, including hearing loss, scoliosis, hip dysplasia, restless legs syndrome, and tremor, can also be present in CMTD patients (3). As the most common inherited disorder involving the peripheral nerves, the prevalence of CMTD is about 1 in 2,500 worldwide (4). Currently, variants in four genes (*Peripheral Myelin Protein 22, Gap Junction Beta 1, Myelin Protein Zero, and Mitofusin 2*), are responsible for over 90% of CMT patients (5).

The *Myelin Protein Zero* (*MPZ*) gene is located on chromosome 1q23.3, and it consists of 6 exons, spanning approximately 6,369 kilobases. This gene is specifically expressed in Schwann cells of the peripheral nervous system and encodes a type I transmembrane glycoprotein that is a major structural component of the peripheral myelin sheath (6, 7). Acting as an adhesion molecule, the MPZ protein functions like molecular glue, playing a role in tightly packing the myelin around nerve cells, which wrap around and insulate peripheral

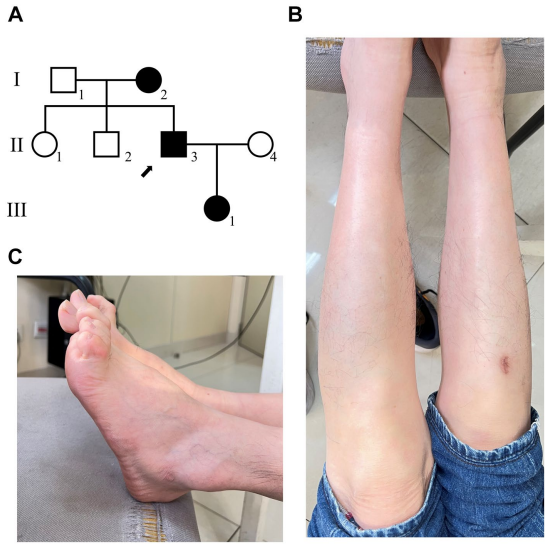

FIGURE 1
The clinical diagnosis of the proband. **(A)** Family diagram of patients with disease, and the arrow shows the proband. **(B)** The morphology of the patient's feet has significantly high arches. **(C)** The patient has calf muscle atrophy.

nerves (7). Currently, approximately 5% of CMTD patients result from variants in *MPZ* (8–10). Additionally, some studies have also reported that *MPZ* variants can lead to other polyneuropathies, such as Dejerine–Sottas syndrome and congenital hypomyelinating nesuropathy (11, 12).

Here, we studied a Chinese family presenting with distal atrophy and weakness. Whole exome sequencing revealed a novel variant (NM_000530.8, c.145C>A/p.His49Asn) in the *MPZ* gene within the proband. Sanger sequencing additionally confirmed the presence of this novel variant in other affected family members, suggesting co-segregation. Furthermore, bioinformatics software predicted that this newly identified *MPZ* variant is deleterious.

2 Case report

2.1 Clinical description

The family, including seven people were investigated in this study (Figure 1A). The proband (II-3), a 52 years-old male from Jiangsu province in eastern China. The proband came to our clinic 1 year ago (November 2022). According to his own account, he began to realize that exercise was more difficult seven years ago (at the age of 45). The condition slowly worsened until it was difficult to walk, so he came to our hospital for consultation.

Clinical examination reveals: the proband's lower limbs exhibit an inverted bottle shape, noticeable atrophy of the calf muscles, and spinal curvature. The proband has no dislocation, but the arches are markedly elevated, displaying claw-like deformities in the toes. The patient experiences difficulties in movement, demonstrating an abnormal striding gait and poor limb balance. The patient has weaknesses in the lower limb muscles, reduced strength in the arms, but no limb tremors. Both Achilles tendon reflex and knee-jerk reflex

TABLE 1 Motor nerve conduction velocities of EMG result.

MNCV		Latency (ms)	Amplitude (mv)	CV (m/s)	F-wave latency (ms)
Ulnar nerve. Left	Wrist-ADM	2.99	7.80		40.30
	Below elbow-wrist	11.20	5.90	34.10	
Ulnar nerve. Right	Wrist-ADM	3.85	5.60		42.40
	Below elbow-wrist	11.30	5.10	37.60	
Median nerve. Left	Wrist-APB	6.57	3.50		44.50
	Elbow-wrist	13.10	2.50	38.30	
Median nerve. Right	Wrist-APB	5.45	5.10		45.10
	Elbow-wrist	12.80	4.10	34.00	
Tibial nerve. Left	Ankle-AH	5.58	9.30		52.00
	Popliteal-ankle	18.90	5.30	34.50	
Tibial nerve. Right	Ankle-AH	6.35	6.90		52.70
	Popliteal-ankle	21.50	3.40	27.10	
Nervi peroneal is common. Left	Below knee-tibialis anterior	4.52	2.30		
	Upon knee-below knee	6.90	2.20	42.00	
Nervi peroneal is common. Right	Below knee-tibialis anterior	6.96	0.75		
	Upon knee-below knee	9.76	1.39	35.70	

are diminished, and there is a decrease in pinprick sensation (Figures 1B,C). Electromyography (EMG) indicated multiple symmetrical peripheral nerve lesions, particularly myelin damage. Peripheral motor nerve conduction velocity (MNCV) was moderately impaired (Table 1), alongside reduced sensory nerve conduction velocities (SNCV) in the upper limb (Table 2). In addition, autoimmune peripheral neuropathy and paraneoplastic nerve

TABLE 2 Sensory nerve conduction velocities of EMG result.

SNCV		Latency (ms)	Amplitude (mv)	CV (m/s)
Ulnar nerve. Left	Finger V-wrist	4.79	2.1	24.7
Ulnar nerve. Right	Finger V-wrist	4.25	3.8	34.6

syndrome were excluded by examining ganglioside antibody spectrum (GM1, GD1b, GQ1b, GM2, GM3, GD1a, GT1b, Sulfatide, GM4, GD2, GD3, GT1a) and paraneoplastic nerve syndrome spectrum [Hu, Yo, Ri, CV2, PNMA2 (Ma-2/Ta), amphiphysin, recoverin, SOX1, titin, Zic4, GAD65, Tr (DNER)] in serum and cerebrospinal fluid. A family history investigation indicated that his mother (I-2) also suffered from mobility impairment and calf muscle atrophy. Additionally, his daughter (III-1) occasionally experiences muscle weakness in her limbs.

As a result, patients are diagnosed with Charcot–Marie–Tooth disease. CMT cannot be effectively treated, so none of the patients were hospitalized. Patients are advised to increase their intake of vitamins B1 and B12. A follow-up was conducted 1 year later. There was no significant change in the patient's condition.

2.2 Genetic analysis

Initially, multiplex ligation-dependent probe amplification was employed to exclude copy number variants in two candidate genes, *Kinesin Family Member 1B* and *Peripheral Myelin Protein 22*, which are commonly associated with copy number variations in CMTD patients (Supplementary Figure S1). Subsequently, the proband underwent whole sequencing to detect potential gene variants. A total of 9.16 GB of data, encompassing 70,012 SNVs/Indels, were identified in the proband. Following the aforementioned data filtering process, 12 variants were retained (Supplementary Table S1). Among these 12 variants, only the novel variant (NM_000530.8, c.145C>A/p.His49Asn) in *MPZ* was deemed to be the underlying genetic anomaly for the family. Sanger sequencing further confirmed the co-segregation of this variant with the affected family members (Figure 2A) and its absence in our 200 control cohorts. This novel variant, resulting in the substitution of histidine with asparagine, was located at a neutral tolerant site and Immunoglobulin-like domain of protein zero (IgV_P0) (Figure 2B). We predicted and compared the protein structure after the p.His49Asn variant (Figure 2C), based on the latest reports of IgV_P0 domain (PDBid: 8iia (13)). Surface potential analysis additionally revealed that variant altered the surface charge of the MPZ protein (Figure 2C). According to ACMG guideline, the variant belongs to Likely pathogenic (PM1 + PM2 + PP1 + PP3) (14).

3 Discussion and conclusion

Charcot–Marie–Tooth disease (CMTD) comprises several subtypes, including CMT dominant intermediate D (CMTDID), a rare form defined by motor nerve conduction velocity (MNCV) falling within the intermediate range of 25–45 m/s (1, 15). This subtype was initially reported in 1999 within a 4-generation Macedonian family. The family exhibited a symmetrical pattern of distal muscle atrophy, weakness, and sensory impairment, more pronounced in the lower limbs and to a lesser extent in the upper limbs, besides, the youngest patients only 34 years old (16). In our study, the proband showed myelin damage in both motor and sensory nerves, with MNCV ranging from 27–42 m/s. Whole exome sequencing and Sanger sequencing further confirmed that the *MPZ* variant (NM_000530.8, c.145C>A/p.His49Asn) was the genetic anomaly responsible for the family's condition. Our research may broaden the variant spectrum of *MPZ* and aid in genetic counseling and early diagnosis for CMT disease patients.

MPZ protein, an integral membrane glycoprotein, primarily connects adjacent lamellae to stabilize myelin assembly (17). It serves as the principal structural component of peripheral myelin and is exclusively expressed in Schwann cells (18). The MPZ protein is composed of three domains: a singular Immunoglobulin V-Type-like extracellular domain, a lone transmembrane domain, and a single cytosolic domain (19). Previous studies have indicated that the majority of pathogenic *MPZ* variants can trigger the unfolded protein response and endoplasmic reticulum retention (7). In our investigation, the novel variant (NM_000530.8, c.145C>A/p.His49Asn) in *MPZ* was situated in the extracellular IgV_P0 domain (Figure 2B). Crystallographic analysis of the extracellular domain of MPZ revealed its capacity to form interactions, resulting in homotetramer structures which are supported by recent solution-based studies using SEC, SAXS, and NMR (13, 20). Further, one recent study indicated that the extracellular domains of the MPZ protein form an 8-mer responsible with a potential involvement in membrane adhesion (13). The novel variant's alteration of the MPZ protein's charge may potentially influence the stabilization of membrane layers in compact myelin and adhesion between layers, further leading to demyelination (Figure 2C). Also, MPZ plays a crucial role in the development of myelin structure. Variants in *MPZ* could potentially impact the normal formation of myelin, consequently disturbing the interactions between Schwann cells and axons, ultimately resulting in abnormal axon (7). Interestingly, the earliest identified CMTDID patients carried the D35Y variant (16). The shortest distance between D35 and H49 (B conformation) is 4 angstroms, and the shortest distance between D35 and N49 is only 3.6 angstroms (Figure 2C). Therefore, there may be a relationship between CMTDID disease and residue contact of these two positions. In addition, Veneri et al. (21) found that the increase of glycosylation sites in MPZ can impair its function and lead to loosen myelin. Mutations in H49N produce an NCS sequence that belongs to the glycosylation motif (N-X-S/T), resulting in excessively glycosylation of MPZ. CMTDID reported in this study belongs to the intermediate type (16), showing both mild demyelinating lesions and mild axonal abnormalities.

Currently, a total of 180 variants in the *MPZ* gene have been reported in patients displaying various phenotypes. Through summarizing these reported *MPZ* variants, we observed that the majority of cases (78.2%) carrying *MPZ* variants exhibited Charcot–Marie–Tooth (CMT) phenotypes. Additionally, 7.4% of carriers presented with Dejerine–Sottas syndrome, and 0.8% displayed Roussy–Levy syndrome. Within 78.2% of carriers manifesting CMT diseases, a mere 0.4% of patients showed the CMT dominant intermediate D (CMTDID) subtype (HGMD database: https://www.

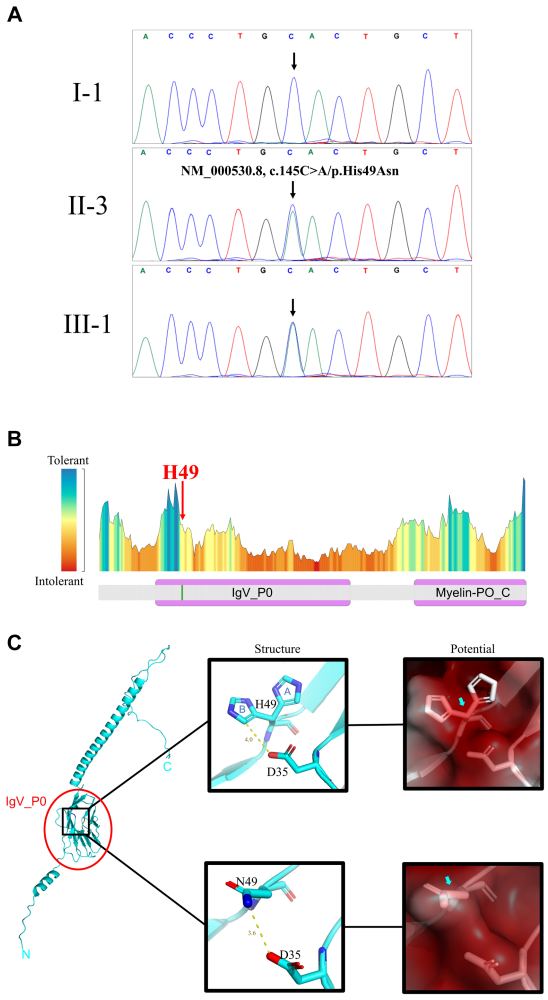

FIGURE 2
Gene and protein analysis. **(A)** Sanger sequencing results for I-1 (unaffected +/+), II-3 (affected +/−), and III-1 (affected +/−) patients (see Figure 1A for pedigree). **(B)** Predicted residue tolerance in the MPZ protein obtained using MetaDome. H49 is predicted to be of neutral tolerance to mutations. MPZ contains two domains: immunoglobulin-like domain of protein zero (IgV_P0) and Myelin-PO glycoprotein cytoplasmic C-term (Myelin-PO_C) by Conserved Domain Search prediction. **(C)** H49 is located on the IgV_P0 domain shown on the full length MPZ model (left panel). The atomic conformation (middle panels) and the surface electrostatic potential energy (right panels) change with the H49N variant. In the middle panels, blue "A" and "B" indicate 2 conformations of H49 in the crystal structure. Yellow line and text indicate the distance between atoms on side chains at positions 35 and 49 (angstrom). The blue and red atoms represent negative and positive charges, respectively. The variation of H49N causes the side chain charge from negative to become neutral. In the right panels, red means positive, blue means negative, and white means neutral. The surface potential prediction is slight changed from positive to neutral.

hgmd.cf.ac.uk/ac/index.php). This scarcity underscores the rarity of CMTDID subtypes identified among *MPZ* variant carriers. In this context, we identified a novel *MPZ* variant (NM_000530.8, c.145C>A/p.His49Asn) in a CMTDID patient, thereby reporting a unique case arising from a novel *MPZ* variant. This contributes to the expanding pool of recognized CMTDID patients and furthers our understanding of this subtype.

In MPZ+/− mice, neuropathy develops in adulthood, displaying minimal nerve conduction slowing and mild demyelination, akin to patients with *MPZ* variants (22, 23). Recently, Shackleford et al. created a new *MPZ* variant (p.T124M) knock-in mouse model, revealing impaired motor performance, reduced compound motor action potential amplitudes, and axonal damage, albeit with normal nerve conduction velocities (24). The distinctions between MPZ+/− mice and MPZ (p.T124M) knock-in mice underscore the intricate role of *MPZ* in CMT disease development, implying that this study's primary constraint lies in its absence of functional research.

In summation, our study employed whole exome sequencing and Sanger sequencing to identify a novel *MPZ* variant (NM_000530.8, c.145C>A/p.His49Asn) in a Chinese family afflicted by CMT disease. Subsequent analysis validated this variant as the cause of a rare CMT subtype known as CMTDID. Our work enhances the diversity of *MPZ* variant profiles and the roster of recognized CMTDID patients, contributing to a deeper comprehension of the relationship between *MPZ* and CMTDID.

Data availability statement

The datasets presented in this article are not readily available because of ethical and privacy restrictions. Requests to access the datasets should be directed to the corresponding authors.

Ethics statement

The studies involving humans were approved by the Ethics Committee of the Affiliated Hospital of Yangzhou University, Yangzhou, China. The studies were conducted in accordance with the local legislation and institutional requirements. The participants provided their written informed consent to participate in this study. Written informed consent was obtained from the individual(s) for the publication of any potentially identifiable images or data included in this article.

Author contributions

GH-C: Data curation, Formal analysis, Investigation, Software, Validation, Visualization, Writing – original draft. M-FZ: Data curation, Formal analysis, Investigation, Methodology, Software, Validation, Visualization, Writing – original draft. YDo: Writing – review & editing. L-LF: Methodology, Writing – review & editing. Y-HL: Writing – review & editing. YDe: Conceptualization, Funding acquisition, Project administration, Resources, Supervision, Validation, Writing – review & editing. L-LT: Conceptualization, Funding acquisition, Project administration, Resources, Supervision, Validation, Writing – review & editing.

Funding

The author(s) declare financial support was received for the research, authorship, and/or publication of this article. This research was supported by the National Natural Science Foundation of China (82201394); the Open Research Fund of State Key Laboratory of Hybrid Rice (Wuhan University) (KF202202); Research Project of the Hunan Provincial Health Commission (202103012102); Central

South University Graduate Students' Independent Exploration and Innovation Project (2023ZZTS0571).

Acknowledgments

The authors are grateful to the patients who agreed to participate in the study for their assistance.

Conflict of interest

The authors declare that the research was conducted in the absence of any commercial or financial relationships that could be construed as a potential conflict of interest.

Publisher's note

Supplementary material

The Supplementary material for this article can be found online at: https://www.frontiersin.org/articles/10.3389/fneur.2024.1319962/full#supplementary-material

References

1. Berciano J, García A, Gallardo E, Peeters K, Pelayo-Negro AL, Álvarez-Paradelo S, et al. Intermediate Charcot–Marie–Tooth disease: an electrophysiological reappraisal and systematic review. *J Neurol*. (2017) 264:1655–77. doi: 10.1007/s00415-017-8474-3

2. Volodarsky M, Kerkhof J, Stuart A, Levy M, Brady LI, Tarnopolsky M, et al. Comprehensive genetic sequence and copy number analysis for Charcot–Marie–Tooth disease in a Canadian cohort of 2517 patients. *J Med Genet*. (2021) 58:284–8. doi: 10.1136/jmedgenet-2019-106641

3. Pareyson D, Marchesi C. Diagnosis, natural history, and management of Charcot–Marie–Tooth disease. *Lancet Neurol*. (2009) 8:654–67. doi: 10.1016/S1474-4422(09)70110-3

4. Barreto LCLS, Oliveira FS, Nunes PS, de França Costa IMP, Garcez CA, Goes GM, et al. Epidemiologic study of Charcot–Marie–Tooth disease: a systematic review. *Neuroepidemiology*. (2016) 46:157–65. doi: 10.1159/000443706

5. Herrmann DN. Experimental therapeutics in hereditary neuropathies: the past, the present, and the future. *Neurotherapeutics*. (2008) 5:507–15. doi: 10.1016/j.nurt.2008.07.001

6. Moss KR, Bopp TS, Johnson AE, Höke A. New evidence for secondary axonal degeneration in demyelinating neuropathies. *Neurosci Lett*. (2021) 744:135595. doi: 10.1016/j.neulet.2020.135595

7. Shy ME, Jáni A, Krajewski K, Grandis M, Lewis RA, Li J, et al. Phenotypic clustering in MPZ mutations. *Brain*. (2004) 127:371–84. doi: 10.1093/brain/awh048

8. Hayasaka K, Himoro M, Sato W, Takada G, Uyemura K, Shimizu N, et al. Charcot–Marie–Tooth neuropathy type 1B is associated with mutations of the myelin P_0 gene. *Nat Genet*. (1993) 5:31–4. doi: 10.1038/ng0993-31

9. Auer-Grumbach M, Strasser-Fuchs S, Robl T, Windpassinger C, Wagner K. Late onset Charcot–Marie–Tooth 2 syndrome caused by two novel mutations in the MPZ gene. *Neurology*. (2003) 61:1435–7. doi: 10.1212/01.WNL.0000094197.46109.75

10. Seeman P, Mazanec R, Huehne K, Suslíková P, Keller O, Rautenstrauss B. Hearing loss as the first feature of late-onset axonal CMT disease due to a novel P0 mutation. *Neurology*. (2004) 63:733–5. doi: 10.1212/01.WNL.0000134605.61307.DE

11. Hayasaka K, Himoro M, Sawaishi Y, Nanao K, Takahashi T, Takada G, et al. *De novo* mutation of the myelin P_0 gene in Dejerine–Sottas disease (hereditary motor and sensory neuropathy type III). *Nat Genet*. (1993) 5:266–8. doi: 10.1038/ng1193-266

12. Auer-Grumbach M, Strasser-Fuchs S, Wagner K, Körner E, Fazekas F. Roussy–Lévy syndrome is a phenotypic variant of Charcot–Marie–Tooth syndrome IA associated with a duplication on chromosome 17p11.2. *J Neurol Sci*. (1998) 154:72–5. doi: 10.1016/S0022-510X(97)00218-9

13. Sakakura M, Tanabe M, Mori M, Takahashi H, Mio K. Structural bases for the Charcot–Marie–Tooth disease induced by single amino acid substitutions of myelin protein zero. *Structure*. (2023) 31:1452–1462.e4. doi: 10.1016/j.str.2023.08.016

14. Miller DT, Lee K, Abul-Husn NS, Amendola LM, Brothers K, Chung WK, et al. ACMG SF v3.2 list for reporting of secondary findings in clinical exome and genome sequencing: a policy statement of the American College of Medical Genetics and Genomics (ACMG). *Genet Med*. (2023) 25:100866. doi: 10.1016/j.gim.2023.100866

15. Young P, De Jonghe P, Stögbauer F, Butterfass-Bahloul T. Treatment for Charcot–Marie–Tooth disease. *Cochrane Database Syst Rev*. (2008) 2008:CD006052. doi: 10.1002/14651858.CD006052.pub2

16. Mastaglia FL, Nowak KJ, Stell R, Phillips BA, Edmondston JE, Dorosz SM, et al. Novel mutation in the myelin protein zero gene in a family with intermediate hereditary motor and sensory neuropathy. *J Neurol Neurosurg Psychiatry*. (1999) 67:174–9. doi: 10.1136/jnnp.67.2.174

17. Howard P, Feely SME, Grider T, Bacha A, Scarlato M, Fazio R, et al. Loss of function MPZ mutation causes milder CMT1B neuropathy. *J Peripher Nerv Syst*. (2021) 26:177–83. doi: 10.1111/jns.12452

18. Lei L, Han D, Gong S, Zheng J, Xu J. *Mpz* gene suppression by shRNA increases Schwann cell apoptosis *in vitro*. *Neurol Sci*. (2010) 31:603–8. doi: 10.1007/s10072-010-0341-2

19. Lemke G, Axel R. Isolation and sequence of a cDNA encoding the major structural protein of peripheral myelin. *Cell*. (1985) 40:501–8. doi: 10.1016/0092-8674(85)90198-9

20. Ptak CP, Peterson TA, Hopkins JB, Ahern CA, Shy ME, Piper RC. Homomeric interactions of the MPZ Ig domain and their relation to Charcot–Marie–Tooth disease. *Brain*. (2023) 146:5110–23. doi: 10.1093/brain/awad258

21. Veneri FA, Prada V, Mastrangelo R, Ferri C, Nobbio L, Passalacqua M, et al. A novel mouse model of CMT1B identifies hyperglycosylation as a new pathogenetic mechanism. *Hum Mol Genet*. (2022) 31:4255–74. doi: 10.1093/hmg/ddac170

22. Giese KP, Martini R, Lemke G, Soriano P, Schachner M. Mouse P_0 gene disruption leads to hypomyelination, abnormal expression of recognition molecules, and degeneration of myelin and axons. *Cell*. (1992) 71:565–76. doi: 10.1016/0092-8674(92)90591-Y

23. Wrabetz L, Feltri ML, Quattrini A, Imperiale D, Previtali S, D'Antonio M, et al. P_0 glycoprotein overexpression causes congenital hypomyelination of peripheral nerves. *J Cell Biol*. (2000) 148:1021–34. doi: 10.1083/jcb.148.5.1021

24. Shackleford GG, Makoukji J, Grenier J, Liere P, Meffre D, Massaad C. Differential regulation of Wnt/beta-catenin signaling by liver X receptors in Schwann cells and oligodendrocytes. *Biochem Pharmacol*. (2013) 86:106–14. doi: 10.1016/j.bcp.2013.02.036

frontiers | Frontiers in Neurology

TYPE Case Report
PUBLISHED 20 March 2024
DOI 10.3389/fneur.2024.1362013

OPEN ACCESS

EDITED BY
Ryan Davis,
Kolling Institute, Australia

REVIEWED BY
David Manser,
The University of Sydney, Australia
Rei Yasuda,
Kyoto Prefectural University of Medicine, Japan
Ferdy Cayami,
Diponegoro University, Indonesia
James E. Goldman,
Columbia University, United States

*CORRESPONDENCE
Giovanni Ristori
✉ giovanni.ristori@uniroma1.it

RECEIVED 27 December 2023
ACCEPTED 05 March 2024
PUBLISHED 20 March 2024

CITATION
Romano C, Morena E, Petrucci S, Diamant S, Marconi M, Travaglini L, Zanni G, Piane M, Salvetti M, Romano S and Ristori G (2024) Case report: A novel mutation of glial fibrillary acidic protein gene causing juvenile-onset Alexander disease.
Front. Neurol. 15:1362013.
doi: 10.3389/fneur.2024.1362013

Case report: A novel mutation of glial fibrillary acidic protein gene causing juvenile-onset Alexander disease

Carmela Romano[1], Emanuele Morena[2], Simona Petrucci[3,4], Selene Diamant[2], Martina Marconi[2], Lorena Travaglini[5], Ginevra Zanni[6], Maria Piane[3,4], Marco Salvetti[2,7], Silvia Romano[2] and Giovanni Ristori[2,8]*

[1]Department of Human Neurosciences, Sapienza University of Rome, Sant'Andrea Hospital, Rome, Italy, [2]Department of Neurosciences, Mental Health and Sensory Organs, Sapienza University of Rome, Sant'Andrea Hospital, Rome, Italy, [3]Department of Clinical and Molecular Medicine, Faculty of Medicine and Psychology, Sapienza University of Rome, Rome, Italy, [4]S. Andrea University Hospital, Rome, Italy, [5]Laboratory of Medical Genetics, Bambino Gesù Children's Hospital, IRCCS, Rome, Italy, [6]Genetics and Rare Diseases Research Division, Unit of Neuromuscular and Neurodegenerative Disorders, Bambino Gesù Children's Hospital, IRCCS, Rome, Italy, [7]IRCCS Istituto Neurologico Mediterraneo (INM) Neuromed, Pozzilli, Italy, [8]Neuroimmunology Unit, IRCCS Fondazione Santa Lucia, Rome, Italy

Alexander disease (AxD) is a rare inherited autosomal dominant (AD) disease with different clinical phenotypes according to the age of onset. It is caused by mutations in the glial fibrillary acid protein (GFAP) gene, which causes GFAP accumulation in astrocytes. A wide spectrum of mutations has been described. For some variants, genotype–phenotype correlations have been described, although variable expressivity has also been reported in late-onset cases among members of the same family. We present the case of a 19-year-old girl who developed gait ataxia and subtle involuntary movements, preceded by a history of enuresis and severe scoliosis. Her mother has been affected by ataxia since her childhood, which was then complicated by pyramidal signs and heavily worsened through the years. Beyond her mother, no other known relatives suffered from neurologic syndromes. The scenario was further complicated by a complex brain and spinal cord magnetic resonance imaging (MRI) pattern in both mother and daughter. However, the similar clinical phenotype made an inherited cause highly probable. Both AD and autosomal recessive (AR) ataxic syndromes were considered, lacking a part of the proband's pedigree, but no causative genetic alterations were found. Considering the strong suspicion for an inherited condition, we performed clinical exome sequencing (CES), which analyzes more than 4,500 genes associated with diseases. CES evidenced the new heterozygous missense variant c.260 T > A in exon 1 of the glial fibrillary acidic protein (GFAP) gene (NM_002055.4), which causes the valine to aspartate amino acid substitution at codon 87 (p. Val87Asp) in the GFAP. The same heterozygous variant was detected in her mother. This mutation has never been described before in the literature. This case should raise awareness for this rare and under-recognized disease in juvenile–adult cases.

KEYWORDS

Alexander disease, leukodystrophy, GFAP mutation, astrocytes, ataxia

1 Introduction

Alexander disease (AxD) is a very rare inherited leukodystrophy with a progressive course. Its prevalence is not well known, and the only population-based prevalence estimate is one in 2.7 million (1). AxD is caused by mutations in the *glial fibrillary acid protein (GFAP) gene,* located in chromosome 17q21, which encodes a type III intermediate filament protein that is predominantly expressed in astrocytes. The most reported variants are point mutations at exon 1 (54%), exon 4 (31%), and exons 8, 6, and 5 (7, 4, and 3%, respectively). The *GFAP* variants act as gain-of-function mutations that break up the dimerization of astrocytes' intermediate filaments, causing abnormal protein aggregation, called Rosenthal fibers, in the astrocyte cytoplasm (2). The Rosenthal fibers, which are aggregates of GFAP, heat shock protein 27 (HSP27), and alpha B-crystallin, are the pathological hallmark of the disease (3). The accumulation of Rosenthal fibers causes astrocyte dysfunction (4). However, other mechanisms, apart from protein aggregation, seem to be responsible for AxD pathology. It seems in fact that GFAP mutations cause proteasome activity inhibition, chemokine, and nitric oxide production, and consequently, oxidative stress, activation of cell stress patterns, and changes in astrocyte morphology. Furthermore, these mutant astrocytes promote an inflammatory environment in the CNS (5). Whatever the cause, the damage begins in the astrocytes and then extends beyond involving other cellular elements through probably microglial activation (2). All these changes are responsible for white matter degeneration and neuronal loss (5).

AxD usually has well-defined clinical characteristics in infants and children, but it can also be present in adults with non-specific neurological manifestations. Based on these different age-related clinical spectrums, four clinical groups were distinguished: neonatal form, infantile form, juvenile form, and adult form (2, 6). The neonatal form is characterized by neurodevelopmental delay and regression, seizures, and gastrointestinal manifestations with a rapid progression to death within 2 years; the infantile form presents with variable developmental issues, seizures, ataxia, hyperreflexia, spasticity, hydrocephalus, and megalencephaly; the juvenile form is characterized by mild developmental delay, bulbar signs, vomiting, scoliosis, autonomic dysfunction, spasticity, ataxia, and epilepsy; and the adult form presents with bulbar or pseudobulbar findings (palatal myoclonus, dysphagia, dysphonia, dysarthria, or slurred speech), motor/gait abnormalities with pyramidal tract signs, or cerebellar abnormalities (2, 6). In 2001, Van der Knaap et al. identified, in a population of infantile-onset AxD, five magnetic resonance imaging (MRI) criteria to diagnose AxD: 1. extensive cerebral white matter abnormalities with a frontal preponderance; 2. periventricular rim of decreased signal intensity on T2-weighted images and elevated signal intensity on T1-weighted images; 3. abnormalities of the basal ganglia and thalami, such as swelling or atrophy; 4. brain stem abnormalities, particularly involving the medulla and midbrain; 5. contrast enhancement of one or more of the following: ventricular lining (*Garland-like feature*), periventricular rim, frontal white matter, optic chiasm, fornix, basal ganglia, thalamus, dentate nucleus, and brain stem (7).

Furthermore, several MRI studies in AxD showed significant differences in radiological presentation between infant and juvenile/adult-onset, with a predominant atrophy and signal alterations in the brainstem and upper spinal cord in juvenile/adult-onset, as well as fewer supratentorial periventricular white matter abnormalities in infantile-onset (8).

In 2011, a new classification was proposed based on the distribution of lesions and the age of onset (9), dividing AxD into two types: type I, characterized by frontal lobe distribution and infantile-onset; type II, characterized by hindbrain predominance of lesions and a more variable age of onset (juvenile and adult). To date, several case reports have described the most common MRI alterations found in type II AxD: 1. significant atrophy of the medulla and spinal cord; 2. involvement of the dentate with less frequent coexisting cerebellar white matter change (10); 3. poor involvement of white matter compared to type I AxD; 4. pial FLAIR signal abnormality, most often concentrated in the medulla; 5. enhancement of middle cerebellar peduncle and brainstem; 6. bilateral involvement of middle cerebellar peduncle, which is a non-specific MRI feature of AxD but is present in several other neurodegenerative diseases (multiple system atrophy, spinocerebellar ataxia, Wilson disease (WD), etc.); 7. "Tadpole atrophy," consisting of atrophy of the medulla and cervical spinal cord with a relative sparing of the pons; 8. medullary signal change (myelopathy is a common clinical presentation in these patients) associated with spinal atrophy (also enhancement may be present), which leads to a strong suspicion of AxD (8, 11).

The diagnosis of AxD may be suspected in patients with suggestive clinical and radiological features, but it requires genetic confirmation. Nowadays, the use of next-generation sequencing (NGS) technologies is increasing the diagnostic rate.

We report the case of a young woman who developed ataxia, involuntary movements, enuresis, and scoliosis as her main symptoms and signs. Her mother had a similar clinical pattern. The set of clinical, radiological, and anamnestic data leads us to suspect a genetic cause. The clinical exome sequencing (CES) evidenced a new heterozygous missense variant c.260T > A in exon 1 of the *GFAP* gene (NM_002055.4) that causes the valine to aspartate amino acid substitution at codon 87 (p. Val87Asp) in the GFAP both in our patients and in her mother. This mutation has never been described before in the literature.

2 Case presentation

A 19-year-old girl (III:1, Figure 1) came to our neurological clinic for the recent appearance of mild imbalance and involuntary movements in her face and upper limbs.

The patient reported, in her medical history, scoliosis, and episodes of enuresis since she was 13 years old. Moreover, her aunt reported some episodes characterized by lack of attention, in which the patient seemed "lost in her thoughts," but gave a prompt response when asked. She had normal psychomotor development, and she succeeded in graduating from high school despite some learning difficulties.

Exploring the familiar history, we discovered that her mother (II:3, Figure 1) had a previous diagnosis of primary progressive multiple sclerosis (PPMS) with an unclear clinical course. The first symptom experienced by the mother since her childhood seemed to be ataxia; however, through the years, weakness and stiffness in both legs became the leading symptoms, with a rapid worsening until bedding and percutaneous endoscopic gastrostomy (PEG) feeding when she was 40 years old. Because of her critical clinical condition,

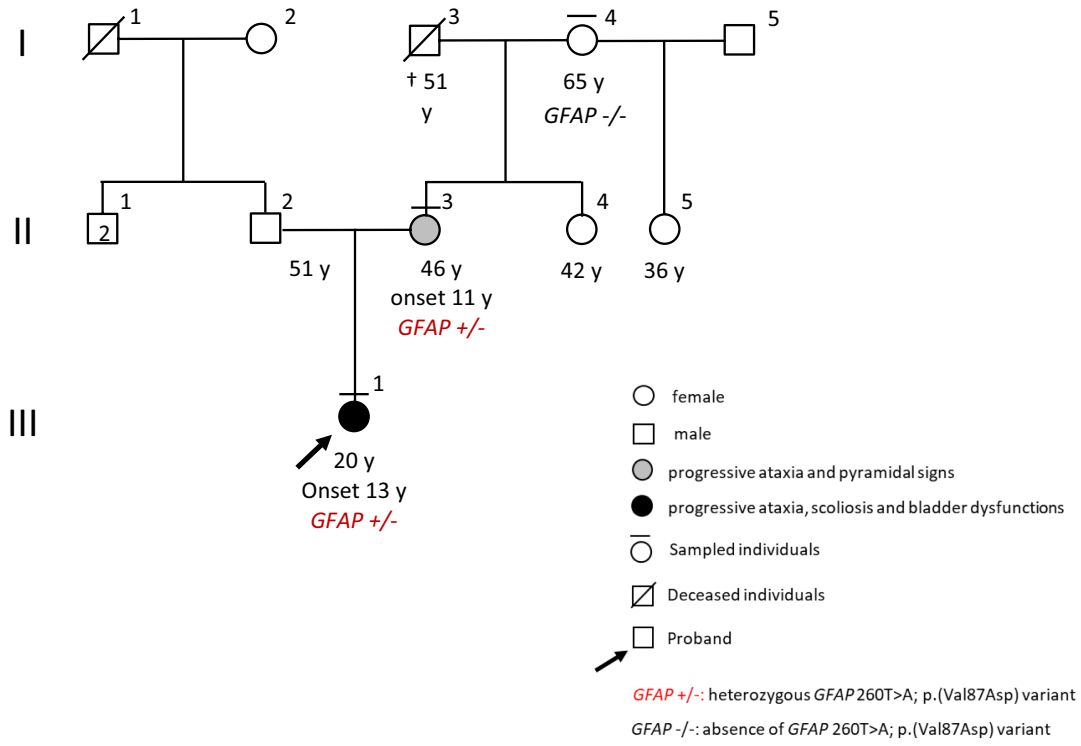

FIGURE 1
Pedigree.

we were not able to perform a neurological examination for the mother. However, the last neurological examination performed some years ago in another clinic evidenced spastic paraparesis, slurred speech, and dysphagia. No maternal relatives were referred to have neurologic diseases except for the mother, and no information was available about the father or the paternal branch (Figure 1).

The neurological examination of our patient mainly evidenced difficulties in balance and walking, with significant difficulty performing tandem test walking. Moreover, we evidenced a clear nystagmus in the horizontal gaze bilaterally, a clonus at the ankles with a plantar cutaneous reflex in extension bilaterally, and sporadic dystonic movements in her face and upper limbs.

Therefore, our patient's presentation with a complex syndrome with prominent cerebellar ataxia, which was phenotypically similar to that of her mother, made an inherited cause highly probable. Nonetheless, we also investigated the possible causes of acquired ataxias, such as vitamin deficiency, autoimmune, and viral causes.

The proband's pedigree was partially informative; therefore, both autosomal dominant (AD) and autosomal recessive (AR) ataxic syndromes were considered consanguinity, and/or pseudo-dominant inheritance could not be excluded.

We first assessed the most common AD cerebellar ataxias, but the repeat expansion testing excluded any pathogenic amplification in the *ATXN1*, *ATXN2*, *ATXN3*, *CACNA1A*, *ATXN7*, *PPP2R2B,* and *TBP* genes, and no damaging variants in the *KCNC3* and *FXN* genes were detected. Therefore, we performed a NGS analysis for the ataxia-related genes. However, we found no causative genetic alterations.

In the meantime, the patient performed further exams, including a brain and spinal cord MRI. The MRI evidenced limited T2-hyperintensities involving the periventricular and temporal insular white matter in both hemispheres, and, more interestingly, the T2-hyperintensities also involved basal ganglia, middle cerebellar peduncles, and the area around the IV ventricle; no enhancement was identified in these areas. Moreover, it showed cerebellar vermal and spinal cord atrophy (Figure 2).

Based on the basal ganglia alterations at MRI, as well as on the clinical evidence of cerebellar involvement and dystonia, we performed a ceruloplasmin and copper level dosage and a molecular analysis of the *ATP7B* gene to investigate WD, a rare AR disorder of copper metabolism. However, even these tests resulted in a negative result.

In addition, the patient performed uroflowmetry, which showed neurogenic bladder disease; neuropsychological tests, which evidenced some difficulties with planning skills and episodic memory; and a VideoEEG during sleep, which showed not-induced, rare epileptic spike-and-wave discharges that spread over all of the brain with no clinical correlations.

At this point, we obtained a mother's MRI, performed at the age of 41 years old. This MRI evidenced white matter abnormalities around the IV ventricle, more limited white matter abnormalities in the supratentorial periventricular area, and pial T2-hyperintensities were described in the brainstem and cerebellum; a severe atrophy of the brainstem, cerebellum (especially the vermis), and cervical spinal cord was described (Figure 2). However, the mother's MRI accounted for the advanced phase of the disease, and no previous imaging was available.

Even if the MRI patterns of our patient and her mother did not overlap entirely, despite the comparison being made between MRIs performed at different ages and stages of the disease, there

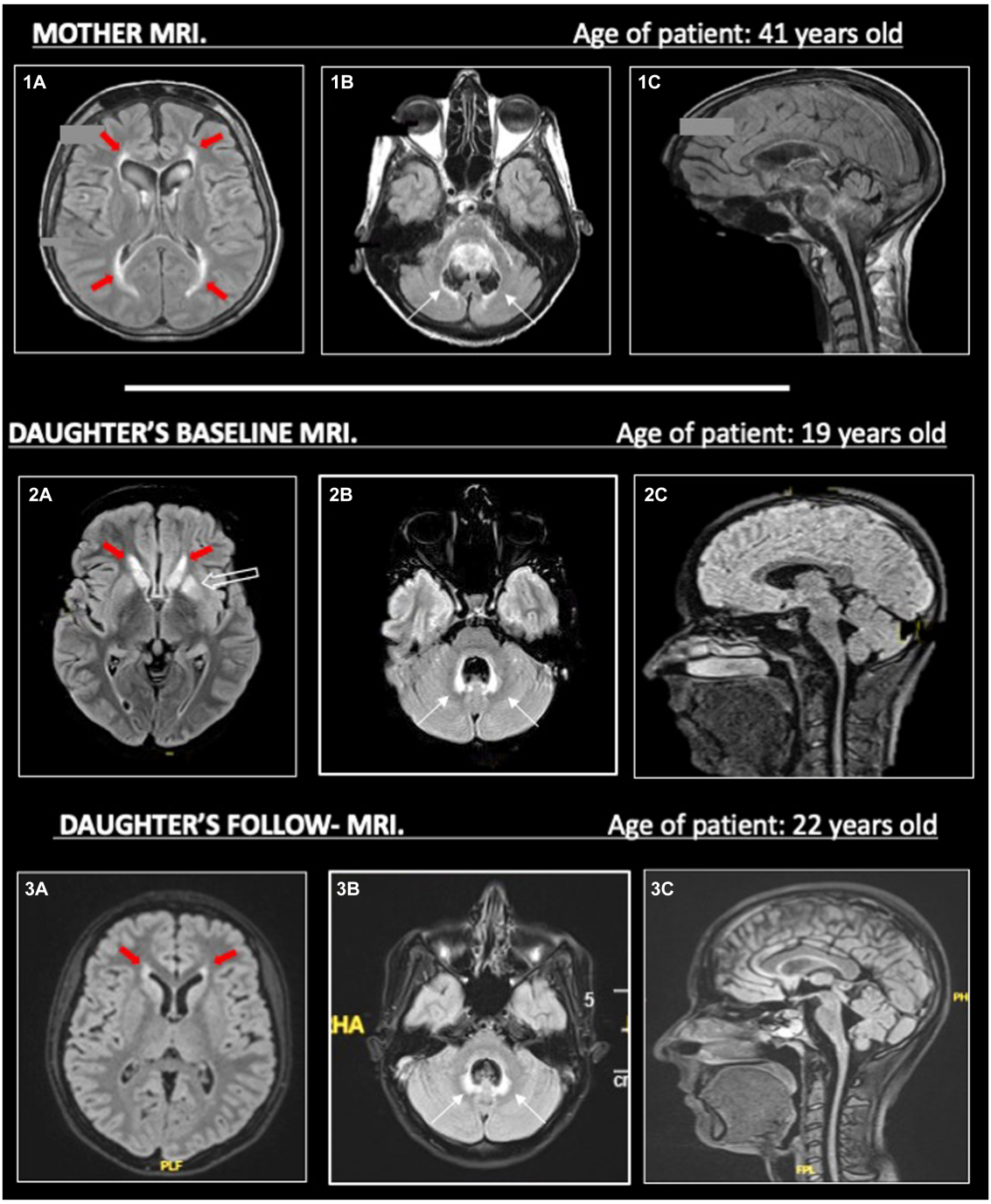

FIGURE 2
On the left (1a, 2a, 3a), we show T2-hyperintense symmetric periventricular lesions (red-filled arrows) in both mother and daughter. In (2a), we can see T2-hyperintensities in the basal ganglia (empty arrow) of the daughter, less evident in her MRI follow-up in 2023 (3a). On the central column (1b, 2b, 3b), widespread atrophy of the cerebellar vermis is evident in both mother and daughter (1b, 2b), without evident worsening in the follow-up MRI (3b) in the daughter. T2-hyperintensities around the IV ventricle (thin black arrows) are more pronounced in the daughter than the mother, maybe due to a higher cerebellar vermis atrophy. On the right (1c, 2c, 3c), in the sagittal images, we can see prominent atrophy of the cerebellum, brainstem (with spare of pons) and cervical spinal cord. All MRI sequences are FLAIR, apart from (1c) (T1).

was a strong suspicion for an inherited neurodegenerative condition, including leukodystrophies (12).

Therefore, we decided to perform CES, a diagnostic targeted sequencing test that analyzes more than 4,500 genes associated with diseases, by NGS (TruSightONE Expanded Sequencing Kit, Illumina).

The CES evidenced the new heterozygous missense variant c.260 T > A in exon 1 of *GFAP* (NM_002055.4), which causes the valine to aspartate amino acid substitution at codon 87 (p. Val87Asp) in the glial fibrillary acidic protein. No further damaging variants were found in the other analyzed genes. The *GFAP* variant was confirmed

in the proband and investigated in the mother (II:3, Figure 1) and in the grandmother (I:4, Figure 1) by Sanger sequencing. This analysis identified the substitution also in the mother, but not in the healthy grandmother (Figure 1, pedigree). Damaging variants in *GFAP* (MIM * 1377 80, chromosome) are responsible for Alexander's disease (AxD, MIM # 203450), a rare AD neurodegenerative disorder caused by glial fibrillary acidic protein accumulation in astrocytes.

3 Discussion

AxD is a very rare inherited leukodystrophy with a progressive and fatal clinical course due to a mutation in the *GFAP gene,* which encodes an intermediate filament protein that is predominantly expressed in astrocytes (2).

AxD clinical presentation is heterogeneous, and different members of the same family may have variable phenotypes. This clinical heterogeneity depends on different variants of the mutation and on different ages of onset (6).

In this case report, ataxia was the leading symptom in the proband and the first clinical manifestation in her mother, which progressively worsened through the years. The management of inherited ataxias may be challenging for clinicians due to the wide clinical phenotypes and the continuous discovery of new genetic mutations. Clinical findings are not sufficient for the diagnosis, and, in the absence of a clear familiar history, misdiagnosis is quite common. In our case, for example, the mother was previously misdiagnosed with PPMS.

The diagnostic process was further complicated by the incomplete knowledge of the patient's pedigree and the complex neuroimaging patterns in the patient and her mother, taken in different stages of the disease. As illustrated in Figure 2, the predominant atrophy of the brainstem with a spare of pons (tadpole atrophy), the atrophy of the cerebellum and spinal cord, the pial and sub-pial alterations of the brainstem, and the few white matter abnormalities may have suggested the possibility of a type II AxD.

In the end, the CES analysis evidenced the new heterozygous missense variant c.260 T > A in exon 1 of the *GFAP* gene (NM_002055.4). According to the American College of Medical Genetics and Genomic Guidelines, this variant can be classified as likely pathogenic (13). Indeed, i) the c.260T > A in *GFAP* we found in the proband and her mother has never been described to date, either in general population or AxD cases (pathogenic moderate criteria 2, PM2); ii) it is in a mutational hot spot domain of the protein (pathogenic moderate criteria 1, PM1), iii) it is considered pathogenic by the most relevant pathogenicity scores (MetaLR 0.94; Revel 0.93) (pathogenic supporting criteria 3, (PP3); iv) different amino acidic changes at the same codon (p. Val87Ile; p.Val87Leu; p.Val87Gly) were previously described in late-onset AxD patients (pathogenic moderate criteria 5, PM5) (8, 14–16).

These data (PM1, PM2, PM5, PP1, PP3 PP4), together with the maternal segregation and the clinical features of the two women compatible with *GFAP*-related phenotypes (pathogenic supporting 1, PP1, and pathogenic supporting criteria 4, PP4), are in favor of a damaging role of the p.Val87Asp substitution in determining the disease (13).

Currently, our patient is receiving symptomatic treatments such as physical therapy and anti-epileptic drugs (AEDs), and she has overall clinical stability. To date, unfortunately, there are no disease-modifying treatments available for AxD, even if a Phase 1–3 multi-center trial testing antisense oligonucleotides is now ongoing (17).

This clinical case expands the known variable genotype–phenotype correlation in AxD, reporting a new variant causing juvenile AxD, and it should raise awareness for this rare and under-recognized disease in juvenile–adult cases.

Data availability statement

The datasets presented in this article are not readily available because of ethical and privacy restrictions. Requests to access the datasets should be directed to the corresponding author.

Ethics statement

Ethical review and approval was not required for the study on human participants in accordance with the local legislation and institutional requirements. Written informed consent from the patients/participants or patients/participants' legal guardian/next of kin was not required to participate in this study in accordance with the national legislation and the institutional requirements. Written informed consent was obtained from the individual(s) for the publication of any potentially identifiable images or data included in this article.

Author contributions

CR: Conceptualization, Investigation, Writing – original draft. EM: Data curation, Investigation, Writing – original draft, Conceptualization. SP: Investigation, Investigation, Data curation, Writing – original draft. SD: Data curation, Methodology, Writing – review & editing. MM: Data curation, Methodology, Writing – review & editing. LT: Formal analysis, Methodology, Supervision, Writing – review & editing. GZ: Formal analysis, Methodology, Supervision, Writing – review & editing. MP: Supervision, Writing – review & editing. MS: Writing – review & editing, Supervision. SR: Writing – review & editing, Supervision. GR: Conceptualization, Data curation, Writing – review & editing, Investigation, Supervision.

Funding

The author(s) declare that no financial support was received for the research, authorship, and/or publication of this article.

Acknowledgments

The authors thank the patient and her family for providing us with consent to publish the case and the images.

Conflict of interest

The authors declare that the research was conducted in the absence of any commercial or financial relationships that could be construed as a potential conflict of interest.

The author(s) declared that they were an editorial board member of Frontiers, at the time of submission. This had no impact on the peer review process and the final decision.

Publisher's note

References

1. The Alexander Disease Study Group in JapanYoshida T, Sasaki M, Yoshida M, Namekawa M, Okamoto Y, et al. Nationwide survey of Alexander disease in Japan and proposed new guidelines for diagnosis. *J Neurol*. (2011) 258:1998–2008. doi: 10.1007/s00415-011-6056-3

2. Kuhn J, Cascella M (2022). Alexander disease. StatPearls, Treasure Island (FL): StatPearls Publishing. Available at: http://www.ncbi.nlm.nih.gov/books/NBK562242/

3. Hagemann TL, Connor JX, Messing A. Alexander disease-associated glial fibrillary acidic protein mutations in mice induce Rosenthal fiber formation and a white matter stress response. *J Neurosci*. (2006) 26:11162–73. doi: 10.1523/JNEUROSCI.3260-06.2006

4. Hagemann TL, Powers B, Mazur C, Kim A, Wheeler S, Hung G, et al. Antisense suppression of glial fibrillary acidic protein as a treatment for Alexander disease. *Ann Neurol*. (2018) 83:27–39. doi: 10.1002/ana.25118

5. Sosunov A, Olabarria M, Goldman JE. Alexander disease: an astrocytopathy that produces a leukodystrophy. *Brain Pathol*. (2018) 28:388–98. doi: 10.1111/bpa.12601

6. Srivastava S, Waldman A, Naidu S (1993). Alexander Disease. Available at: https://www.ncbi.nlm.nih.gov/books/NBK1172

7. van der Knaap MS, Naidu S, Breiter SN, Blaser S, Stroink H, Springer S, et al. Alexander disease: diagnosis with MR imaging. *AJNR Am J Neuroradiol*. (2001) 22:541–52.

8. Graff-Radford J, Schwartz K, Gavrilova RH, Lachance DH, Kumar N. Neuroimaging and clinical features in type II (late-onset) Alexander disease. *Neurology*. (2014) 82:49–56. doi: 10.1212/01.wnl.0000438230.33223.bc

9. Prust M, Wang J, Morizono H, Messing A, Brenner M, Gordon E, et al. GFAP mutations, age at onset, and clinical subtypes in Alexander disease. *Neurology*. (2011) 77:1287–94. doi: 10.1212/WNL.0b013e3182309f72

10. Farina L, Pareyson D, Minati L, Ceccherini I, Chiapparini L, Romano S, et al. Can MR imaging diagnose adult-onset Alexander disease? *AJNR Am J Neuroradiol*. (2008) 29:1190–6. doi: 10.3174/ajnr.A1060

11. Oh HY, Yoon RG, Lee JY, Kwon O, Lee W-W. Characteristic MR imaging features and serial changes in adult-onset Alexander disease: a case report. *J Korean Soc Radiol*. (2023) 84:736–44. doi: 10.3348/jksr.2021.0015

12. Schiffmann R, van der Knaap MS. Invited article: an MRI-based approach to the diagnosis of white matter disorders. *Neurology*. (2009) 72:750–9. doi: 10.1212/01.wnl.0000343049.00540.c8

13. Richards S, Aziz N, Bale S, Bick D, das S, Gastier-Foster J, et al. Standards and guidelines for the interpretation of sequence variants: a joint consensus recommendation of the American College of Medical Genetics and Genomics and the Association for Molecular Pathology. *Genet Med*. (2015) 17:405–24. doi: 10.1038/gim.2015.30

14. Suzuki H, Yoshida T, Kitada M, Ichihashi J, Sasayama H, Nishikawa Y, et al. Late-onset Alexander disease with a V87L mutation in glial fibrillary acidic protein (GFAP) and calcifying lesions in the sub-cortex and cortex. *J Neurol*. (2012) 259:457–61. doi: 10.1007/s00415-011-6201-z

15. Okamoto Y, Mitsuyama H, Jonosono M, Hirata K, Arimura K, Osame M, et al. Autosomal dominant palatal myoclonus and spinal cord atrophy. *J Neurol Sci*. (2002) 195:71–6. doi: 10.1016/s0022-510x(01)00687-6

16. Yoshida T, Tomozawa Y, Arisato T, Okamoto Y, Hirano H, Nakagawa M. The functional alteration of mutant GFAP depends on the location of the domain: morphological and functional studies using astrocytoma-derived cells. *J Hum Genet*. (2007) 52:362–9. doi: 10.1007/s10038-007-0124-7

17. Ionis Pharmaceuticals, Inc. "A Phase 1–3, Double-Blind, Randomized, Placebo-Controlled Study to Evaluate the Efficacy, Safety, Pharmacokinetics and Pharmacodynamics of Intrathecally Administered Zilganersen (ION373) in Patients with Alexander Disease," clinicaltrials.gov, Clinical trial registration NCT04849741, 2024. Available at: https://clinicaltrials.gov/study/NCT04849741

frontiers | Frontiers in Neurology

TYPE Case Report
PUBLISHED 08 April 2024
DOI 10.3389/fneur.2024.1347289

OPEN ACCESS

EDITED BY
Huifang Shang,
Sichuan University, China

REVIEWED BY
Qiheng He,
Capital Medical University, China
Valeria Capra,
Giannina Gaslini Institute (IRCCS), Italy

*CORRESPONDENCE
Feres Chaddad-Neto
✉ fereschaddad@hotmail.com

RECEIVED 30 November 2023
ACCEPTED 14 March 2024
PUBLISHED 08 April 2024

CITATION
Jong-A-Liem GS, Sarti THM, dos Santos MG, Giacon LMT, Wuo-Silva R, Baeta AM, de Campos Filho JM and Chaddad-Neto F (2024) Case report: Association between PTEN-gene variant and an aggressive case of multiple dAVFs. *Front. Neurol.* 15:1347289. doi: 10.3389/fneur.2024.1347289

Case report: Association between PTEN-gene variant and an aggressive case of multiple dAVFs

Glaucia Suzanna Jong-A-Liem[1,2], Talita Helena Martins Sarti[1,2], Mariusi Glasenapp dos Santos[3], Luciano Marcus Tirotti Giacon[4], Raphael Wuo-Silva[1], Alex Machado Baeta[5], José Maria de Campos Filho[2] and Feres Chaddad-Neto[1,2]*

[1]Department of Neurology and Neurosurgery, Universidade Federal de São Paulo, São Paulo, SP, Brazil, [2]Department of Neurosurgery, Hospital Beneficência Portuguesa de São Paulo, São Paulo, SP, Brazil, [3]Department of Neurosurgery, Universidade Federal de Santa Maria, Santa Maria, RS, Brazil, [4]Department of Neuroradiology, Hospital Beneficência Portuguesa de São Paulo, São Paulo, SP, Brazil, [5]Department of Neurology, Hospital Beneficência Portuguesa de São Paulo, São Paulo, SP, Brazil

Introduction: Mutations of the phosphatase and tensin homolog (PTEN) gene have been associated with a spectrum of disorders called PTEN hamartoma tumor syndrome, which predisposes the individual to develop various types of tumors and vascular anomalies. Its phenotypic spectrum includes Cowden syndrome (CS), Bannayan–Riley–Ruvalcaba syndrome (BRRS), Proteus syndrome, autism spectrum disorders (ASD), some sporadic cancers, Lhermitte–Duclos disease (LDD), and various types of associated vascular anomalies.

Clinical presentation: A previously healthy 27-year-old woman was experiencing visual scintillating scotomas and mild chronic headaches for the past 2 years. The initial computed tomographic (CT) and magnetic resonance imaging (MRI) scans did not reveal any abnormalities, but the possibility of pseudotumor cerebri was considered. Furthermore, a cerebral angiogram showed a posterior fossa dural arteriovenous fistula (dAVF), which was initially treated through embolization. However, in spite of proper treatment, this patient experienced multiple recurrent dAVFs in different locations, requiring multiple embolizations and surgeries. Despite exhibiting altered cerebral perfusion and hemodynamics, the patient did not display any significant symptoms until she experienced a sudden stroke resulting from deep venous thrombosis, which was not associated with any medical procedures or medication use. A comprehensive analysis was performed due to the aggressive nature of the dAVFs. Surprisingly, exome sequencing of a blood sample revealed a PTEN gene variant in chromosome 10, indicative of Cowden syndrome. However, no tumors or other vascular lesions were detected in other systems that would constitute Cowden syndrome.

Conclusion: The rapid formation of multiple and complex dAVFs, coupled with not meeting the criteria for any other PTEN-related syndrome, unequivocally leads to the presentation of a novel phenotype of the PTEN germline variant.

KEYWORDS

pseudotumor cerebri, gene variant, AV fistulas, dural arteriovenous fistula (DAVF), PTEN gene mutation

1 Introduction

The phosphatase and tensin homolog (PTEN) gene is a tumor suppressor gene that inhibits the PI3K/AKT/mTOR and vascular endothelial growth factor (VEGF) signaling pathways, which control cell growth, migration, apoptosis, and angiogenesis (1). Mutations of this gene have been associated with a spectrum of disorders called PTEN hamartoma tumor syndrome and predisposes the individual with the syndrome to develop various types of tumors and vascular anomalies. As this gene is expressed in almost all tissues and cell types, this condition usually involves multiple systems and, therefore, neurological anomalies are quite common.

These PTEN germline mutations are very rare, and their phenotypic spectrum includes Cowden syndrome (CS), Bannayan–Riley–Ruvalcaba syndrome (BRRS), Proteus syndrome, autism spectrum disorders (ASD), some sporadic cancers, Lhermitte–Duclos disease (LDD), and various types of vascular anomalies (2).

This case report, therefore, presents a novel phenotypic expression of the PTEN gene in a previously healthy adult with multiple and complex multiple dural arteriovenous fistulas (dAVFs).

2 Clinical presentation

A 27-year-old female lawyer was experiencing visual scintillating scotomas and subtle chronic headaches for the last 2 years. The patient had no comorbidities, no family history of cancer syndromes, and did not use continuous medication. An ophthalmologic investigation revealed her condition to be bilateral papilledema and the patient was referred to a neurologist. The initial computed tomographic (CT) and magnetic resonance imaging (MRI) scans were normal and raised the possibility of pseudotumor cerebri, which required supplemental analysis with digital subtracted angiography (DSA). In this examination, a dural arteriovenous fistula (dAVF) was detected in the posterior fossa, which was successfully embolized, resulting in occlusion without complications. The patient was discharged with no acquired deficit (mRS 1).

After 1 year, the headaches reoccurred, and the patient was readmitted. In DSA, a new and highly complex dAVF was detected in the supratentorial region, affecting meningeal branches of the external carotid artery, the meningohypophyseal trunk, the ascending pharyngeal and occipital arteries, and both transverse sinuses near the Torcula and superficial cortical veins (Figure 1). Therefore, she underwent a new session of embolization without any complications and was discharged without headaches (mRS 1).

Again, 1 month later, she was readmitted for the third time due to the emergence of a new symptom: tinnitus. A new DSA procedure revealed the presence of a new cortical dAVF in the patient, which was treated with another session of embolization without any complications. The patient was discharged and recovered from the tinnitus but continued to experience a mild headache. As the dAVF pattern changed and symptoms worsened over time, the patient underwent a fourth session of embolization after 3 months and a fifth session after 6 months for the same reasons.

Following the completion of the fifth session, the magnetic resonance angiography (MRA) analysis revealed the continued presence of multiple and intricate dAVFs. These dAVFs were supplied by arteries stemming from the right middle meningeal artery, right internal maxillary artery, and occipital artery (Figure 2). Additionally, these dAVFs were directly linked to the right transverse, sigmoid sinus, straight sinus, superior petrosal sinus, and superior sagittal sinus, all of which showed arterial flow. Furthermore, the deep venous drainage, medullary, and cortical veins exhibited signs of venous congestion and indirect indications of brain swelling.

Therefore, the patient underwent a ventriculoperitoneal (VP) shunt with an initial threshold of 150 mmHg. The surgery was uneventful, and the patient was discharged with minor symptoms.

The patient suffered a generalized seizure and fell into a coma during a routine neuroimaging check-up 2 months later. New CT scans revealed a small infarct in the left frontal region with indications of hemorrhagic transformation. MR angiography and venography tests showed tortuous and partial thrombosis in the following veins: the right basal vein of Rosenthal, the sylvian superficial vein, the frontobasal vein, and the right internal jugular

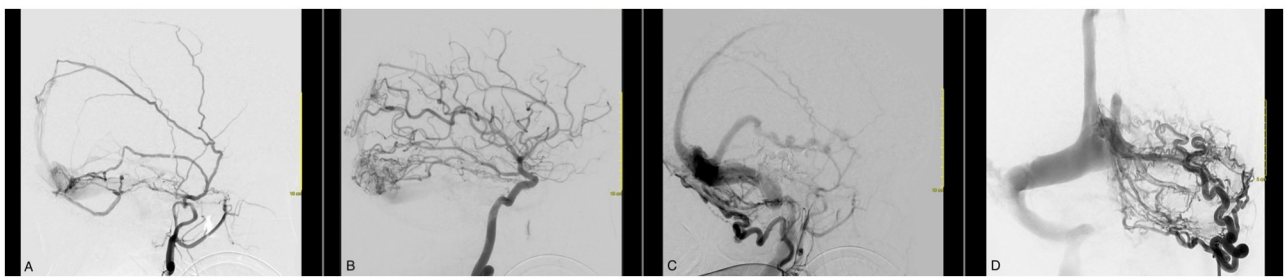

FIGURE 1
Cerebral angiography with a selective left external carotid artery (ECA) catheterization evidencing an AVF between branches of the external carotid artery and the superficial venous system. Venous congestion and reflux are evident in the Labbe vein and up until the posterior third of the superior sagittal sinus. **(A)** The meningeal branches of ECA in fistulous communication with the superior sagittal sinus and transverse sinus. **(B)** The cortical branches of the ICA in fistulous communication with the superior sagittal and transverse sinus. **(C, D)** A very enlarged occipital artery with multiple branches in fistulous communication with the transverse and sigmoid sinus.

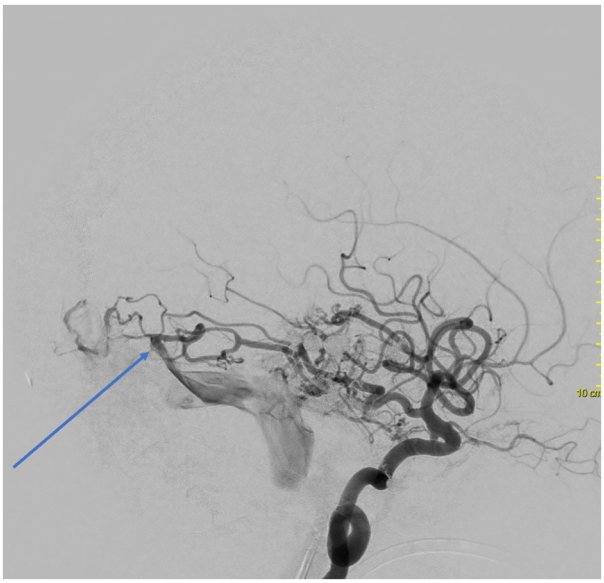

FIGURE 2
Cerebral angiography with a selective left internal carotid artery catheterization evidencing an AVF between branches of the posterior cerebral artery and the Labbe vein.

bulb. Despite the VP shunt being in the correct position, there were still signs of increased intracranial pressure (ICP).

The patient was kept under sedation for neuroprotection and presented with multiple neurological complications secondary to the mass cerebral venous thrombosis. Despite prolonged periods of anticoagulation therapy, she remained in a comatose condition. A new MRI evidenced the persistence of extensive brain swelling and ischemic parenchymal injury. Given the aggressiveness of the dAVFs and the poor outcome, the patient underwent rheumatologic, immunologic, hematologic, and genetic investigations. The first of these investigations was unremarkable. However, the genetic exome sequencing of her blood sample revealed a pathological variant in the PTEN gene compatible to Cowden syndrome. The patient underwent a full-body screening, which did not reveal any tumors or other vascular lesions in other systems.

The patient's family provided informed consent to publish this case, which was also authorized by the hospital's ethics committee.

3 Discussion

The most common neurological phenotypic expressions associated with the PTEN germline mutation manifest as follows.

Macrocephaly is a common finding (80%) in CS and happens to be 100% present in BRRS (3, 4). Lynch et al. studied BRRS in six children with extreme macrocephaly. Four parents of these children also carried the PTEN mutation and asymptomatic extreme macrocephaly as well (3). Hence, we affirm that macrocephaly of idiopathic cause can be an early marker for PTEN mutation-linked disorders (5). Developmental delay is also typical and associated with the macrocephalic finding. Children and adults in these cases have presented a lower intelligence quotient (IQ) score. Objectively, this intellectual disability, measured with an IQ score of 75, is also a minor criterion for the diagnosis of CS (6). ASD, remarkably in association with macrocephaly, has also been linked to PTEN mutation. One in five patients with ASD-macrocephalic have been diagnosed with a PTEN mutation. In these ASD cases, macrocephaly seems to be more severe compared to the non-PTEN-mutated group (7). Individuals with PTEN-related ASD also show anatomical differences, with an increase in cortical white matter and a distinctive neurocognitive and behavioral phenotype, including delayed language development, poor working memory and processing speed, and adaptive and sensory abnormalities (8, 9). Epilepsy has been mentioned in some cases (4, 10, 11) but is not as common in this population.

Lhermitte–Duclos disease (LDD) is the most common brain tumor that develops in adult CS patients. Once identified and confirmed, it is considered a pathognomonic finding for CS (6). This benign lesion occurs in around 35% of the CS patients, and only ∼250 cases have been published (12). On T2-MRI, we identify a classic alternating pattern of high and low signal, giving it a striated appearance that is said to resemble "tiger stripes." This tigroid appearance on T2 imaging distinguishes LDD from other more common primary cerebellar gliomas that destroy the delicate folial pattern of the cerebellum (13). These lesions are benign and progress through a slow growth. Surgical treatment is only required in symptomatic cases (12, 14). In the NIH Genetic Testing Registry, PTEN mutations have also been linked to the appearance of familial meningioma and other predisposing genes. There have been cases of CS associated with meningioma (10). However, whether the meningioma is genuinely associated with the PTEN mutation or is an incidental finding is unclear (15).

Asymptomatic cavernous malformations (cavernoma or cavernous angioma) and developmental venous anomalies (venous angioma) are common, and many cases were reported with these conditions in patients with CS (10). One case of a giant ruptured fusiform middle cerebral artery aneurysm was also reported in a CS patient; however, the PTEN gene mutation was not confirmed because the patient and his family did not consent to genetic testing (16). Two cases of spinal AVF associated with LDD have been reported. Rupture or steal phenomena of the AVF in a cervical location can have devastating clinical consequences. Both cases were very similar in feeding and drainage patterns and could represent a different phenotype (17–19). Non-neurological AVM has been reported in many CS and BRRS cases (20). Real intracranial AVM has not been reported yet. A French CS multicenter study found six patients (in a series of 20) harboring vascular malformation (10). Therefore, the association of PTEN mutations and vascular anomalies is consistent with the growing evidence that PTEN modulates angiogenesis (20).

The literature review for the present study revealed that only a limited number of cases identified a correlation between the PTEN variant and dAVFs. These few cases exhibited the syndromes mentioned earlier. An adult with classic CS experienced a generalized seizure caused by bleeding from multiple dural and epidural high-flow AVFs. This patient underwent five sessions of embolization uneventfully but unfortunately passed away due to severe status epilepticus (21). Another study reported that

a 14-year-old with BRRS, who manifested with diplopia and papilledema, was diagnosed with pseudotumor cerebri, similar to the reported case in our study. Despite the signs of increased ICP, no MRI or MR angiogram abnormalities were noted. Because the patient in our study worsened over time, new studies identified dAVF connecting meningeal branches of the middle meningeal artery to the transverse sinus bilaterally. She underwent two sessions of embolization and had a good recovery (22). Acquired dAVF has also been reported in CS in a postop of a brainstem cavernoma. In this case, the manipulated dura underwent neovascularization, creating anomalous communications between dural arteries and cerebellar cortical veins. This patient was reapproached to treat the dAVF. This case suggests that postoperative angiogenesis may cause AVF in patients with CS (23). Determining whether PTEN insufficiency alone or other molecular factors in the PI3K/Akt/VEGF signaling contribute to these angiogenic formations is difficult (24).

Our case, different from the ones mentioned in the literature, did not meet the criteria for any PTEN gene syndrome. Whole-body screening did not identify any cutaneous or visceral lesions, which would fulfill the criteria for CS. She was normocephalic and had no history of developmental delay. Because she was a lawyer, we deduce that the patient previously had an average IQ. Additionally, this case has a unique presentation of rapidly formed multiple and new dAVFs. Despite compromised venous drainage, venous congestion, and chronic perfusion shortages, the patient remained relatively asymptomatic. She only progressed to a more severe neurological state when experiencing acute bleeding secondary to venous thrombosis. Interestingly, her cerebral perfusion adapted rapidly to the collaterals and responded highly to hemodynamic changes after every embolization. This complex formation of dAVF corroborates with the suspicion of physiopathology that PTEN modulates angiogenesis.

It is important to emphasize that this mutation is relatively rare (25).

Of the few cases previously published associated with dAVF, typical PTEN syndromic patients were involved. Hence, we advocate the novelty of this case: (1) Despite the PTEN variant, the patient did not fulfill the criteria for any syndrome; and (2) the rapid and aggressive formation of new dAVFs is not typical. More studies are necessary to understand how to manage patients who present with such dAVFs.

4 Conclusion

The previously reported dAVF cases with PTEN variant were linked to syndromic PTEN mutations. We describe a case of a previously healthy adult with multiple and complex dAVFs as a new phenotype.

Data availability statement

The datasets presented in this article are not readily available because of ethical and privacy restrictions. Requests to access the datasets should be directed to the corresponding author.

Ethics statement

The studies involving humans were approved by the Ethics and Research Committee of the Federal University of São Paulo. The studies were conducted in accordance with the local legislation and institutional requirements. The participants provided their written informed consent to participate in this study. Written informed consent was obtained from the individual(s) for the publication of any potentially identifiable images or data included in this article.

Author contributions

GJ-A-L: Conceptualization, Investigation, Writing – original draft, Writing – review & editing. TS: Formal analysis, Investigation, Writing – review & editing. MS: Data curation, Methodology, Writing – review & editing. LG: Data curation, Methodology, Writing – review & editing. RW-S: Writing – review & editing. AB: Data curation, Investigation, Writing – review & editing. JC: Resources, Validation, Writing – review & editing. FC-N: Project administration, Supervision, Validation, Writing – review & editing.

Funding

The author(s) declare that no financial support was received for the research, authorship, and/or publication of this article.

Acknowledgments

We would like to thank all the microvascular fellows for their support with this work.

Conflict of interest

The authors declare that the research was conducted in the absence of any commercial or financial relationships that could be construed as a potential conflict of interest.

Publisher's note

All claims expressed in this article are solely those of the authors and do not necessarily represent those of their affiliated organizations, or those of the publisher, the editors and the reviewers. Any product that may be evaluated in this article, or claim that may be made by its manufacturer, is not guaranteed or endorsed by the publisher.

References

1. Plamper M, Gohlke B, Woelfle J. PTEN hamartoma tumor syndrome in childhood and adolescence-a comprehensive review and presentation of the German pediatric guideline. *Mol Cell Pediatr.* (2022) 9:3. doi: 10.1186/s40348-022-00135-1

2. Tan WH, Baris HN, Burrows PE, Robson CD, Alomari AI, Mulliken JB, et al. The spectrum of vascular anomalies in patients with PTEN mutations: implications for diagnosis and management. *J Med Genet.* (2007) 44:594–602. doi: 10.1136/jmg.2007.048934

3. Lynch NE, Lynch SA, McMenamin J, Webb D. Bannanyan-Riley-Ruvalcaba syndrome: a cause of extreme macrocephaly and neurodevelopmental delay. *Arch Dis Child.* (2009) 94:553–4. doi: 10.1136/adc.2008.155663

4. Hendriks YMC, Verhallen JTCM, van der Smagt JJ, Kant SG, Hilhorst Y, Hoefsloot L, et al. Bannanyan-Riley-Ruvalcaba syndrome: further delineation of the phenotype and management of PTEN mutation-positive cases. *Fam Cancer.* (2003) 2:79–85. doi: 10.1023/A:1025713815924

5. Starink TM, van der Veen JP, Arwert F, de Waal LP, de Lange GG, Gille JJ, et al. The Cowden syndrome: a clinical and genetic study in 21 patients. *Clin Genet.* (1986) 29:222–33. doi: 10.1111/j.1399-0004.1986.tb00816.x

6. Pilarski R, Burt R, Kolman W, Pho L, Shannon KM, Swisher E. Cowden syndrome and the PTEN hamartoma tumor syndrome: systematic review and revised diagnostic. *J Natl Cancer Inst.* (2013) 105:1607–16. doi: 10.1093/jnci/djt277

7. Mester JL, Tilot AK, Rybicki LA, Frazier TW, Eng C. Analysis of prevalence and degree of macrocephaly in patients with germline PTEN mutations and of brain weight in Pten knock-in murine model. *Eur J Hum Genet.* (2011) 19:763–8. doi: 10.1038/ejhg.2011.20

8. Busch RM, Srivastava S, Hogue O, Frazier TW, Klaas P, Hardan A, et al. Developmental synaptopathies consortium. *Transl Psychiatry.* (2019) 9:253. doi: 10.1038/s41398-019-0588-1

9. Frazier TW, Embacher R, Tilot AK, Koenig K, Mester J, Eng C. Molecular and phenotypic abnormalities in individuals with germline heterozygous PTEN mutations and autism. *Mol Psychiatry.* (2015) 20:1132–8. doi: 10.1038/mp.2014.125

10. Lok C, Viseux V, Francoise M, Richard MA, Gondry-Jouet C, Deramond H, et al. Brain magnetic resonance imaging in patients with Cowden syndrome. *Medicine.* (2005) 84:129–36. doi: 10.1097/01.md.0000158792.24888.d2

11. Prats-Sánchez LA, Hervás-García JV, Becerra JL, Lozano M, Castaño C, Munuera J, et al. Multiple intracranial arteriovenous fistulas in Cowden Syndrome. *J Stroke Cerebrovasc Dis.* (2016) 25:e93–4. doi: 10.1016/j.jstrokecerebrovasdis.2016.03.048

12. Khandput U, Huntoon K, Smith-Cohn M, Shaw A, Elder JB. Bilateral recurrent dysplastic cerebellar gangliocytoma (Lhermitte-Duclos Disease) in Cowden Syndrome: a case report and literature review. *World Neurosurg.* (2019) 127:319–25. doi: 10.1016/j.wneu.2019.03.131

13. Zhang HW, Zhang YQ, Liu XL, Mo YQ, Lei Y, Lin F, et al. MR imaging features of Lhermitte-Duclos disease: case reports and literature review. *Medicine.* (2022) 101:e28667. doi: 10.1097/MD.0000000000028667

14. Joo G, Doumanian J. Radiographic findings of dysplastic cerebellar gangliocytoma (Lhermitte-Duclos Disease) in a woman with Cowden Syndrome: a case study and literature review. *J Radiol Case Rep.* (2020) 14:1–6. doi: 10.3941/jrcr.v14i3.3814

15. Yehia L, Eng C, Adam MP, Feldman J, Mirzaa GM, Pagon RA, et al. PTEN Hamartoma Tumor Syndrome. In: Bean LJH, Gripp KW, Amemiya A, editors. *GeneReviews.* Seattle, WA: University of Washington, Seattle (2001).

16. Toh K, Suzuki K, Miyaoka R, Kitagawa T, Saito T, Nakano Y, et al. Giant cerebral aneurysm in a patient with Cowden syndrome treated with surgical clipping. *World Neurosurg.* (2019) 126:336–40. doi: 10.1016/j.wneu.2019.02.245

17. Almubarak AO, Haq AU, Alzahrani I, Shail EA. Lhermitte-duclos disease with cervical arteriovenous fistula. *J Neurol Surg A Cent Eur Neurosurg.* (2019) 80:134–7. doi: 10.1055/s-0038-1670636

18. Akiyama Y, Ikeda J, Ibayashi Y, Nonaka T, Asai Y, Houkin K. Lhermitte-Duclos disease with cervical paraspinal arteriovenous fistula. *Neurol Med Chir.* (2006) 46:446–9. doi: 10.2176/nmc.46.446

19. Bae BG, Kim HJ, Lee SG, Choi JR, Hwang C, Lee JH, et al. A novel PTEN mutation in a Korean patient with Cowden syndrome and vascular anomalies. *Acta Derm Venereol.* (2011) 91:88–90. doi: 10.2340/00015555-0994

20. Turnbull MM, Humeniuk V, Stein B, Suthers GK. Arteriovenous malformations in Cowden syndrome. *J Med Genet.* (2005) 42:e50. doi: 10.1136/jmg.2004.030569

21. Srinivasa RN, Burrows PE. Dural arteriovenous malformation in a child with Bannayan-Riley-Ruvalcaba Syndrome. *Am J Neuroradiol.* (2006) 27:1927–9.

22. Moon K, Ducruet AF, Crowley RW, Klas K, Bristol R, Albuquerquer FC. Complex dural arteriovenous fistula in Bannayan-Riley-Ruvalcaba syndrome. *J Neurosurg Pediatr.* (2013) 12:87–92. doi: 10.3171/2013.3.PEDS12551

23. Sadahiro H, Ishihara H, Goto H, Oka F, Shirao S, Yoneda H, et al. Postoperative dural arteriovenous fistula in a patient with Cowden disease: a case report. *J Stroke Cerebrovasc Dis.* (2014) 23:572–5. doi: 10.1016/j.jstrokecerebrovasdis.2013.04.021

24. Kar S, Samii A, Bertalanffy H. PTEN/PI3K/Akt/VEGF signaling and the cross talk to KRIT1, CCM2, and PDCD10 proteins in cerebral cavernous malformations. *Neurosurg Rev.* (2015) 38:229–36. doi: 10.1007/s10143-014-0597-8

25. Busa T, Milh M, Degardin N, Girard N, Sigaudy S, Longy M, et al. Clinical presentation of PTEN mutations in childhood in the absence of family history of Cowden syndrome. *Eur J Paediatr Neurol.* (2015) 19:188–92. doi: 10.1016/j.ejpn.2014.11.012

frontiers | Frontiers in Neurology

TYPE Case Report
PUBLISHED 18 April 2024
DOI 10.3389/fneur.2024.1349861

OPEN ACCESS

EDITED BY
Huifang Shang,
Sichuan University, China

REVIEWED BY
Barbara Garavaglia,
IRCCS Carlo Besta Neurological Institute Foundation, Italy
Saurabh Srivastav,
Rice University, United States

*CORRESPONDENCE
Kang Du
✉ dukangyn@126.com

RECEIVED 07 December 2023
ACCEPTED 18 March 2024
PUBLISHED 18 April 2024

CITATION
Cai D, Wu H, Huang B, Xiao W and Du K (2024) A novel variant of *PLA2G6* gene related early-onset parkinsonism: a case report and literature review. *Front. Neurol.* 15:1349861. doi: 10.3389/fneur.2024.1349861

A novel variant of *PLA2G6* gene related early-onset parkinsonism: a case report and literature review

Dapeng Cai, Haohao Wu, Baogang Huang, Weiwei Xiao and Kang Du*

Department of Neurology, Qujing First People's Hospital, Qujing, Yunnan, China

This study reported a case of early-onset parkinsonism associated with a novel variant of the PLA2G6 gene. The boy first started showing symptoms at the age of 11, with gait instability and frequent falls. As the disease progressed, his gait instability worsened, and he developed difficulties with swallowing and speaking, although there was no apparent decline in cognitive function. An MRI of the head revealed significant atrophy of the cerebellum. The initial diagnosis for the boy was early-onset parkinsonism, classified as Hoehn-Yahr grade 5.Genomic sequencing of the patient indicated that he had compound heterozygous variations in the PLA2G6 gene: c.1454G>A (p.Gly485Glu) and c.991G>T (p.Asp331Tyr). Pedigree analysis revealed that his younger brother also carried the same variant, albeit with milder symptoms. The patient's unaffected mother was found to be a carrier of the c.991G>T variant. Additionally, this study reviewed 62 unrelated families with PLA2G6 gene-related early-onset parkinsonism. The analysis showed a higher proportion of female probands, with a mean age of onset of ~23.0 years. Primary symptoms were predominantly bradykinesia and psychosis, with tremors being relatively rare. Cerebellar atrophy was observed in 41 patients (66.1%). Among the reported mutations, the most common mutation was c.991G>T, presenting in 21 families (33.9%), followed by c.2222G>A in eight families (12.9%). Other mutations were less common. Notably, the c.991G>T mutation was exclusive to Chinese families and was a prevalent mutation among this population. The initial symptoms varied significantly among patients with different mutations.

KEYWORDS

***PLA2G6*, early-onset parkinsonism, cerebellar atrophy, hot spot mutation, heterogeneity**

1 Introduction

Early-onset parkinsonism (EOP) is a neurodegenerative disease related to genetic factors. PLA2G6 gene mutation is considered to be one of the pathogenic genes involved in the development of EOP (1). Autosomal recessive EOP caused by mutations in the PLA2G6 gene is called PLA2G6-associated Neurodegeneration (PLAN) (2, 3). These include Infantile neuroaxonal dystrophy (INAD), Atypical neuroaxonal dystrophy (ANAD), and EOP (4). In this study, a case of EOP caused by a novel PLA2G6 gene mutation was reported, and previous reports of EOP related to this gene were reviewed.

2 Case presentation

A 22-year-old male patient was admitted to the hospital due to gait abnormality and frequent falls. The patient developed the above symptoms at the age of 11, and his motor development was slightly worse than that of his peers. After that, the patient's gait instability was aggravated, dysphagia and dysarthria gradually appeared, without obvious cognitive decline, and no special diagnosis and treatment were given. The patient's anomalies of gait and weakness of extremities were further aggravated, manifested as frequent falls, requiring bed rest or wheelchair. The patient's articulation disorder and deglutition disorders were aggravated compared with the previous ones, and the cognitive decline was presented, but he could still communicate normally with his family members. The proband's father died of trauma. Prior to his death, he denied the anomalies of gait, muscle weakness and other symptoms. The proband's younger brother began to have gait instability at the age of 11, and his motor development since childhood was slightly worse than that of his peers. At the age of 20, he can still walk normally, live independently, but his muscle tension is symmetrically increased. The proband's mother had a head trembling a few months ago, without other special discomforts. The patient's cranial magnetic resonance imaging (MRI) examination in September 2022 revealed cerebellar atrophy. The diagnosis of Parkinson's syndrome was made, and the Hoehn-Yahr grade was 5.

The nervous system physical examination revealed that the patient had normal vital signs, clear mind, but had severe dysarthria. The orientation of time, character and place was normal, the calculation and comprehension were decreased. The cranial nerves examination did not reveal any abnormalities. The distal and proximal muscle strength of both upper limbs was grade 3, the distal and proximal muscle strength of both lower limbs was grade 2, the symmetry of muscle tension of both upper limbs was increased, the muscle tension of both lower limbs was decreased, the tendon reflex of both upper limbs was brisk, the tendon reflex of both lower limbs was absent, the Rossolimo's sign of both upper limbs was positive, the pathological sign of both lower limbs was negative, the meningeal irritation sign was negative, and the patient had no sensory abnormalities and ataxia signs in the physical examination. Wide base gait, slow movement, reduced swing arms of both hands, and unilateral assistance during walking. The patient could not cooperate to complete the bilateral finger-nose test, heel-knee-tibia test, and pull-back test.

The results of auxiliary examination suggest that: there were no abnormalities in hematuria, stool routine, biochemical indicators, homocysteine, ceruloplasmin, hepatitis, syphilis, HIV, coagulation function, autoimmune antibody spectrum, and cardiac ultrasound. MRI plain scan and contrast-enhancement of the head indicated brain atrophy, especially in the bilateral cerebellar hemispheres (Figure 1C).

The patient's whole genome sequencing suggested that the PLA2G6 gene compound heterozygous variants c.1454G > A (p.Gly485Glu), c.991G > T (p.Asp331Tyr) (Figures 1A, B). The results of pedigree verification suggested that the proband's brother was consistent with the proband's results. The proband's mother was a asymptomatic carrier of the variant of PLA2G6 gene c.991G > T. The proband's father failed to perform pedigree verification due to unexpected death, which was consistent with the role of family co-segregation. The variant of c.991G > T has been previously reported as a pathogenic variation (5), however, the variant of c.1454G > A has not been reported. The Mutation Taster software predicted it as a pathogenic variation, and the probability was 0.9999; this variant was not found in ExAC and Thousand Human Genome Database, and the conservation analysis suggested that it was highly conserved (Figure 1D).

The patient was finally diagnosed with PLA2G6 gene-related early-onset Parkinson's syndrome. The patient was treated with madopa 62.5 mg tid gradually increased to 125 mg tid orally. After 2 months of follow-up, the patient's gait abnormality was slightly improved compared with the previous one, and the disease did not progress significantly.

3 Literature review

In this study, the keywords "PLA2G6," "parkinsonism," and "Parkinson" were searched through "Pubmed," "Wanfang Medicine," and "China National Knowledge Infrastructure" databases. The literature of PLA2G6 gene-related EOP patients reported in Chinese and English was reviewed. A total of 62 families, including 30 Chinese families, were reviewed, and the clinical and genetic characteristics of the probands in all families were summarized (Table 1).

By reviewing the literature, it was found that among the 62 probands, the male to female ratio was 2: 3, and the average onset age of male patients was 22.9 ± 8.7 years old. The average age of onset in women was 23.0 ± 8.5 years. There were 51 cases (82.2%) with movement disorder as the initial symptom, including 27 cases (43.5%) with gait disorder, 10 cases (16.1%) with gait instability, and 11 cases (17.7%) with limb trembling. There were 14 cases (22.6%) with depression, dysphoria, and other emotional instability as the initial symptoms. All probands were examined by cranial MRI, and 41 (66.1%) patients had cerebellar atrophy.

Among the 30 cases of national probands, the male to female ratio was 3:2, and the average onset age of male patients was 22.9 ± 8.9 years. The average age of onset in women was 22.9 ± 8.8 years. The most common mutation was c.991 G > T mutation in 21 families (70%), followed by c.967 G > A mutation in three families (10 %), c.1077 G > A mutation in three families (10%), and other mutations were rare. The most common clinical manifestations were movement disorder in 30 cases (100%), including gait disorder in 17 cases (56.7%), limb trembling in 19 cases (63.3%), and mental and behavioral disorders in 24 cases (80%). Among them, movement disorder was the most common symptom, with 28 cases (93.3%).

Among the 15 European and American probands, the ratio of male to female was 1:14. The most common clinical manifestations were movement disorder in 15 cases (100 %) and mental and behavioral disorders in 14 cases (93.3 %). Among them, mental and behavioral disorders were the most common symptoms, a total of 14 cases (93.3 %).

Of the 14 probands from the Middle East and western Asia, the ratio of male to female was 5: 9. The most common clinical

10.3389/fneur.2024.1349861

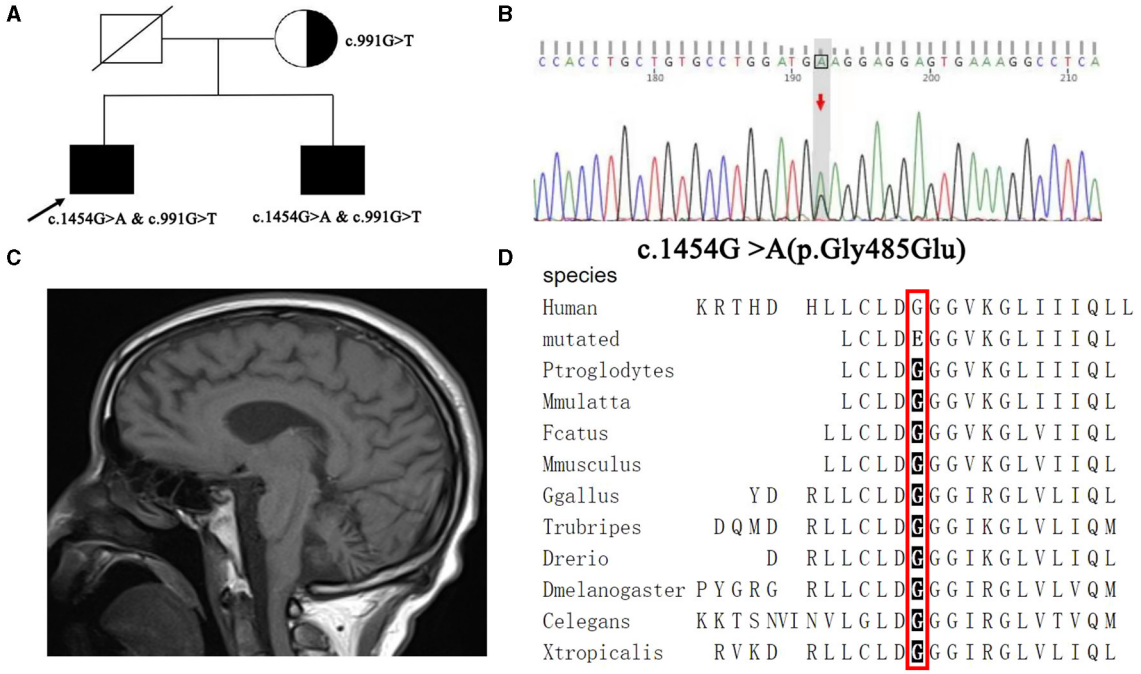

FIGURE 1
(A) Family diagram of the proband; **(B)** Another complex heterozygous variation of proband c.1454G>A with Sanger sequencing; **(C)** Cerebellar atrophy can be seen in the sagittal T1WI phase of the proband's head MRI; **(D)** The conservative analysis of this variant suggests that it is highly conservative.

symptoms were movement disorder (10 cases, 71.4%) and mental and behavioral disorders (13 cases, 92.9%). The most common symptoms were movement disorder (nine cases, 64.3%) and mental and behavioral disorders (seven cases, 50%).

Among the reported mutations, the most common mutation was c.991G > T in 21 families (33.9%), followed by c.2222G > A in eight families (12.9%), and other mutation types were rare. Among them, the c.991 G > T mutation only was found in Chinese, and the c.2222 G > A mutation was mainly distributed in the Middle East, western Asia and other countries. Among them, the ratio of male to female in the proband with c.991G > T mutation was 13:8. There were 15 cases (71%) of compound heterozygous mutations and six cases (29%) of homozygous mutations. The average age of onset of patients with compound heterozygous mutations was 23.1 ± 9.2 years old, and the most common initial symptom was movement disorder in seven cases (46.7%). There were 14 cases (93.3%) with dystonia and 10 cases (66.7%) with mental and behavioral disorders. The average age of patients with homozygous mutations was 32.5 ± 4.5 years old, and the initial symptoms were atypical, including one case of gait disorder (16.7%) and one case of movement disorder (16.7%). There were six cases (100%) of dystonia and three cases (50%) of mental and behavioral disorders. Among the probands with compound heterozygous mutations, there were 14 cases (93%) of cerebellar atrophy, and no cerebellar atrophy was found in the probands with homozygous mutations. The male to female ratio of the proband with c.2222G > A mutation was 1:7, all of which were homozygous mutations. The average age of onset was 23.3 ± 7.6 years. The most common initial symptoms were mental and behavioral disorders in seven cases (87.5%), including dysphoria, depression and other symptoms in 6 cases (75.0%). There were five cases (62.5%) of dystonia and eight cases (100%) of mental and behavioral disorders. A total of four probands had cerebellar atrophy (50%).

In addition, among all the probands, 9 (33%) patients with homozygous mutations had cerebellar atrophy, and 36 (85%) patients with compound heterozygous mutations had cerebellar atrophy.

4 Discussion

PLA2G6 gene is located in 22q13.1 region, about 6.0 Mb, containing 17 exons, encoding 85 ku cytosolic $Ca2^{+}$ independent phospholipids A2 (iPLA2). There are two forms of iPLA2-A and iPLA2-β. The iPLA2-β enzyme is closely related to neurodegenerative diseases, and different mutation sites can lead to different degrees of changes in iPLA2-β enzyme. This leads to different clinical phenotypes of PLAN (31). The mutation types of this gene include missense mutation, truncation mutation and copy number variation, but the specific mechanism of this mutation is not clear (31). Previous studies have shown that the pathogenesis of EOP caused by PLA2G6 gene may be the loss of iPLA2 enzyme protein function caused by PLA2G6 gene mutation, which in turn causes phospholipid metabolism disorder of nerve cell membrane, intracellular iron deposition, lipid peroxidation, mitochondrial inner membrane damage, and Golgi morphological changes, eventually leading to a large number of apoptosis of dopaminergic neurons, decreased dopamine secretion, and the

TABLE 1 A retrospective analysis of *PLA2G6* gene-related EOP literature has been reported.

Family number	Family source	Sex	Age of onset (years)	Initial symptom	Clinical manifestation	Head MRI	Treatment	Variant 1	Variant 2	Author/ year
1	English	F	26	Cognitive decline, movement disorder, clumsiness, frequent falls, trembling, and dysarthria	Cognitive decline, dystonia, movement disorder, and rigidity	Normal	Levodopa/effective	c.2222G>A	c.2222G > A	Paisan-Ruiz et al. 2009 (6)
2	English	F	18	Cognitive decline, dysphoria, and movement disorder	Gait disorder, dystonia, and mental disorder	Normal	Levodopa/effective	c.2239C > T	c.2239C > T	Paisan-Ruiz et al. 2009 (6)
3	Iranian	M	25	Gait disorder	Gait disorder, dystonia, and cognitive decline	Normal	NA	c.1894C>T	c.1894C>T	Sina et al. 2009 (7)
4	Japanese	F	20	Resting tremor and gait instability	Resting tremor, movement disorder, rigidity, anomalies of posture, gait disorder, depression, mental disorder, and cognitive decline	Normal	NA	c.216C>A	c.1904G>A	Yoshino et al. 2010 (8)
5	Japanese	M	25	Movement disorder and gait disorder	Resting tremor, movement disorder, rigidity, anomalies of posture, gait disorder, and cognitive decline	Normal	NA	c.1354C>T	c.1904G>A	Yoshino et al. 2010 (8)
6	French	F	18	Depression	Dystonia, depression, dyspraxia, and frequent falls	Cerebellar atrophy.	NA	c.4C>A	Del Ex 3	Bower et al. 2011 (9)
7	Chinese	M	37	Gait disorder	Resting tremor, movement disorder, rigidity, anomalies of posture, and gait disorder	Normal	NA	c.991G>T	c.991G>T	Shi et al. 2011 (5)
8	Scandinavian	F	22	Depression	Resting tremor, movement disorder, rigidity, anomalies of posture, gait disorder, depression, mental and behavioral disorders, cognitive decline, and dystonia	Normal	NA	c.G238A	c.G238A	Agarwal et al. 2012 (10)
9	Chinese	F	19	Movement disorder and gait disorder	Resting tremor, severe muscle rigidity, movement disorder, defective coordination, trembling, mental and behavioral disorders, and dysarthria	Cerebellar atrophy.	Levodopa/effective	c.991G>T	c.1077G>A	Lu et al. 2012 (11)
10	Chinese	F	8	Movement disorder and gait disorder	Resting tremor, severe muscle rigidity, movement disorder, defective coordination, mental and behavioral disorders and dysarthria	Cerebellar atrophy.	Levodopa/effective	c.991G>T	c.1078G>A	Lu et al. 2012 (11)

(Continued)

10.3389/fneur.2024.1349861

TABLE 1 (Continued)

Family number	Family source	Sex	Age of onset (years)	Initial symptom	Clinical manifestation	Head MRI	Treatment	Variant 1	Variant 2	Author/ year
11	Chinese	F	30	Movement disorders	Severe muscle rigidity, movement disorder, defective coordination, and mental and behavioral disorders	Normal	Levodopa/effective	c.991G>T	c.991G>T	Lu et al. 2012 (11)
12	English	F	18	Movement disorder and gait disorder	Defective coordination, dysarthria, dysphagia, rigidity, and movement disorder	Cerebellar atrophy.	NA	c.109C>T	c.1078_3C>A	Paisán-Ruiz et al. 2012 (12)
13	Greek	F	22	Dysphoria and visual illusion	Dysphoria, trembling, movement disorder, and frequent falls	Cerebellar atrophy.	Levodopa/effective	c.1715C>T	c.1715C>T	Paisán-Ruiz et al. 2012 (12)
14	The white race	F	3	Gait instability	Dystonia, muscle rigidity, gait instability, and dysphoria	Cerebellar atrophy.	NA	c.2370T>G	c.691G>C	Illingworth et al. 2014 (13)
15	American	F	25	Trembling, gait disorder, and depression	Dystonia, dysphagia, depression, dysphoria and mental disorder	Cerebellar atrophy.	Levodopa/Invalid	c.2222G>A	c.2222G>A	Virmani et al. 2014 (14)
16	Italian	F	27	Gait disorder, movement disorder, dysarthria, and dysphoria	Movement disorder, frequent falls, rigidity, dystonia, dysphoria, mental disorder, and cognitive impairment	Normal	Levodopa/effective	c.1547C>T	c.1547C>T	Malaguti et al. 2015 (15)
17	Chinese	M	36	Gait disorder	Gait disorder, dystonia, movement disorder, and rigidity	Normal	Levodopa/effective	c.991G>T	c.991G>T	Xie et al. 2015 (16)
18	Chinese	M	36	Static tremor	Resting tremor, dystonia, movement disorder, and rigidity	Normal	Levodopa/effective	c.991G>T	c.991G>T	Xie et al. 2015 (16)
19	Koreans	F	22	Gait instability and dysarthria	Dystonia, disorder, frequent falls, and dysarthria	Normal	Levodopa/effective	c.1039G>A	c.1670C>T	Kim et al. 2015 (17)
20	Turks	F	27	Movement disorder	Dystonia, Resting tremor, movement disorder, rigidity, anomalies of posture, gait disorder, movement disorder, depression, mental disorder, and cognitive decline	Normal	NA	c.2239C>T	c.2239C>T	Giri et al. 2016 (18)

(Continued)

10.3389/fneur.2024.1349861

TABLE 1 (Continued)

Family number	Family source	Sex	Age of onset (years)	Initial symptom	Clinical manifestation	Head MRI	Treatment	Variant 1	Variant 2	Author/ year
21	Arab	F	26	Gait disorder	Dystonia, depression, and movement disorder	Normal	NA	c.2222G>A	c.2222G>A	Bohlega et al. 2016 (19)
22	German	F	21	Gait disorder	Movement disorder and gait disorder	Cerebellar atrophy.	Levodopa/effective	c.610-1G>T	c.1627C>T	Klein et al. 2016 (20)
23	Indian	M	9	Cognitive decline and trembling	Dystonia and defective coordination	Cerebellar atrophy.	Levodopa/effective	c.1946G>A	c.1946G>A	Kapoor et al. 2016 (21)
24	Saudi Arabia	F	26	Depression and movement disorder	Resting tremor, movement disorder, rigidity, anomalies of posture, gait disorder, depression, mental and behavioral disorders, and cognitive decline	Normal	NA	c.2222G>A	c.2222G>A	Bohlega et al. 2016 (19)
25	Chinese	M	27	Gait disorder	Resting tremor, movement disorder, rigidity, anomalies of posture, and gait disorder	Cerebellar atrophy.	Levodopa/effective	c.668C>T	c.1915G>A	Chen et al. 2018 (22)
26	Chinese	M	29	Gait disorder	Anomalies of posture, gait disorder, movement disorder, trembling, dysarthria, and dystonia	Cerebellar atrophy.	NA	c.991G>T	c.1982C>T	Chen et al. 2018 (22)
27	Chinese	M	30	Gait disorder and frequent falls	Rigidity, movement disorder, frequent falls, cognitive decline, and gait disorder	Cerebellar atrophy.	Levodopa/effective	c. 991G>T	c.1472+1G>A	Shen et al. 2019 (23)
28	Kuwaitians	F	17	Mental disorder, depression, and dysphoria	Mental disorder, depression, dysphoria, rigidity, Dystonia, gait instability, and frequent falls	Cerebellar atrophy.	Levodopa/effective	c.2215G>C	c.2215G>C	Kamel et al. 2019 (24)
29	Chinese	M	17	Dystonia, dysarthria, and cognitive decline	Frequent falls, mental disorder, dysarthria, dystonia, and epilepsy	Cerebellar atrophy.	NA	c.991G>T	c.238G>A	Ma et al. 2019 (25)
30	Indian	F	3	Gait disorder and cognitive decline	Rigidity, slow development, gait instability, and cognitive decline	Cerebellar atrophy.	NA	c.1798C>T	c.2357C>T	Jain et al. 2019 (26)

(Continued)

10.3389/fneur.2024.1349861

TABLE 1 (Continued)

Family number	Family source	Sex	Age of onset (years)	Initial symptom	Clinical manifestation	Head MRI	Treatment	Variant 1	Variant 2	Author/ year
31	Chinese	F	30	Movement disorder	Resting tremor, movement disorder, rigidity, anomalies of posture, depression, mental disorder, cognitive decline, and gait disorder	Normal	Levodopa/effective	c.991G>T	c.991G>T	Chu et al. 2020 (27)
32	Chinese	F	26	Clumsiness	Resting tremor, movement disorder, rigidity, anomalies of posture, depression, mental and behavioral disorders, cognitive decline, and gait disorder	Normal	Levodopa/effective	c.991G>T	c.991G>T	Chu et al. 2020 (27)
33	Chinese	M	31	Depression	Dysarthria, movement disorder, and dystonia	Cerebellar atrophy.	Levodopa/effective	c.991G>T	c.1077G>A	Chu et al. 2020 (27)
34	Chinese	F	34	Resting tremor and fatigue	Resting tremor, movement disorder, and memory decline	Normal	Levodopa/effective	c.1321T>C	c.856delT	Gao et al. 2020 (28)
35	Chinese	F	25	Lower extremity weakness and movement disorder	Resting tremor, rigidity, movement disorder, and memory decline	Normal	Levodopa/effective	c.856delT	c.856delT	Gao et al. 2020 (28)
36	English	F	27	Dystonia	Dystonia, cognitive decline, anxiety, and depression	Cerebellar atrophy.	Levodopa/effective	c.956C>T	c.1061T>C	Magrinelli et al. 2022 (29)
37	English	F	29	Trembling and executive dysfunction	Resting tremor, movement disorder, rigidity, and mental disorder	Cerebellar atrophy.	Levodopa/effective	c.238G>A	c.1924A>G	Magrinelli et al. 2022 (29)
38	Indian	F	21	Trembling and mental and behavioral disorders	Resting tremor, movement disorder, rigidity, and mental disorder	Cerebellar atrophy.	Levodopa/effective	c.673C>T	c.2311G>A	Magrinelli et al. 2022 (29)
39	Indian	M	29	Trembling	Resting tremor, movement disorder, rigidity, and mental disorder	Cerebellar atrophy.	Levodopa/effective	c.1937C >T	c.1937C>T	Magrinelli et al. 2022 (29)
40	Indian	F	25	Trembling	Resting tremor, movement disorder, rigidity, and mental disorder	Cerebellar atrophy.	Levodopa/effective	c.2370T > G	c.1511C>T	Magrinelli et al. 2022 (29)

(Continued)

10.3389/fneur.2024.1349861

TABLE 1 (Continued)

Family number	Family source	Sex	Age of onset (years)	Initial symptom	Clinical manifestation	Head MRI	Treatment	Variant 1	Variant 2	Author/ year
41	Indian	F	15	Depression and dysphoria	Anomalies of posture, cognitive decline, dysphoria, depression, mental disorder, and anxiety	Cerebellar atrophy.	Levodopa/effective	c.2222G>A	c.2222G>A	Magrinelli et al. 2022 (29)
42	Pakistani	F	23	Dysphoria	Dysarthria, cognitive decline, dysphoria, depression, urinary dysfunction, and anxiety	Cerebellar atrophy.	Levodopa/effective	c.2222G>A	c.2222G>A	Magrinelli et al. 2022 (29)
43	Pakistani	F	21	Dysphoria and depression	Cognitive decline, myoclonus, dysphoria, depression, and anxiety	Normal	Levodopa/effective	c.2222G>A	c.2222G>A	Magrinelli et al. 2022 (29)
44	German	M	22	Dyspraxia and gait instability	Dyspraxia, gait instability, dysarthria, and cognitive decline	Cerebellar atrophy.	Levodopa/effective	c.1021G>A	c.1898C>T	Magrinelli et al. 2022 (29)
45	Indian	M	21	Mental disorder and dysphoria	Spasm of eyelid, dysarthria, mental and behavioral disorders, and anxiety	Cerebellar atrophy.	Levodopa/effective	c.2222G>A	c.2222G>A	Magrinelli et al. 2022 (29)
46	Pakistani	M	31	Gait disorder, frequent falls	Myoclonus and cognitive decline	Cerebellar atrophy.	Levodopa/effective	c.2239C>T	c.2239C>T	Magrinelli et al. 2022 (29)
47	Hungarian	F	3	Gait instability and dysarthria	Gait instability, dysphagia, movement disorder, mental deterioration, trembling, dysphoria, and anxiety	Cerebellar atrophy.	NA	c.1864C>T	c.1798C>T	Toth-Bencsik et al. 2021 (30)
48	Chinese	M	29	Dyspraxia, gait disorder, and rigidity	Constipation, dreaminess, dysphoria, olfactory impairment, gait disorder, dyspraxia, and rigidity	Normal	Levodopa/effective	c.991G>T	c.1A>G	Chen et al. 2022 (31)
49	Chinese	M	20	Movement disorder	Anomalies of posture, gait disorder, trembling, movement disorder, rigidity, dysarthria, and cognitive decline	Cerebellar atrophy.	Levodopa/effective	c.991G>T	c.1117G>A	Cheng et al. 2022 (2)
50	Chinese	M	29	Gait disorder	Anomalies of posture, gait disorder, resting tremor, movement disorder, rigidity, and dysarthria	Cerebellar atrophy.	Levodopa/effective	c.991G>T	c.1915delG	Cheng et al. 2022 (2)
51	Chinese	M	31	Dysarthria	Anomalies of posture, gait disorder, resting tremor, rigidity, dysarthria, cognitive decline, and gait disorder	Cerebellar atrophy.	Levodopa/effective	c.967G>A	c.1450G>T	Cheng et al. 2022 (2)

(Continued)

10.3389/fneur.2024.1349861

TABLE 1 (Continued)

Family number	Family source	Sex	Age of onset (years)	Initial symptom	Clinical manifestation	Head MRI	Treatment	Variant 1	Variant 2	Author/ year
52	Chinese	F	35	Movement disorder	Anomalies of posture, gait disorder, resting tremor, movement disorder, rigidity, dysarthria, and cognitive decline	Cerebellar atrophy.	NA	c.991G>T	c.1631T>C	Cheng et al. 2022 (2)
53	Chinese	F	6	Gait disorder	Anomalies of posture, gait disorder, trembling, and cognitive decline	Cerebellar atrophy.	NA	c.991G>T	c.1427+2T>A	Cheng et al. 2022 (2)
54	Chinese	M	15	Gait disorder	Anomalies of posture, gait disorder, trembling, movement disorder, rigidity, dysarthria, and cognitive decline	Cerebellar atrophy.	NA	c.1077G>A	c.1670C>T	Cheng et al. 2022 (2)
55	Chinese	M	24	Gait instability, movement disorder, and reduced expression	Movement disorder, gait instability, reduced expression, and cognitive decline	Cerebellar atrophy.	Levodopa/effective	c.991G>T	c.1427 + 1G>A	Lili Gao et al. 2022 (3)
56	Chinese	F	29	Gait instability, lower extremity weakness, and rigidity	Rigidity, movement disorder, frequent falls, cognitive decline, dysarthria, ocular paralysis, lower extremity weakness, and gait disorder	Cerebellar atrophy.	Levodopa/effective	c.967G>A	c.116G>A	Wan et al. 2022 (32)
57	Chinese	M	14	Gait instability	Gait instability, dysarthria, and mental disorder	Cerebellar atrophy.	Levodopa/Invalid	c.2120dupA	c.2071C>G	Wan et al. 2022 (32)
58	Chinese	F	3	Lower extremity weakness	Lower extremity weakness, rigidity, and mental disorder	Cerebellar atrophy.	NA	c.238G>A	c.1534T>A	Wan et al. 2022 (32)
59	Chinese	M	28	Muscle rigidity and resting tremor	Rigidity, resting tremor, movement disorder, and gait disorder	Cerebellar atrophy.	Levodopa/effective	c.991G>T	c.1054_1058delinsCTGGCCAGGAG	Ma et al. 2022 (33)
60	Chinese	M	30	Gait disorder, movement disorder, and dysarthria	Gait disorder, movement disorder, dysarthria, and frequent falls	Cerebellar atrophy.	Levodopa/effective	c.967G>A	c.1450G>T	Ma et al. 2022 (33)
61	Chinese	F	31	Gait instability, movement disorder, and trembling	Resting tremor, rigidity, movement disorder, and frequent falls	Cerebellar atrophy.	Levodopa/Invalid	c.991G>T	c.1771C>T	Ma et al. 2022 (33)
62	Chinese	M	11	Gait instability, movement disorder, and slow development	Gait disorder, dysphagia, slow development, severe dysarthria, and dystonia	Cerebellar atrophy.	Levodopa/effective	c.991G>T	c.1454G>A	This article

F, female; M, male; NA, not available.

10.3389/fneur.2024.1349861

presence of Lewy bodies formed by misfolding and aggregation of α-synuclein in surviving neurons, leading to the occurrence of EOP (34, 35).

After reviewing the literature, this study showed that there were slightly more female patients with PLA2G6 gene-related EOP than male patients, and all of them had similar age of onset. The average age of onset was about 22 years old. The patients of EOP usually had gait disorder and movement disorder as the initial symptoms, but the resting tremor was relatively rare. As the disease progressed, it might be accompanied by symptoms such as rigidity, cognitive decline, mental and behavioral disorders (36–38). The majority of patients responded well to levodopa preparations, but the incidence of dyskinesia and symptom fluctuations reported in the literature was high and occurred earlier (34).

Based on retrospective analysis, it was found that the most common mutation in Chinese people was c.991G > T. One of the mutations reported in this study was also this variant. The mutation accounted for more than half of the Chinese pedigrees reported. It was further confirmed that the c.991G > T was the hot spot mutation of the PLA2G6 gene in China (2, 27), suggesting that this mutation had a founder effect in Chinese patients. The most common mutation reported abroad was c.2222G > A, which was mainly found in the Middle East and western Asia, including Arab, Saudi Arabia, India, Pakistan and other countries. The most common symptoms of c.991G > T mutation-related patients were movement disorder and gait disorder. Patients with c.2222G > A mutation usually had cognitive impairment, anxiety, depression, dysphoria, and other mental disorders, accompanied by a small amount of movement disorders. It was found that among the EOP probands caused by PLA2G6 gene, the probands with mental and behavioral disorders in Europe and America, western Asia and the Middle East were significantly higher than those in Chinese probands, which further confirmed the correlation between the clinical phenotype of EOP and different genotypes (29). However, Cheng et al. suggested that it might also be due to the complex phenotypic characteristics of Chinese patients, which could easily cover up symptoms such as myoclonus, cognitive decline and mental and behavioral disorders (2), suggesting that the evaluation of cognitive and mental disorders in EOP patients should be strengthened in clinical work.

In this study, 21 probands with c.991G > T mutation reported previously were further analyzed. It was found that patients with c.991G > T mutation usually had movement disorder, gait disorder and other symptoms as the first symptoms, followed by aggravation of symptoms and dystonia, resting tremor and other motor symptoms and non-motor symptoms. Among them, patients with c.991 G > T homozygous mutation occurred about 10 years later than those with compound heterozygous mutation. Furthermore, the initial symptoms were atypical and the clinical manifestations were milder. All of them were sensitive to levodopa treatment, which was consistent with previous studies (3, 11, 16). In addition, this study found that almost all of the probands with compound heterozygous mutations at this variant had cerebellar atrophy, while no cerebellar atrophy occurred in the six homozygous mutant probands, further suggesting that the clinical manifestations of patients with homozygous mutations at this variant were relatively mild. Previous *in vitro* cell experiments showed that c.991G > T mutant cells still retained 30% iPLA2β enzyme activity compared with wild-type cells, but the iPLA2β enzyme activity in H597fx69 cells expressing frameshift mutations only retained 6% (39). Because different mutation sites have different effects on iPLA2β enzyme activity, the reason for the difference between the two may be that another heterozygous mutation site outside the c.991 G > T mutation site has a greater effect on iPLA2β enzyme activity. The PLA2G6 protease activity of patients is higher than that of patients with heterozygous mutations, but more *in vitro* experiments of non-frameshift mutations are needed for further verification in the future. Therefore, we hypothesize that heterozygous and homozygous mutations in the PLA2G6 gene have different effects on the activity of iPLA2β enzyme, and the proportion of iPLA2β enzyme activity loss can partially explain that homozygous mutation probands have relatively benign clinical and neuroimaging phenotypes compared with heterozygous mutation probands (16).

This study also found that 64.8% of the probands showed brain atrophy on head MRI, but most studies showed that only a small number of EOP probands showed iron deposition on head MRI (31, 37, 40). From a pathological point of view, PLAN is characterized by the depletion of neurons in the cerebellar cortex, accompanied by astrocyte proliferation, axonal spheroids in the central and peripheral nervous system, and progressive brain iron deposition (2), cerebellar atrophy is the earliest sign on head MRI, while the signs of brain iron deposition in the basal ganglia often appear later. This may be the reason why MRI cerebellar atrophy signs are common and iron deposition signs are rare in EOP probands (2). Some researchers found that pro-inflammatory cytokines were significantly up-regulated, microglial activation, and reactive astrocyte proliferation were found in the pathological tissues of patients. Therefore, it is believed that inflammatory response is involved in the pathological process of cerebellar atrophy, and it is speculated that early anti-inflammatory treatment may help to delay the progression of cerebellar atrophy in patients with Parkinson's syndrome (41).

Another compound heterozygous mutation c.1454G > A in the PLA2G6 gene of the proband in this study has not been reported. Like most other EOP patients with PLA2G6 compound heterozygous mutations, the symptoms of PLA2G6 gene-related EOP in this patient were basically similar. The onset of the disease was 11 years old, with gait disorder, and the clinical manifestation was dystonia-Parkinson syndrome. The genetic test results of the proband's younger brother were consistent with those of the proband, and the age of onset was 11 years old. However, the clinical symptoms of the proband's younger brother were significantly lighter than those of the proband. The initial symptoms were anomalies of gait, and he could walk normally and take care of himself with the progression of the disease, and were not accompanied by symptoms such as dysphonia and dysphagia. It was speculated whether the proband had more susceptible genes than his younger brother, such as GBA, MAPT, SNCA, etc., leading to more severe clinical symptoms (42). In addition, different hormone levels could also affect the progression of Parkinson's disease (29). Considering that the living environment and habits of the proband and the proband's brother were roughly the same, this might also be one of the reasons for the clinical differences between the two.

Although the incidence of EOP is not high, the morbidity and mortality are very high (38), and most patients have a good response to treatment such as madopar 5–10 years after onset (3). This study also found that the vast majority of PLA2G6 gene-related EOP responds to levodopa treatment, but the delayed use of levodopa will increase the incidence of dyskinesia, and the switching period fluctuation is more obvious (33). Therefore, early diagnosis is of great significance for early initiation of anti-Parkinson therapy.

Because the sample size of most studies on PLA2G6 gene-related EOP in Chinese population is relatively small (3, 16, 27), this leads to limitations in the clinical and phenotypic comparison of different PLA2G6 gene mutation reviews in this study. The clinical and genetic characteristics of PLA2G6 gene-related EOP patients in China will be more clear in future multicenter large sample studies.

5 Conclusion

In conclusion, this study reported a case of early-onset parkinsonism caused by a novel variant of PLA2G6 gene and reviewed previous reports. This expands the genetic pedigree of the disease and increased clinicians' understanding of the clinical and genetic characteristics of early-onset parkinsonism.

Data availability statement

The datasets presented in this article are not readily available because of ethical and privacy restrictions. Requests to access the datasets should be directed to the corresponding author.

Ethics statement

The studies involving humans were approved by the Ethics Committee of Qujing First People's Hospital. The studies were conducted in accordance with the local legislation and institutional requirements. Written informed consent for participation in this study was provided by the participants' legal guardians/next of kin. Written informed consent was obtained from the individual(s), and minor(s)' legal guardian/next of kin, for the publication of any potentially identifiable images or data included in this article.

Author contributions

DC: Conceptualization, Data curation, Formal analysis, Writing – original draft. HW: Conceptualization, Methodology, Supervision, Writing – review & editing. BH: Conceptualization, Methodology, Supervision, Writing – review & editing. WX: Data curation, Methodology, Writing – review & editing. KD: Conceptualization, Formal analysis, Funding acquisition, Investigation, Methodology, Software, Supervision, Validation, Writing – review & editing.

Funding

The author(s) declare financial support was received for the research, authorship, and/or publication of this article. This study was supported by the Yunnan Provincial Department of Education Science Research Funding (No. 2023Y0702).

Conflict of interest

The authors declare that the research was conducted in the absence of any commercial or financial relationships that could be construed as a potential conflict of interest.

Publisher's note

References

1. Riboldi GM, Frattini E, Monfrini E, Frucht SJ, Di Fonzo A. A practical approach to early-onset Parkinsonism. *J Parkinsons Dis.* (2022) 12:1–26. doi: 10.3233/JPD-212815

2. Cheng HL, Chen YJ, Xue YY, Wu ZY, Li HF, Wang N. Clinical characterization and founder effect analysis in Chinese patients with phospholipase A2-associated neurodegeneration. *Brain Sci.* (2022) 12:50517. doi: 10.3390/brainsci12050517

3. Gao L, Shi C, Lin Q, Wu Y, Hu L, Wang M, et al. Case report: a case of PLA2G6 gene-related early-onset Parkinson's disease and review of literature. *Front Neurosci.* (2022) 16:1064566. doi: 10.3389/fnins.2022.1064566

4. Deng X, Yuan L, Jankovic J, Deng H. The role of the PLA2G6 gene in neurodegenerative diseases. *Ageing Res Rev.* (2023) 89:101957. doi: 10.1016/j.arr.2023.101957

5. Shi CH, Tang BS, Wang L, Lv ZY, Wang J, Luo LZ, et al. PLA2G6 gene mutation in autosomal recessive early-onset parkinsonism in a Chinese cohort. *Neurology.* (2011) 77:75–81. doi: 10.1212/WNL.0b013e318221acd3

6. Paisan-Ruiz C, Bhatia KP, Li A, Hernandez D, Davis M, Wood NW, et al. Characterization of PLA2G6 as a locus for dystonia-parkinsonism. *Ann Neurol.* (2009) 65:19–23. doi: 10.1002/ana.21415

7. Sina F, Shojaee S, Elahi E, Paisan-Ruiz C. R632W mutation in PLA2G6 segregates with dystonia-parkinsonism in a consanguineous Iranian family. *Eur J Neurol.* (2009) 16:101–4. doi: 10.1111/j.1468-1331.2008.02356.x

8. Yoshino H, Tomiyama H, Tachibana N, Ogaki K, Li Y, Funayama M, et al. Phenotypic spectrum of patients with PLA2G6 mutation and PARK14-linked parkinsonism. *Neurology.* (2010) 75:1356–61. doi: 10.1212/WNL.0b013e3181f73649

9. Bower MA, Bushara K, Dempsey MA, Das S, Tuite PJ. Novel mutations in siblings with later-onset PLA2G6-associated neurodegeneration (PLAN). *Mov Disord.* (2011) 26:1768–9. doi: 10.1002/mds.23617

10. Agarwal P, Hogarth P, Hayflick S, MacLeod P, Kuriakose R, McKenzie J, et al. Imaging striatal dopaminergic function in phospholipase A2 group VI-related parkinsonism. *Mov Disord.* (2012) 27:1698–9. doi: 10.1002/mds.25160

11. Lu CS, Lai SC, Wu RM, Weng YH, Huang CL, Chen RS, et al. PLA2G6 mutations in PARK14-linked young-onset parkinsonism and sporadic Parkinson's disease. *Am J Med Genet B Neuropsychiatr Genet.* (2012) 159B:183–91. doi: 10.1002/ajmg.b.32012

12. Paisán-Ruiz C, Li A, Schneider SA, Holton JL, Johnson R, Kidd D, et al. Widespread Lewy body and tau accumulation in childhood and adult onset dystonia-parkinsonism cases with PLA2G6 mutations. *Neurobiol Aging.* (2012) 33:814–23. doi: 10.1016/j.neurobiolaging.2010.05.009

13. Illingworth MA, Meyer E, Chong WK, Manzur AY, Carr LJ, Younis R, et al. PLA2G6-associated neurodegeneration (PLAN): further expansion of the clinical, radiological and mutation spectrum associated with infantile and atypical childhood-onset disease. *Mol Genet Metab.* (2014) 112:183–9. doi: 10.1016/j.ymgme.2014.03.008

14. Virmani T, Thenganatt MA, Goldman JS, Kubisch C, Greene PE, Alcalay RN. Oculogyric crises induced by levodopa in PLA2G6 parkinsonism-dystonia. *Parkinsonism Relat Disord.* (2014) 20:245–7. doi: 10.1016/j.parkreldis.2013.10.016

15. Malaguti MC, Melzi V, Di Giacopo R, Monfrini E, Di Biase E, Franco G, et al. A novel homozygous PLA2G6 mutation causes dystonia-parkinsonism. *Parkinsonism Relat Disord.* (2015) 21:337–9. doi: 10.1016/j.parkreldis.2015.01.001

16. Xie F, Cen Z, Ouyang Z, Wu S, Xiao J, Luo W. Homozygous pD331Y mutation in PLA2G6 in two patients with pure autosomal-recessive early-onset parkinsonism: further evidence of a fourth phenotype of PLA2G6-associated neurodegeneration. *Parkinsonism Relat Disord.* (2015) 21:420–2. doi: 10.1016/j.parkreldis.2015.01.012

17. Kim YJ, Lyoo CH, Hong S, Kim NY, Lee MS. Neuroimaging studies and whole exome sequencing of PLA2G6-associated neurodegeneration in a family with intrafamilial phenotypic heterogeneity. *Parkinsonism Relat Disord.* (2015) 21:402–6. doi: 10.1016/j.parkreldis.2015.01.010

18. Giri A, Guven G, Hanagasi H, Hauser AK, Erginul-Unaltuna N, Bilgic B, et al. PLA2G6 mutations related to distinct phenotypes: a new case with early-onset Parkinsonism. *Tremor Other Hyperkinet Mov.* (2016) 6:363. doi: 10.5334/tohm.289

19. Bohlega SA, Al-Mubarak BR, Alyemni EA, Abouelhoda M, Monies D, Mustafa AE, et al. Clinical heterogeneity of PLA2G6-related Parkinsonism: analysis of two Saudi families. *BMC Res Notes.* (2016) 9:295. doi: 10.1186/s13104-016-2102-7

20. Klein C, Lochte T, Delamonte SM, Braenne I, Hicks AA, Zschiedrich-Jansen K, et al. PLA2G6 mutations and Parkinsonism: long-term follow-up of clinical features and neuropathology. *Mov Disord.* (2016) 31:1927–9. doi: 10.1002/mds.26814

21. Kapoor S, Shah MH, Singh N, Rather MI, Bhat V, Gopinath S, et al. Genetic analysis of PLA2G6 in 22 Indian families with infantile neuroaxonal dystrophy, atypical late-onset neuroaxonal dystrophy and dystonia Parkinsonism complex. *PLoS ONE.* (2016) 11:e155605. doi: 10.1371/journal.pone.0155605

22. Chen YJ, Chen YC, Dong HL, Li LX, Ni W, Li HF, et al. Novel PLA2G6 mutations and clinical heterogeneity in Chinese cases with phospholipase A2-associated neurodegeneration. *Parkinsonism Relat Disord.* (2018) 49:88–94. doi: 10.1016/j.parkreldis.2018.02.010

23. Shen T, Hu J, Jiang Y, Zhao S, Lin C, Yin X, et al. Early-onset Parkinson's disease caused by PLA2G6 compound heterozygous mutation, a case report and literature review. *Front Neurol.* (2019) 10:915. doi: 10.3389/fneur.2019.00915

24. Kamel WA, Al-Hashel JY, Abdulsalam AJ, Damier P, Al-Mejalhem AY. PLA2G6-related parkinsonism presenting as adolescent behavior. *Acta Neurol Belg.* (2019) 119:621–2. doi: 10.1007/s13760-018-1003-z

25. Ma LM, Zhao J, Shi YY, Chen ZZ, Ren ZX, Zhang JW. PLA2G6 compound complicated mutation in an atypical neuroaxonal dystrophy pedigree. *Zhonghua Yi Xue Za Zhi.* (2019) 99:354–8. doi: 10.3760/cma.j.issn.0376-2491.2019.05.007

26. Jain S, Bhasin H, Romani M, Valente EM, Sharma S. Atypical childhood-onset neuroaxonal dystrophy in an Indian girl. *J Pediatr Neurosci.* (2019) 14:90–3. doi: 10.4103/jpn.JPN_91_18

27. Chu YT, Lin HY, Chen PL, Lin CH. Genotype-phenotype correlations of adult-onset PLA2G6-associated neurodegeneration: case series and literature review. *BMC Neurol.* (2020) 20:101. doi: 10.1186/s12883-020-01684-6

28. Gao C, Huang T, Chen R, Yuan Z, Tian Y, Zhang Y, et al. Han Chinese family with early-onset Parkinson's disease carrying novel frameshift mutation and compound heterozygous mutation of PRKN appearing incompatible with MDS clinical diagnostic criteria. *Front Neurol.* (2020) 11:582323. doi: 10.3389/fneur.2020.582323

29. Magrinelli F, Mehta S, Di Lazzaro G, Latorre A, Edwards MJ, Balint B, et al. Dissecting the phenotype and genotype of PLA2G6-related Parkinsonism. *Mov Disord.* (2022) 37:148–61. doi: 10.1002/mds.28807

30. Toth-Bencsik R, Balicza P, Varga ET, Lengyel A, Rudas G, Gal A, et al. New insights of phospholipase A2 associated neurodegeneration phenotype based on the long-term follow-up of a large Hungarian family. *Front Genet.* (2021) 12:628904. doi: 10.3389/fgene.2021.628904

31. Chen T, Chang Y, Cui Z, Yin X, Wang M, Gao Z, et al. Two cases of PLA2G6-associated young onset Parkinson disease. *Chin J Nerv Mental Dis.* (2022) 48:746–9. doi: 10.3969/j.issn.1002-0152.2022.12.008

32. Wan Y, Jiang Y, Xie Z, Ling C, Du K, Li R, et al. Novel PLA2G6 pathogenic variants in Chinese patients with PLA2G6-associated neurodegeneration. *Front Neurol.* (2022) 13:922528. doi: 10.3389/fneur.2022.922528

33. Ma J, Wang X, Wang C. PLA2G6 gene related early onset Parkinson syndrome with cerebellar atrophy: 3 cases report. *Chin J Neurol.* (2022) 55:1292–7. doi: 10.3760/cma.j.cn113694-20220720-00563

34. Jankovic J, Tan EK. Parkinson's disease: etiopathogenesis and treatment. *J Neurol Neurosurg Psychiatry.* (2020) 91:795–808. doi: 10.1136/jnnp-2019-322338

35. Ramanadham S, Ali T, Ashley JW, Bone RN, Hancock WD, Lei X. Calcium-independent phospholipases A2 and their roles in biological processes and diseases. *J Lipid Res.* (2015) 56:1643–68. doi: 10.1194/jlr.R058701

36. Zhao Y, Qin L, Pan H, Liu Z, Jiang L, He Y, et al. The role of genetics in Parkinson's disease: a large cohort study in Chinese mainland population. *Brain.* (2020) 143:2220–34. doi: 10.1093/brain/awaa167

37. Liu H, Wang Y, Pan H, Xu K, Jiang L, Zhao Y, et al. Association of rare heterozygous PLA2G6 variants with the risk of Parkinson's disease. *Neurobiol Aging.* (2021) 101:295–7. doi: 10.1016/j.neurobiolaging.2020.11.003

38. de Oliveira P, Montanaro V, Carvalho D, Martins B, Ferreira A, Cardoso F. Severe early-onset Parkinsonian syndrome caused by PLA2G6 heterozygous variants. *Mov Disord Clin Pract.* (2021) 8:794–6. doi: 10.1002/mdc3.13230

39. Gui YX, Xu ZP, Wen L, Liu HM, Zhao JJ, Hu XY. Four novel rare mutations of PLA2G6 in Chinese population with Parkinson's disease. *Parkinsonism Relat Disord.* (2013) 19:21–6. doi: 10.1016/j.parkreldis.2012.07.016

40. Chan DK, Mok V, Ng PW, Yeung J, Kwok JB, Fang ZM, et al. PARK2 mutations and clinical features in a Chinese population with early-onset Parkinson's disease. *J Neural Transm.* (2008) 115:715–9. doi: 10.1007/s00702-007-0011-6

41. Blanchard H, Taha AY, Cheon Y, Kim HW, Turk J, Rapoport SI. iPLA2beta knockout mouse, a genetic model for progressive human motor disorders, develops age-related neuropathology. *Neurochem Res.* (2014) 39:1522–32. doi: 10.1007/s11064-014-1342-y

42. Parkinson's Disease and Dyskinesia Group NBOC, Parkinson's Disease and Dyskinesia Group NBCM. Chinese expert consensus on diagnoses and treatments of early-onset Parkinson's disease. *Chin J Neuromed.* (2021) 20:109–16. doi: 10.3760/cma.j.cn115354-20201119-00903

frontiers | Frontiers in Neurology

TYPE Case Report
PUBLISHED 31 May 2024
DOI 10.3389/fneur.2024.1344018

OPEN ACCESS

EDITED BY
Huifang Shang,
Sichuan University, China

REVIEWED BY
Rosangela Ferese,
Mediterranean Neurological Institute Neuromed (IRCCS), Italy
Neha Nanda,
Harvard Medical School, United States

*CORRESPONDENCE
Raja Mokdad-Gargouri
raja.gargouri@cbs.rnrt.tn

RECEIVED 24 November 2023
ACCEPTED 08 May 2024
PUBLISHED 31 May 2024

CITATION
Ammous-Boukhris N, Abdelmaksoud-Dammak R, Ben Ayed-Guerfali D, Guidara S, Jallouli O, Kamoun H, Charfi Triki C and Mokdad-Gargouri R (2024) Case report: Compound heterozygous variants detected by next-generation sequencing in a Tunisian child with ataxia-telangiectasia. *Front. Neurol.* 15:1344018. doi: 10.3389/fneur.2024.1344018

Case report: Compound heterozygous variants detected by next-generation sequencing in a Tunisian child with ataxia-telangiectasia

Nihel Ammous-Boukhris[1], Rania Abdelmaksoud-Dammak[1], Dorra Ben Ayed-Guerfali[1], Souhir Guidara[2], Olfa Jallouli[3], Hassen Kamoun[2], Chahnez Charfi Triki[3] and Raja Mokdad-Gargouri[1]*

[1]Laboratory of Eukaryotes' Molecular Biotechnology, Center of Biotechnology of Sfax, University of Sfax, Sfax, Tunisia, [2]Department of Human Genetics, Hedi Chaker Hospital, Sfax, Tunisia, [3]Department of NeuroPediatry, Hedi Chaker Hospital, Sfax, Tunisia

Ataxia-telangiectasia (A-T) is an autosomal recessive primary immunodeficiency disorder (PID) caused by biallelic mutations occurring in the serine/threonine protein kinase (*ATM*) gene. The major role of nuclear *ATM* is the coordination of cell signaling pathways in response to DNA double-strand breaks, oxidative stress, and cell cycle checkpoints. Defects in ATM functions lead to A-T syndrome with phenotypic heterogeneity. Our study reports the case of a Tunisian girl with A-T syndrome carrying a compound heterozygous mutation *c.[3894dupT]; p.(Ala1299Cysfs3;rs587781823)*, with a splice acceptor variant*: c.[5763-2A>C;rs876659489]* in the *ATM* gene that was identified by next-generation sequencing (NGS). Further genetic analysis of the family showed that the mother carried the c.[5763-2A>C] splice acceptor variant, while the father harbored the c.[3894dupT] variant in the heterozygous state. Molecular analysis provides the opportunity for accurate diagnosis and timely management in A-T patients with chronic progressive disease, especially infections and the risk of malignancies. This study characterizes for the first time the identification of compound heterozygous ATM pathogenic variants by NGS in a Tunisian A-T patient. Our study outlines the importance of molecular genetic testing for A-T patients, which is required for earlier detection and reducing the burden of disease in the future, using the patients' families.

KEYWORDS

ataxia-telangiectasia, ATM, mutations, next generation sequencing, targeted sequencing

Introduction

Ataxia-telangiectasia (A-T) is an autosomal recessive multisystem disorder characterized by progressive cerebellar degeneration, variable immunodeficiency, oculocutaneous telangiectasia, cancer susceptibility, and sensitivity to radiation (1, 2).

A-T patients represent a wide range of clinical manifestations, including progressive cerebellar ataxia, radiosensitivity, susceptibility to malignancies, and metabolic disorders. Other abnormalities, such as growth failure, poor pubertal development, insulin-resistant diabetes, gonadal atrophy, lung disease, cutaneous abnormality, and cardiovascular disease, have also been reported in A-T patients (3, 4). A-T patients have poor prognosis, and their survival time is approximately 25 years. The two most common causes of death in these patients are chronic pulmonary diseases and malignancy (5).

This syndrome is caused by biallelic pathogenic mutations in the ataxia-telangiectasia (*ATM*) gene containing 66 exons; of which, 62 are coding exons, spread over 150 kb of genomic DNA, with an open-reading frame of 9,168 nucleotides (6). This gene encodes a large protein (~350 KDa) belonging to the phosphatidylinositol 3-kinase–related protein kinase (PIKK) family including *ATR*, *DNAPKcs*, *mTOR*, and *SMG1* genes (6, 7). As a member of the PIKK family, *ATM* contains a kinase domain positioned between conserved C-terminal domains known as FAT (FRAP, ATR, and TRRAP proteins), PIKK kinase, and FATC domains (7). These domains control ATM's kinase activity by interacting with regulatory proteins and inducing posttranslational modifications (7).

ATM function is important to B-and T-cell receptor development and class switch recombination (CSR) in activated B cells (8). In addition, ATM plays a critical role in the repair of DNA double-strand breaks, the regulation of the cell cycle, the stability of the genome, and the survival of cells (9).

The majority of ATM pathogenic variants are single-nucleotide variant (SNV) alterations, such as frameshift or nonsense variants, which are predicted to truncate the ATM protein (8). Patients carrying these types of ATM mutations develop the classic form of A-T (10, 11).

Other SNV pathogenic variants of ATM include missense and splicing variants. According to the Human Gene Mutation Database, the copy number variation (CNV) or large genomics alterations are detected in approximately 1%–10% of A-T patients (12, 13). However, limited information is available on the co-occurrence of SNV and CNV and its identified role or phenotype burden in A-T patients (8).

This study reports for the first time a case of a Tunisian child diagnosed with A-T syndrome, who carried compound heterozygous ATM pathogenic variants, detected by targeted NGS. The co-segregation of both mutations was analyzed in the parents.

Patient and methods

The proband in this study is a 16-year-old girl who had been followed up since the age of 6 years when she first presented with ocular telangectasia, foot drop, and proximo-distal deficit of both inferior extremities as addressed first to the Pediatric Neurology Department and then to Genetic Department of Hedi Chaker Hospital-Sfax Tunisia. The family pedigree information was gathered, and blood samples were collected from the patient and her parents. The proband had been the subject of various diagnostic tests, including magnetic resonance imaging (MRI) of the brain and cervical region, ultrasound examinations of the heart and abdomen, electroencephalogram (EEG), and blood biochemical analysis involving α-fetoprotein (AFP), immunoglobulin (Ig), and ceruloplasmin level detection.

Written informed consent was obtained from all participants.

DNA extraction and targeted sequencing

The QIAamp DNA Blood Mini kit (Qiagen) was used to extract genomic DNA from 0.4 mL of peripheral blood obtained from the patient and her parents. The instructions of the manufacturer were followed during the extraction process. The resulting DNA was quantified using Qubit 3.0 (Thermo Fisher Scientific).

Briefly, 200 ng of genomic DNA was used to prepare the library using the OncoRisk panel kit, according to the protocol provided by Celemics. This panel includes 31 genes: *APC, ATM, BARD1, BLM, BMPR1A, BRCA1, BRCA2, BRIP1, CDH1, CDK4, CDKN2A, CHEK2, EPCAM, MLH1, MRE11A, MSH2, MSH6, MUTYH, NBN, PALB2, PMS2, PRSS1, PTEN, RAD50, RAD51C, RAD51D, SLX4, SMAD4, STK11, TP53, and VHL.*

Subsequently, the library was quantified with the Qubit® dsDNA HS Assay Kit (Life Technologies). The DNA library was pooled and prepared for sequencing using the MiSeq Reagent Kit v3 (300 cycles) according to the manufacturer's instructions to generate paired-end reads with a read length of 151 bp (Illumina, San Diego, CA). Reads were trimmed to remove low-quality sequences and then aligned to the human reference genome (GRCh37/hg19) using the Burrows–Wheeler alignment (BWA) package. The ATM (NM_000051.3) sequence from the National Center for Biotechnology Information (NCBI) database[1] was used as the reference, and NGS data were analyzed using the BaseSpace Variant Interpreter.[2] SplicAI and SPIP prediction tools were used to evaluate the effect of the splice site acceptor variant (14, 15).

Sanger sequencing

Sanger sequencing was used to confirm the presence of the variants identified by NGS and to investigate co-segregation analysis in the family members. Forward and reverse primers were designed using Primer 3.0 software to amplify the fragments covering the variant region and provided upon request. PCR products were purified and labeled using the BigDye Terminator V3.1 Cycle Sequencing Kit and sequenced on SeqStudio (Applied Biosystems). Sequence analysis was performed using BioEdit software.

Results

Case presentation

The proband *(IV-3)* is a 16-year-old girl who had no pre-, peri-, or post-natal complications and normal cognitive and motor development. She was consulted at the age of 6 years for abnormal

1 http://www.ncbi.nlm.nih.gov

2 https://basespace.illumina.com

movements and has since then followed up for cerebellar ataxia at the Department of Pediatric Neurology and Department of Genetics, at the CHU Hedi Chaker of Sfax, Tunisia. The proband *(IV-3)* had choreic abnormal movements affecting the upper and lower extremities since the age of 4.5 years, and upon examination, she had no facial dysmorphia, normal measurements, dysarthric speech, oculomotor apraxia, and static and kinetic cerebellar syndrome. She had difficulties at school, and due to worsening instability, she became bedridden at the age of 10 years. Ocular telangectasia was observed at 10 years of age, and after a year, she had developed foot drop and proximo-distal deficit of both inferior extremities and choreo-athetosis movements. Brain MRI performed at 3 years of age showed discrete cerebellum atrophy (Figure 1). EMG at the age of 12 years showed no neuropathy but was in favor of myoclonic dystonia. The EEG at the age of 11 years was well-organized, without abnormalities.

Concerning biochemical parameters, the serum alpha-FP levels were significantly increased from 125.2 ng/mL at the age of 6 years to 370 ng/mL at the age of 15 years, whereas the serum level of IgA was significantly decreased. Other biological analyses showed all normal levels of cholesterol, creatinine alkaline, lactate dehydrogenase (LDH), and ceruloplasmin.

The older sister (IV-2) experienced similar symptoms but showed a delay in language and walking ability. She also had tachycardia and suffered from immune deficiency, which was treated with venoglobulin transfusions. She died at the age of 16 years after a cardiac arrest.

There was no known consanguinity in the family, but there were a few cases of blindness. The proband's mother *(III-6)* and aunt *(III-8)* both had breast cancer, and her paternal cousin was treated for autism (Figure 2).

Genetic testing

The blood DNA of the proband was analyzed by NGS using a panel covering 31 genes (*Oncorisk* and *Celemics*) related to human malignancies. Approximately 99.9% of target regions were covered with at least 50X, and the mean region coverage depth was 3570.5. After filtering, two variants in the *ATM* gene, namely, NM_000051.3 *c.[3894dupT];p.(Ala1299Cysfs3;rs587781823)* and c.[5763-2A>C; *rs876659489*], were identified in the patient. According to the ClinVar database and ACMG criteria, the frameshift c.[3894dupT] is located in exon 26/63 and is classified as pathogenic (*class 5, PVS1, PM2,* and *PP5_Very Strong*). This mutation led to a frameshift at residue 1,299, which produced a truncated protein of 1,312 amino acids p. (Ala1299Cysfs3) lacking the FAT, PI3K/PI4K catalytic, and FATC domains. This variant is rare, with a population frequency equal to 0.00000796 (exomes) and 0.000163 (GnomAD).

On the other hand, the c.[5763-2A>C; *rs876659489*] variant is expected to disrupt RNA splicing by affecting an acceptor splice site in intron 38 of the *ATM* gene; thereby, it is classified as a class 5 pathogenic variant according to the ClinVar database and *ACMG* criteria (*PVS1_Moderate, PM2, PP3_Strong,* and *PP5_Very_Strong*). The *SpliceAI* and *SPIP* tools predicted that the *c.[5763-2A>C]* variant results in an acceptor loss with scores = 1 and −0.99, respectively. The population frequency of this variant is 0.000009, as indicated by GnomAD.

In addition, the proband *(IV-3)* carried six other variants in the *ATM* gene: one synonymous missense variant c.[5948A>G];p.(Ser1983=*rs659243*) and five intronic variants, all classified as benign. No other pathogenic variant has been identified in genes included in the NGS panel in the present study.

Furthermore, the DNA of the proband *(IV-3)* and her parents *(III-5 and III-6)* were subjected to Sanger sequencing to (i) confirm the variants found by NGS in the proband and (ii) investigate the heredity of both variants in the parents. Both variants were successfully verified in the proband; in addition, we found that the c.[3894dupT];p.(Ala1299CysfsTer3;*rs587781823*) variant, in the exon 26 of the *ATM* gene, was inherited from her father, and the c.[5763-2A>C *rs876659489*] splice site acceptor variant (intron 38) was inherited from her mother (Figure 3). It is important to mention that in these families, the first-degree relatives over two generations were affected by breast cancer, namely, the proband's mother *(III-6)*, her aunt *(III-8)*, and her grandmother *(II-5)*, but unfortunately, their DNA samples were not available for genetic testing (Figure 2).

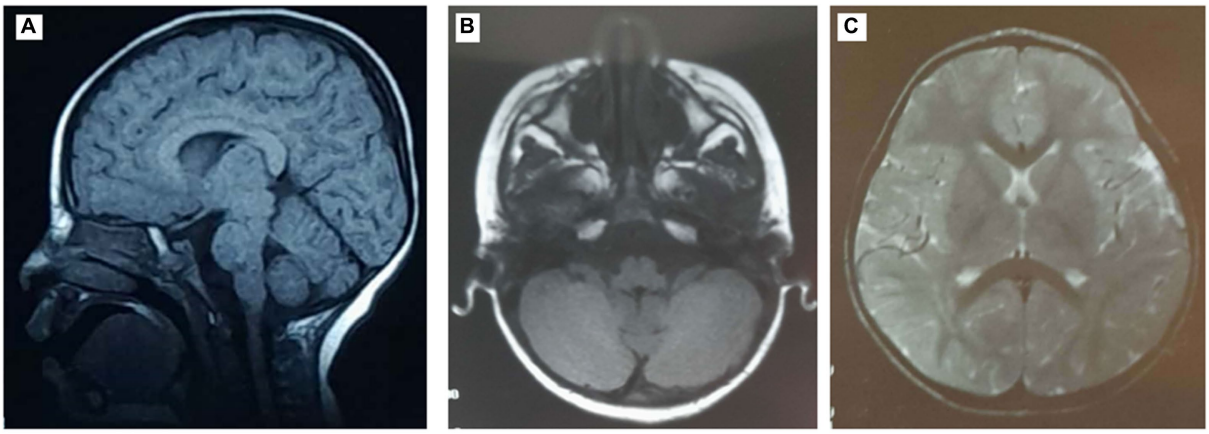

FIGURE 1
Magnetic resonance images (MRIs) of the patient's brain showing discrete cerebellum atrophy. **(A)** Sagittal T1-weighted brain MRI. Axial T1- **(B)** and T2- **(C)** weighted brain MRI.

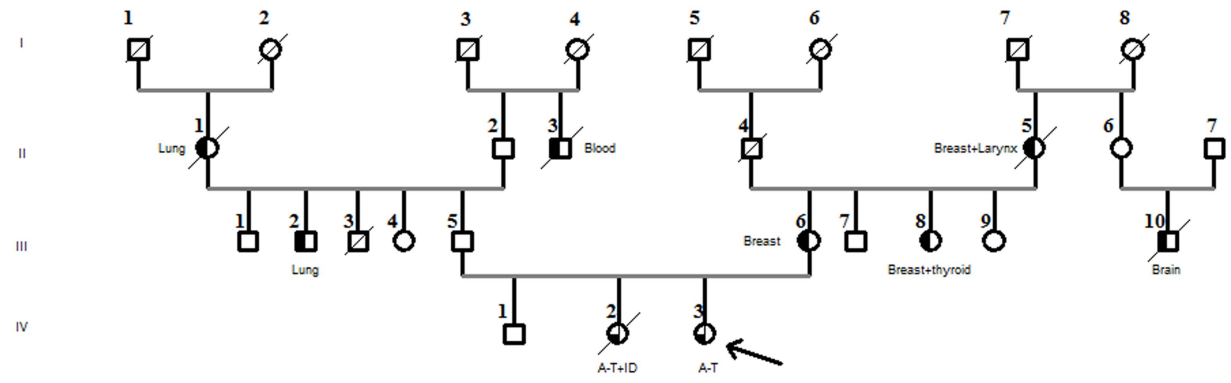

FIGURE 2
Family pedigree diagnosed with the compound heterozygous *ATM* pathogenic variant. The arrow in the pedigree member shows the A-T patient. The sister of the proband had A-T associated with immunodeficiency (A-T + ID). Black half-filled pedigree members indicate cancer cases (cancer types are mentioned in the pedigree).

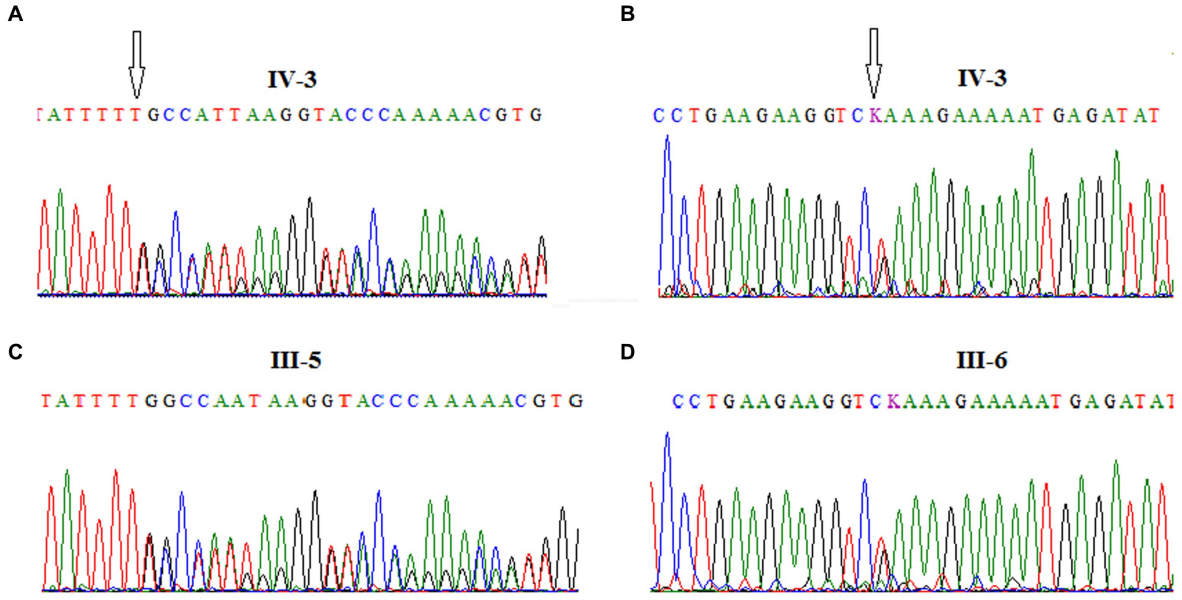

FIGURE 3
Chromatograms showing the frameshift mutation *c.[3894dupT]; p.(Ala1299CysfsTer3; rs587781823)*, in ATM exon 26 identified in the A-T patient **(A)** and her father **(C)** and the splice site acceptor mutation *c.[5763-2A>C; rs876659489]* in ATM exon 39 identified in the A-T patient **(B)** and her mother **(D)**.

Discussion

Ataxia-telangiectasia (A-T) is a rare disorder affecting multiple body systems. Typically, the degeneration of the nervous system begins between 6 and 18 months of age, resulting in being confined to a wheelchair by the age of 10 years. Cerebellar degeneration causes symptoms such as unsteady trunk movements, difficulty walking, lack of coordination, weak muscles, and sudden falls (16). The involuntary movements in A-T patients worsen over time, starting mildly in childhood and becoming more noticeable in adulthood. Movement disorders characterized by reduced movement are less common compared to those with excessive movement. Some patients might develop symptoms resembling Parkinson's disease, such as stiffness and tremors when at rest (17).

It is well known that the mode of inheritance for A-T is autosomal recessive and caused by biallelic mutations in the *ATM* gene. The ATM protein plays a pivotal role in regulating several tumor suppressor proteins, mainly TP53, BRCA1, Chek2, RAD17, RAD9, and NBS1 (18, 19). These proteins, along with ATR kinase, are considered master controllers of cell cycle checkpoint signaling pathways, essential for the cell's response to DNA damage and maintenance of genome stability (19, 20). Thus, when both copies of the *ATM* gene are inactivated (biallelic inactivation), it leads to A-T.

It is important to mention that in Tunisia, only two studies have investigated the clinical, immunological, and molecular (chromosomal instability) features without identifying the causal *ATM* gene mutation (21, 22). Therefore, our study is the first one that reports a Tunisian A-T patient harboring compound heterozygous

mutations in the *ATM* gene, namely, a frameshift *c.[3894dupT];p.(Ala1299CysfsTer3;rs587781823)* and a splice site acceptor variant (*c.[5763-2A>C],rs876659489*). According to the literature, the frameshift variant had been previously identified in a homozygous state in Italian and Polish A-T patients (23, 24).

Globally, most *ATM* gene mutations involve frameshift or nonsense mutations located in the proximal, central, and distal regions of the *ATM* gene (25). Barone et al. demonstrated that the majority of *ATM* missense mutations in A-T are functionally linked to defects in expression and/or inactivation of kinase activity (26). Additionally, Jacquemin et al. showcased that, aside from resulting in the under-expression of the ATM protein, ATM missense mutations caused abnormal cytoplasmic localization of the protein (27).

A recent study on Iranian A-T patients reported that ATM nonsense and frameshift mutations are most frequent, leading to a more severe phenotype than missense or splice-site mutations (28). However, in Chinese A-T patients, the mutational spectrum of ATM is likely to be diverse and different, when largely compared to other ethnic areas (29). Biallelic ATM mutations combining the splice site variant with frameshift, nonsense, or missense mutations were less frequent than other compound mutations. Despite this, there is a recent case report that described a Chinese A-T patient diagnosed at 7 years of age with the compound heterozygous ATM genotype (frameshift combined with splice site ATM variant), who is similar to the proband in our case (30). This Chinese girl presented with growth retardation, ataxia, medium ocular telangiectasia, cerebellar atrophy, elevated serum alpha-fetoprotein (AFP) level, and normal serum levels of immunoglobulins, which are all similar to our proband.

Altogether, our patient had an onset of A-T syndrome at the age of 6 years with slow progression and a lack of basal ganglia manifestations, ruling out immunodeficiency, which may indicate that her mutations led to less severe neurodegenerative effects compared to other mutations in the *ATM* gene.

Furthermore, there is increasing evidence showing that heterozygous mutations in the *ATM* gene are associated with an increased risk of developing a wide spectrum of malignancies, including breast, stomach, and lung cancers (31). We observed that the Tunisian family consists of several members with various types of cancer such as lung, larynx, brain, and breast. In line with this report, we confirmed that the proband's mother, who had breast cancer, carried the pathogenic ATM variant *c.[3894dupT];p.(Ala1299CysfsTer3;rs587781823)*, which is most likely responsible for the malignancy.

Although there is currently no cure for A-T patients, there has been a rapid development of mutation-targeted therapeutic approaches. These advancements bring hope for potential treatment in specific A-T patients with ATM mutations (32). These mutations can be corrected, for example, using antisense morpholino oligonucleotide (AMO), read through compound (RTC), or micro-RNA (33, 34). In fact, AMOs have shown effectiveness in correcting type II and IV splicing mutations (35). Research has also revealed that functional ATM protein can be induced using RTCs to target premature termination codons in cells with ATM heterozygous nonsense mutations (33). Furthermore, gene editing approaches, such as CRISPR/Cas9, have been employed for targeting the ATM gene, offering a promising tool for new therapeutic approaches in treating this disease (36).

These *in vitro* tests shed light on the potential therapeutic applications of customized mutation-targeted therapies for A-T patients in the future. However, it is very important to note that this personalized approach profoundly relies on an exhaustive analysis of ATM gene mutations.

Conclusion

In summary, we report a case of an A-T patient carrying a compound heterozygous mutation c.[3894dupT];p.(Ala1299CysfsTer 3;*rs587781823*) and c.[5763-2A>C *rs876659489*] splice acceptor variant in the *ATM* gene. Our findings extend the genotype spectrum of A-T in the Tunisian population and will allow timely decisions to be made in A-T diagnosis for better therapeutic management.

Data availability statement

The datasets presented in this article are not readily available because of ethical and privacy restrictions. Requests to access the datasets should be directed to the corresponding author.

Ethics statement

The studies involving humans were approved by the Comité de Protection des personnes CHU Hedi Chaker/CHU Habib Bourguiba sfax—Tunisia. The studies were conducted in accordance with the local legislation and institutional requirements. Written informed consent for participation in this study was provided by the participants' legal guardians/next of kin. Written informed consent was obtained from the individual(s), and minor(s)' legal guardian/next of kin, for the publication of any potentially identifiable images or data included in this article.

Author contributions

NA-B: Investigation, Methodology, Writing – original draft, Writing – review & editing. RA-D: Data curation, Investigation, Methodology, Writing – review & editing. DB: Formal analysis, Methodology, Writing – review & editing. SG: Conceptualization, Formal analysis, Writing – review & editing. OJ: Formal analysis, Writing – review & editing. HK: Writing – review & editing. CC: Supervision, Validation, Writing – review & editing. RM-G: Conceptualization, Formal analysis, Supervision, Writing – original draft, Writing – review & editing.

Funding

The author(s) declare that no financial support was received for the research, authorship, and/or publication of this article.

Conflict of interest

The authors declare that the research was conducted in the absence of any commercial or financial relationships that could be construed as a potential conflict of interest.

Publisher's note

References

1. Chaudhary MW, Al-Baradie RS. Ataxia-telangiectasia: future prospects. *Appl Clin Genet*. (2014) 7:159–67. doi: 10.2147/TACG.S35759

2. Nissenkorn A, Levy-Shraga Y, Banet-Levi Y, Lahad A, Sarouk I, Modan-Moses D. Endocrine abnormalities in ataxia telangiectasia: findings from a national cohort. *Pediatr Res*. (2016) 79:889–94. doi: 10.1038/pr.2016.19

3. Su Y, Swift M. Mortality rates among carriers of ataxia-telangiectasia mutant alleles. *Ann Intern Med*. (2000) 133:770–8. doi: 10.7326/0003-4819-133-10-200011210-00009

4. Bott L, Lebreton J, Thumerelle C, Cuvellier J, Deschildre A, Sardet A. Lung disease in ataxia-telangiectasia. *Acta Paediatr*. (2007) 96:1021–4. doi: 10.1111/j.1651-2227.2007.00338.x

5. Crawford TOSkolasky RL, Fernandez R, Rosquist KJ, Lederman HM. Survival probability in ataxia telangiectasia. *Arch Dis Child*. (2006) 91:610–1. doi: 10.1136/adc.2006.094268

6. Gately DP, Hittle JC, Chan GK, Yen TJ. Characterization of ATM expression, localization, and associated DNA-dependent protein kinase activity. *Mol Biol Cell*. (1998) 9:2361–74. doi: 10.1091/mbc.9.9.2361

7. Nanda N, Roberts NJ. ATM serine/threonine kinase and its role in pancreatic risk. *Genes*. (2020) 11:108. doi: 10.3390/genes11010108

8. Bakkenist CJ, Kastan MB. DNA damage activates ATM through intermolecular autophosphorylation and dimer dissociation. *Nature*. (2003) 421:499–506. doi: 10.1038/nature01368

9. Aki T, Uemura K. Cell death and survival pathways involving ATM protein kinase. *Genes*. (2021) 12:581. doi: 10.3390/genes12101581

10. Verhagen MM, Last JI, Hogervorst FB, Smeets DF, Roeleveld N, Verheijen F, et al. Presence of ATM protein and residual kinase activity correlates with the phenotype in ataxia-telangiectasia: a genotype-phenotype study. *Hum Mutat*. (2012) 33:561–71. doi: 10.1002/humu.22016

11. Taylor AM, Lam Z, Last JI, Byrd PJ. Ataxia telangiectasia: more variation at clinical and cellular levels. *Clin Genet*. (2015) 87:199–208. doi: 10.1111/cge.12453

12. Cavalieri S, Funaro A, Porcedda P, Turinetto V, Migone N, Gatti RA, et al. ATM mutations in Italian families with ataxia telangiectasia include two distinct large genomic deletions. *Hum Mutat*. (2006) 27:1061. doi: 10.1002/humu.9454

13. Cavalieri S, Funaro A, Pappi P, Migone N, Gatti RA, Brusco A. Large genomic mutations within the ATM gene detected by MLPA, including a duplication of 41 kb from exon 4 to 20. *Ann Hum Genet*. (2008) 72:10–8. doi: 10.1111/j.1469-1809.2007.00399.x

14. Jaganathan K, Kyriazopoulou Panagiotopoulou S, McRae JF, Darbandi SF, Knowles D, Li YI, et al. Predicting splicing from primary sequence with deep learning. *Cell*. (2019) 176:535–48.e24. doi: 10.1016/j.cell.2018.12.015

15. Leman R, Parfait B, Vidaud D, Girodon E, Pacot L, Le Gac G, et al. SPiP: splicing prediction pipeline, a machine learning tool for massive detection of exonic and intronic variant effects on mRNA splicing. *Hum Mutat*. (2022) 43:2308–23. doi: 10.1002/humu.24491

16. Hoche F, Seidel K, Theis M, Vlaho S, Schubert R, Zielen S, et al. Neurodegeneration in ataxia telangiectasia: what is new? What is evident? *Neuropediatrics*. (2012) 43:119–29. doi: 10.1055/s-0032-1313915

17. Pearson TS. More than Ataxia: hyperkinetic movement disorders in childhood autosomal recessive Ataxia syndromes. *Tremor Other Hyperkin Move*. (2016) 6:368. doi: 10.5334/tohm.319

18. Zolotovskaia MA, Modestov AA, Suntsova MV, Rachkova AA, Koroleva EV, Poddubskaya EV, et al. Pan-cancer antagonistic inhibition pattern of ATM-driven G2/M checkpoint pathway vs other DNA repair pathways. *DNA Repair*. (2023) 123:103448. doi: 10.1016/j.dnarep.2023.103448

19. Phan LM, Rezaeian AH. ATM: Main features, signaling pathways, and its diverse roles in DNA damage response, tumor suppression, and Cancer development. *Genes*. (2021) 12:845. doi: 10.3390/genes12060845

20. Gatti RA, Berkel I, Boder E, Braedt G, Charmley P, Concannon P, et al. Localization of an ataxia-telangiectasia gene to chromosome 11q22-23. *Nature*. (1988) 336:577–80. doi: 10.1038/336577a0

21. Triki C, Feki I, Meziou M, Turki H, Zahaf A, Mhiri C. Clinical, biological and genetic study of 24 patients with ataxia telangiectasia from southern Tunisia. *Rev Neurol*. (2000) 156:634–7.

22. Sfaihi L, Stoppa Lyonnet D, Ben Ameur S, Dubois D'enghien C, Kamoun T, Barbouch MR, et al. Ataxia-telangiectasia in the south of Tunisia: a study of 11 cases. *La Tunisie Medicale*. (2015) 93:511–5.

23. Chessa L, Piane M, Magliozzi M, Torrente I, Savio C, Lulli P, et al. Founder effects for ATM gene mutations in Italian Ataxia telangiectasia families. *Ann Hum Genet*. (2009) 73:532–9. doi: 10.1111/j.1469-1809.2009.00535.x

24. Podralska MJ, Stembalska A, Ślęzak R, Lewandowicz-Uszyńska A, Pietrucha B, Kołtan S, et al. Ten new ATM alterations in polish patients with ataxia-telangiectasia. *Mol Genet Genomic Med*. (2014) 2:504–11. doi: 10.1002/mgg3.98

25. Telatar M, Teraoka S, Wang Z, Chun HH, Liang T, Castellvi-Bel S, et al. Ataxia-telangiectasia: identification and detection of founder-effect mutations in the ATM gene in ethnic populations. *Am J Hum Genet*. (1998) 62:86–97. doi: 10.1086/301673

26. Barone G, Groom A, Reiman A, Srinivasan V, Byrd PJ, Taylor AM. Modeling ATM mutant proteins from missense changes confirms retained kinase activity. *Hum Mutat*. (2009) 30:1222–30. doi: 10.1002/humu.21034

27. Jacquemin V, Rieunier G, Jacob S, Bellanger D, d'Enghien CD, Laugé A, et al. Underexpression and abnormal localization of ATM products in ataxia telangiectasia patients bearing ATM missense mutations. *Eur J Hum Genet*. (2012) 20:305–12. doi: 10.1038/ejhg.2011.196

28. Amirifar P, Ranjouri MR, Pashangzadeh S, Lavin M, Yazdani R, Moeini Shad T, et al. The spectrum of ATM gene mutations in Iranian patients with ataxia-telangiectasia. *Pediatr Allergy Immunol*. (2021) 32:1316–26. doi: 10.1111/pai.13461

29. Huang Y, Yang L, Wang J, Yang F, Xiao Y, Xia R, et al. Twelve novel Atm mutations identified in Chinese ataxia telangiectasia patients. *NeuroMolecular Med*. (2013) 15:536–40. doi: 10.1007/s12017-013-8240-3

30. Shao L, Wang H, Xu J, Qi M, Yu Z, Zhang J. Ataxia-telangiectasia in China: a case report of a novel ATM variant and literature review. *Front Neurol*. (2023) 14:1228810. doi: 10.3389/fneur.2023.1228810

31. Sriramulu S, Ramachandran M, Subramanian S, Kannan R, Gopinath M, Sollano J, et al. A review on role of ATM gene in hereditary transfer of colorectal cancer. *Acta Biomed*. (2019) 89:463–9. doi: 10.23750/abm.v89i4.6095

32. Chessa LMR, Molinaro A. Focusing new Ataxia telangiectasia therapeutic approaches. *J Rare Dis Diagn*. (2016) 2:2. doi: 10.21767/2380-7245.100041

33. Nakamura K, Du L, Tunuguntla R, Fike F, Cavalieri S, Morio T, et al. Functional characterization and targeted correction of ATM mutations identified in Japanese patients with ataxia-telangiectasia. *Hum Mutat*. (2012) 33:198–208. doi: 10.1002/humu.21632

34. Hu H, Gatti RA. Micro RNAs: new players in the DNA damage response. *J Mol Cell Biol*. (2011) 3:151–8. doi: 10.1093/jmcb/mjq042

35. Du L, Gatti RA. Potential therapeutic applications of antisense morpholino oligonucleotides in modulation of splicing in primary immunodeficiency diseases. *J Immunol Methods*. (2011) 365:1–7. doi: 10.1016/j.jim.2010.12.001

36. Nurieva W, Ivanova E, Chehab S, Singh P, Reichlmeir M, Szuhai K, et al. Generation of four gene-edited human induced pluripotent stem cell lines with mutations in the ATM gene to model Ataxia-telangiectasia. *Stem Cell Res*. (2023) 73:103247. doi: 10.1016/j.scr.2023.103247

Frontiers in Neurology

Explores neurological illness to improve patient care

The third most-cited clinical neurology journal explores the diagnosis, causes, treatment, and public health aspects of neurological illnesses. Its ultimate aim is to inform improvements in patient care.

Discover the latest Research Topics

See more →

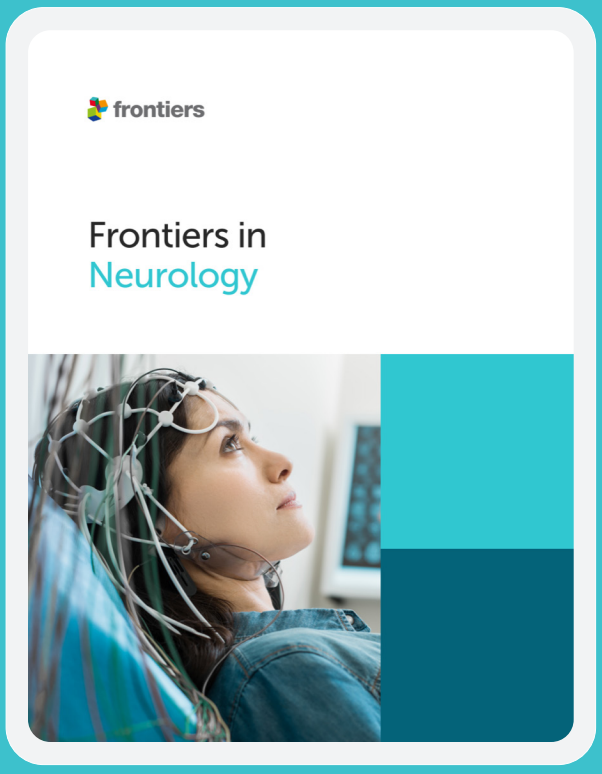

Frontiers

Avenue du Tribunal-Fédéral 34
1005 Lausanne, Switzerland
frontiersin.org

Contact us

+41 (0)21 510 17 00
frontiersin.org/about/contact